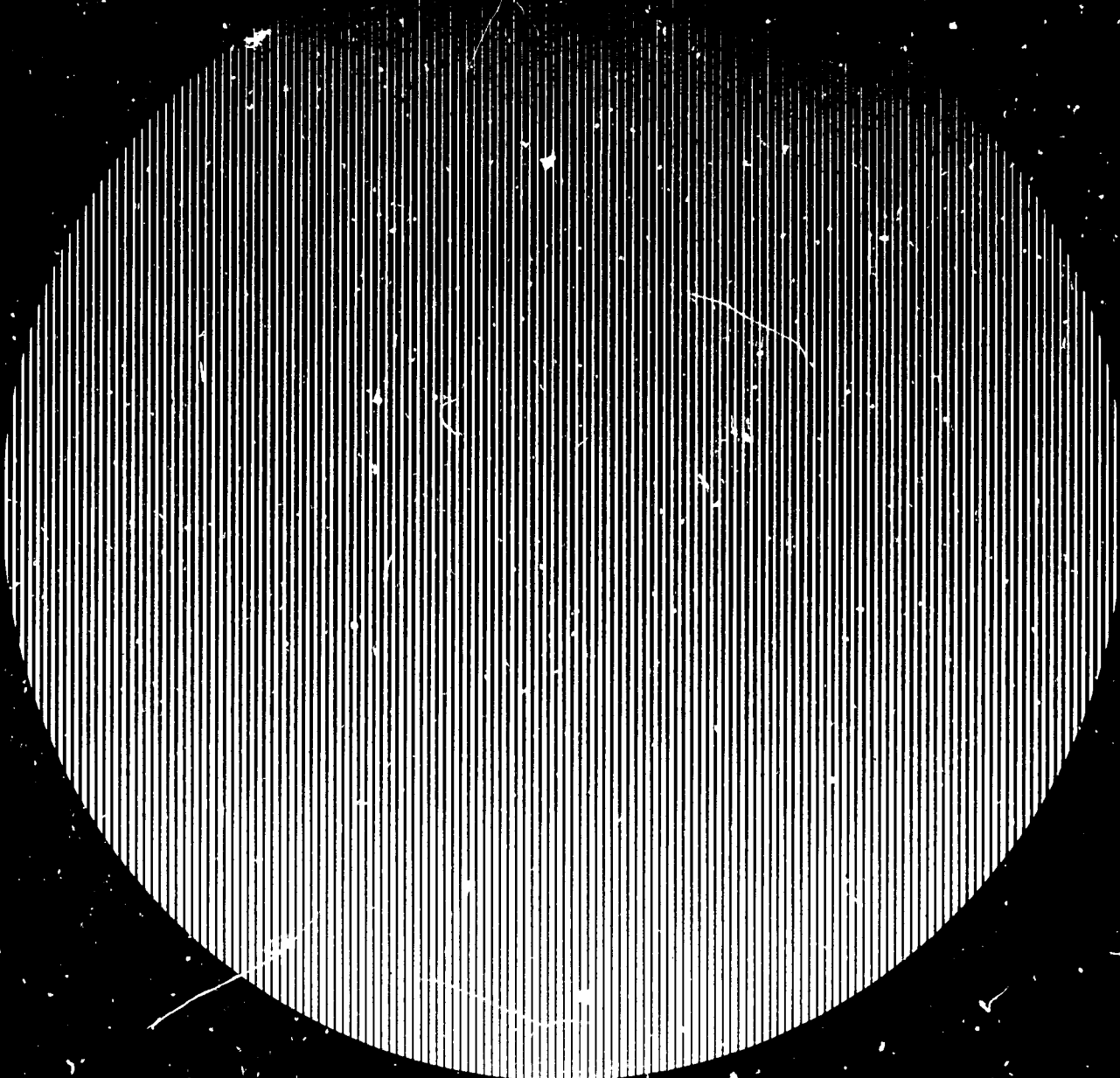


Interaction of the Saturated and Unsaturated Soil Moisture Zones

1. Analytical Solution of the Linearized Richards Equation
2. The Role of Climate in Shaping the Phreatic Surface



2639912/62
6/10/82 10:10 AM

EG-AAD-400
PN-ARM 397
OSP 89965

R82-43

INTERACTION OF THE SATURATED AND UNSATURATED SOIL MOISTURE ZONES

1. ANALYTICAL SOLUTION OF THE LINEARIZED RICHARDS EQUATION
2. THE ROLE OF CLIMATE IN SHAPING THE PHREATIC SURFACE

by

Scott Alan Miller

and

Peter S. Eagleson

RALPH M. PARSONS LABORATORY

HYDROLOGY AND WATER RESOURCE SYSTEMS

Report Number 284

Prepared under the support of the M.I.T. Technology Adaptation Program, which is funded through a grant from the Agency for International Development, United States Department of State.

August 1982

ABSTRACT

In Part I, dimensionless analytical expressions are derived describing the hydrologic processes and the moisture distribution of a high water table unsaturated soil column, by linearizing Richards' equation. The finite Fourier transform method is used to solve for the moisture content, which is the basis for the solutions for the depth-averaged moisture content, ponding time, boundary fluxes and their integral quantities. The effects of transpiration are included through three models of soil-water extraction by plants. Simplified, physically-based expressions for infiltration rate and ponding time which include water table effects, are proposed in the appendix.

Examples of the solutions are presented and several cases are compared with a numerical finite-element model of the non-linear problem. Fitted parameter estimates are compared with analytical expressions from the literature. Comparisons are for average moisture content, ponding time and cumulative infiltration. Good to excellent agreement is found for all cases. The exfiltration solutions, with and without vegetation, are untested.

In Part II, the dynamic relation between soil-moisture, water table depth, and accretion to groundwater is studied. Derived relations between the moisture content, water table depth, and net accretion are compared over a range of climate and soil types. These are used in a one-dimensional non-linear finite-difference model for the water table shape and the longer run influence of climate upon it. The boundaries are constant potentials.

The water table is shown to have an influence for depths from less than one meter to over one hundred meters, with the greater influence for clay soils and larger potential evaporation rates. Climate-induced water table depressions and swamplands are shown to be dependent upon the unsaturated zone water balance and upon the hydraulic conductivity of the soil. Case studies for the water table-water balance model use data from the El-Gizera and Bahr-el-Ghazal regions of Sudan.

In both parts of this work, dimensionless parameters are developed to describe when the water table influences the water balance of unsaturated soil and when the climate influences the water table shape.

ACKNOWLEDGEMENTS

This work has been sponsored by the M.I.T. Technology Adaptation Program, which is funded through a grant from the Agency for International Development, United States Department of State.

This report contains the work performed by Scott A. Miller for his Master's thesis submitted to the Department of Civil Engineering at M.I.T. The research was supervised by Dr. Peter S. Eagleson, Professor of Civil Engineering.

The authors thank the many people who aided the completion of this work. We acknowledge in particular the technical assistance of Dr. P. Christopher D. Milly and the help of Ms. Anne L. Clee, who typed this report, and Ms. Antoinette DiRenzo, who assisted in the preparation of the document.

PREFACE

This report is one of a series of publications which describe various studies undertaken under the sponsorship of the Technology Adaptation Program at the Massachusetts Institute of Technology,

The United States Department of State, through the Agency for International Development, awarded the Massachusetts Institute of Technology a contract to provide support at M. I. T. for the development, in conjunction with institutions in selected developing countries, of capabilities useful in the adaptation of technologies and problem-solving techniques to the needs of those countries. This particular study describes research conducted in conjunction with Cairo University, Cairo, Egypt.

In the process of making this TAP supported study some insight has been gained into how appropriate technologies can be identified and adapted to the needs of developing countries per se, and it is expected that the recommendations developed will serve as a guide to other developing countries for the solution of similar problems which may be encountered there.

Fred Moavenzadeh

Program Director

TABLE OF CONTENTS

	<u>Page No.</u>
TITLE PAGE	1
ABSTRACT	2
ACKNOWLEDGEMENT	4
PREFACE	5
TABLE OF CONTENTS	6
LIST OF FIGURES	10
LIST OF TABLES	13a
NOTATION	14
Chapter 1 INTRODUCTION	26
Chapter 2 OBJECTIVES	27
2.1 Motivation	27
2.2 Problem Formulation	29
Chapter 3 SOIL MOISTURE MOVEMENT	33
3.1 Introduction	33
3.2 Literature Review	34
3.2.1 Boundary Fluxes	34
3.2.2 Infiltration Process	34
3.2.3 Drainage Process	51
3.2.4 Exfiltration Process	52
3.2.5 Transpiration Process	53
3.3 Qualitative Description	61
3.3.1 Zones of Soil Moisture Movement	61
3.3.2 Processes of Soil Moisture Movement	64
3.4 Derivation of the Mathematical Model	68
3.4.1 Governing Equation	68
3.4.2 Boundary Conditions	72
3.4.3 Initial Condition	75
3.4.4 Vegetal Transpiration Sink	78

	3.5	Linearizing the Model	81
	3.5.1	Problem Presentation	81
	3.5.2	Dimensionless Parameterization	86
Chapter 4		SOLVING THE LINEAR PROBLEM	91
	4.1	Solving for Moisture Content Distribution	91
	4.1.1	General Solution Method	91
	4.1.2	Initial Condition	95
	4.1.3	Boundary Conditions	98
	4.1.4	Root Sink Terms	100
	4.1.5	Moisture Content Distribution	102
	4.2	Deriving Dynamic Equations	105
	4.2.1	General Method	105
	4.2.2	Boundary Fluxes and Volumes	107
	4.2.3	Infiltration Equations	112
	4.2.4	Ponding Time	114
		4.2.4.1 Ponding time: method one	114
		4.2.4.2 Ponding time: method two	115
	4.2.5	Exfiltration Equations	117
	4.2.6	Drying Time	118
		4.2.6.1 Drying time: method one	118
		4.2.6.2 Drying time: method two	119
	4.2.7	Percolation	120
	4.2.8	Capillary Rise	122
	4.2.9	Depth-Average Moisture Content	124
	4.2.10	Vegetal Moisture Uptake	126
Chapter 5		RESULTS	127
	5.1	Introduction	127
	5.2	Summary of Dimensionless Groupings	127
	5.3	Finite Domain Determination	129
	5.4	Convergence	140
	5.4.1	Series Convergence	140
	5.4.2	Boundary Convergence	142
	5.5	Numerical Examples	145
	5.5.1	Soil-Water Depletion	145
		5.5.1.1 Drainage	145
		5.5.1.2 Drainage plus transpiration by plants	147

5.5.1.3	A comparison of drainage and transpiration with drainage and bare soil evaporation	149
5.5.2	Infiltration	151
5.5.2.1	Ponding time	151
5.5.2.2	Infiltration capacity	152
5.5.3	Water loss at the soil surface	156
5.5.3.1	Drying time	156
5.5.3.2	Exfiltration capacity	157
5.5.4	Two period process: simulation prototype	158
5.6	Comparisons with a Numerical Solution	160
5.6.1	Introduction	160
5.6.2	Ponded infiltration into yolo light clay for two water table depths	162
5.6.2.1	Parameter estimation	162
5.6.2.2	Soil data	164
5.6.2.3	Dimensionless parameters	165
5.6.2.4	Volume of infiltrated moisture	166
5.6.2.5	Average moisture content	170
5.6.3	Infiltration of rainfall (pre-ponded) into yolo light clay	176
5.6.3.1	Ponding time preliminaries	176
5.6.3.2	Ponding time results	178
5.6.3.3	Average moisture content for rainfall infiltration ($i/K_1 < 1$)	181
Chapter 6	CLIMATE-WATER TABLE COUPLING	184
6.1	Introduction	184
6.2	Literature Review	185
6.3	Problem Formulation and Assumptions	188
6.3.1	Problem Statement	188
6.3.2	Groundwater Model Assumptions	189
6.3.3	Capillary Rise Model	191
6.3.4	Percolation Rate Model	192
6.4	Analytical Solutions	195
6.4.1	Steady State Flow with Accretion	195
6.4.2	Steady State Flow with Accretion and Point Pumping	197
6.4.3	Transient Flow with Accretion	198

6.5	Finite Difference Model	200
6.5.1	Discretization Procedure	200
6.5.2	Iteration Procedure	208
6.5.3	Convergence Requirement	209
6.6	Results	211
6.6.1	Similarity Parameters	211
6.6.2	Water Balance Results	213
6.6.2.1	Water table-dependent quantities for CSV Systems	213
6.6.3	Results of Coupled Groundwater - Water Balance Models	228
6.6.3.1	Methodology	228
6.6.3.2	Results	233
6.6.3.3	Convergence	241
Chapter 7	SUMMARY, CONCLUSIONS AND RECOMMENDATIONS FOR FUTURE RESEARCH	244
7.1	Summary	244
7.2	Conclusions	245
7.3	Recommendations for Future Research	246
REFERENCES		248
Appendix A	A.1 Similarity to Horton's Infiltration Law	260
	A.2 Infiltration Law for Shallow Water Table Soils	262
	A.3 Ponding Time using Horton's Law	263
	A.4 Ponding Time for Shallow Water Table Conditions	264
Appendix B	Listing of Computer Code	265

LIST OF FIGURES

<u>Figure No.</u>	<u>Title</u>	<u>Page No.</u>
2.1	Two-dimensional, idealized swampland water balance.	28
2.2	Soil moisture fluxes.	30
2.3	Two-dimensional idealized phreatic aquifer bounded by two rivers.	32
3.1	Infiltration rate for a simple soil system.	37
3.2	Wetting front approximation by method of Green and Ampt.	39
3.3	Soil-moisture retention curves.	39
3.4	Diffusivity models.	47
3.5	Volumetric evapotranspiration accounting model.	55
3.6	Subsurface water classification.	62
3.7	Subsurface water classification for shallow water table soil column.	65
3.8	Gravity drainage with a deep water table.	66
3.9	Gravity drainage with a shallow water table.	66
3.10	Infiltration with an intermediate depth water table.	69
3.11	Infiltration with a shallow water table.	69
3.12	Root sink models.	82
5.1	Sensitivity of Equation (4.166) to number of series terms for a draining shallow soil column ($Z^0 = 1$, $e_p^0 = 0$, $n_e = .35$, uniform $\theta_0 = .25$).	141
5.2	Sensitivity of Equation (4.122) to water table depth and number of series terms for infiltration ($i^0 = 2$, $n_e = .35$, hydrostatic θ_0).	143

<u>Figure No.</u>	<u>Title</u>	<u>Page No.</u>
5.3	Sensitivity of Equation (4.166) to vegetation and surface evaporation for a draining wet shallow soil column ($Z^0 = 1$, $n_e = .35$, uniform $\theta_o = .30$, $n = 100$).	146
5.4	Infiltration into a shallow soil column using Equation (4.68) ($Z^0 = 2$, $i^0 = 2$, $n_e = .35$, hydrostatic θ_o , $n = 200$).	153
5.5	Sensitivity of Equation (4.122) to approximation (4.121) by comparison with Equation (4.118) for infiltration into a shallow soil column ($i^0 = 3$, $n_e = .35$, hydrostatic θ_o , $n = 100$).	153
5.6	Sensitivity of Equation (4.114) to water table depth for infiltration into a shallow soil column ($n_e = .40$, hydrostatic θ_o , $z^0 = .02Z^0$, $n = 100$).	155
5.7	Sensitivity of Equation (4.135) to water table depth for exfiltration from a wet shallow soil column ($n_e = .40$, uniform $\theta_o = .35$, $z^0 = 0$, $n = 101$).	155
5.8	Storm-interstorm sequence using Equation (4.166) ($Z^0 = 1$, $i^0 = .3$, $e_p^0 = .3$, $n_e = .35$, uniform $\theta_o = .2$, $n = 100$).	159
5.9	Cumulative infiltration comparing Equation (4.117) with the numerical non-linear solution using Philip's D_+ ($n_e = .26$, hydrostatic θ_o , $n = 100$).	168
5.10	Cumulative infiltration comparing Equation (4.117) with the numerical non-linear solution using Eagleson's D_* ($n_e = .2$, hydrostatic θ_o , $n = 100$).	169
5.11	Bare soil infiltration comparing Equation (4.167) with the numerical non-linear solution using Philip's D_* ($n_e = .26$, uniform $\theta_o = .13$, $n = 100$).	172
5.12	Bare soil infiltration comparing Equation (4.167) with the numerical non-linear solution using Eagleson's D_* ($n_e = .26$, uniform $\theta_o = .13$, $n = 100$).	173
5.13	Bare soil infiltration comparing Equations (4.167) with the numerical non-linear solution using fitted D_* ($n_e = .26$, uniform $\theta_o = .13$, $n = 100$).	175

<u>Figure No.</u>	<u>Title</u>	<u>Page No.</u>
5.14	Infiltration comparison of ponding time equation (4.122) with the numerical non-linear solution: sensitivity to water table depth and rainfall intensity ($n_e = .26$, hydrostatic θ_o , Philip's D_* , $n = 100$).	179
5.15	Infiltration comparing Equation (4.166) with the numerical non-linear solution using fitted i^0 ($n_e = .26$, uniform $\theta_o = .13$, Philip's D_* , $n = 100$).	182
6.1	Water balance equilibrium with no net annual recharge and a year long rainy season ($\Lambda = 1$).	217
6.2	Water balance equilibrium with no net annual recharge and a half year rainy season ($\Lambda = 1$).	217
6.3	Water balance equilibrium with no net annual recharge for El-Gizera soil ($\Lambda = 1$, $T_1 = 157$ days, $e_p = 1.6$ m/year).	221
6.4	Water table-dependent water balance, Clinton, MA.	223
6.5	Water table-dependent water balance, Santa Paula, CA.	223
6.6	Water table-dependent water balance, Bahr el Ghazal.	225
6.7	Water table-dependent water balance, El-Gizera, Sudan.	226
6.8	Water table-dependent water balance, El-Gizera ($M = M_o$).	226
6.9	Water table-dependent recharge rates, Clinton, MA.	229
6.10	Water table-dependent recharge rates, Santa Paula, CA.	230
6.11	Water table-dependent water loss rates, El-Gizera, Sudan.	231
6.12	Water table-dependent recharge rates, El-Gizera, Sudan.	232
6.13	Climate-induced steady-state water table depression, El-Gizera, Sudan ($L = 100$ km, $K_1 = 73$ m/year, $t = 500$ years).	234

<u>Figure No.</u>	<u>Title</u>	<u>Page No.</u>
6.14	Climate-induced steady-state water table depression, El-Gizera, Sudan ($L = 2$ km, $K_1 = 73$ m/year, $t = 500$ years).	235
6.15	Climate-induced steady-state water table depression, El-Gizera, Sudan ($L = 2$ km, $K_1 = 365$ m/year, $t = 500$ years).	235
6.16	Climate-induced steady-state water table shape with non-uniform land surface and initial water table slope, El-Gizera, Sudan ($L = 100$ km, $K_1 = 73$ m/year, $t = 500$ years).	237
6.17	Water table depression due to pumping, El-Gizera, Sudan ($L = 100$ km, $K_1 = 73$ m/year, $t = 42$ years).	238
6.18	Steady-state water table depression due to pumping, El-Gizera, Sudan ($L = 4.5$ km, $K_1 = 73$ m/year, $t = 50$ years).	238
6.19	Steady-state recharge mound; Bahr-el-Ghazal, Sudan ($L = 6$ km, $K_1 = 142$ m/year, $t = 500$ years).	239
6.20	Steady-state recharge mound; Bahr el Ghazal, Sudan ($L = 6$ km, $K_1 = 71$ m/year, $t = 500$ years).	239
6.21	Comparison of steady-state water table shape between the finite difference model and Equation (6.15) ($L = 100$ km, $K_1 = 126.1$ m/year, $Q_N = .01$ m/year).	240

LIST OF TABLES

<u>Table No.</u>	<u>Title</u>	<u>Page No.</u>
6.1	Soil Parameters	219
6.2	Water Balance Data	227
6.3	Groundwater Model Inputs	242

NOTATION

- NOTE: 1. Symbols not included in the list are defined in the text wherever they are used.
2. Multiple uses of the same symbol are distinguished by the context of the usage.
3. Dimensions are indicated in parentheses by force (F), mass (M), length (L), time (T), temperature (deg) and dimensionless (-).
4. Generally used subscripts and superscripts are listed at the end of the notation. First, find the variable in the notation and if the subscript is not included, check the subscript section.

a	Kostiakov model parameter (L^2T^{-1})
a	distance of well from $x = 0$ (L)
a_2	linear model parameter ($=k/D_*$) (L^{-1})
A	sinusoidal initial condition parameter (-)
<u>A</u>	coefficient matrix
A_{BC}	boundary condition solution integral (-)
A_1	Green-Ampt model parameter (L^2T^{-1})
A_2	Philip model parameter (LT^{-1})
A_3	moisture content solution coefficient
b	Kostiakov model parameter (-)
<u>b</u>	coefficient matrix (LT^{-1})
b_0	root sink model parameter (T^{-1})
b_1	root sink model parameter (L^{-2})

<u>B</u>	coefficient matrix (-)
B	coefficient term for capillary rise expression (-)
B_1	Green-Ampt model parameter (LT^{-1})
B_2	Philip model parameter (L)
B_3	moisture content solution coefficient
c	pore disconnectedness index (-)
c_1	Thornthwaite model parameter ($IT^{-1}deg^{-1}$)
C	Green-Ampt model parameter (L)
\bar{C}	solution term incorporating boundary and depth-dependent transpiration sink effects (-)
d	deep seepage rate (LT^{-1})
d	diffusivity index (-)
D	hydraulic diffusivity of soil moisture (L^2T^{-1})
$D(\beta_m)$	normalizing coefficient for solution eigenfunction (L)
D_e	hydraulic diffusivity for exfiltration (L^2T^{-1})
D_i	hydraulic diffusivity for infiltration (L^2T^{-1})
D_*	linearized (constant) hydraulic diffusivity (L^2T^{-1})
e_p	potential bare soil evaporation rate (LT^{-1})
e_{p_v}	potential vegetation transpiration rate (LT^{-1})
e_T	evapotranspiration rate (LT^{-1})
e_{T_L}	evapotranspiration rate at land surface (LT^{-1})
e_{T_o}	evapotranspiration rate at water surface (LT^{-1})
e_{T_p}	potential evapotranspiration rate (LT^{-1})
e_{T_s}	evapotranspiration rate from soil moisture (LT^{-1})
e_v	constant vegetation transpiration rate (LT^{-1})

e_v^*	maximum transpiration rate (LT^{-1})
E_s	cumulative bare soil exfiltration (L)
E_{ss}	cumulative bare soil exfiltration for soil-controlled process (L)
E_T	cumulative evapotranspiration (L)
E_{TA}	annual volume of evapotranspiration (L)
E_v	cumulative transpiration (L)
E_{vc}	cumulative transpiration with climate-controlled surface process (L)
E_{vs}	cumulative transpiration with soil-controlled surface process (L)
\underline{f}	accretion matrix (LT^{-1})
f_c	asymptotic infiltration rate (LT^{-1})
f_e^*	exfiltration capacity (LT^{-1})
$f_{e,i}$	initial exfiltration capacity (LT^{-1})
$f_{e,ss}$	steady state exfiltration capacity (LT^{-1})
f_i	infiltration rate (LT^{-1})
f_i^*	infiltration capacity or infiltration rate for soil-controlled process (LT^{-1})
$f_{i,i}^*$	initial infiltration capacity (LT^{-1})
$f_{i,ss}^*$	steady state infiltration capacity (LT^{-1})
f_o	initial constant flow rate in unsaturated zone (LT^{-1})
f_o	initial infiltration rate (LT^{-1})
f_o	initial drainage rate (LT^{-1})
\bar{F}	integral transform of initial condition (-)
g	acceleration due to gravity (LT^{-2})
g	boundary condition matrix (LT^{-1})

g_r	vegetal extraction rate of soil moisture (T^{-1})
$g_{r,max}$	maximum vegetal extraction rate of soil moisture (T^{-1})
$g_{r,1}$	reduced maximum vegetal extraction rate (T^{-1})
G	dimensionless vegetal extraction parameter
\bar{G}	integral transform of depth-dependent transpiration sink term (-)
G_R	dimensionless vegetal extraction rate (-)
G_1	dimensionless maximum vegetal extraction rate
G_2	transformed concentration-dependent vegetal sink term (Eqn. 3.122)
G_{11}	dimensionless root sink parameter (Eqn. 3.114)
G_{12}	dimensionless root sink parameter (Eqn. 3.115)
G_{21}	dimensionless root sink parameter (Eqn. 3.117)
G_{22}	dimensionless root sink parameter (Eqn. 3.118)
h	height of water table above reference level (L)
\underline{h}	water table height matrix (L)
\bar{h}	average phreatic surface elevation (L)
$h(o)$	initial moisture content at the landsurface (-)
h_L	height of river above datum at $x = L$ (L)
h_s	water table elevation above datum (L)
h_o	height of river above datum at $x = 0$ (L)
h_o	height of surface retention water (L)
H	height of land surface above datum (L)
H_c	land surface height above reference level halfway between two reservoirs (L)

H_L	land surface height above reference level at $x = L$ (L)
H_0	land surface height above reference level at $x = 0$ (L)
H_1	depth of ponded infiltration above land surface (L)
H_1	land surface boundary condition linearized solution parameter (-)
H_2	water table boundary condition linearized solution parameter (-)
i	uniform rainfall rate (LT^{-1})
I	cumulative infiltration (L)
I_s	cumulative infiltration for soil-controlled process (L)
J_1	general solution term for fluxes and contents (-)
J_2	general solution term for cumulative quantities (-)
k	hydraulic conductivity coefficient for linear model (LT^{-1})
k_i	fitted parameter for linear ponding time model (LT^{-1})
k_{ij}	saturated soil permeability to water (L^2)
k_{rw}	relative permeability with respect to saturation (L^2)
k_v	plant coefficient (-)
k_1	time constant for infiltration/exfiltration rate equation (T^{-1})
K	hydraulic conductivity of soil moisture (LT^{-1})

K	"resaturated" hydraulic conductivity or gravity drainage rate (LT^{-1})
\bar{K}	temporal average hydraulic conductivity at the land surface (LT^{-1})
$K(\beta_m, z)$	eigenvalue of solution to linearized problem (-)
$K(1)$	maximum or saturated hydraulic conductivity (LT^{-1})
K_{wo}	hydraulic conductivity at field capacity (LT^{-1})
K_o	initial hydraulic conductivity (LT^{-1})
K_1	maximum hydraulic conductivity (LT^{-1})
L	distance between rivers (L)
m	pore size distribution index (-)
m	iteration number (-)
m_H	mean storm depth (L)
m_i	mean storm intensity (LT^{-1})
m_{t_b}	mean time between storms (T)
m_{t_r}	mean storm duration (T)
m_v	mean number of storms (-)
m_τ	mean annual rainy season length (T)
m_1	moisture content solution coefficient
M	vegetated fraction of land surface (-)
M_d	difference between maximum and initial moisture contents (-)

M_o	optimal vegetated fraction of land surface (-)
M_1	the total increase in moisture content from the initial to the steady state during capillary rise (no evapotranspiration) (-)
n	soil porosity (-)
n_e	effective porosity (-)
n_1	moisture content solution coefficient
$N(t)$	drainage rate through water table (LT^{-1})
\vec{N}	atmospheric flux vector, positive into soil (LT^{-1})
p	percolation rate to phreatic aquifer (LT^{-1})
p_b	bubbling pressure (Bear, 1979, p. 197) (FL^{-2})
p_c	capillary pressure of air-water interface in unsaturated soil (FL^{-2})
P_L	precipitation rate onto land surface (LT^{-1})
P_N	net percolation rate to saturated zone (LT^{-1})
p_w	water pressure (FL^{-2})
P_o	precipitation rate onto water surface (LT^{-1})
P_A	annual volume of precipitation (L)
P_s	seasonal volume of precipitation (L)
q	soil-moisture downward flow rate or apparent velocity (LT^{-1})
\vec{q}	apparent velocity vector of the porous medium (LT^{-1})
Q	volumetric flow rate between rivers (L^2)
Q	cumulative soil-moisture volume crossing a horizontal section of the unsaturated zone (L)
Q_{IN}	volumetric flow rate into a control volume (L^2T^{-1})
Q_N	net accretion rate into phreatic aquifer (LT^{-1})
Q_{OUT}	volumetric flow rate out of a control volume (L^2T^{-1})

Q_p	pumping rate of well (L^2T^{-1})
Q_{pI}	volumetric flow rate from reservoir of $h = h_o$ to well (L^2T^{-1})
Q_{pII}	volumetric flow rate from reservoir of $h = h_L$ to well (L^2T^{-1})
Q_v	uniform, distributed water table accretion from all sources (LT^{-1})
r_g	groundwater runoff rate (LT^{-1})
r_s	surface runoff rate (LT^{-1})
R_{GA}	annual volume of groundwater runoff (L)
R_{SA}	annual volume of surface runoff (L)
s_w	degree of soil-moisture saturation (-)
s_o	space and time averaged local soil moisture content (-)
S	sorptivity ($LT^{-1/2}$)
S_{AV}	average capillary suction at wetting front (L)
S_e	exfiltration sorptivity ($LT^{-1/2}$)
S_i	infiltration sorptivity ($LT^{-1/2}$)
S_y	specific yield of aquifer (-)
t	time (T)
t_c	soil parameter, dividing short and long time events (T)
t_c	contact time or time when $z_F = z_c$ (T)
t_d	drying time (T)
t_f	duration of previous process (T)
t_{grav}	time dividing dominance of capillary and gravity forces (T)
t_L	time when wetting front reaches the water table (T)
t_r	storm duration (T)
t_o	ponding time (T)
t^*	time defined by $I(t^*) = it_o$ (T)

t^+	time at which surface retention moisture has evaporated (T)
T	transmissivity (L^2T^{-1})
T_1	number of days per year of capillary rise (T)
\bar{T}	linearized transmissivity (L^2T^{-1})
\bar{T}_a	average ambient air temperature (deg)
v	percolation rate (LT^{-1})
v_c	percolation rate with climate-controlled surface process (LT^{-1})
v_s	percolation rate with soil-controlled surface process (LT^{-1})
V_D	cumulative drainage to water table (L)
$V_{D,C}$	cumulative drainage to water table for climate-controlled process (L)
$V_{D,S}$	cumulative drainage to water table for soil-controlled process (L)
$V_{D,\infty}$	total drainable volume of water in the unsaturated zone (L)
V_s	stored volume of soil-moisture in unsaturated zone (L)
v_{sc}	stored volume of soil-moisture with climate-controlled surface process (L)
V_{ss}	stored volume of soil-moisture with soil-controlled surface process (L)
$V_{ss,0}$	initial volume of soil moisture in unsaturated zone (L)
V_w	cumulative capillary rise from water table (L)
V_{wc}	cumulative capillary rise with climate-controlled surface process (L)
V_{ws}	cumulative capillary rise with soil-controlled surface process (L)
w	capillary rise rate from water table (LT^{-1})
w_c	capillary rise rate with climate-controlled surface process (LT^{-1})
w_s	capillary rise rate with soil-controlled surface process (LT^{-1})

w_o	long-term average capillary rise rate (LT^{-1})
\bar{w}	seasonal (annual) average capillary rise rate (LT^{-1})
W	relative transpiration rate (-)
x	distance from reservoir of height, h_o (L)
x_i	direction of moisture flow (L)
x_j	direction of pressure gradient (L)
x_m	distance from $x = 0$ to the extreme water table depth (L)
z	depth from land surface (L)
z_c	contact depth or depth to water table/intermediate zone interface (L)
z_F	wetting front penetration depth over an event period (L)
$\left. \begin{matrix} z_i \\ z_{max} \\ z_o \end{matrix} \right\}$	maximum wetting front penetration depth (L)
Z	water table depth from land surface (L)
Z_r	effective root zone depth (L)
Z_o	depth to top of capillary fringe ($Z_o = Z_o(p_b)$) (L)
β_m	eigenvalue for moisture content solution to linear problem (-)
β	scaling factor for time step equation (-)
γ	index of water table influence (-)
γ_{max}	maximum value for water table influence index (-)
δ	vegetation transpiration sink model parameter (L)
θ	volumetric moisture content (L)
θ_{an}	moisture content when anaerobiosis occurs (-)
θ_{AV}	depth-averaged moisture content (-)
θ_B	moisture content at either land surface or water table boundary (-)
θ_{BC1}	contribution of land surface boundary condition to moisture content (-)

θ_{BC2}	contribution of water table boundary condition to moisture content (-)
θ_d	moisture content dividing soil- and climate-controlled transpiration (-)
θ_e	effective soil-moisture content (-)
θ^o	transformed moisture content (-)
θ_i	initial moisture content at the land surface (-)
θ_{IC}	contribution of initial condition to moisture content (-)
θ_{ll}	minimum soil moisture content (-)
θ_s	removal of moisture content due to vegetal transpiration sink (-)
θ_{ss}	maximum moisture content at land surface (-)
θ_w	wilting point soil-water content (-)
θ_{wo}	irreducible water content or field capacity (-)
θ_o	initial moisture content (-)
θ_1	maximum moisture content (-)
$\theta_{1,z}$	maximum moisture content at the water table (-)
$\theta_{1,0}$	maximum moisture content at the land surface (-)
$\bar{\theta}$	time-average moisture content at land surface (-)
κ	parameter of water balance model (-)
Λ	groundwater loss index (-)
Λ_m	maximum value of groundwater loss index (-)
μ_w	dynamic viscosity of water (FTL^{-2})
ρ_w	isothermal water density (ML^{-3})
τ	characteristic residence time of water in aquifer (T)
ϕ	Boltzmann similarity variable ($LT^{-1/2}$)
ϕ_c	similarity contact variable ($LT^{-1/2}$)

ϕ_e	desorption diffusivity (L^2T^{-1})
ϕ_i	sorption diffusivity (L^2T^{-1})
ψ	matric potential (L)
ψ_o	maximum matric potential (L)
ψ_1	matric potential at saturation or bubbling pressure matric potential (L)

Subscripts (except when explicitly indicated in the notation)

j	pressure gradient index
e	effective moisture content index (subtracting field capacity)
T	transformed variable index for diffusion equation analogy
f	solution index for flux (third type) surface boundary condition
c	solution index for concentration (first type) surface boundary condition
u	solution index for uniform initial condition
s	solution index for sinusoidal initial condition
h	solution index for hydrostatic initial condition
,l	solution index for linearly depth-dependent root sink
,e	solution index for exponentially depth-dependent root sink
o	index for initial moisture content solution
ss	index for steady state process

Superscripts

o	dimensionless
---	---------------

INTRODUCTION

The unsaturated soil moisture zone is the physical link between the land surface and the saturated groundwater zone of the soil-water system. The moisture dynamics of the unsaturated zone determine the volume of water entering the groundwater regime and the volume which is rejected in either overland flow or evaporation. The distribution of soil moisture in the unsaturated zone, resulting from the interactions of the climate-soil-vegetation-groundwater systems determines, in part, the potential for vegetation growth. This is critical when assessing the potential for regional agricultural development. The dynamics of chemical transport in the unsaturated zone, determined, in part, by soil moisture dynamics, influence the pollutant level in the saturated regime.

At present, the saturated and unsaturated zones are usually treated by separate analyses. The contribution of the unsaturated zone to the saturated one is often considered as an exogenous, lumped input, called net accretion. The influence of the saturated zone on the unsaturated zone, and ultimately on the hydrology and agricultural output of a region, is usually ignored in analyses of storm events and is treated only in the steady state case for interstorm events. For a more accurate assessment of the physical (and chemical) behavior of each zone the dynamic interactions should be modelled, particularly in cases of high water tables.

Chapter 2

OBJECTIVES2.1 Motivation

To simulate high water table fluctuations in swampy regions, models of the dynamic soil moisture behavior are needed. Simulation of the water table behavior involves a water balance of the region around the swampland. A two-dimensional idealized water balance is seen in Figure 2.1. In that figure

p_L = precipitation rate onto land surface

p_O = precipitation rate onto water surface

e_{T_L} = evapotranspiration rate at land surface

e_{T_O} = evapotranspiration rate at water surface

r_S = surface runoff rate

r_g = groundwater runoff rate

d = deep seepage rate

h_S = water table elevation above datum

Z = water table depth from land surface

p_N = net percolation to saturated zone

A water balance of the unsaturated zone determines the volume of surface runoff and percolation which is generated from the region around the swamp. These are inputs to a saturated zone and swamp water balance used to calculate water table fluctuations. A one-dimensional, vertical, idealized flux balance of the unsaturated

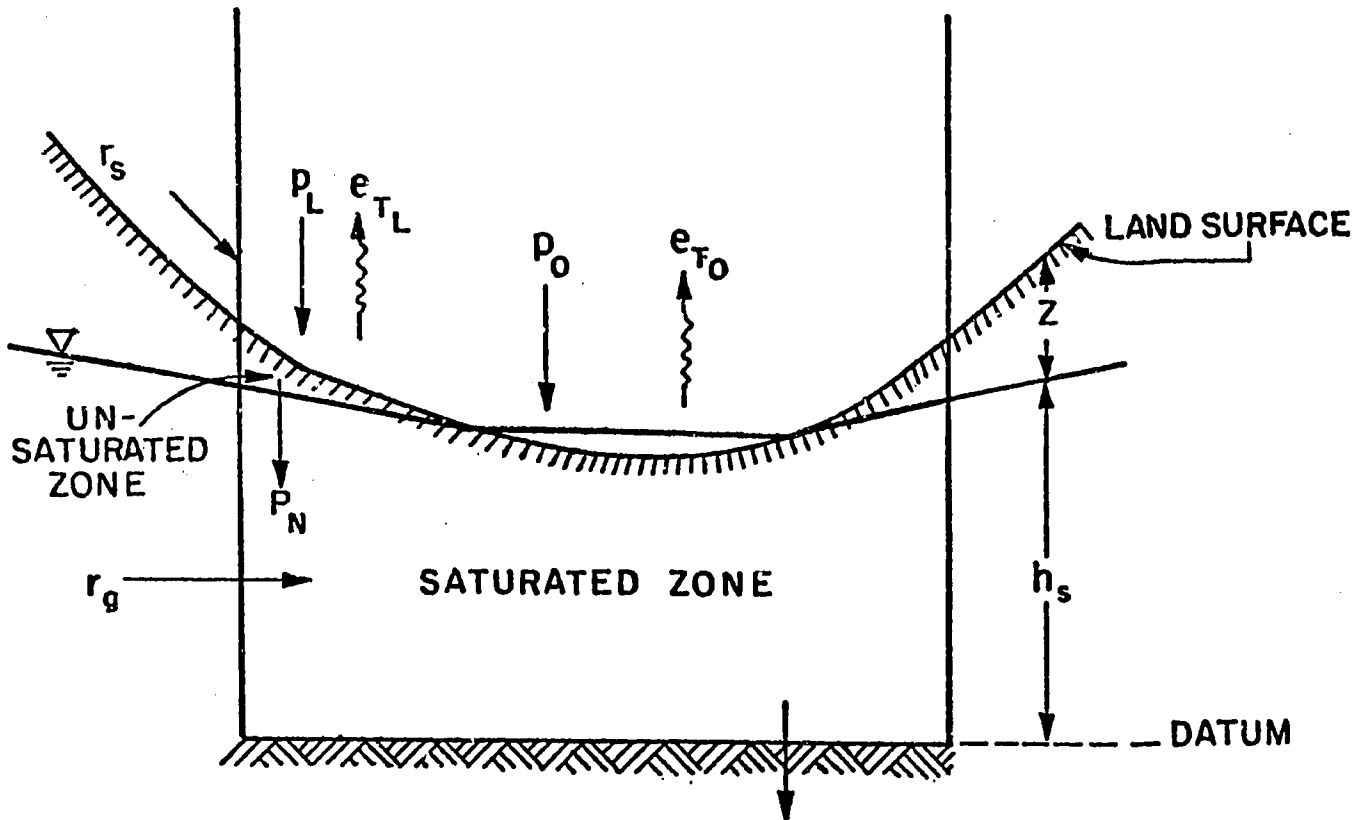


Figure 2.1

TWO-DIMENSIONAL, IDEALIZED SWAMPLAND WATER BALANCE

zone is seen in Figure 2.2, where

$$e_{T_s} = \text{evapotranspiration rate from soil moisture}$$

$$f_i(t) = \text{infiltration rate}$$

$$Z_o = \text{depth to top of capillary fringe}$$

To calculate surface runoff and net percolation, mathematical expressions are needed for these fluxes. Such expressions need to account for the effects of the high water table and vegetation. To generate understanding of transient swamp behavior, the relations should be theoretically, rather than empirically, motivated.

For agricultural planning, it is also useful to know the factors governing the shape and depth of the water table. One important question is to what extent the climate, soil and vegetation influence these features. In the El-Gizera region of Sudan, maximum water table depths of over 100 meters are measured. The question posed is whether this condition could be due to the climate-soil-vegetation system or whether alternative explanations such as leakage, pumping or measurement error must be sought.

2.2 Problem Formulation

Two specific objectives are sought in this work:

The first objective is to see if useful analytical expressions for the flux terms, $f_i(t)$, $e_{T_s}(t)$, $p_N(t)$, shown in Figure 2.2, may be derived from the simplified physics of moisture flow in the unsaturated zone, incorporating both a high water table condition and vegetation. The goal is to solve the linearized Fokker-Planck equation with land surface and water table boundary conditions. The derived flux

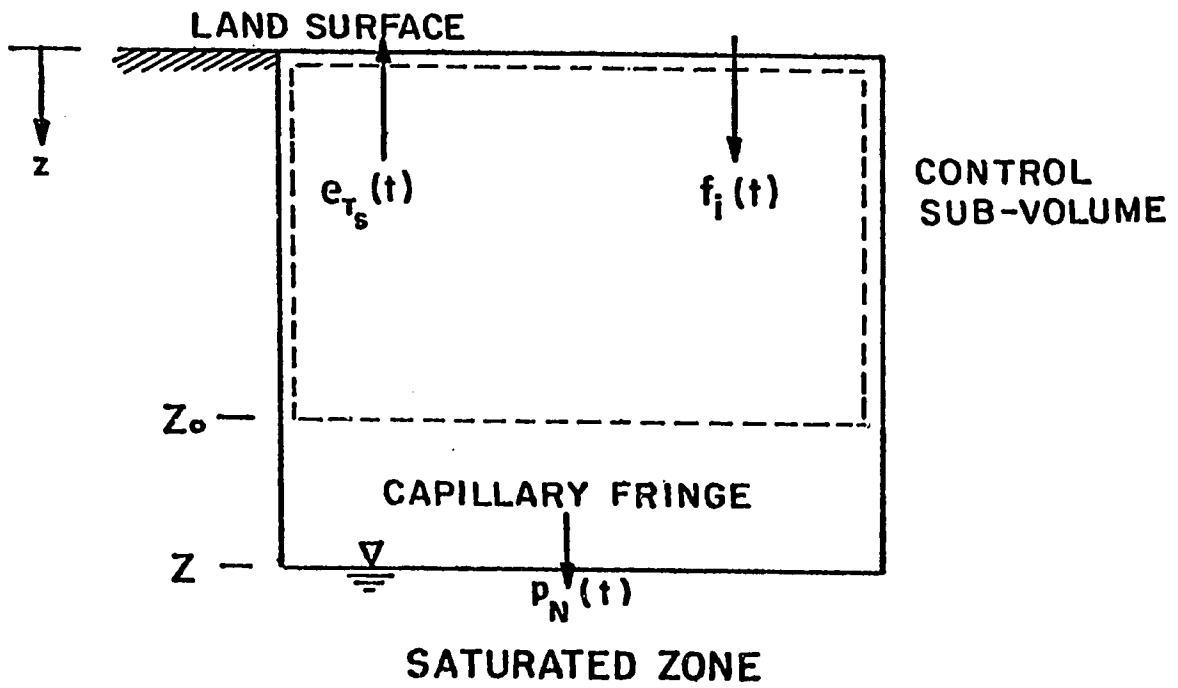


Figure 2.2
SOIL MOISTURE FLUXES

expressions are to be compared with a numerical solution.

The second objective is to account for the effects of climate on the phreatic surface shape in terms of parameters of the soil and vegetation. The goal is to determine under what generalized conditions the phreatic surface will be concave or convex and to ascertain the amplitude of its displacement. The two-dimensional, idealized basin under study is shown in Figure 2.3, where

L = distance between rivers

h_0 = height of river at $x = 0$, above datum (impermeable
aquifer bottom)

h_L = height of river at $x = L$, above datum

x = horizontal distance

p = percolation to phreatic aquifer

w = capillary rise from phreatic aquifer

Q = volumetric flow rate from rivers

H = height of land surface above datum

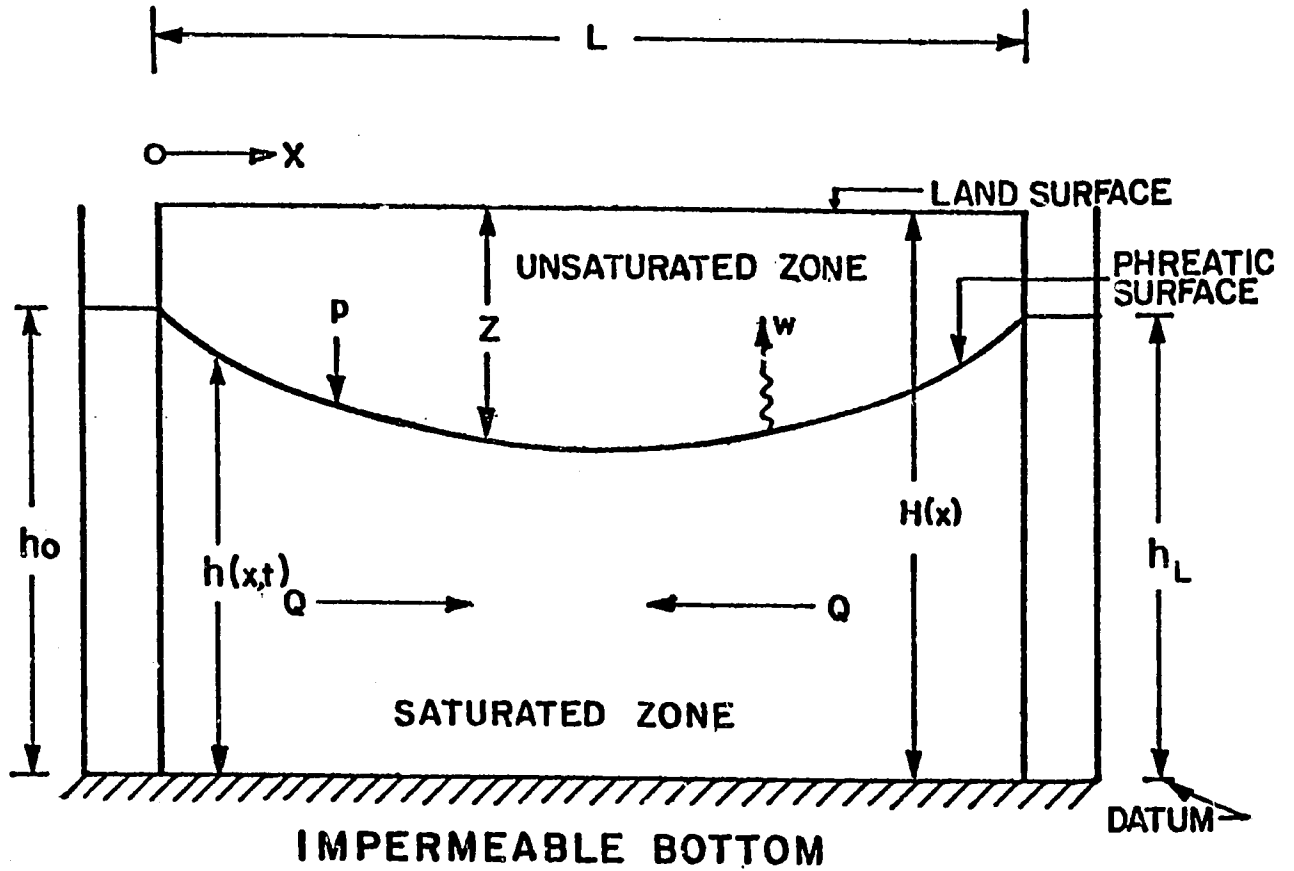


Figure 2.3

TWO-DIMENSIONAL, IDEALIZED PHREATIC AQUIFER
BOUNDED BY TWO RIVERS

Chapter 3

SOIL MOISTURE MOVEMENT3.1 Introduction

Motivated by our interest in swamp drainage, we wish to account for the effects of the water table and vegetation on the soil moisture volumes and fluxes. Certain processes must be modelled in order to simulate catchment dynamics. These are (Dooge, 1973):

1. Infiltration
2. Percolation to the water table
3. Change in level of soil moisture zone storage
4. Exfiltration through bare soil
5. Transpiration by plants
6. Loss of water from water table

These processes are discussed here both qualitatively and mathematically. Expressions for their one-dimensional transient behavior are derived from simplifications of the commonly accepted mathematical model of soil physics, the Fokker-Planck equation. The alternative to an analytical solution of the mathematical model is a numerical one, which is costly in computer time and requires much input data (Skaggs, 1978). For reasons of numerical stability, such a model requires incremental time steps on the order of seconds for processes lasting hours and days, and for simulations of periods of several years (Skaggs, 1978). Though the numerical solution may

incorporate many complexities of the soil physics, another drawback is that "it still remains for the investigator to organize the results and discern the pattern in them" (Philip, 1969b).

3.2 Literature Review

3.2.1 Boundary Fluxes

In general, expressions for moisture fluxes across the boundaries of the unsaturated zone fit into one of four categories: naive, intuitive, frankly empirical or physically-based (Childs, 1969). Reviews of the most common flux expressions are plentiful (Chow, 1964), (Whistler and Bouwer, 1970), (Dooge, 1973), (Hillel, 1980), (Kutilek, 1980). To see if an expression may be modified to account for a high water table and a root sink, it is helpful to review the assumptions and general method of some representative flux expressions. While most expressions for these fluxes, in the literature, are for deep water table systems, some of the methods used are applicable to shallow water table cases.

Of interest in hydrological modelling are the time integrals of the moisture fluxes, or cumulative volumes of moisture crossing the boundaries, which are also presented below for some cases.

3.2.2 Infiltration Process

To calculate the total volume of moisture infiltrated into a simple soil system^{*} in a storm period, two mathematical models are

* A simple soil system is one with no surface retention, and which is homogeneous and isotropic.

needed:

(a) Before the landsurface is saturated, all the rainfall is infiltrated, making the process climate-controlled. (This means the moisture flux rate into the soil is the rainfall rate).

(b) At a characteristic ponding time, the landsurface is assumed to be saturated. The soil no longer is able to infiltrate all the rainfall, and surface runoff may be produced. Since the soil properties determine the infiltration rate after surface saturation, this is referred to as the soil-controlled process. A low intensity rainstorm may never saturate the soil surface.

To account for the total volume of moisture infiltrated during a storm, one must know

$$I \equiv it_0 + I_s(t; t_0) \quad t = t_r \quad (3.1)$$

where

$$I_s(t; t_0) = \int_{t_0}^t f_i^*(t') dt' \quad (3.2)$$

and

- I = total infiltrated volume of water during a storm
- f_i^* = infiltration rate for soil -controlled process
- I_s = infiltrated volume for soil-controlled process
- i = uniform rainfall rate
- t_0 = ponding time
- t_r = storm duration

$I_s(t)$ and $f_i^*(t)$ are known as the 'Law of Infiltration' (Childs, 1969). Most soil-moisture flux modelling research is devoted to finding accurate 'Infiltration Laws' for a variety of conditions (Philip, 1969a). Recent efforts are concerned with expressions for t_0 (Kutilek, 1980). Knowing t_0 is equivalent to having knowledge of the climate-controlled infiltrated moisture volume (Mein and Larson, 1973).

Figure 3.1 graphically presents the shape of an infiltration law, typical for either deep or shallow water tables. It also shows the volume of moisture infiltrated during the climate-controlled process and soil-controlled process. A requirement for models of $f_i^*(t)$ is 'to account for the rapid decrease [of $f_i^*(t)$] from initially very high values and, for uniform soils, the asymptotic approach to an ultimate constant value,' as seen in Figure 3.1 (Childs, 1969).

A commonly used infiltration law based on a naive model of soil moisture movement is that of Green and Ampt (1911). In this model, the soil moisture zone is conceived of as a bundle of parallel capillary tubes. The expression, $f_i^*(t)$, is stated implicitly as $f_i^*(I_s(t))$. The $f_i^*(I)$ expression is

$$f_i^* = A_1/I_s + B_1 \quad (3.3)$$

where

A_1, B_1 = physically-based model parameters

$I_s(t)$ is implicitly expressed by

$$t = \{I_s - C[\ln(1 + I_s/C)]\}/B \quad (3.4)$$

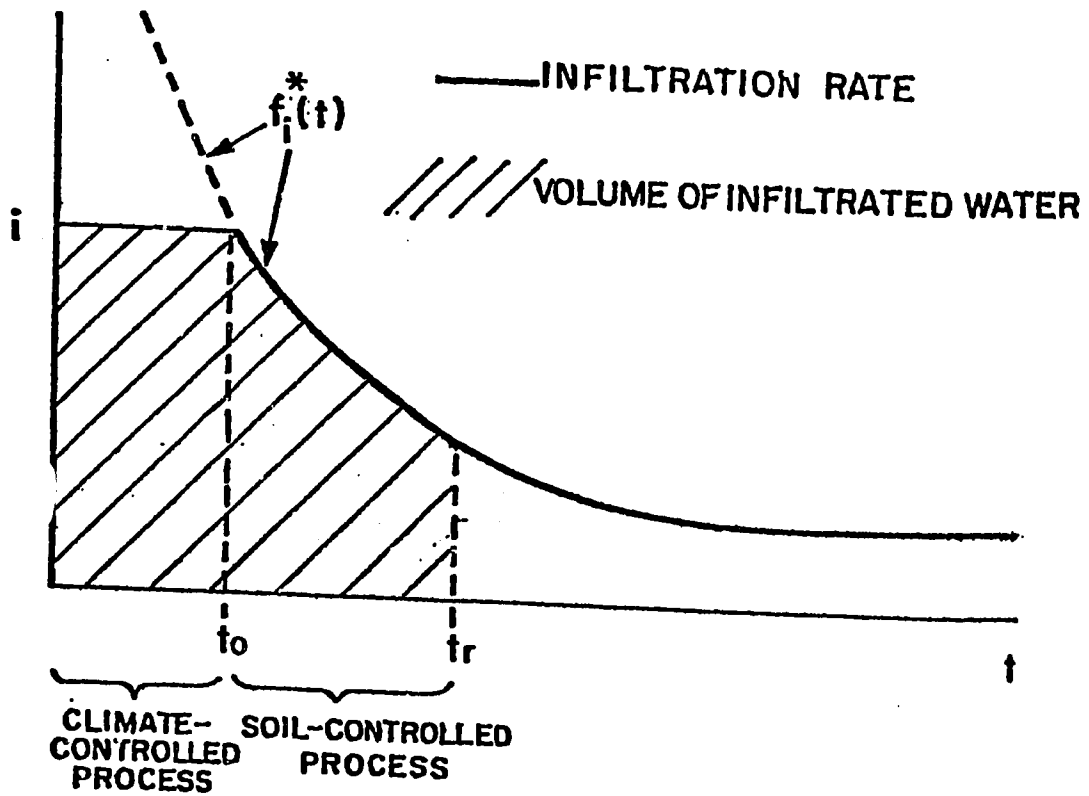


Figure 3.1

INFILTRATION RATE FOR A SIMPLE SOIL SYSTEM

where

C = physically-based model parameter.

Over the last several years, expressions (3.3) and (3.4) have been derived from a more widely accepted and successfully tested conception of soil moisture movement. The parameters may be independently determined from soil properties if the soil-water system fulfills the model's assumptions which are:

1. the infiltrated moisture front advances only by advection
2. the wetting front may be approximated by a step-wise drop from maximum moisture content to the initial moisture content
3. the soil column is effectively semi-infinite with an approximately uniform initial condition

The assumed moisture distribution for this model is shown in Figure 3.2. The correspondingly assumed moisture characteristic curve is compared with the curves typical for two soil type extremes in Figure 3.3. This model is more appropriate for sandy type soils than clay soils.

The Green and Ampt model is applicable for the shallow water table condition. Equation (3.4) may be expressed in series form (Dooge, personal communication with P. S. Eagleson)

$$\left[\frac{B_1^2}{C} \right] t = \sum_{m=2}^{\infty} \frac{(-1)^m}{m} \left[\frac{B_1^2 I_s}{C} \right]^m \quad (3.5)$$

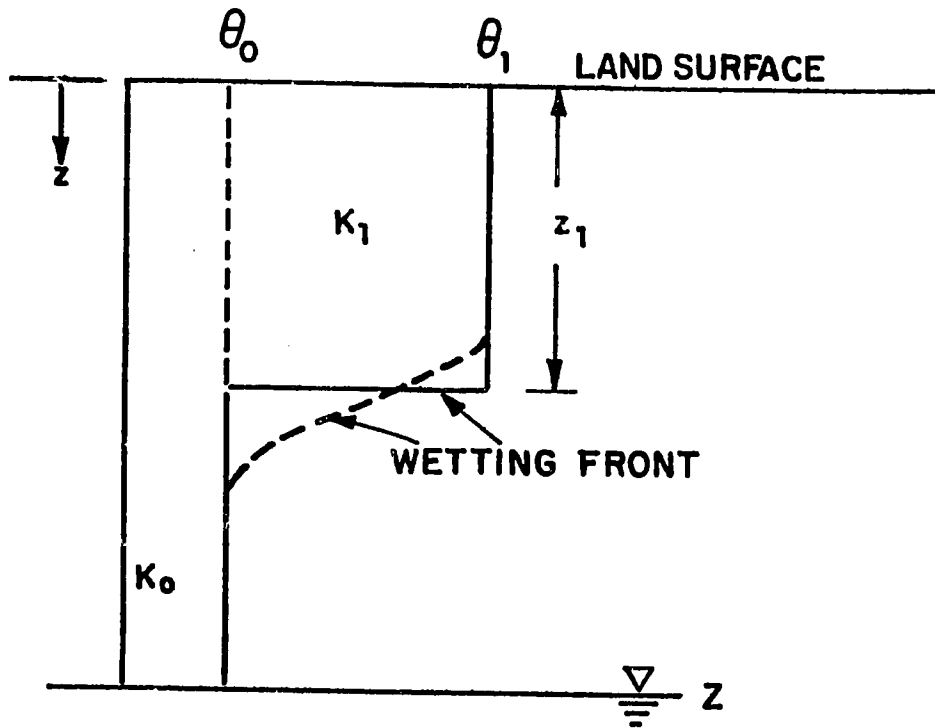


Figure 3.2

WETTING FRONT APPROXIMATION
BY METHOD OF GREEN AND AMPT

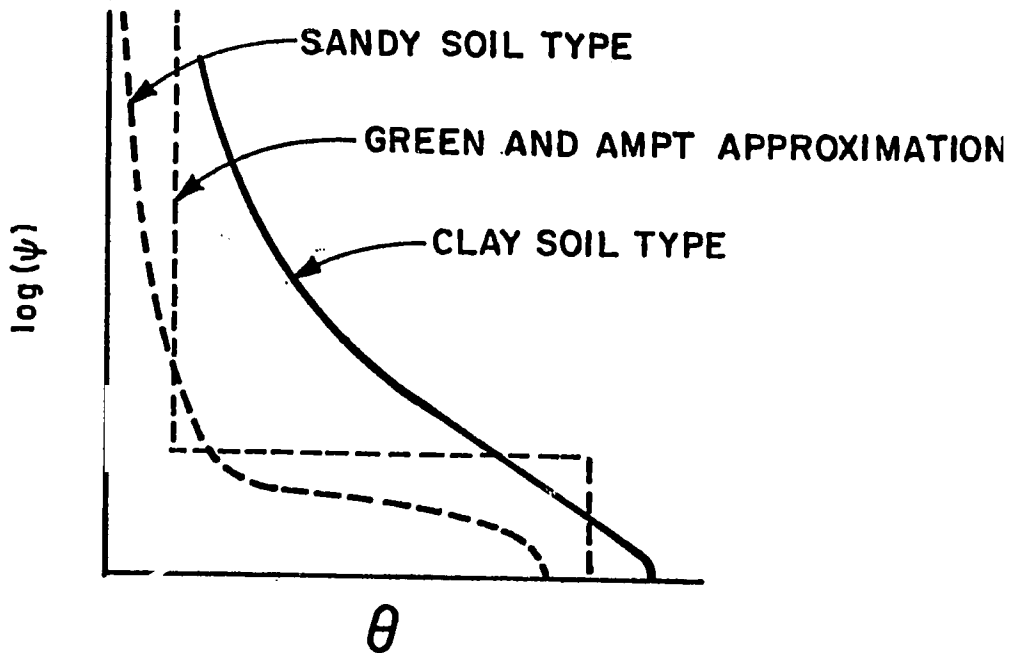


Figure 3.3

SOIL MOISTURE RETENTION CURVES

For the semi-infinite domain, the series is highly convergent for early time or when the initial hydraulic conductivity approaches the maximum hydraulic conductivity. Only the first term of the series is needed. The flux expression, Equation (3.3), becomes an explicit function of time,

$$f_i^* = \left(\frac{C}{2t} \right)^{1/2} + K_o \quad (3.6)$$

where

K_o = initial hydraulic conductivity

For the shallow water table case, or finite domain, an expression for $f_i^*(t)$ is found implicitly for early time using two terms of Equation (3.5), and a replacement of assumption (3) by an assumption and a boundary condition.

3a. the initial moisture flow rate in the soil column is constant, either upward or downward

3b. at the water table the soil is saturated

The flux expression, $f(z_f(t))$, is

$$f_i^*(z_F(t)) = K_1 \left(\frac{(1-f_o/K_o) Z + H_1}{z_f} \right) + \frac{f_o K_1}{K_o} \quad (3.7)$$

where

K_1 = hydraulic conductivity above wetting front

f_o = initial constant flow rate in unsaturated zone

H_1 = depth of ponded infiltration above land surface

z_F = depth from land surface to wetting front

The wetting front is the advecting front of infiltrated water.

The expression for $z_F(t)$ involves the introduction of the linearized Fokker-Planck equation as a simplified model of the soil-moisture movement for the initial condition, in addition to the above assumptions. The resulting relation is

$$\frac{1}{2} \left(\frac{z_F}{Z} \right)^2 - \frac{1}{3} \left(\frac{z_F}{Z} \right)^3 = \frac{D_* t}{Z^2} \quad (3.8)$$

where

D_* = linearized hydraulic diffusivity

The time, t_L , at which the wetting front reaches the water table is calculated by this model to be

$$t_L = \frac{1}{6} \frac{Z^2}{D_*} \quad (3.9)$$

If all the above assumptions are met by the soil-water system, the model may be used with physically meaningful parameters. For most cases, the parameters need to be fitted to the model using field data. In this manner, the simplified equation (3.3) is used in the shallow water table case, with the parameters estimated for each depth and rainfall rate, along with a variety of other physically realistic cases (Skaggs, 1978), (Hillel and Gardner, 1969), (Childs and Bybordi, 1969), (Bouwer, 1969).

This model also yields an expression for ponding time, for the semi-infinite domain (Mein and Larson, 1973), (Kutilek, 1980), which is

$$t_o = S_{AV} M_d / [(f_o/K_1) - 1] f_o \quad f_o > K_1 \quad (3.10)$$

where

$$M_d = (\theta_1 - \theta_0) \quad (3.11)$$

and

S_{AV} = average wetting front capillary suction

θ_1 = maximum moisture content

θ_0 = initial moisture content

Another frequently used infiltration law, of the intuitive type, is Horton's Equation, based on a decay process analogy (Horton, 1939). For a simple soil system and a semi-infinite medium,

$$f_i^*(t) = (f_0 - f_c) \exp(-k_1 t) + f_c \quad (3.12)$$

where

f_c = asymptotic infiltration rate

f_0 = initial infiltration rate

k_1 = model parameter

This model assumes the rate of decay of the infiltration rate is exponential and that there is a constant initial infiltration rate. It may be applied to high water table soils using parameters fitted for each depth and rainfall rate of interest. This model may be derived from simplified soil moisture movement physics, assuming a linearized diffusivity (Eagleson, 1970).

Unlike the parametric models motivated by physical reasoning, frankly empirical models are developed solely to fit a curve (Ghosh, 1980). Kostikov's equation is the most famous example (Kostikov, 1932)

$$f_i^*(t) = a/t^b \quad (3.13)$$

where

a, b = fitted model parameters

While Equation (3.13) fits data only in early time, a recent empirical model, in dimensionless form, fits data over the entire time range (Collis-George, 1977). For deep water tables and simple soil systems, the parameters may be found independently from field measurements. The model is

$$I_s^0(t^0) = (\tanh t^0)^{1/2} \quad (3.14)$$

where

$$\begin{aligned} I_s^0 &= \text{dimensionless quantity of infiltrated moisture} \\ &= (I(t) - \bar{K}t)/I_0 \end{aligned} \quad (3.15)$$

$$\begin{aligned} t^0 &= \text{dimensionless time} \\ &= t/t_c \end{aligned} \quad (3.16)$$

and

I_0 = parameter of infiltration equation

\bar{K} = temporal average hydraulic conductivity at the land surface

t_c = soil parameter, dividing short and long time events

Explicit analysis of the physics of soil-water movement results in several infiltration law expressions, the most famous of which is that of Philip (Philip, 1957c), (Philip, 1969a), (Hillel, 1980).

For early time, the volumetric infiltration expression is

$$I_s(t) = St^{1/2} + A_2 \quad (3.17)$$

and large time

$$I_s(t) = B_2 + K_1 t \quad (3.18)$$

where

S = sorptivity, a soil parameter

A_2, B_2 = model parameters

For simple soils, a uniform initial condition and a semi-infinite domain, A_2, B_2 and S are measurable soil parameters. The models are derived from two solutions of the one-dimensional non-linear Fokker-Planck equation, the generally accepted equation for soil moisture movement in the unsaturated zone (Childs, 1969). This equation is

$$\frac{\partial \theta}{\partial t} = \frac{\partial}{\partial z} \left(D(\theta) \frac{\partial \theta}{\partial z} \right) - \frac{dK}{d\theta} \frac{\partial \theta}{\partial z} \quad (3.19)$$

where

$$D(\theta) = - K(\theta) \frac{d\psi}{d\theta} \quad (3.20)$$

and

$D(\theta)$ = soil moisture diffusivity function

$K(\theta)$ = hydraulic conductivity function

ψ = capillary potential

The similarity solution method, used to derive the soil sorptivity term, S , from the mathematics, cannot be applied to the finite water table case. The key to the method involves a transformation of variables to reduce the problem from two variables to one variable. The only valid transformation is the Boltzmann transformation (Philip, 1969a), which is

$$\phi = zt^{-1/2} \quad (3.21)$$

When Equation (3.21) is applied to the lower boundary in the semi-infinite case, $\phi \rightarrow \infty$ as $z \rightarrow \infty$, but for the finite domain case,

$$t \geq 0 \quad z = Z \quad \theta = \theta_1 \quad (3.22)$$

is transformed into

$$t \geq 0 \quad \phi = Zt^{-1/2} \quad \theta = \theta_1 \quad (3.23)$$

preventing the reduction of the number of variables to one.

A second technique of the physically-based models not applicable for the finite water table case is that of describing the quantity of infiltrated water by

$$I_s(t) = K_o t + \int_{\theta_0}^{\theta_1} z(\theta, t) d\theta \quad (3.24)$$

where

$$\int_{\theta_0}^{\theta_1} z d\theta = \text{the change in soil-moisture storage due to infiltration, for the semi-infinite domain}$$

For the finite domain case integrating from θ_0 to θ_1 includes not only infiltrated water but water from the capillary fringe which leads to an overestimated amount of infiltrated water. It also assumes that an initial uniform moisture content, θ_0 , may be defined over part of the soil column.

Linearizing Equation (3.19) permits the derivation of an infiltration expression for the high water table case from the soil physics, as the Boltzmann transformation is no longer needed. The linearized equation of motion is

$$\frac{\partial \theta_*}{\partial t} = D_* \frac{\partial^2 \theta_*}{\partial z^2} - k \frac{\partial \theta_*}{\partial z} \quad (3.25)$$

where we assume for the semi-infinite case

$$k = \frac{dK}{d\theta} = \frac{K_1 - K_0}{\theta_1 - \theta_0} \quad (3.26)$$

and

$$D_* = D(\theta)$$

k and D_* are independent soil properties only where the assumptions are approximated by the real system. D_* and the diffusivity assumed by the Green and Ampt model are compared with the $D(\theta)$ relation for a representative real soil in Figure 3.4. In the figure, θ_{w0} = irreducible water content or field capacity (Bear, 1979). Note that the linearized model is best suited for the lower moisture content range or small changes in θ over the entire range, while the other model is only valid where the soil saturation is at the maximum value (Philip, 1969a).

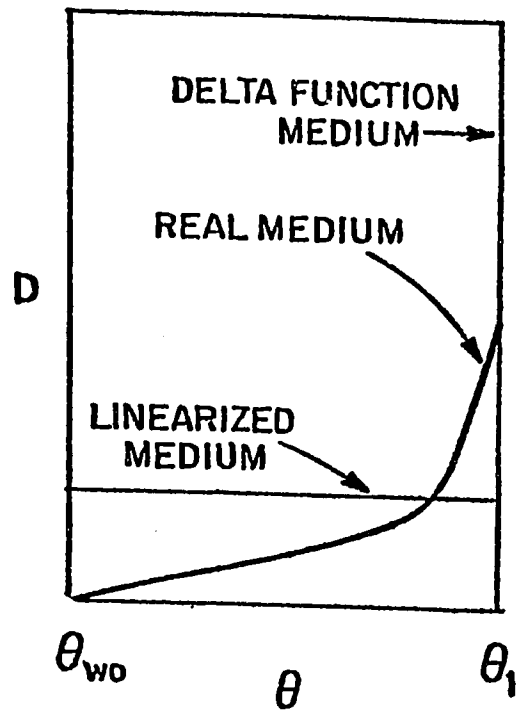


Figure 3.4

DIFFUSIVITY MODELS

Estimating D_* and k , when the linearizing assumptions are not adhered to, requires consideration of initial and boundary moisture contents. For the semi-infinite case, explicit expressions for D_* and k are derived by matching D_* to the known early time solution of the non-linear problem and k to the large time solution (Philip, 1969a). For the finite domain case, values of D_* and k may be fitted for a variety of initial and boundary conditions by matching the $I_s(t)$ curve generated by the analytical solution to the linear problem either to data or to the numerical solution for the non-linear problem.

Solutions for the linearized problem for the semi-infinite domain are derived in different ways by various authors (Dooge, 1973), (Eagleson, 1970), (Philip, 1969a), (Carslaw and Jaeger, 1959). The short and long time expansion methods of Philip (1969b) are often useful for simplifying the solution.

In the finite domain, expressions for the wetting front location are useful as indicators for when the front meets the capillary fringe. This characteristic time indicates when the domain effectively becomes finite. Expressions for the wetting front in a semi-infinite domain include (Eagleson, 1978c),

$$z_f = 4(Dt)^{1/2} + \frac{K_o t}{n_e} \quad (3.27)$$

where

z_f = maximum wetting front penetration depth

n_e = effective porosity

Another expression is (Braester, 1973)

$$z_F = f_o t / (\bar{\theta}_1 - \theta_o) \quad (3.28)$$

where

$\bar{\theta}_1$ = time-averaged surface moisture content

Both expressions are derived from the linearized Fokker-Planck equation, though Equation (3.27) is for a saturated surface moisture content and Equation (3.28) is for a constant surface moisture flux boundary condition.

Infiltration equations are also derived from analytical solutions for $\theta(z, t)$. Solutions exist for $\theta(z, t)$ using the non-linear Fokker-Planck equation, Equation (3.19) and approximations of it, for a variety of initial and boundary conditions (Babu, 1976), (Brutsaert, 1976), (Philip and Knight, 1974), (Braester, 1973), (Parlange, 1971b).

To estimate ponding time for the infiltration process, the common, semi-empirical method is known as the "time-compression approximation" (Reeves and Miller, 1975). It consists of two steps:

1. The volume of water actually infiltrated at $t = t_o$ must equal the volume of infiltrated water predicted by the infiltration law when $f_i^*(t) = i$, the constant rainfall rate.

2. At t_o , $f_i^*(t - t^*) = f_i^*(t^*) = i$, where t^* is the time when $f_i^*(t^*) = i$, if the model, $f_i^*(t)$, were valid from the start of the rain-storm.

The method may be applied to any infiltration law, $f_i^*(t)$, including one derived for a shallow water table. Using a law for the

semi-infinite domain, applicable for early time (Philip, 1957c),

$$f_i^*(t) = \frac{1}{2} St^{-1/2} + A \quad (3.29)$$

Condition (1) preserves the infiltrated volume,

$$\int_0^{t^*} f_i^*(t) dt = it_0 \quad (3.30)$$

Interpreting Equation (3.29) from $0 < t < t^*$ results in Equation (3.17),

$$St^{*1/2} + At^* = it_0 \quad (3.31)$$

Condition (1) relates the two characteristic times,

$$t_0 = \frac{St^{*1/2} + At^*}{i} \quad (3.32)$$

Equation (3.29) states

$$f_i^*(t^*) = \frac{1}{2} St^{*-1/2} + A \quad (3.29)$$

or

$$t^* = \frac{S^2}{4(f_i^*(t^*) - A)^2} \quad (3.33)$$

Condition (2) says $f_i^*(t^*) = i$ at $t = t_0$. Substituting Equation (3.33) into Equation (3.32) results in,

$$t_0 = \frac{S_i^2}{2i(i-A)} \left| 1 + \frac{A}{2(i-A)} \right| \quad (3.34)$$

When $i \gg A$, Equation (3.34) is simplified to

$$t_o \approx \frac{S_i^2}{2(i-A)^2} \quad (3.35)$$

Ponding time may also be estimated from the solution to the Fokker-Planck equation subject to a flux boundary condition at the land surface. Equation (3.35) is identical with the solution to the linearized diffusion equation, except the term $\frac{1}{2}$ is replaced by $\frac{\pi^2}{16}$ (Eagleson, 1978e).

3.2.3 Drainage Process

For gravity drainage of infiltrated water, a naive conceptual model of soil moisture movement, similar to that of Green and Ampt (1911), is used to develop a cumulative drainage expression for a semi-infinite domain (Youngs, 1960). The expression is

$$V_D(t) = V_{D,\infty} [1 - \exp(-f_o t / V_{D,\infty})] \quad (3.36)$$

where

V_D = cumulative volume of water draining into water table

$V_{D,\infty}$ = total drainable volume of water in the unsaturated zone

f_o = initial drainage rate

A physically-based model is an approximation of a series solution to the linearized Fokker-Planck equation for a finite domain (Whistler and Bouwer, 1970), (Gardner, 1962), and is expressed by

$$V_D(t) = V_{D,\infty} \left[1 - \frac{8}{\pi^2} \exp - \left(\frac{K\pi^2 t}{4V_{D,\infty}} \right) \right] \quad (3.37)$$

where

K = "resaturated" hydraulic conductivity; for a drained and rewet soil column

3.2.4 Exfiltration Process

Most work on the exfiltration process is for the steady-state capillary rise phenomenon, where the moisture is taken from the saturated zone (Gardner, 1958). An analysis of the linearized Fokker-Planck equation has yielded one transient capillary rise expression (Philip, 1969c). In dimensionless notation

$$v_w^o = \frac{1}{2} \left[\pi^{-1/2} t^o{}^{1/2} e^{-t^o} + \frac{1}{2} \operatorname{erfc} t^o{}^{1/2} - t^o \operatorname{erfc} t^o{}^{1/2} \right] \quad (3.38)$$

where

$$t^o = \left(\frac{k^2}{4D_*} \right) t = \frac{S^2}{16M_1^2} t \quad (3.39)$$

$$v_w^o = \frac{V_w + K_o t}{4M_1} \quad (3.40)$$

and

$$M_1 = \int_{\theta_o}^{\theta_1} \int_{\theta_o}^{\theta_1} \frac{D(\theta') d\theta'}{K(\theta') - K_o} d\theta \quad (3.41)$$

Here z is defined positive upward. We define

M_1 = the increase in total moisture content from the initial state to the steady state.

M_1 may be computed from the equilibrium profile directly, (Philip, 1969c). For the shallow water table case, it may also be used as a parameter to match the linear and non-linear models in an integral sense.

Exfiltration from the soil column itself may be computed in a manner analogous with that of Equation (3.17) (Eagleson, 1978d).

3.2.5 Transpiration Process

Analytical soil moisture movement models incorporating plant transpiration, used mainly in analyses of agricultural development, are relatively uncommon. The two basic approaches are accounting for transpiration separately, and explicitly accounting for vegetation in the mathematical model (Molz, 1981), (Eagleson, 1978d), (Skaggs, 1978), (Lomen and Warrick, 1976).

The most simplified model evaluates bare soil loss and transpiration loss in a purely volumetric sense (Skaggs, 1978). The model lumps the bare soil evaporation rate and transpiration rate together. The potential rate is empirically determined from an elementary model (Thorntwaite, 1948),

$$e_{T_p} = c\bar{T}_a \quad (3.42)$$

where

$$e_{T_p} = e_p + k_v e_p \quad (3.43)$$

and

e_{T_p} = potential evapotranspiration rate

e_p = potential bare soil evaporation rate

k_v = plant coefficient

\bar{T}_a = average temperature per period (e.g., hour, day)

c_1 = fitted model parameter

Referring to Figure 3.5, the evapotranspiration rate is calculated by assuming

1. $e_T = e_{T_P}$ if $w(Z) = e_{T_P}$, where $w(Z)$ is the rate of capillary rise as a function of water table depth. $w(Z)$ is calculated using an approximate analytical steady state solution (Gardner, 1958).

$$2. \quad \begin{aligned} e_T &= e_{T_P} \quad (\text{for } w < e_{T_P}) \quad \text{until } \theta(Z_r) = \theta_{ll} \\ e_T &= w \quad (\text{for } w < e_{T_P}) \quad \text{after } \theta(Z_r) = \theta_{ll} \end{aligned}$$

The model parameters are

Z_r = effective root zone depth per crop.

θ_{ll} = minimum moisture content, approximately equal to the wilting point.

A dry zone is created moving vertically downward until no extractable moisture remains in the root zone. Then the moisture supply is equal to the capillary rise. The dry zone is the first filled during the storm event.

In the root zone, the deficit must be calculated against an initial condition assumed in this model to be the "drained to equilibrium" initial condition. Another feature of this model is that $Z_r = Z_r(t)$ may be used to simulate crop growth periods.

The advantage of this model is its simplicity, and the drawback is that it is a purely steady-state model, where the soil limiting condition is parameterically, not physically derived. The analysis brings out some other general issues in evapotranspiration modelling, notably what constitutes a shallow water table, and over what space and time domains may a water table be considered in equilibrium. In a local

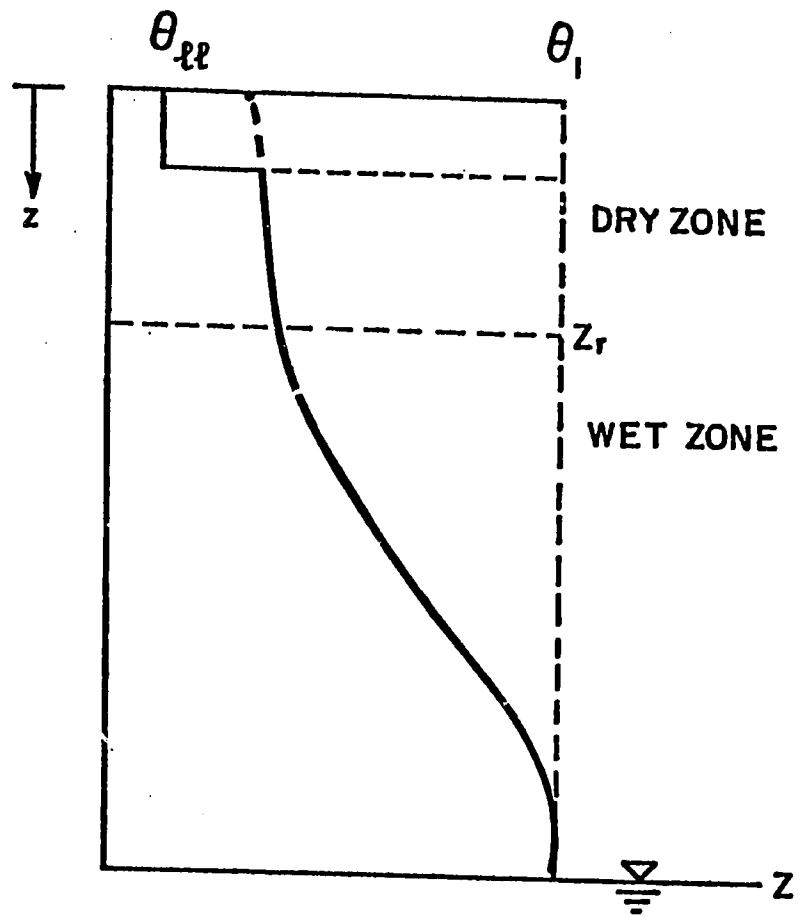


Figure 3.5

VOLUMETRIC EVAPOTRANSPIRATION ACCOUNTING MODEL

model, water table depth is a function of local infiltration/exfiltration conditions, while in a regional study the lateral transmissivity contributes toward the maintenance of a smooth water table surface. The rate at which the water table is fluctuating compared with the response time of the capillary fringe partially determines whether the equilibrium initial condition is appropriate. Considering it could take days for equilibrium to be reached, both the equilibrium initial condition and the steady state approach to evapotranspiration modelling may be inadequate.

Following Whistler et al (1968), a second exfiltration model accounting for vegetation is based on the one-dimensional Fokker-Planck equation, with an added sink term. This model states

$$\frac{\partial \theta}{\partial t} = \frac{\partial}{\partial z} \left(D(\theta) \frac{\partial \theta}{\partial z} \right) - \frac{\partial K(\theta)}{\partial z} - g_r(\theta, z, t) \quad (3.44)$$

where

$g_r(\theta, z, t; \text{parameters})$ = sink function due to moisture uptake
by plants

Simplifying assumptions leading to an analytical approximation are (Eagleson, 1978d):

1. Water table depth $z = Z$ is deeper than both root zone depth $z = Z_r$ and penetration depth, $z = z_f$, delineating the soil-water zone from the intermediate zone. The column is treated as effectively semi-infinite.

2. Uniform initial condition and constant concentration boundary conditions.

3. Plant roots are uniformly distributed over the root zone depth and plants, covering a fraction, M_1 , of the land surface, are distributed uniformly over the surface. Further assuming that the extraction rate is independent of depth and time, over an event's duration,

$$g_r(z, \theta) = g_r = \text{const.} \quad (3.45)$$

It may be removed from the governing equation, (3.44), and more easily handled in the surface boundary condition (Lomen and Warrick, 1978).

This results in an expression for the volume of moisture exfiltrated similar to Equation (3.24),

$$E_s(t) = \int_{\theta_1}^{\theta_0} z d\theta - [K_o + Me_v]t \quad (3.46)$$

where

$E_s(t)$ = cumulative volume of exfiltrated water

M = vegetated fraction of land surface

e_v = constant vegetation transpiration rate

and

$\int_{\theta_1}^{\theta_0} z dt$ = the change in soil moisture storage in the root zone
for the semi-infinite domain

Solving Equation (3.19) for z , the exfiltration rate equals,

$$f_e^*(t) \approx \frac{1}{2} S_e t^{-1/2} - \frac{1}{2} [K_1 + K_o] - Me_v \quad (3.47)$$

Solving the linearized desorption problem for the semi-infinite

domain, with a root sink of strength Me_V/Z_r , for $0 < z < Z_r$, Eagleson (1978d) derived,

$$f_e^*(t) = \frac{1}{2} S_e t^{-1/2} - [2Me_V/Z_r][D_e t/\pi]^{1/2} \quad (3.48)$$

where

$$S_e = 2(\theta_o - \theta_1)(D_e/\pi)^{1/2} \quad (3.49)$$

Over a reasonable range of data, we may neglect the second term of Equation (3.48), making $f_e^*(t)$ due solely to desorption (Eagleson, 1978c).

In this model,

S_e = exfiltration sorptivity

D_e = exfiltration diffusivity

In Equation (3.47), $K_o = 0$ and for the range of average interstorm durations, $K_1 \ll S_e t^{-1/2}$ (Eagleson, 1978c). We let S_e be defined by the linearized desorption parameter, S_e , of Equation (3.49). Finally adding a term for capillary rise from the water table by linear superposition, an expression for exfiltration is developed, involving the processes of desorption, transpiration and capillary rise,

$$f_e^*(t) = \frac{1}{2} S_e t^{-1/2} - Me_V + w \quad t > t_d \quad (3.50)$$

where

t_d = drying time, time at which the land surface is assumed to become dry

This model accounts for the 'dry zone' of the previous model with an explicit time dependent, physically derived term. This is not applicable in the high water table system, though the approach may be modified to do so as is done in this analysis.

Drying time may be explicitly derived in a similar manner to ponding time, including vegetation effects, for the deep water table case (Eagleson, 1978d). Starting from Equation (3.50), we let

$$W(\theta) = \frac{e_{p_v}}{e_p} = k_v \quad (3.51)$$

where

$W(\theta)$ = relative transpiration rate per area of vegetated surface

e_{p_v} = potential vegetation transpiration rate

k_v = plant coefficient

The total evapotranspired volume of moisture in an interstorm period is composed of that volume evaporated from bare soil and that volume transpired,

$$E_T = (1-M)E_S + ME_V \quad (3.52)$$

where

E_T = total volume of moisture lost to the atmosphere

E_S = volume of moisture lost by bare soil evaporation

E_V = volume of moisture transpired by plants

Integrating (3.50) and substituting this and Equation (3.51) into Equation (3.52),

$$E_T = \{(1-M) S_e (t - t^+)^{1/2} + (w - Mk_v e_p)(t - t^+)\} + Mk_v e_p (t - t^+) \quad \text{for } t - t^+ \leq t_d \quad (3.53)$$

where

t_d = time after surface retention moisture evaporates

As with the ponding time analysis, at t_d ,

$$f_e^*(t_d) = e_p \quad (3.54)$$

Solving Equation (3.53) for t_d , and using Equation (3.50), we obtain

$$t_d = \frac{S_e^2}{2e_p^2(1+Mk_v - w/e_p)} \left(1 - M + \frac{M^2k_v + (1-M)w/e_p}{2(1+Mk_v - w/e_p)} \right) \quad (3.55)$$

The above method separates the effects of bare soil evaporation from transpiration, unlike the previous model.

One analysis derives an explicit relationship for moisture uptake by plants, accounting for the high water table in the steady state (Lomen and Warrick, 1976). The root sink term is assumed to be

$$g_r(\theta) = b_0 + b_1 D_* (\theta - \theta_0) \quad (3.56)$$

where

b_0, b_1 = model parameters

It is used in a linearized Fokker-Planck equation. The uptake is defined by

$$e_v = \int_0^{z_1} g_r(\theta(z)) dz \quad (3.57)$$

where

e_v = plant transpiration rate

The solution for $\theta(z)$ is substituted in Equation (3.56) and integrated as in Equation (3.57).

The result is of the form,

$$e_v = b_1 [(A_3/m_1)(e^{m_1 z} - 1) + (B_3/n_1)(e^{n_1 z} - 1)] \quad (3.58)$$

where

A_3, B_3, m_1, n_1 = coefficients of the solution for $\theta(z)$

with

$$\theta(z) = \frac{1}{D_*} (D_* \theta_o + A_3 e^{m_1 z} + B_3 e^{n_1 z} - b_o/b_1) \quad (3.59)$$

Note that the level of solution complexity increases as more phenomena are incorporated into the model (e.g., vegetation, high water table).

3 3 Qualitative Description

3.3.1 Zones of Soil Moisture Movement

Below the land surface, there are four regimes of soil moisture movement, divided into two zones, as shown in Figure 3.6. With our interest in the zone of aeration, we restrict the discussion to vertical moisture movement, which predominates in this zone.

The soil water subzone is characterized by a fluctuating wetting front induced by the sequence of storm and interstorm periods.

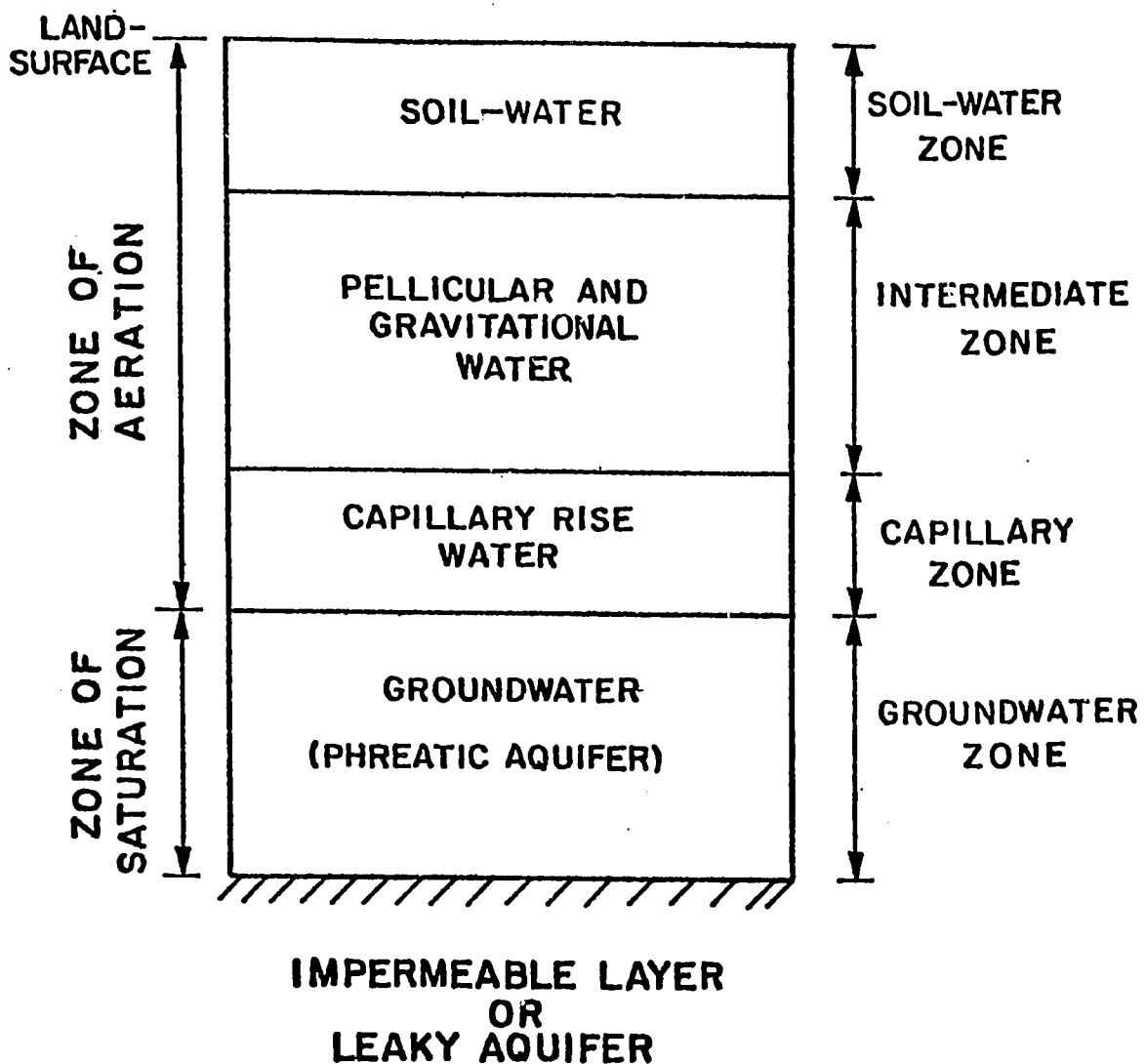


Figure 3.6

SUBSURFACE WATER CLASSIFICATION

This zone also contains the root zone, where vegetation receives its water supply. This is where the modelling of the transient soil moisture behavior is of most interest.

The time scale of the remaining subzones is much longer than that of the soil water zone. The intermediate zone passes moisture between the soil moisture zone and aquifer system at a slowly varying rate, determined by its relatively uniform moisture content. The capillary zone acts as a smooth transition zone between the saturated zone and zone of aeration, with a typically constant moisture distribution.

The thickness of these zones is very dependent on soil type, climate, geology and vegetation under natural conditions. For example, the capillary zone or capillary fringe can range in thickness from 2-5 cm for coarse sand to 2-4 meters for clays (Bear, 1979).

Several combinations of factors may yield a narrow zone of aeration bounded by a shallow water table and a partially-vegetated landsurface. At some point, the boundary between the capillary fringe and the soil-water zone becomes indistinct, preventing the modelling of the moisture fluxes in each zone separately, as was done with several of the models in Section 3.2. The level of interaction between the zones may be an annually varying phenomenon, particularly under non-steady climate or modified hydrological conditions.

The root zone thickness and type of plants in a region are affected by the shallow water table condition. Unlike the deep water table case, where the vegetation characteristics are determined by the soil-water zone activity, the proximity of the capillary fringe to the landsurface allows roots to enter this zone. Root penetration will be

limited by the anaerobic conditions of the lower capillary fringe. The zones of the shallow water table case are seen in Figure 3.7.

3.3.2 Processes of Soil Moisture Movement

The rate of drainage of infiltrated water differs between a deep and a shallow water table due to the reduced or absent intermediate zone in the latter case (see Figure 3.7). For a deep water table, the drainage rate is a function of the soil moisture content of the intermediate zone (Eagleson, 1978c). This content is often used as the uniform initial condition for infiltration models (Philip, 1969a). When the water table is high, the drainage rate is dependent on the fluctuating soil moisture content of the soil-water zone, which makes its transient behavior more important than in the other case. The distinction is displayed in Figures 3.8 and 3.9, where

z = depth from land surface

Z = depth to water table

θ = volumetric moisture content

θ_0 = moisture content of drained soil

θ_1 = moisture content at saturation

$K(\theta)$ = hydraulic conductivity or gravity drainage rate.

While the drainage rate is higher for the shallow water table case, it is somewhat affected by entrapped air (Morel-Seytoux and Ghanji, 1974).

The rate of infiltration also differs between the deep and shallow water table cases. In the former case, infiltration is into a

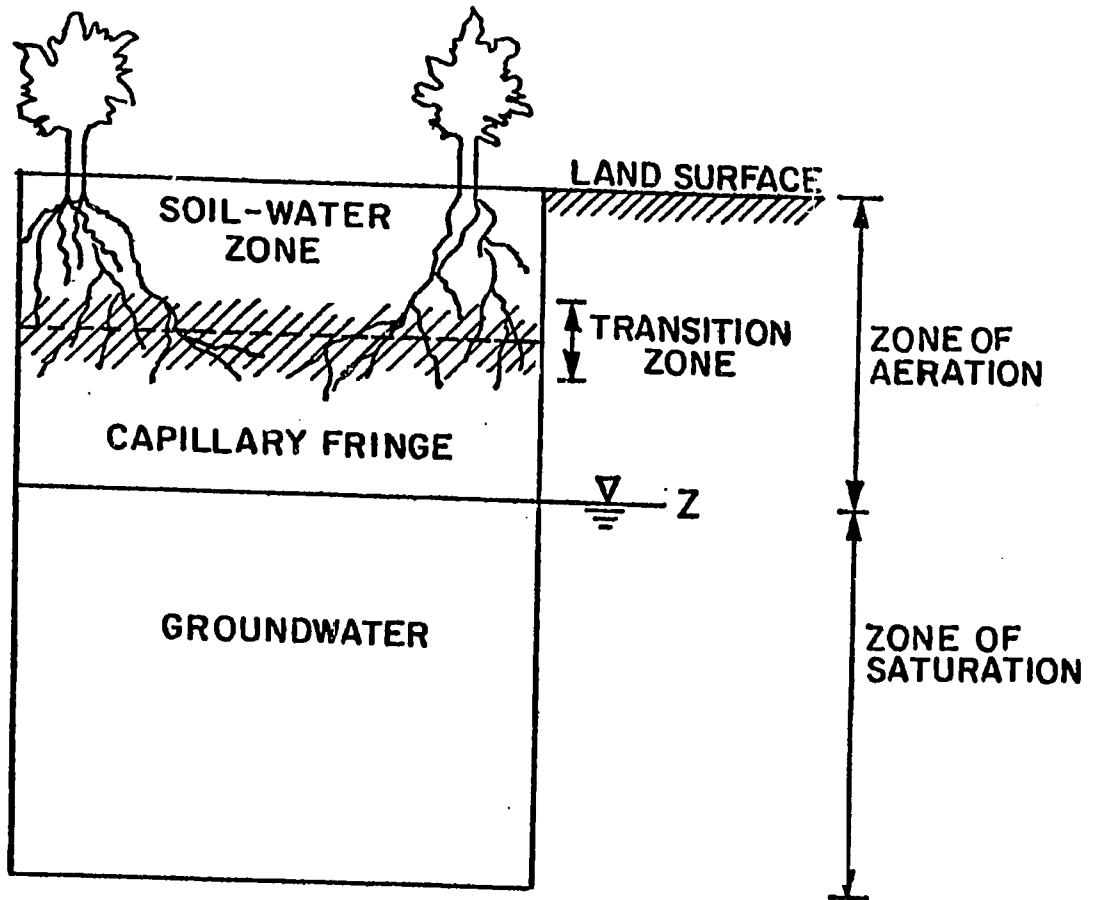


Figure 3.7

SUBSURFACE WATER CLASSIFICATION
FOR SHALLOW WATER TABLE SOIL COLUMN

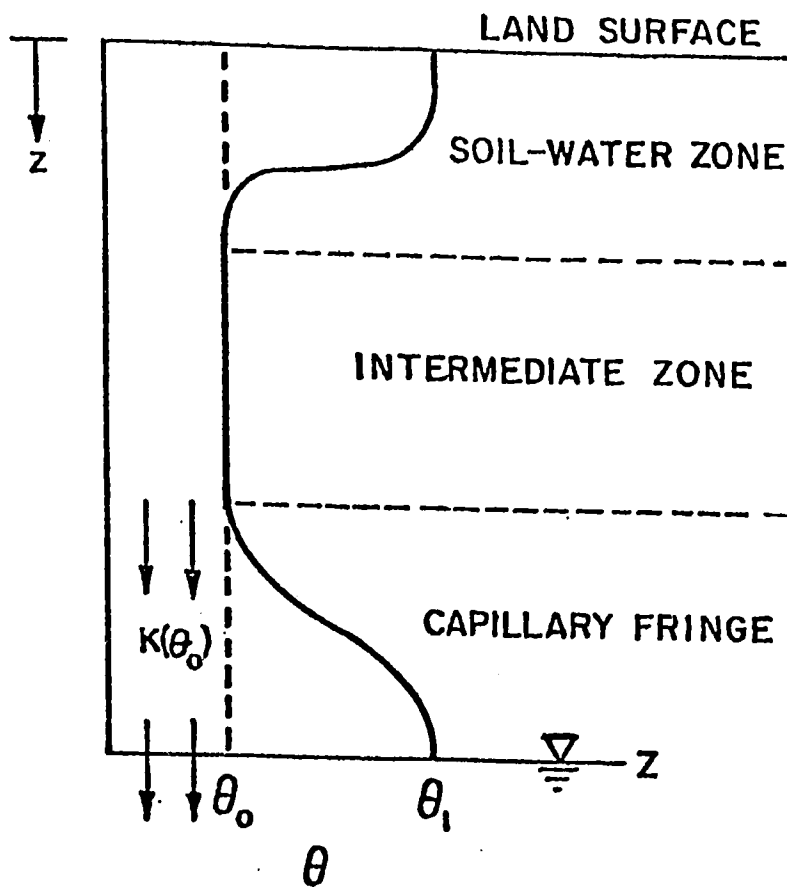


Figure 3.8

GRAVITY DRAINAGE WITH A DEEP WATER TABLE

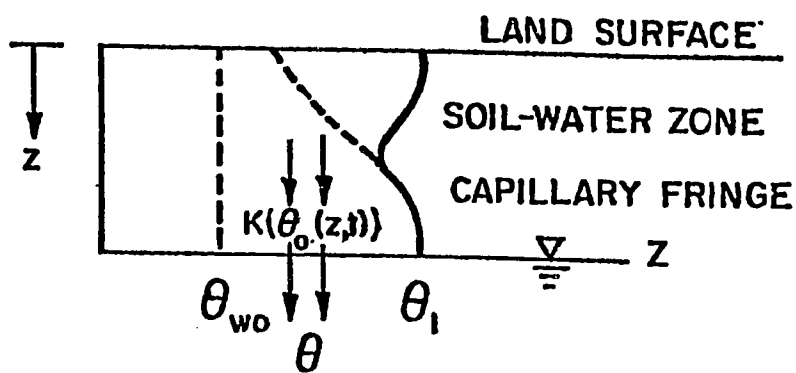


Figure 3.9

GRAVITY DRAINAGE WITH A SHALLOW WATER TABLE

soil of uniform initial moisture content, which may be viewed as extending infinitely downward. In the latter case, the infiltration is into a soil with an initially spatially distributed moisture content, as seen by the dotted line in Figure 3.9. Infiltration into a soil where moisture content increases with depth is reduced below that for a spatially uniform initial moisture content (Philip, 1969a). The shape of this initial moisture distribution is determined by the moisture retention characteristic of the soil (Bear, 1979). In this case, the column cannot be assumed semi-infinite.

The exfiltration rate is also affected by the altered initial moisture content. Here the increased initial content serves as a moisture supply, yielding higher exfiltration rates for the shallow water table cases. The presence of the water table also delays or eliminates the onset of the drying time.

The characteristic times of the infiltration process are influenced by the water table depth, as seen in Figures 3.10 and 3.11. Ponding time is reached sooner with a shallow water table, basically because of the reduced available pore space. Ponding time is when θ_{surface} is at point A.

The time at which the wetting front interacts with the capillary fringe, effectively defining when the semi-infinite domain assumption is invalid, is also a function of water table depth, along with soil properties. It is meaningless in cases like that shown in Figure 3.11, where the capillary zone reaches the land surface.

Figures 3.10 and 3.11 show typical steps in an infiltration process. In early steps moisture movement is primarily due to the capillarity, or matric potential gradient. In later steps, after the land surface is saturated, gravity plays the dominant role in moisture movement. In the shallow water table case of Figure 3.11 capillarity plays a relatively more important role as saturation is reached in early time. As with drainage, entrapped air is a significant infiltration factor.

3.4 Derivation of the Mathematical Model

3.4.1 Governing Equation

Using the terminology of Bear (1979), we develop the equation of moisture movement. The equation of continuity for the unsaturated zone is

$$\frac{\partial}{\partial t} (n s_w) - \frac{\partial}{\partial x_i} (q_i) = 0 \quad (3.60)$$

where

n = soil porosity

s_w = degree of moisture saturation

q = soil moisture flow rate

x_i = direction of pressure gradient

i = flow direction index

The general expression of Darcy's law for the three-dimensional flow of moisture in the unsaturated zone is

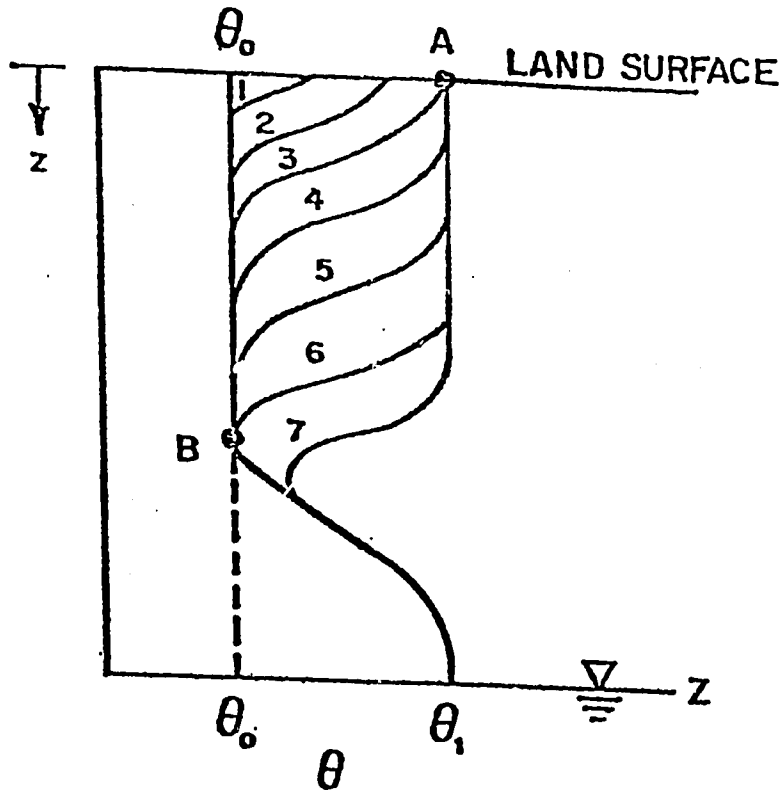


Figure 3.10

INFILTRATION WITH AN INTERMEDIATE DEPTH WATER TABLE

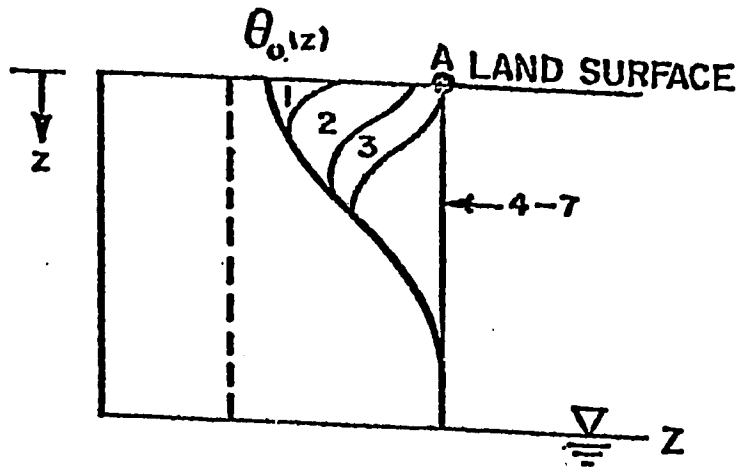


Figure 3.11

INFILTRATION WITH A SHALLOW WATER TABLE

$$q_i = k_{ij} \frac{k_{rw}(s_w)}{\mu_w} \left(\frac{\partial p_w}{\partial x_j} + \rho_w g \frac{\partial z}{\partial x_j} \right) \quad (3.61)$$

where

p_w = water pressure

z = depth from landsurface

ρ_w = isothermal water density

k_{ij} = saturated soil permeability to water

k_{rw} = relative permeability with respect to saturation

μ_w = dynamic viscosity of water

g = acceleration due to gravity

j = pressure gradient index

Substituting Equation (3.61) into Equation (3.60) results in the three-dimensional equation of motion for moisture flow in the unsaturated porous medium,

$$\frac{\partial}{\partial t} (ns_w) - \frac{\partial}{\partial x_i} \left(k_{ij} \frac{k_{rw}(s_w)}{\mu_w} \left(\frac{\partial p_w}{\partial x_j} + \rho_w g \frac{\partial z}{\partial x_j} \right) \right) = 0 \quad (3.62)$$

Equation (3.62) is based on the assumptions that:

1. the porous medium is a continuum of representative elementary volumes (REV) (Bear, 1979)
2. air and vapor transport are neglected
3. thermo-osmotic effects are neglected
4. the solid matrix is rigid and stable
5. moisture movement is due only to a piezometric head gradient

Equation (3.62) is simplified to

$$\frac{\partial \theta}{\partial t} - \frac{\partial}{\partial z} (K(\theta) \frac{\partial}{\partial z} \phi) = 0 \quad (3.63)$$

by further assuming:

6. an isotropic and homogeneous porous medium

7. ρ_w is constant

In Equation (3.63)

$$\phi = z - \psi \quad (3.64)$$

where

$$\psi = -p_w/\gamma = p_c/\gamma > 0 \quad (3.65)$$

and

ψ = matric potential

p_c = capillary pressure of air-water interface

$K(\theta)$ is a highly nonlinear function and subject to hysteresis effects. In this analysis, we neglect hysteresis by treating the wetting and drying processes separately. Neglecting hysteresis permits $\theta(\psi)$ to be a unique function (Bear, 1979).

Substituting Equation (3.64) into (3.63) yields,

$$\frac{d\theta}{d\psi} \frac{\partial \psi}{\partial t} + \frac{\partial}{\partial z} [K(\theta) \frac{\partial \psi}{\partial z} - K(\theta)] = 0 \quad (3.66)$$

or

$$\frac{\partial \theta}{\partial t} - \frac{\partial}{\partial z} [D(\theta) \frac{\partial \theta}{\partial z} - K(\theta)] = 0 \quad (3.19)$$

where

$$D(\theta) = -K(\theta) \frac{d\psi}{d\theta} \quad (3.67)$$

In this analysis, Equation (3.19) is used because of its similarity to the advection-diffusion equation and because $K(\theta)$ is more mathematically well-behaved compared with $K(\psi)$, (Klute, 1952a), (Bear, 1979). The complete nonlinear model accounting for the effects of capillarity, gravity and moisture uptake by plants is represented by Equation (3.44).

3.4. Boundary Conditions

Since the one-dimensional governing equation is of the second order in space and first order in time, we need two boundary conditions and one initial condition to find a unique solution. Physically the unsaturated zone is bounded by the land surface and the phreatic surface. The boundaries of the model are those of the macroscopic continuum, not those described by the dynamics of the fluid and the solid. This means that the one-dimensional model is assumed to represent a finite horizontal area, not just a point.

Mathematically, the surface boundary condition is derived from Darcy's Law for the macroscopic porous medium. This is a valid model if the flow velocities are sufficiently small. In the vertical direction, for a horizontal land surface continuity requires

$$\vec{N} \cdot lz = \vec{q} \cdot lz \quad (3.68)$$

where

\vec{N} = the atmospheric flux vector

\vec{q} = the porous medium apparent velocity vector

lz = vertical directional vector

For a horizontal land surface, $N = N(t)$, where $N(t)$ is a positive downward flux scalar. From the vertical one-dimensional Darcy's Law,

$$\vec{q} \cdot lz = q = K(\theta) \frac{\partial \psi}{\partial z} + K(\theta) \quad (3.69)$$

and for a homogeneous soil, neglecting hysteresis,

$$q = -D(\theta) \frac{\partial \theta}{\partial z} + K(\theta) \quad (3.70)$$

where positive is defined downward, and q is the scalar apparent velocity of the soil moisture.

Substituting Equation (3.70) into Equation (3.68),

$$N = -D(\theta) \frac{\partial \theta}{\partial z} + K(\theta) \quad (3.71)$$

When $N > 0$, the problem is one of infiltration. For $N < 0$, the problem is one of exfiltration. And when $N = 0$, a drainage problem is defined. For an infiltration problem, as the process proceeds $\frac{\partial \theta}{\partial z}$ approaches zero. To match a climate determined constant rainfall rate, $N = i$, $K(\theta)$ and $D(\theta)$ must increase. The corresponding increase in θ is bounded by θ_1 , when all the surface layer pores are filled. At this point $N = N(t)$, determined by the soil characteristics. The surface

boundary is more simply defined at this time by

$$\theta = \theta_1 \quad z = 0 \quad (3.72)$$

The excess rainfall in reality may accumulate through surface ponding or leave as surface runoff. This model assumes the rainfall excess is all surface runoff. If ponding were important, the model would need to have ψ as the dependent variable.

For infiltration,

$$-D(\theta) \frac{\partial \theta}{\partial z} \geq 0 \quad (3.73)$$

thus, if $N \leq K(\theta_1)$, Equation (3.71) is the boundary condition over the storm duration.

For an exfiltration problem,

$$-D(\theta) \frac{\partial \theta}{\partial z} \leq 0 \quad (3.74)$$

As $\frac{\partial \theta}{\partial z}$ approaches zero, $K(\theta)$ must decrease to meet the climate demand. The lower bound occurs at θ_{wo} , the moisture field capacity, where $K(\theta_{wo}) = 0$. At this time, the boundary condition is

$$\theta = \theta_{wo} \quad z = 0 \quad (3.75)$$

At the water table,

$$N(t) = -D(\theta) \frac{\partial \theta}{\partial z} + K(\theta) \quad (3.76)$$

where

$N(t)$ = drainage rate through the water table

and $\frac{\partial \theta}{\partial z}$ is not known before solving for $\theta(z,t)$. We do know that the

water table is defined by

$$\psi = 0 \quad z = Z \quad (3.77)$$

which corresponds with

$$\theta = \theta_1 \quad z = Z \quad (3.78)$$

Expression (3.78) is the second boundary condition.

It may be more convenient to apply the bottom boundary condition, not at the water table, but where $\psi = \psi_{\text{bubbling}}$. For ψ less than this, $\theta \approx \theta_1$. For $\psi > \psi_{\text{bubbling}}$, $\frac{d\theta}{d\psi}$ differs more significantly from zero. This may be done if $(\psi = 0) - (\psi = \psi_{\text{bubbling}})$ corresponds with a known distance from the water table.

3.4.3 Initial Condition

Since the aim of the analysis is to derive accurate analytical expressions for moisture fluxes, not moisture distributions, the initial condition need only preserve the properties important to the fluxes, their rates and associated volumes. Separate initial conditions are needed for the infiltration and exfiltration processes.

For the infiltration problem, if we assume the previous exfiltration or drainage process continues until equilibrium is reached, we may use the hydrostatic equilibrium initial condition. Assuming the upward flow velocity is negligible, equilibrium results in a pressure distribution linear with depth. It may be derived from Darcy's Law that, in hydrostatic equilibrium,

$$\psi = Z - z \quad (3.79)$$

where

Z = depth to the water table

This results in an initial distribution of $\theta(z)$ depending on the moisture characteristic curve, $\theta(\psi)$. The curve used depends on the approximate model used to encode the soil physics or the data accessible for the soil.

For both infiltration and exfiltration, we may use a two step process which preserves both the volume of moisture in the soil column and the moisture content at the boundaries. The initial volume of soil moisture is calculated from the depth-averaged final soil moisture content of the previous time period, as

$$V_{ss,0} = \int_0^Z \theta(z', t_f) dz' \quad (3.80)$$

where

t_f = duration of previous process

$V_{ss,0}$ = initial volume of soil moisture

This volume is used to fit a sinusoidal curve whose boundaries are fixed by the given values of moisture content at the boundaries.

This initial condition is described functionally by,

$$h(z) = \frac{n-h(0)}{Z} z + h(0) + A \sin\left(\pi\left(\frac{z}{Z} + 1\right)\right) \quad (3.81)$$

where

$$\begin{aligned} h(o) &= \text{initial moisture content at the land surface} \\ &= \theta(0, t_f) \end{aligned}$$

and

$$n = \text{porosity}$$

$$\begin{aligned} \theta(o, t_f) &= \text{final soil moisture content at the land surface} \\ &\text{for the previous process} \end{aligned}$$

$$A = \text{fitted parameter}$$

The value of A is set to conserve the initial soil moisture volume. The initial volume is equal to the depth integral of the initial distribution

$$\int_0^Z \left\{ \frac{n-h(o)}{Z} z + h(o) + A \sin\left[\pi\left(\frac{z}{Z} + 1\right)\right] \right\} dz = V_{ss,o} \quad (3.82)$$

Integrating the linear terms of the LHS yields,

$$\int_0^Z \left[\frac{n-h(o)}{Z} z + h(o) \right] dz = \frac{n+h(o)}{2} Z \quad (3.83)$$

Solving Equation (3.82) for A results in

$$A = \frac{V_{ss,o} - \frac{n+h(o)}{2} Z}{\int_0^Z \sin\left[\pi\left(\frac{z}{Z} + 1\right)\right] dz} \quad (3.84)$$

where (Gradshteyn and Ryzhik, 1980)

$$\int_0^Z \sin\left[\pi\left(\frac{z}{Z} + 1\right)\right] dz = -\frac{2Z}{\pi} \quad (3.85)$$

We may reduce Equation (3.84) to

$$A = \frac{\pi}{4} [n + h(o) - 2\theta_{AV}(t_f)] \quad (3.86)$$

where

θ_{AV} = the average moisture content at the end of the previous process

$$= V_{ss,0}/Z$$

For soil controlled exfiltration $h(o) = \theta_{wo}$, the field capacity. For soil-controlled infiltration, $h(o) = n$. $h(o)$ varies between those two for the climate-controlled cases.

This initial condition may be compared with the simpler uniform initial condition, $\theta_{AV}(t_f)$, which preserves only the volume of soil moisture. The sinusoidal initial condition accounts for the fact that some process has occurred earlier and that the capillary fringe exists. Of course, the more complex initial condition results in a more complex solution.

3.4.4 Vegetal Transpiration Sink

The extraction of soil-water by plants must be accounted for volumetrically and incorporated into the moisture flux expressions. Assuming that plants transpire at a rate which is independent of moisture potential, moisture content or time, two empirical extraction functions express moisture uptake as a function of depth. The models differ in how they model the decay of root density with depth. These models assume that root depth, root density and the transpiration rate primarily govern moisture uptake by plants. They assume also that the average

root depth is approximately constant over an event period. Molz and Remson (1971) model a linearly decaying root density with depth, contained in the following sink term expression,

$$g_r(z) = \frac{1.8 e_v}{z_r} - \frac{1.6 e_v}{z_r^2} z \quad 0 < z < z_r \quad (3.87)$$

with

$$e_v = k_v e_p \quad (3.88)$$

where

e_v = transpiration rate per unit area of soil surface

k_v = plant coefficient

Raats (1976) models an exponentially decaying root density with depth by,

$$g_r(z) = (e_v/\delta) \exp(-z/\delta) \quad (3.89)$$

where

δ = a parameter fitted to preserve the volume of moisture transpired.

Another empirical extraction function assumes the plant transpiration rate is a function of soil moisture content. Feddes et al (1976) use a piecewise linear function,

$$g_r(\theta) = \begin{cases} 0 & , \quad 0 \leq \theta \leq \theta_w \\ g_{r,\max} \left(\frac{\theta - \theta_w}{\theta_d - \theta_w} \right) & , \quad \theta_w < \theta \leq \theta_d \\ g_{r,\max} & , \quad \theta_d < \theta \leq \theta_{an} \\ 0 & \theta_{an} < \theta \leq \theta_l \end{cases} \quad (3.90)$$

where

$$g_{r,\max} = 2e_v^*/Z_r \quad (3.91)$$

and

$g_{r,\max}$ = maximum soil moisture vegetal extraction rate (t^{-1})

e_v^* = maximum transpiration rate per unit area of soil surface

θ_w = soil water content at wilting

θ_d = moisture content dividing soil-water and climate controlled transpiration processes

θ_{an} = moisture content at which anaerobic soil-water-conditions occur (the anaerobiosis point).

The regions of validity are defined by the matric potentials associated with each characteristic moisture content, which are plant species dependent.

The model assumes that the moisture flux into the plant roots is proportional to the soil-plant potential gradient, which is approximated by the linear moisture content gradient given by Equation (3.90).

Equation (3.91) for $g_{r,\max}$ requires the assumption that for shallow water tables under steady state and dry surface conditions the maximum transpiration rate equals 50% of the climatic demand (Feddes et al, 1976). This is calculated from typical steady state moisture distributions and the associated $g_r(\theta)$ curve. This curve is approximated by a linear function. With this assumption

$$e_v \equiv \int_0^{z_r} g_{r,\max}(\theta(z,t)) dz \approx \frac{1}{2} z_r g_{r,\max} \quad (3.92)$$

where

$g_{r,\max}(\theta)$ = the $g_r(\theta)$ distribution yielding maximal transpiration

Assuming transpiration is steady at the maximal value, Figure 3.12 shows a comparison of the above three root sink expressions, $g_r(z)$, under exfiltration conditions. The primary difference between the first two models and the third is that the first group emphasizes root density and the latter the flow gradient into the roots.

The empirical nature of the above models requires that the parameters be calibrated within the context of the soil moisture movement model (Molz, 1981).

3.5 Linearizing the Model

3.5.1 Problem Presentation

We linearize the governing equation (3.44),

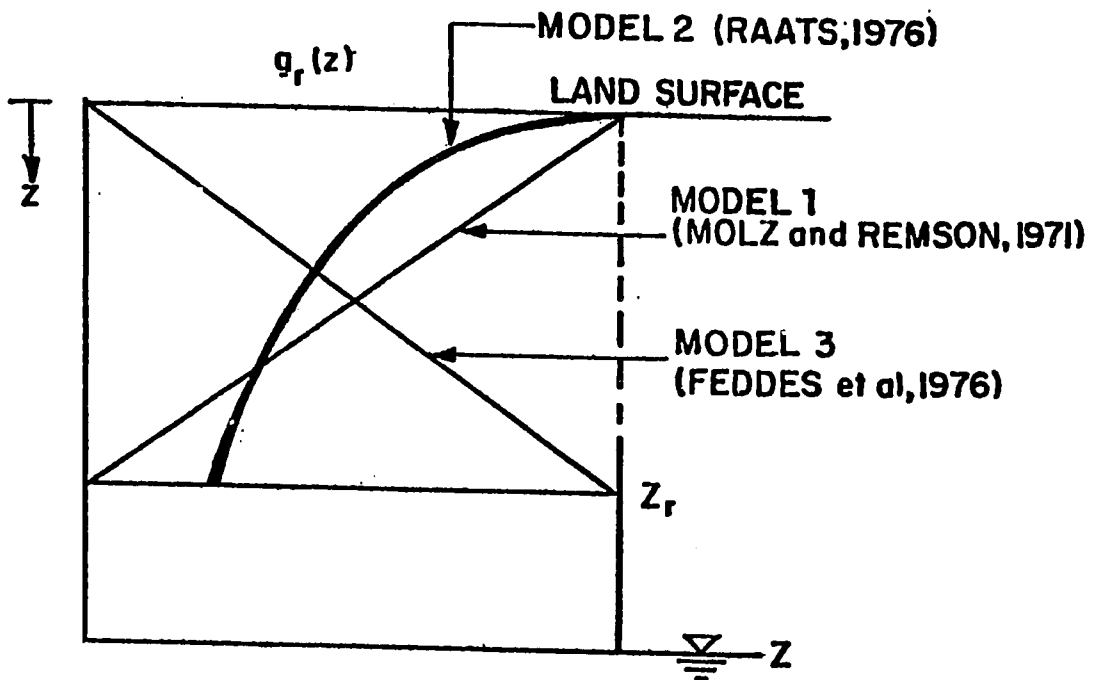


Figure 3.12

ROOT SINK MODELS

$$\frac{\partial \theta}{\partial t} = \frac{\partial}{\partial z} \left(D(\theta) \frac{\partial \theta}{\partial z} \right) - \frac{dK(\theta)}{d\theta} \frac{\partial \theta}{\partial z} - g_r(\theta, z, t) \quad (3.44)$$

by letting

$$D(\theta) \approx D_* = \text{constant}$$

and (3.26a)

$$\frac{dK(\theta)}{d\theta} \approx k = \text{constant}$$

The linearized equation is,

$$\frac{\partial \theta}{\partial t} = D_* \frac{\partial^2 \theta}{\partial z^2} - k \frac{\partial \theta}{\partial z} - g_r(\theta, z, t) \quad (3.25)$$

By integrating expression (3.26) for k , we find

$$K(\theta) = k(\theta - \theta_o) + K_{wo} \quad (3.93)$$

where

K_{wo} = hydraulic conductivity at $\theta = \theta_{wo}$

Evaluating k at $\theta = \theta_1$ defines k parametrically to be

$$k = \frac{K_1 - K_{wo}}{\theta_1 - \theta_{wo}} \quad (3.26b)$$

where

K_1 = maximum hydraulic conductivity

According to Gardner (1958), Equation (3.26b) results also from the assumption that

$$K(\psi) = K_1 \exp(-a_2\psi). \quad (3.94)$$

Using Equation (3.20), we may solve for the assumed moisture characteristic curve $\theta(\psi)$, where

$$D(\theta) = -K(\psi) \frac{d\psi}{d\theta} \quad (3.20)$$

Substituting Equations (3.26) and (3.93) into Equation (3.20), separating the variables and integrating θ from θ_{wo} to θ and ψ from ψ_1 to ψ results in

$$D_*(\theta - \theta_{wo}) = [K(\psi) - K(\psi_0)]/a_2 \quad (3.95)$$

where

ψ_0 = maximum capillary potential

At $\theta = n$, $\psi = \psi_0$ and

$$a_2 = \frac{K_1 - K_{wo}}{D_* n_e} = k/D_* \quad (3.96)$$

where

$$n_e = \theta_1 - \theta_{wo} \quad (3.97)$$

Substituting Equations (3.94) and (3.96) into Equation (3.95), the resulting moisture characteristic for the model is

$$\theta_e = n_e \left(\frac{K_1}{K_1 - K_{wo}} \right) [\exp(-a_2\psi) - \exp(-a_2\psi_0)] \quad (3.98)$$

where

$$\begin{aligned}\theta_e &= \text{effective moisture content} \\ &= \theta - \theta_{w0}\end{aligned}\quad (3.99)$$

Assuming there is no flow at $\theta = \theta_{w0}$, $K(\theta_{w0}) = K(\psi_0) = 0$ and

$$\theta_e = n_e \exp\left(-\frac{K_1}{D_* n_e} \psi\right) \quad (3.100)$$

If the root sink term is expressed by either Equation (3.87) or (3.89), no changes need be made for it, but if Equation (3.90) is used, it must also be linearized. To do this, we assume

$$\theta_w \approx \theta_{w0} \quad (3.101)$$

and

$$\theta_d \approx \theta_{an} \approx \theta_1 \quad (3.102)$$

With these assumptions, Equation (3.90) reduces to

$$g_r(\theta) = g_{r,1} \theta_e \quad (3.103)$$

where

$$g_{r,1} = g_{r,\max}/n_e = 2e^*/Z_r n_e \quad (3.104)$$

with

$g_{r,1}$ = vegetal extraction function parameter

The linearized flux boundary condition is

$$N - K_{w0} = -D_* \frac{\partial \theta_e}{\partial z} + k \theta_e \quad (3.105)$$

The concentration boundary conditions are already linear.

In terms of θ_e , they are

$$\theta_e = n_e \quad (3.72)$$

and

$$\theta_e = 0 \quad (3.75)$$

The sinusoidal and uniform initial conditions are also acceptable for a linear model, where $h(z)$ is replaced by $h_e(z)$ and θ_{AV} by $\theta_{e,AV}$. The hydrostatic initial condition is readily found from the derived moisture characteristic curve of the linear model. Substituting Equation (3.79) into Equation (3.99) and using the relation (3.96), the expression is

$$h_e(z) = n_e \exp[-a_2(Z-z)] \quad (3.106)$$

3.5.2 Dimensionless Parameterization

To simplify the problem, we define dimensionless space and time parameters by

$$z^o = \frac{kz}{D_*} \quad (3.107)$$

$$t^o = \frac{k^2 t}{D_*} \quad (3.108)$$

These reduce Equation (3.25) to

$$\frac{\partial \theta_e}{\partial t^o} = \frac{\partial^2 \theta_e}{\partial z^o{}^2} - \frac{\partial \theta_e}{\partial z^o} - G_R \quad (3.109)$$

where

G_R = dimensionless vegetal extraction function

and

$$G_R(z^0) = \left(\frac{D_*}{k^2} \right) g_r(z) \quad (3.110)$$

for the depth-dependent root-sink and

$$G_R(\theta_e) = G_1 \theta_e \quad (3.111)$$

for the moisture-content dependent root sink. Here

G_1 = dimensionless model parameter

$$= (D_*/k^2 n_e) g_{r,max} \quad (3.112)$$

For the root sink Equation (3.87)

$$G_R(z^0) = G_{11} - G_{12}z^0 \quad (3.113)$$

where the dimensionless parameters are

$$G_{11} = 1.8 \left(\frac{D_* e_v}{k^2 z_r} \right) \quad (3.114)$$

and

$$G_{12} = 1.6 \left(\frac{D_* e_v}{k^2 z_r} \right) \quad (3.115)$$

For the root sink of Equation (3.89),

$$G_R(z^0) = G_{21} \exp(-G_{22} z^0) \quad (3.116)$$

where the dimensionless parameters are

$$G_{21} = D_* e_v / k^2 \delta \quad (3.117)$$

and

$$G_{22} = D_*/k\delta \quad (3.118)$$

We may convert Equation (3.109) into a diffusion equation using the following transformation of variables (Kirkham and Powers, 1972). For the concentration-dependent root sink,

$$\theta^0 = \theta_e \exp[-z^0/2 + (1/4 + G_1)t^0] \quad (3.119)$$

where

$$\theta^0 = \text{transformed volumetric moisture content}$$

For the depth-dependent moisture content, we may set $G_1 = 0$.

When substituting Expression (3.119) into Equation (3.109), the problem is reduced to

$$\frac{\partial \theta^0}{\partial t^0} = \frac{\partial^2 \theta^0}{\partial z^{0^2}} \quad (3.120)$$

for the concentration-dependent case and

$$\frac{\partial \theta^0}{\partial t^0} = \frac{\partial^2 \theta^0}{\partial z^{0^2}} - G_2(z^0, t^0) \quad (3.121)$$

for the depth-dependent case, where

$$\begin{aligned} G_2(z^0, t^0) &= \text{transformed sink term} \\ &= G_R(z^0) \exp(-z^0/2 + t^0/4) \end{aligned} \quad (3.122)$$

The dimensionless flux boundary condition from Equation (3.105) is

$$-\frac{\theta_e}{z^0} + \theta_e = N^0 \quad (3.123)$$

where dimensionless flux is defined by

$$N^0 \equiv \frac{1}{k} (N - K_{wo}) = n_e \left(\frac{N - K_{wo}}{K_1 - K_{wo}} \right) \quad (3.124)$$

Transforming this boundary condition by Equation (3.119) results in

$$-\frac{\theta^0}{z^0} + \frac{1}{2} \theta^0 = N_T^0 \quad z^0 = 0 \quad (3.125)$$

where

$$N_T^0 = N^0 \exp[(1/4 + G_1)t^0] \quad (3.126)$$

The transformed concentration boundary condition at the water table is

$$\theta_{1,z}^0 = n_e \exp[-z^0/2 + (1/4 + G_1)t^0] \quad (3.127)$$

For infiltration at the land surface

$$\theta_{1,0}^0 = n_e \exp[(1/4 + G_1)t^0] \quad (3.128)$$

and for exfiltration

$$\theta^0 = 0 \quad (3.129)$$

The uniform initial condition is transformed into

$$h^0(z^0) = \theta_{e,AV} \exp(-z^0/2) \quad (3.130)$$

The sinusoidal initial condition using the dimensionless depth variable is

$$h_e(z^0) = h_e(o) + (n_e - h_e(o)) (z^0/Z^0) + A \sin(\pi(z^0/Z^0 + 1)) \quad (3.131)$$

where

$$z^0 = kz/D_*$$

The transformed sinusoidal initial condition is

$$h^0(z^0) = h_e(z^0) \exp(-z^0/2) \quad (3.132)$$

The dimensionless hydrostatic initial condition is

$$h_e(z^0) = n_e \exp(z^0 - Z^0) \quad (3.133)$$

Its transformed equivalent is

$$h^0(z^0) = n_e \exp(z^0/2 - Z^0) \quad (3.134)$$

SOLVING THE LINEAR PROBLEM4.1 Solving for Moisture Content Distributions

4.1.1 General Solution Method

All of the several methods used for solving linear partial differential equations make use of the superposition concept. This permits one to separately account for the boundary conditions, the initial conditions and the sink term (Carslaw and Jaeger, 1959). The Finite Fourier Transform (FFT) approach is adapted here because it is relatively easy to use, clearly separating the effects of the various imposed conditions, and because it is flexible enough to incorporate a wide variety of conditions, including problems of two or three spatial dimensions (Ölcer, 1964), (Ölcer, 1965), (Ozisik, 1967), (Cleary and Adrian, 1973).

For this analysis, we may describe the three transformed governing equations, two boundary conditions and three initial conditions with the following general problem statement. The governing equation is

$$\frac{\partial \theta^0}{\partial t^0} = \frac{\partial^2 \theta^0}{\partial z^0{}^2} - G_2(z^0, t^0) \quad (4.1)$$

The boundary conditions are, for the flux surface boundary

$$-\frac{\partial \theta^0}{\partial z^0} + \frac{1}{2} \theta^0 = N_T^0(t^0) \quad (4.2)$$

and for the concentration boundary, either at the land surface or the water table

$$\theta^0 = \theta_B^0(t^0) \quad (4.3)$$

where $\theta_B^0(t)$ may differ at the two boundaries.

The initial conditions are generalized as

$$\theta^0 = h^0(z^0) \quad (4.4)$$

The general solution to this problem, using the FFT method, is given by (Cleary, 1977)

$$\theta^0(z^0, t^0) = \sum_{m=0}^{\infty} (K(\beta_m, z^0)/D(\beta_m)) \exp(-\beta_m^2 t^0) [\bar{F}(\beta_m) + \int_0^{t^0} \exp(\beta_m^2 t^0) A_1(\beta_m, t^0) dt^0] \quad (4.5)$$

where, for the flux surface boundary condition

$$A_1(\beta_m, t^0) = \left[K(\beta_m, z^0) \Big|_{z^0=0} N_T^0(t^0) - \frac{dK(\beta_m, z^0)}{dz^0} \Big|_{z^0=z^0} \theta_{1,z^0}^0 \right] - \bar{G}(\beta_m, t^0) \quad (4.6)$$

and for the concentration surface boundary condition

$$A_1(\beta_m, t^0) = \left[\frac{dK(\beta_m, z^0)}{dz^0} \Big|_{z^0=0} \theta_{1,0}^0 - \frac{dK(\beta_m, z^0)}{dz^0} \Big|_{z^0=z^0} \theta_{1,z^0}^0 \right] - \bar{G}(\beta_m, t^0) \quad (4.7)$$

where

$G(\beta_m, t) =$ integral transform of the depth-dependent root sink

$$= \int_0^{z^0} K(\beta_m, z^0) [G_2(z^0, t^0)] dz^0 \quad (4.8)$$

and

$$\begin{aligned}\bar{F}(\beta_m) &= \text{integral transform of the initial condition} \\ &= \int_0^{z^0} K(\beta_m, z^0) h^0(z^0) dz^0\end{aligned}\quad (4.9)$$

When the sink term is a function only of soil moisture content

$$\bar{G}(\beta_m, t^0) = 0 \quad (4.10)$$

$K(\beta_m, z^0)$ is the eigenfunction for this problem defined generally by

$$K(\beta_m, z^0) = \beta_m \cos \beta_m z^0 + H_1 \sin \beta_m z^0 \quad (4.11)$$

and normalized by

$$D(\beta_m) = \frac{1}{2} [(\beta_m^2 + H_1^2)(z^0 + \frac{H_2}{\beta_m^2 + H_2^2}) + H_1] \quad (4.12)$$

where β_m is the eigenvalue corresponding to the eigenfunction, which is defined implicitly by

$$\tan \beta_m z^0 = \frac{\beta_m (H_1 + H_2)}{\beta_m^2 - H_1 H_2} \quad (4.13)$$

with H_1 and H_2 determined from the boundary conditions.

For the flux surface boundary condition, Equation (4.2), and the concentration bottom boundary condition, Equation (3.127), Ozisik (1967) shows that Equation (4.11) may be reduced to

$$K(\beta_m, z^0) = \sin \beta_m (Z^0 - z^0) \quad (4.14)$$

and Equation (4.12) simplifies to

$$D_F(\beta_m) = \frac{1}{2} \left[\frac{Z^0 (\beta_m^2 + H_1^2) + H_1}{\beta_m^2 + H_1^2} \right] \quad (4.15)$$

where

$$H_1 = 1/2 \quad (4.16)$$

For this case, Equation (4.13) reduces to

$$\beta_m \cot \beta_m Z^0 = -H_1 \quad (4.17)$$

For the concentration surface and water table boundary conditions, expressed generally by Equation (4.3)

$$K(\beta_m, z^0) = \sin \beta_m z^0 \quad (4.20)$$

and

$$D_c(\beta_m) = Z^0/2. \quad (4.21)$$

The eigenvalues are explicitly defined by

$$\beta_m = m\pi/Z^0 \quad m = 1, 2, 3 \quad (4.22)$$

The total transformed moisture content for the linear model, which is the sum of the contributions from the initial and boundary conditions and the loss from the moisture sink is expressed by

$$\theta^0(z^0, t^0) = \theta_{IC}^0(z^0, t^0) + \theta_{BC1}^0(z^0, t^0) + \theta_{BC2}^0(z, t^0) - \theta_S^0(z^0, t^0) \quad (4.23)$$

where

$\theta_{IC}^0(z^0, t^0)$ = the transformed moisture content due to the
initial condition

$\theta_{BC1}^0(z^0, t^0)$ = the transformed moisture content due to the
surface boundary condition

$\theta_{BC2}^0(z^0, t^0)$ = the transformed moisture content due to the
water table condition

$\theta_S^0(z^0, t^0)$ = the transformed moisture content due to the
depth-dependent root sink

The advantage of separating the components like this is that the effect of each on the total response may be separately studied.

4.1.2 Initial Condition

In general

$$\theta_{IC}^0 = \sum_{m=0}^{\infty} K(\beta_m, z^0) \exp(-\beta_m^2 t^0) \bar{F}(\beta_m)/D(\beta_m) \quad (4.24)$$

which is dependent on the boundary conditions used. For the flux surface boundary condition with the concentration water table boundary condition, substituting Equation (4.14) for $K(\beta_m, z^0)$, using the uniform initial condition of Equation (3.129)

$$\begin{aligned} \bar{F}_{uf}(\beta_m) &= \theta_{e,AV} \int_0^{z^0} \sin \beta_m (Z^0 - z^0) \exp(-z^0/2) dz^0 \\ &= \theta_{e,AV} F_1(Z^0)/p_1 \end{aligned} \quad (4.25)$$

where

$$F_1(Z^0) = \beta_m \exp(-Z^0/2) + \sin\beta_m Z^0 \quad (4.26)$$

and

$$p_1 = 1/4 + \beta_m^2 \quad (4.27)$$

Using the transformed sinusoidal initial condition, Equation

(3.131)

$$F_{sf}(\beta_m) = \int_0^{Z^0} \sin\beta_m (Z^0 - z^0) [(p_2 + p_3 z^0 + A \sin[\pi(z^0/Z^0 + 1)])] \exp(-z^0/2) dz^0 \quad (4.28)$$

$$= \frac{p_2}{p_1} F_1(Z^0) + \frac{p_3}{p_1} F_2(Z^0) + \frac{A}{2} \frac{F_4(Z^0) - (\pi(Z^0 - \beta_m))}{1/4 + (\pi/Z^0 - \beta_m)^2} - \frac{F_4(Z^0) + (\pi/Z^0 + \beta_m)}{1/4 + (\pi/Z^0 + \beta_m)^2} \quad (4.29)$$

where

$$p_2 = h_e(0) \quad (4.30)$$

$$p_3 = (n_e - h_e(0))/Z^0 \quad (4.31)$$

$$F_2(Z^0) = [\beta_m \exp(-Z^0/2) (Z^0 + 1/p_1) + F_3(Z^0)/p_1] \quad (4.32)$$

and

$$F_3(Z^0) = [1/4 - \beta_m^2] \sin\beta_m Z^0 - \beta_m \cos\beta_m Z^0$$

$$F_4(Z^0) = \frac{1}{2} [\exp(-Z^0/2) + 1] \quad (4.33)$$

With the transformed hydrostatic initial condition of

Equation (3.133)

$$F_{hf}(\beta_m) = \int_0^{Z^0} n_e \exp(-Z^0) \sin \beta_m (Z^0 - z^0) \exp(z^0/2) dz^0 \quad (4.34)$$

$$= [n_e \beta_m \exp(-Z^0/2)]/p_1 \quad (4.35)$$

For the concentration surface boundary condition with the concentration water table boundary condition, substituting Equation (4.20) for $K(\beta_m, z^0)$, using the uniform initial condition of Equation (3.129)

$$\begin{aligned} F_{uc}(\beta_m) &= \theta_{e,AV} \int_0^{Z^0} \sin \beta_m z^0 \exp(-z^0/2) dz^0 \\ &= \theta_{e,AV} \beta_m F_5(Z^0)/p_1 \end{aligned} \quad (4.36)$$

where

$$F_5(Z^0) = 1 - (-1)^m \exp(-Z^0/2) \quad (4.37)$$

Using the transformed sinusoidal initial condition of Equation (3.131)

$$\begin{aligned} F_{sc}(\beta_m) &= \int_0^{Z^0} \sin \beta_m z^0 [p_2 + p_3 z^0 + A \sin[\pi(z^0/Z^0 + 1)]] \exp(-z^0/2) dz^0 \\ &= p_2 \beta_m F_5(Z^0)/p_1 + p_3 \beta_m F_6(Z^0)/p_1 \\ &\quad + \pi A \left[\frac{(m+1)F_7(Z^0)}{1/4 + \beta_{m+1}^2} - \frac{(m-1)F_7(Z^0)}{1/4 + \beta_{m-1}^2} \right] \end{aligned} \quad (4.38)$$

where

$$F_6(Z^0) = 1/p_1 - (-1)^m \exp(-Z^0/2) (Z^0 + 1/p_1) \quad (4.39)$$

$$F_7(Z^0) = 1 + (-1)^m \exp(-Z^0/2) \quad (4.40)$$

With the transformed hydrostatic initial condition,

$$\begin{aligned} \bar{F}_{hc}(\beta_m) &= \int_0^{Z^0} n_e \exp(-Z^0) \sin \beta_m z^0 \exp(z^0/2) dz^0 \\ &= n_e \beta_m \exp(-Z^0) F_8(Z^0)/p_1 \end{aligned} \quad (4.41)$$

where

$$F_8(Z^0) = 1 - (-1)^m \exp(Z^0/2) \quad (4.42)$$

4.1.3 Boundary Conditions

The general expression for the contribution of the boundary conditions to the transformed moisture content is

$$\theta_{BC}^0 = \sum_{m=0}^{\infty} K(\beta_m, z^0) \exp(-\beta_m^2 t^0) A_{BC}(\beta_m, t^0) / D(\beta_m) \quad (4.43)$$

where

A_{BC} = integral defined by the boundary condition

For the flux surface boundary condition

$$\begin{aligned} A_{BC1,F}(\beta_m, t^0) &= \int_0^{t^0} \exp(\beta_m^2 t^{0'}) (K(\beta_m, z^0))_{z^0=0} N_T^0 dt^{0'} \\ &= N^0 C_1(t^0) \sin \beta_m Z^0 \end{aligned} \quad (4.44)$$

where

$$\begin{aligned} C_1(t^0) &= \int_0^{t^0} \exp(p_4 t^{0'}) dt^{0'} \\ &= (\exp(p_4 t^0) - 1) / p_4 \end{aligned} \quad (4.45)$$

and

$$p_4 = 1/4 + G_1 + \beta_m^2 \quad (4.46)$$

For the contribution from the water table boundary condition, with the flux surface boundary condition

$$\begin{aligned} A_{BC2,F}(\beta_m, t^0) &= \int_0^{t^0} \exp(\beta_m^2 t^{0'}) \left(- \frac{dK(\beta_m, z^0)}{dz^0} \right)_{z^0=Z^0} \theta_{1,Z^0}^0(t^{0'}) dt^{0'} \\ &= n_e \beta_m C_1(t^0) \exp(-Z^0/2) \end{aligned} \quad (4.47)$$

and

$$\left. \frac{dK(\beta_m, z^0)}{dz^0} \right|_{z^0=Z^0} = \frac{d}{dz^0} (\sin \beta_m (Z^0 - z^0)) \Big|_{z^0=Z^0} = -\beta_m \quad (4.48)$$

With the surface concentration boundary condition, for infiltration

$$\begin{aligned} A_{BC1,C}(\beta_m, t^0) &= \int_0^{t^0} \exp(\beta_m^2 t^{0'}) \left(\frac{dK(\beta_m, z^0)}{dz^0} \right)_{z^0=0} \theta_{1,0}^0(t^{0'}) dt^{0'} \\ &= n_e \beta_m C_1(t^0) \end{aligned} \quad (4.49)$$

where

$$\left. \frac{dK(\beta_m, z^0)}{dz^0} \right|_{z^0=0} = \frac{d}{dz^0} (\sin \beta_m z^0) \Big|_{z^0=0} = \beta_m \quad (4.50)$$

and for exfiltration

$$A_{BC1,C}(\beta_m, t^0) = 0 \quad (4.51)$$

For the water table contribution with the surface concentration boundary condition

$$A_{BC2,C}(\beta_m, t^0) = \int_0^{t^0} \exp(\beta_m^2 t^0) \left(- \frac{dK(\beta_m, z^0)}{dz^0} \right)_{z^0=Z^0} \theta_{1,Z^0}^0(t^0) dt^0$$

$$= -(-1)^m n_e \beta_m C_1(t^0) \exp(-Z^0/2) \quad (4.52)$$

where

$$\left. \frac{dK(\beta_m, z^0)}{dz^0} \right|_{z^0=Z^0} = (-1)^m \beta_m \quad (4.53)$$

4.1.4 Root Sink Terms

For the depth-dependent root sinks, we set $G_1 = 0$ and account for the vegetal moisture extraction by

$$\theta_s^0 = \sum_{m=0}^{\infty} K(\beta_m, z^0) \exp(-\beta_m^2 t^0) R(\beta_m, t^0) / D(\beta_m) \quad (4.54)$$

where

$$R(\beta_m, t^0) = \int_0^{t^0} \exp(\beta_m^2 t^0) \bar{G}(\beta_m, t^0) dt^0 \quad (4.55)$$

For the flux surface boundary condition and the concentration water table boundary condition, using the linear sink expression (3.113)

$\bar{G}(\beta_m, t^0)$ is evaluated to be

$$\bar{G}_{L,F}(\beta_m, t^0) = \int_0^{Z^0} \sin \beta_m (Z^0 - z^0) [G_{11} - G_{12} z^0] \exp[-z^0/2 + t^0/4] dz^0$$

$$= \{G_{11} F_1(Z^0) - G_{12} F_2(Z^0)\} \exp(t^0/4) / p_1 \quad (4.56)$$

and

$$R_{L,F}(\beta_m, t^0) = \{G_{11}F_1(Z^0) - G_{12}F_2(Z^0)\} C_1(t^0) \quad (4.57)$$

Using the exponential sink expression (3.116) with the same boundary conditions results in

$$\begin{aligned} \bar{G}_{E,F}(\beta_m, t^0) &= \int_0^{Z^0} \sin\beta_m(Z^0 - z^0) [G_{21} \exp(-G_{22}z^0)] \exp(-z^0/2 + t^0/4) dz^0 \\ &= G_{21}F_9(Z^0) \exp(t^0/4)/p_5 \end{aligned} \quad (4.58)$$

where

$$F_9(Z^0) = \beta_m \exp[-(1/2 + G_{22})Z^0] - (1 + G_{22}) \sin\beta_m Z^0 \quad (4.59)$$

$$p_5 = (1/2 + G_{22})^2 + \beta_m^2 \quad (4.60)$$

and

$$R_{E,F}(\beta_m, t^0) = G_{21}F_9(Z^0) C_1(t^0)/p_5 \quad (4.61)$$

With the concentration surface and water table boundary conditions, the linear root sink results in

$$\begin{aligned} \bar{G}_{L,C}(\beta_m, t^0) &= \int_0^{Z^0} \sin\beta_m z^0 [G_{11} - G_{12}z^0] \exp(-z^0/2 + t^0/4) dz^0 \\ &= [G_{11}F_5(Z^0) - G_{12}F_6(Z^0)] \beta_m \exp(t^0/4)/p_1 \end{aligned} \quad (4.62)$$

and

$$R_{L,C}(\beta_m, t^0) = [G_{11}F_5(Z^0) - G_{12}F_6(Z^0)]\beta_m C_1(t^0)/p_1 \quad (4.63)$$

With the same boundary conditions and the exponential sink term the expressions are

$$\begin{aligned} G_{E,C}(\beta_m, t^0) &= \int_0^{z^0} \sin\beta_m z^0 [G_{21} \exp(-G_{22}z^0)] \exp(-z^0/2 + t^0/4) dz^0 \\ &= G_{21}\beta_m F_{10}(Z^0) \exp(t^0/4)/p_5 \end{aligned} \quad (4.64)$$

where

$$F_{10}(Z^0) = 1 - (-1)^m \exp[-(1/2 + G_{22})Z^0] \quad (4.65)$$

and

$$R_{E,C}(\beta_m, t^0) = G_{21}\beta_m F_{10}(Z^0)C_1(t^0)/p_5 \quad (4.66)$$

4.1.5 Moisture Content Distribution

Moisture content distributions from the linearized model are calculated by substituting the above expressions for the transformed moisture contents into Equation (4.23), and inserting that equation into Equation (3.119) to yield

$$\theta_e(z^0, t^0) = (\theta_{IC}^0 + \theta_{BCI}^0 + \theta_{BC}^0 - \theta_S^0) \exp[z^0/2 - (1/4 + G_1)t^0] \quad (4.67)$$

With the flux surface boundary condition, concentration water table boundary condition, and concentration-dependent sink term, the solution for any initial condition is reducible to

$$\theta_{e,f} = \exp(z^0/2) \sum_0^{\infty} (\sin \beta_m (Z^0 - z^0)) \{ \exp(-p_4 t^0) [\bar{F}(\beta_m) - F_{11}/p_4] + F_{11}/p_4 \} / D_F(\beta_m) \quad (4.68)$$

where

$$\left. \begin{aligned} F_{uf}(\beta_m) &= [\text{Equation (4.25)}] \\ F_{sf}(\beta_m) &= [\text{Equation (4.29)}] \\ F_{hf}(\beta_m) &= [\text{Equation (4.35)}] \end{aligned} \right\} \quad (4.68a)$$

and

$$F_{11}(Z^0) = N^0 \sin \beta_m Z^0 + \beta_m n_e \exp(-Z^0/2) \quad (4.68b)$$

With the same boundary conditions and any initial condition, including the linear vegetal sink results in

$$\theta_{e,f} = \exp(z^0/2) \sum_0^{\infty} (\sin \beta_m (Z^0 - z^0)) \{ \exp(-p_4 t^0) [F(\beta_m) - (F_{11} - (G_{11}F_1 - G_{12}F_2)/p_1)/p_4] + [F_{11} - (G_{11}F_1 - G_{12}F_2)]/p_4 \} / D_F(\beta_m) \quad (4.69)$$

Substituting the exponential vegetal sink for the linear one results in

$$\theta_{e,f} = \exp(z^0/2) \sum_0^{\infty} \sin \beta_m (Z^0 - z^0) \{ \exp(-p_4 t^0) [\bar{F}(\beta_m) - (F_{11} - G_{21}F_9/p_5)/p_4] + [F_{11} - G_{21}F_9/p_5]/p_4 \} / D_F(\beta_m) \quad (4.70)$$

With the concentration surface and water table boundary conditions and the concentration-dependent sink term, the infiltration solution for any initial condition is

$$\theta_{e,c} = \exp(z^0/2) \sum_0^{\infty} (\sin \beta_m z^0) \{ \exp(-p_4 t^0) [\bar{F}(\beta_m) - n_e \beta_m F_5 / p_4] + n_e \beta_m F_5 / p_4 \} / D_c(\beta_m) \quad (4.71)$$

where

$$\left. \begin{aligned} F_{uc}(\beta_m) &= [\text{Equation (4.36)}] \\ F_{sc}(\beta_m) &= [\text{Equation (4.38)}] \\ F_{hc}(\beta_m) &= [\text{Equation (4.41)}] \end{aligned} \right\} \quad (4.71a)$$

For exfiltration replace F_5 by F_{12} where

$$F_{12}(Z^0) = -(-1)^m \exp(-Z^0/2) \quad (4.72)$$

With the same boundary conditions and any initial condition, using the linear vegetal sink results in

$$\begin{aligned} \theta_{e,c} = \exp(z^0/2) \sum_0^{\infty} (\sin \beta_m z^0) \{ \exp(-p_4 t^0) [F(\beta_m) - \beta_m (n_e F_5 - (G_{11} F_5 - G_{12} F_6) / p_1) / p_4] \\ + \beta_m [n_e F_5 - (G_{11} F_5 - G_{12} F_6) / p_1] / p_4 \} / D_c(\beta_m) \end{aligned} \quad (4.73)$$

Using the exponential sink, rather than the linear, yields

$$\begin{aligned} \theta_{e,c} = \exp(z^0/2) \sum_0^{\infty} (\sin \beta_m z^0) \{ \exp(-p_4 t^0) [\bar{F}(\beta_m) - \beta_m (n_e F_5 - G_{21} F_{10} / p_5) / p_4] \\ + \beta_m [n_e F_5 - G_{21} F_{10} / p_5] / p_4 \} / D_c(\beta_m) \end{aligned} \quad (4.74)$$

With these expressions for moisture content, we may derive expressions for moisture fluxes, volumes and characteristic times.

4.2 Deriving Dynamic Equations

4.2.1 General Method

Darcy's Law is used to derive expressions for moisture fluxes across the unsaturated zone boundaries. The general dimensionless expression for the linear model is

$$q^o = - \frac{\partial \theta_e}{\partial z^o} + \theta_e \quad (3.123a)$$

where

$$\begin{aligned} q^o &= \frac{1}{k} (q - K_{wo}) \\ &= n_e \left(\frac{q - K_{wo}}{K_1 - K_{wo}} \right) \end{aligned} \quad (3.124)$$

and

q^o = dimensionless rate of downward flow

The corresponding cumulative quantity of moisture passing a horizontal cross-section in a given time period is dimensionlessly found by

$$Q^o = \int_{t_1^o}^{t_2^o} q^o(z^o, t^o) dt^o \quad (4.75)$$

where

Q^o = dimensionless cumulative quantity of moisture passing across a horizontal cross-section at elevation z^o during the time $(t_2^o - t_1^o)$

and

$$Q^0 = \frac{n_e}{D} \left(\frac{Q - K_{wo}(t_2 - t_1)}{K_1 - K_{wo}} \right) \quad (4.76)$$

The volume of moisture in the unsaturated zone at a given time is found from

$$V_s^0 = \int_0^0 \theta_e(z^0, t^0) dz^0 \quad (4.77)$$

where

V_s^0 = dimensionless stored quantity of moisture in unsaturated zone.

The depth-averaged moisture content of a given time is expressed by

$$\theta_{e,AV}^0(t^0) = V_s^0 / Z^0 \quad (4.78)$$

where

$\theta_{e,AV}^0$ = depth-averaged moisture content at time, t^0 .

The volume of moisture transpired over a time period is defined by

$$E_v^0 = \int_{t_1^0}^{t_2^0} \int_0^0 G_R(z^0, t^0) dz^0 dt^0 \quad (4.79)$$

where

E_v^0 = dimensionless quantity of transpired moisture

For the concentration-dependent vegetation sink

$$E_v^0 = G_1 \int_{t_1^0}^{t_2^0} \int_0^{z^0} \theta_e(z^0, t^0) dz^0 dt^0 \quad (4.80)$$

while for the depth-dependent sinks

$$E_v^0 = e_{p_v}^0 (t_2^0 - t_1^0) \quad (4.81)$$

where

$$\begin{aligned} e_{p_v}^0 &= \text{constant dimensionless vegetal transpiration rate} \\ &= \int_0^{z^0} G_R(z^0, t^0) dz^0 \end{aligned} \quad (4.82)$$

Ponding or drying time may be found from the flux surface boundary condition solution for θ_e , setting $\theta_e = \theta_{e,1}$ for infiltration and $\theta_e = 0$ for exfiltration and solving for t^0 . Or else we may use the time compression approximation discussed in Section 3.2.1.

4.2.2 Boundary Fluxes and Volumes

We may simplify the general flux and volume expressions, (3.123a) and (4.75), for the flow at the boundaries by making use of the known boundary conditions. For surface infiltration after ponding time and at the water table over all time, the saturation condition is $\theta_e = n_e$. Rearranging Equation (3.96), n_e may be defined as a dimensionless flow parameter

$$\begin{aligned} n_e &= \frac{1}{k} (K_1 - K_{wo}) \\ &\equiv K_1^0 \end{aligned} \quad (4.83)$$

where

K_1^0 = dimensionless saturated hydraulic conductivity.

Substituting K_1^0 for θ_e in the flow equation simplifies Equation (3.96) to

$$q^0 - K_1^0 = - \frac{\partial \theta_e}{\partial z^0} \quad \text{for } \theta_e = n_e \quad (4.84)$$

For surface exfiltration after drying time, the surface boundary condition, $\theta_e = 0$, simplifies Equation (3.96) to

$$q^0 = - \frac{\partial \theta_e}{\partial z^0} \quad \text{for } \theta_e = 0 \quad (4.85)$$

The right hand side (RHS) of Equations (4.84) and (4.85) may be expanded by substituting Equation (3.119) for θ_e . Differentiating with respect to depth results in

$$\frac{\partial \theta_e}{\partial z^0} = \exp(z^0/2 - (1/4 + G_1)t^0) \frac{\partial \theta^0}{\partial z^0} + \theta_e/2 \quad (4.86)$$

Applying the boundary conditions to Equation (4.86) and substituting this equation both in Equations (4.84) and (4.85) yields, for surface infiltration or flow across the water table

$$q^0 - K_1^0/2 = -\exp(z^0/2 - (1/4 + G_1)t^0) \frac{\partial \theta^0}{\partial z^0} \quad \text{for } \theta_e = n_e \quad (4.87)$$

where

$z^0 = 0$ for surface infiltration

$z^0 = Z^0$ for the water table flux

and for surface exfiltration, with $z^0 = 0$,

$$q^0 = -\exp(z^0/2 - (1/4 + G_1)t^0) \frac{\partial \theta^0}{\partial z^0} \quad \text{for } \theta_e = 0 \quad (4.88)$$

The general solution for the RHS of Equations (4.87) and (4.88) is concisely represented by performing the substitution

$$\exp[-(1/4 + G_1)t^0] \theta^0(z^0, t^0) = \sum_{m=1}^{\infty} J_1(\beta_m, t^0) K(\beta_m, z^0) \quad (4.89)$$

where

$$\begin{aligned} J_1 &= \text{time-dependent term of } \theta_e(z^0, t^0) \text{ and } q(z^0, t^0) \\ &= [(\bar{F} - \bar{C}) \exp(-p_4 t^0) + \bar{C}] / D(\beta_m) \end{aligned} \quad (4.90)$$

The transformed initial condition for the assumed initial conditions of Section 3.4.3 is, for the flux surface boundary condition

$$\bar{F}_f = [\text{Equations (4.68a)}] \quad (4.91)$$

and

$$D_f = [\text{Equation (4.15)}] \quad (4.92)$$

and for the concentration surface boundary condition

$$\bar{F}_c = [\text{Equations (4.71a)}] \quad (4.93)$$

and

$$D_c = z^0/2 \quad (4.94)$$

where

\bar{C} = transformed boundary condition and root sink term

For the surface flux boundary condition and concentration-dependent root sink term

$$\bar{C}_{f,c} = F_{11}/p_4 \quad (4.95)$$

For the same surface boundary condition and the linear root sink term

$$C_{f,\ell} = (F_{11} - (G_{11}F_1 - G_{12}F_2))/p_4 \quad (4.96)$$

With the exponential root sink term

$$\bar{C}_{f,e} = (F_{11} - (G_{21}F_9/p_5))/p_4 \quad (4.97)$$

Using the surface concentration boundary condition and the concentration-dependent root sink term, for infiltration

$$\bar{C}_{c,c} = n_e \beta_m F_5/p_4 \quad (4.98)$$

For exfiltration

$$\bar{C}_{c,c} = n_e \beta_m F_{12}/p_4 \quad (4.99)$$

With the linear root sink, for infiltration

$$\bar{C}_{c,\ell} = \beta_m [n_e F_5 - (G_{11}F_5 - G_{12}F_6)/p_1]/p_4 \quad (4.100)$$

and for exfiltration

$$\bar{C}_{c,\ell} = \beta_m [n_e F_{12} - (G_{11}F_5 - G_{12}F_6)/p_1]/p_4 \quad (4.101)$$

The exponential root sink results in

$$\bar{C}_{c,e} = \beta_m (n_e F_5 - G_{21} F_{10}/p_5)/p_4 \quad (4.102)$$

For exfiltration,

$$C_{c,e} = \beta_m (n_e F_{12} - G_{21} F_{10}/p_5)/p_4 \quad (4.103)$$

Substituting Equation (4.89) into the RHS of Equations (4.87) and (4.88) results in simple general expressions for the boundary fluxes valid for any of the initial condition, boundary condition at the other end or root sink term used, provided the concentration boundary condition is applied on the side of interest. The results in our cases are

$$q^0 - K_1^0/2 = -\exp(z^0/2) \sum_{m=1}^{\infty} J_1(t^0) \left[\frac{\partial}{\partial z^0} K(\beta_m, z^0) \right] \quad \text{for } \theta_e = n_e \quad (4.104)$$

and for surface exfiltration

$$q^0 = -\exp(z^0/2) \sum_{m=1}^{\infty} J_1(t^0) \left[\frac{\partial}{\partial z^0} K(\beta_m, z^0) \right] \quad \text{for } \theta_e = 0 \quad (4.105)$$

When both boundary conditions are concentration type

$$\frac{\partial}{\partial z^0} K(\beta_m, z^0) = \beta_m \cos \beta_m z^0 \quad (4.106)$$

and for the surface flux boundary condition

$$\frac{\partial}{\partial z^0} K(\beta_m; z^0) = -\beta_m \cos \beta_m (Z^0 - z^0) \quad (4.107)$$

The corresponding simplified quantity of moisture passing a horizontal cross-section found by substituting Equations (4.104) and (4.105) into Equation (4.25) is

$$Q^0(t_2^0) - Q^0(t_1^0) = K_1^0(t_2^0 - t_1^0)/2 - \exp(z^0/2) \sum_{m=1}^{\infty} J_2(t_2^0; t_1^0) \left[\frac{\partial}{\partial z^0} K(\beta_m, z^0) \right] \quad \text{for } \theta_e = n_e \quad (4.108)$$

and for surface exfiltration

$$Q^0(t_2^0) - Q^0(t_1^0) = -\exp(z^0/2) \sum_{m=1}^{\infty} J_2(t_2^0; t_1^0) \left[\frac{\partial}{\partial z^0} K(\beta_m, z^0) \right] \quad \text{for } \theta_e = 0 \quad (4.109)$$

where, in both cases

$$J_2 = [(\bar{F} - \bar{C})(\exp(-p_4 t_1^0) - \exp(-p_4 t_2^0))/p_4 + \bar{C}(t_2^0 - t_1^0)]/D(\beta_m) \quad (4.110)$$

where the terms \bar{F} , \bar{C} and D are defined above.

4.2.3 Infiltration Equations

The dimensionless infiltration rate derived from the linear model is defined at $z^0 = 0$ and for all time by

$$f_i^0(t^0) = \begin{cases} i^0 & \text{for } 0 < t^0 < t_0^0 \\ f_i^{0*} & \text{for } t_0^0 < t^0 \end{cases} \quad (4.111)$$

where

$$\begin{aligned} i^0 &= \text{dimensionless uniform rainfall rate} \\ &= \frac{1}{k} (i - K_{wo}) \end{aligned} \quad (4.112)$$

and

$$\begin{aligned} t_0^0 &= \text{dimensionless ponding time} \\ &= k^2 t_0 / D_* \end{aligned} \quad (4.113)$$

Since we assume a saturated land surface after ponding time, we may use Equation (4.106) in Equation (4.107) to define

$$f_i^{0*}(t^0) = K_1^0/2 - \sum_{m=1}^{\infty} (\beta_m \cos \beta_m z^0) J_1(t^0) \quad \text{at } z^0 = 0 \quad (4.114)$$

The corresponding infiltrated quantity is

$$I^0(t^0) = \begin{cases} i^0 t^0 & 0 < t^0 \leq t_0^0 \\ i^0 t_0^0 + I_S^0(t^0; t_0^0) & \text{for } t_0^0 < t^0 \end{cases} \quad (4.115)$$

where

$$\begin{aligned} I_S^0(t^0; t_0^0) &= \text{dimensionless infiltrated quantity for the time} \\ &\quad \text{period after ponding} \\ &= (k/D_*) [I_S(t^0; t_0^0) - K_{w0}(t^0 - t_0^0)] \end{aligned} \quad (4.116)$$

where

$$I_S = \text{infiltrated volume from } t_0 \text{ until } t > t_0.$$

From Equation (4.106) in Equation (4.108), the solution from the linear model is

$$I_S^0(t^0; t_0^0) = K_1^0(t^0 - t_0^0)/2 - \sum_{m=1}^{\infty} (\beta_m \cos \beta_m z^0) J_2(t^0, t_0^0) \quad \text{for } z^0 = 0 \quad (4.117)$$

4.2.4 Ponding Time

4.2.4.1 Ponding time: method one

Ponding time is defined to occur when the soil surface first saturates during infiltration. Using the surface flux boundary condition expression for moisture content, we may solve for t_0^0 by setting $\theta_e = n_e$ at $z^0 = 0$. Using the general solution for $\theta_{e,f}$

$$n_e = \sum_{m=1}^{\infty} \sin\beta_m z^0 [(\bar{F} - \bar{C}) \exp(-p_4 t) + \bar{C}] / D_F(\beta_m) \quad (4.118)$$

To solve for time, which appears only in the exponential term, we rearrange the equation to

$$n_e - \theta_{ss} = \sum_{m=1}^{\infty} \sin\beta_m z^0 [(\bar{F} - \bar{C}) \exp(-p_4 t)] / D_F(\beta_m) \quad (4.119)$$

where

$$\begin{aligned} \theta_{ss} &= \text{surface steady state moisture content, if the saturation} \\ &\quad \text{limit were not imposed} \\ &= \lim_{t \rightarrow \infty} \theta_o \\ &= \sum_{m=1}^{\infty} (\sin\beta_m z^0) \bar{C} / D_F(\beta_m) \end{aligned} \quad (4.120)$$

where

$$\theta_o = \text{surface moisture content, under the surface flux boundary} \\ \text{condition}$$

To solve for time explicitly, we assume the series converges approximately at some finite series length, m_{\max} , and that

$$\begin{aligned} \exp(-p_{4_i} t^0) &\approx \exp(-p_{4_m} t^0) && \text{for } m \leq m_{\max} \\ &\approx 0 && \text{for } m > m_{\max} \end{aligned} \quad (4.121)$$

where

$\exp(-p_{4_m} t^0)$ = m^{th} exponential term in series

Using Equation (4.121) in Equation (4.119), we may remove the term $\exp(-p_{4_i} t^0)$ from the series, divide by the series term and take the natural logarithm of both sides of the equation to find an approximate ponding time expression to be

$$t_o^0 \approx - \left[\ln \left(\frac{\theta_e - \theta_{ss}}{\theta_i - \theta_{ss}} \right) \right] / p_{4_1} \quad (4.122)$$

where

θ_i = initial moisture content at the soil surface

$$= \sum_{m=1}^{\infty} (\sin \beta_m Z^0) \bar{F}/D_F(\beta_m) \quad (4.123)$$

4.2.4.2 Ponding time: method two

Ponding time is also calculated using the time-compression approximation discussed in Section 3.2.1. First we preserve the infiltrated quantity of moisture by setting

$$I_s^0(t^{0*}; 0) = i^0 t_o^0 \quad (4.124)$$

where

t^{0*} = dimensionless time when

$$f_i^{0*}(t^{0*}) = i^0 \quad (4.125)$$

To solve for $t_0^0 = t_0^0(t_0^*)$ we modify approximation (4.121) and assume

$$\begin{aligned} \exp(-p_{4_1} t_0^0)/p_{4_1} &\approx \exp(-p_4 t_0^0)/p_4 && \text{for } m \leq m_{\max} \\ &\approx 0 && \text{for } m > m_{\max} \end{aligned} \quad (4.126)$$

We then substitute Equation (4.117) into Equation (4.124) and find

$$t_0^0 = \frac{1}{i_0^0} \{f_{i,ss}^{0*} t_0^{0*} + (f_{i,i}^{0*} - f_{i,ss}^{0*})[1 - \exp(-p_4 t_0^{0*})]/p_4\} \quad (4.127)$$

where

$$\begin{aligned} f_{i,ss}^{0*} &= \lim_{t_0^0 \rightarrow \infty} f_i^{0*}(t_0^0) \\ &= K_1^0/2 - \sum_{m=1}^{\infty} (\beta_m \cos \beta_m Z^0) \bar{C}/D_c(\beta_m) \end{aligned} \quad (4.128)$$

and

$$\begin{aligned} f_{i,i}^{0*} &= \lim_{t_0^0 \rightarrow 0} f_i^{0*}(t_0^0) \\ &= K_1^0/2 - \sum_{m=1}^{\infty} (\beta_m \cos \beta_m Z^0) \bar{F}/D_c(\beta_m) \end{aligned} \quad (4.129)$$

Next we invert Equation (4.114) to solve for $t_0^{0*} = t_0^{0*}(f_i^{0*})$, using approximation (4.126) and relation (4.125). The result is

$$t_0^{0*} \approx -\ln \left[\frac{i_0^0 - f_{i,ss}^{0*}}{f_{i,i}^{0*} - f_{i,ss}^{0*}} \right] / p_4 \quad (4.130)$$

The ponding time expression, $t_0^0(i_0^0, Z^0)$ found by substituting Equation (4.130) into Equation (4.127) is

$$t_o^o = \frac{1}{i_o^o} \left\{ f_{i,i}^{o*} - i_o - f_{i,ss}^{o*} \ln \left[\frac{i_o^o - f_{i,ss}^{o*}}{f_{i,i}^{o*} - f_{i,ss}^{o*}} \right] \right\} / p_4 \quad i_o^o < f_{i,i}^{o*} \quad (4.131)$$

The primary advantage of the second method is that it guarantees continuity of flux rate and infiltrated volume over all time. Its major disadvantage is its added complexity.

4.2.5 Exfiltration Equations

The dimensionless bare soil exfiltration rate at $z^o = 0$ is defined over all time by

$$f_e^o(t^o) = \begin{cases} e_p^o & \text{for } 0 < t^o < t_d^o \\ f_e^{o*} & t_d^o < t^o \end{cases} \quad (4.132)$$

where

$$\begin{aligned} e_p^o &= \text{dimensionless uniform evaporation rate} \\ &= \frac{1}{k} (e_p - K_{wo}) \end{aligned} \quad (4.133)$$

and

$$\begin{aligned} t_d^o &= \text{dimensionless drying time} \\ &= k^2 t_d / D_* \end{aligned} \quad (4.134)$$

The exfiltration capacity occurring for a dry soil at the land surface (defined to be positive outward), is obtained by substituting Equation (4.106) into Equation (4.105), as

$$f_e^{o*}(t^o) = -q^o(t^o) = \sum_{m=1}^{\infty} (\beta_m \cos \beta_m z^o) J_1(t^o) \quad \text{at } z^o = 0 \quad (4.135)$$

The bare soil exfiltrated volume corresponding to the above fluxes is

$$E_S^0(t^0) = \begin{cases} e_p^0 t^0 & 0 < t^0 < t_d^0 \\ e_p^0 t_d^0 + E_{SS}(t^0; t_d^0) & \text{for } t_d^0 < t^0 \end{cases} \quad (4.136)$$

where

$$\begin{aligned} E_{SS}^0(t^0; t_d^0) &= \text{dimensionless exfiltrated quantity after drying} \\ &\quad \text{time} \\ &= (k/D_*) [E_{SS}(t^0; t_d^0) - K_{wo}(t^0 - t_d^0)] \end{aligned} \quad (4.137)$$

where

$$E_{SS}(t^0; t_d^0) = \text{bare soil exfiltrated volume from } t_d^0 \text{ until } t^0 > t_d^0$$

Using Equation (4.106) in Equation (4.109)

$$E_{SS}^0(t^0; t_d^0) = \sum_{m=1}^{\infty} (\beta_m \cos \beta_m z^0) J_2(t^0; t_d^0) \quad \text{for } z^0 = 0 \quad (4.138)$$

defined positive for flow out of the column.

4.2.6 Drying Time

4.2.6.1 Drying time: method one

Drying time is defined to occur when the soil surface first dries. An expression for the drying time is found in a manner equivalent to that for ponding time from the flux surface boundary condition moisture content expression when

$$\theta_e = 0 \quad \text{at} \quad z^0 = 0 \quad (4.139)$$

Substituting the general moisture content expression for $\theta_{e,f}$ from Section 4.1.5 (Equation (4.162)) into Equation (4.139) and solving for t_d^0 yields

$$t_d^0 \approx - \left[\ln \left(\frac{-\theta_{ss}}{\theta_i - \theta_{ss}} \right) \right] / p_4 \quad (4.140)$$

where the parameters are defined as in Section 4.2.4.1 and approximation (4.121) is invoked.

4.2.6.2 Drying time: method two

We apply the time-compression approximation to the drying time problem in the same manner as for the infiltration problem. First, matching the actual amount of moisture exfiltrated to that predicted by the model results in

$$E_{ss}(t^{0*}; 0) = e_p^0 t_d^0 \quad (4.141)$$

where we assume

$$f_e^{0*}(t^{0*}) = e_p^0 \quad (4.142)$$

Adopting approximation (4.126) and solving for $t_d^0 = t_d^0(t^{0*})$ by substituting Equation (4.138) into Equation (4.141), we find

$$t_d^0 = \frac{1}{e_p^0} \{ f_{e,ss}^{0*} t^{0*} + (f_{e,i}^{0*} - f_{e,ss}^{0*}) [1 - \exp(-p_4 t^{0*})] / p_4 \} \quad (4.143)$$

where, for fluxes defined positive out of the soil column

$$f_{e,ss}^{o*} = \sum_{m=1}^{\infty} (\beta_m \cos \beta_m z^o) \bar{C}/D_c(\beta_m) \quad z^o = 0 \quad (4.144)$$

and

$$f_{e,i}^{o*} = \sum_{m=1}^{\infty} (\beta_m \cos \beta_m z^o) \bar{F}/D_c(\beta_m) \quad z^o = 0 \quad (4.145)$$

Solving for $t^{o*}(e_p^o)$ by substituting Equation (4.135) into Equation (4.142) and using approximation (4.121), we see that

$$t^{o*} \approx - \ln \left[\frac{e_p^o - f_{e,ss}^{o*}}{f_{i,ss}^* - f_{e,ss}^*} \right] / p_4 \quad (4.146)$$

After substituting Equation (4.146) into Equation (4.143) and simplifying the result, the drying time expression is

$$t_d^o = \frac{1}{e_p^o} \left\{ f_{e,i}^{o*} - e_p^o - f_{e,ss}^* \ln \left[\frac{e_p^o - f_{e,ss}^{o*}}{f_{e,i}^{o*} - f_{e,ss}^{o*}} \right] \right\} / p_4 \quad (4.147)$$

4.2.7 Percolation

Percolation of soil water through the water table is assumed to occur at the inception of infiltration. Unlike percolation into a deep phreatic aquifer, the shallow water table percolation rate is a function of surface boundary condition and time. The dimensionless percolation rate is

$$v^o(t^o) = \begin{cases} v_c^o(t^o) & \text{for } 0 < t^o < t_o^o \\ v_s^o(t^o) & \text{for } t_o^o < t^o \end{cases} \quad (4.148)$$

where

v^o = dimensionless percolation rate

v_c^0 = dimensionless percolation rate under climate-controlled infiltration

and

v_s^0 = dimensionless percolation rate under soil-controlled infiltration

There is no mechanism to insure continuity of $v^0(t^0)$ at $t^0 = t_0^0$ other than matching $v_c^0(t_0^0) = v_s^0(t_0^0)$. For very large t_0^0 , we approximate v^0 by v_c^0 , and for very early t_0^0 , we approximate v^0 by v_s^0 .

For the flux surface boundary condition, at $z^0 = Z^0$, we have the percolation rate from Equation (4.107) in Equation (4.104) which is

$$v_c^0(t^0) = K_1^0/2 + \exp(Z^0/2) \sum_{m=1}^{\infty} [\beta_m \cos \beta_m (Z^0 - z^0)] J_1(t^0) \text{ at } z^0 = Z^0 \quad (4.149)$$

With the concentration surface boundary condition assumed valid from $t^0 = 0$, the percolation rate, from Equation (4.106) in Equation (4.104), is

$$v_s^0(t^0) = K_1^0/2 - \exp(Z^0/2) \sum_{m=1}^{\infty} (\beta_m \cos \beta_m z^0) J_1(t^0) \quad (4.150)$$

The steady state percolation rate is defined by

$$v_{c,ss}^0 = K_1^0/2 + \exp(Z^0/2) \sum_{m=1}^{\infty} [\beta_m \cos \beta_m (Z^0 - z^0)] \bar{C}/D_F(\beta_m) \text{ for } z^0 = Z^0 \quad (4.151)$$

for the flux surface boundary condition and

$$v_{s,ss}^0 = K_1^0/2 - \exp(Z^0/2) \sum_{m=1}^{\infty} (\beta_m \cos \beta_m z^0) \bar{C}/D_C(\beta_m) \text{ for } z^0 = Z^0 \quad (4.152)$$

for the concentration boundary condition.

The corresponding dimensionless quantity of percolating water at $z^0 = Z^0$ is

$$V_D^0(t^0) = \begin{cases} V_{Dc}^0(t^0) & \text{for } 0 < t^0 \leq t_0^0 \\ V_{Dc}^0(t_0^0) + V_{Ds}(t^0; t_0^0) & \text{for } t_0^0 < t^0 \end{cases} \quad (4.153)$$

where

V_{Dc}^0 = dimensionless quantity of percolating water at the water table under climate-controlled infiltration

$$= \left(\frac{k}{D_*}\right) [V_{Dc}(t^0) - K_{wo}(t^0)] \quad (4.154)$$

From Equation (4.107) in Equation (4.108),

$$V_{Dc}^0 = K_1^0(t^0)/2 - \exp(Z^0/2) \sum_{m=1}^{\infty} [\beta_m \cos \beta_m (Z^0 - z^0)] J_2(t^0; 0) \quad (4.155)$$

and

V_{Ds}^0 = dimensionless quantity of percolating water at the water table under soil-controlled infiltration

$$= (k/D_*) (V_{Ds}(t^0) - K_{wo}(t^0)) \quad (4.156)$$

From Equation (4.106) in Equation (4.108)

$$V_{Ds} = K_1^0(t^0 - t_0^0)/2 - \exp(Z^0/2) \sum_{m=1}^{\infty} (\beta_m \cos \beta_m z^0) J_2(t^0; 0) \quad z^0 = Z^0 \quad (4.157)$$

4.2.8 Capillary rise

Capillary rise is assumed to start at the inception of an

interstorm period. The rates calculated from the linear model vary depending on the surface boundary condition. The dimensionless capillary rise rate at $z^0 = Z^0$ is

$$w^0(t^0) = \begin{cases} w_c^0(t^0) & \text{for } 0 < t^0 < t_d^0 \\ w_s^0(t^0) & \text{for } t_d^0 < t^0 \end{cases} \quad (4.158)$$

where

w^0 = dimensionless capillary rise rate

w_c^0 = dimensionless capillary rise rate for climate-controlled exfiltration

and

w_s^0 = dimensionless capillary rise rate for soil-controlled exfiltration

For the flux surface boundary condition, the capillary rise rate at $z^0 = Z^0$ is represented by substituting Equation (4.107) into Equation (4.105). If the evaporation rate is low enough, capillary rise may not occur in the interstorm period.

For the concentration-surface boundary condition, the capillary rise rate is represented by using Equation (4.106) in Equation (4.105).

The steady state capillary rise rates are expressed by Equations (4.151) and (4.152) with the differences being in the sign of the flux in Equation (4.151) and in a slightly different \bar{C} in Equation (4.152).

The dimensionless quantities of capillary rise water at $z^0 = Z^0$ are

$$V_w^0(t^0) = \begin{cases} V_{wc}(t^0) & \text{for } 0 < t^0 < t_d^0 \\ V_{wc}(t_d^0) + V_{ws}(t^0; t_d^0) & \text{for } t_d^0 < t^0 \end{cases} \quad (4.159)$$

where

V_{wc}^0 = dimensionless quantity of capillary rise under climate-controlled exfiltration

$$= \left(\frac{k}{D_*}\right) (V_{w,c}(t^0) - K_{wo} t^0) \quad (4.160)$$

$$= [\text{Equation (4.109)}] \quad (4.161)$$

and

V_{ws}^0 = dimensionless quantity of capillary rise under soil controlled exfiltration

$$= \left(\frac{k}{D_*}\right) (V_{w,s}(t^0) - K_{wo}(t^0)) \quad (4.162)$$

$$= [\text{Equation (4.109)}]$$

4.2.9 Depth-Averaged Moisture Content

The depth-averaged moisture content is used to calculate changes in soil moisture storage and to calculate initial condition parameters. Expressed in terms of quantity of moisture stored in the soil moisture zone it is

$$V_s^0(t^0) = \begin{cases} V_{s,c}^0(t^0) & \text{for } 0 < t^0 \leq t_0^0 \\ V_{s,s}^0(t^0) & t_0^0 < t^0 \end{cases} \quad (4.163)$$

where

$V_{s,c}^0$ = dimensionless quantity of moisture stored in the
unsaturated zone for the climate-controlled surface flux

$V_{s,s}^0$ = dimensionless volume of moisture stored in the
unsaturated zone for the soil-controlled surface flux

and

$$V_s^0 = kV_s/D_* \quad (4.164)$$

Expressing the moisture content solutions, presented in Section 4.1.5, generally by

$$\theta_e = \exp(z^0/2) \sum_{m=1}^{\infty} K(\beta_m, z^0) J_1(t^0) \quad (4.165)$$

and substituting this into Equation (4.77), we calculate the average moisture contents in the soil water zone.

Under the flux surface boundary condition

$$V_{s,c}^0(t^0) = \sum_{m=1}^{\infty} \exp(Z^0/2) \beta_m [(\bar{F} - \bar{C}) \exp(-p_4 t^0) + \bar{C}] / p_1 \quad (4.166)$$

and under the concentration surface boundary condition

$$V_{s,s}^0(t^0) = \sum_{m=1}^{\infty} \beta_m [1 - (-1)^m \exp(Z^0/2)] [(\bar{F} - \bar{C}) \exp(-p_4 t^0) + \bar{C}] / p_4 \quad (4.167)$$

As with percolation, no mechanism assures $V_{s,c}^0(t^0) = V_{s,s}^0(t^0)$ other than by arbitrarily setting them equal.

The above expressions are valid for both infiltration and exfiltration processes.

Depth-averaged moisture content is

$$\theta_{e,AV} = V_s^0(t^0) / Z^0 \quad (4.78)$$

4.2.10 Vegetal Moisture Uptake

The only time-dependent moisture uptake rate considered here is for the concentration-dependent root sink. The dimensionless quantity of moisture uptake by plants over the entire time domain is represented by

$$E_V^0(t^0) = \begin{cases} E_{V,c}^0(t^0) & \text{for } 0 < t^0 \leq t_d^0 \\ E_{V,c}^0(t_d^0) + E_{V,s}(t^0; t_d^0) & \text{for } t_d^0 < t^0 \end{cases} \quad (4.168)$$

where

$E_{V,c}^0$ = dimensionless moisture uptake for flux surface boundary condition

$E_{V,s}^0$ = dimensionless moisture uptake for concentration surface boundary condition

and

$$E_V^0 = (k/D_*)E_V(t^0) \quad (4.169)$$

Integrating $V_s^0(t^0)$ over dimensionless time and multiplying by G_1 yields the uptake quantities predicted by the linear model. These are, for the flux surface boundary condition

$$E_{V,c}^0(t^0) = G_1 \sum_{m=1}^{\infty} \exp(Z^0/2) \beta_m J_2(t^0)/p_1 \quad (4.170)$$

and, for the concentration surface boundary condition

$$E_{V,s}^0(t^0; t_d^0) = G_1 \sum_{m=1}^{\infty} \beta_m [1 - (-1)^m \exp(Z^0/2)] J_2(t^0; t_d^0)/p_1 \quad (4.171)$$

Chapter 5

RESULTS5.1 Introduction

A linearized model of soil moisture movement in the unsaturated zone has been developed which incorporates the effects of the water table. From the basic solution for moisture content, expressions have been derived for the dynamics of the moisture fluxes. The result is a comprehensive set of equations which accounts for all of the processes of Section 3.1.

Presentation of the solutions and results in dimensionless format is a direct benefit of analytical solutions. It also aids understanding of the process and the model by showing similar relations among parameters (i.e., the solution is independent of soil type).

5.2 Summary of Dimensionless Groupings

The dimensionless parameters of these solutions are summarized here for convenient reference in presentation of the results:

$$z^o = \frac{kz}{D_*} \quad \text{depth} \quad (3.107)$$

$$Z^o = \frac{kZ}{D_*} \quad \text{depth to water table}$$

$$t^o = \frac{k^2 t}{D_*} \quad \text{time} \quad (3.108)$$

$$t_o^o = \frac{k^2 t_o}{D_*} \quad \text{ponding time (drying time = } t_d^o) \quad (4.113)$$

$$G_R = \left(\frac{D_*}{k^2}\right) g_r \quad \text{vegetal extraction rate} \quad (3.110)$$

$$G_1 = \frac{2}{n_e} \left(\frac{D_* e_v}{k^2 Z_r}\right) \quad \text{maximum concentration-dependent} \\ \text{vegetal extraction rate} \quad (3.112)$$

$$G_{11} = 1.8 \left(\frac{D_* e_v}{k^2 Z_r}\right) \quad \text{uniform vegetal extraction} \\ \text{parameter} \quad (3.114)$$

$$G_{12} = 1.6 \left(\frac{D_* e_v}{k^2 Z_r}\right) \quad \text{linear vegetal extraction} \\ \text{parameter} \quad (3.115)$$

$$G_{21} = \frac{D_* e_v}{k^2 \delta} \quad \text{Raaf's uniform vegetal} \\ \text{extraction parameter} \quad (3.117)$$

$$G_{22} = \frac{D_*}{k \delta} \quad \text{vegetal extraction decay} \\ \text{rate} \quad (3.118)$$

$$N^0 = \frac{1}{k} (N - K_{wo}) \quad \text{vertical flux} \quad (3.124)$$

where

$$\begin{aligned} N &= i && \text{infiltration} \\ &= e_p && \text{exfiltration} \\ &= v_c && \text{percolation} \\ &= w && \text{capillary rise} \\ Q^0 &= \frac{kQ}{D_*} && \text{volumetric flux rate} \quad (4.76) \end{aligned}$$

where

$$\begin{aligned} Q &= I_s && \text{infiltration} \\ &= E_s && \text{exfiltration} \\ &= V_D && \text{percolation} \\ &= V_w && \text{capillary rise} \\ V_s^0 &= \frac{k V_s}{D_*} && \text{volume of moisture in soil column} \end{aligned}$$

$$\theta_{e,AV}^0 = V_s^0/Z^0$$

average soil moisture content in soil column

$$E_v^0 = \frac{k E_v}{D_*}$$

volume of transpired moisture

$$K_1^0 = n_e$$

asymptotic flow rate (4.83)

5.3 Finite Domain Determination

5.3.1 Introduction

Before we explore the response of the derived quantities to the water table depth, we will examine the dimensionless region where the water table influences the soil moisture zone processes. Over what dimensionless depths should the region be viewed as finite and what range of physical depths do these correspond to? We may find an expression for these depths indirectly by considering the relation between the penetration depth (or wetting front location) and the water table depth, for infiltration into a semi-infinite medium.

5.3.2 Dimensionless Wetting Front Depth

We assume a medium may be treated as semi-infinite if $z_{\max} \ll Z$, where z_{\max} is the maximum penetration depth of the wetting front over the event duration of interest, and Z is the depth to the water table. Where this does not hold we may say the region is finite.

Derived from the same linearization procedure adopted here are two expressions for z_{\max} for infiltration into a semi-infinite medium, described in Section 3.2.1. One developed by Braester (1973) for the constant surface flux boundary condition is

$$z_{\max} = N t / (\bar{\theta}_1 - \theta_0) \quad (3.28)$$

where

N = rainfall rate

$\bar{\theta}_1$ = time-averaged surface moisture content

and

θ_0 = initial uniform moisture content

For infiltration of a step change in surface moisture content (constant surface concentration), Eagleson (1970, 1978d) derived the expression

$$z_{\max} = 4(D_*t)^{1/2} + \frac{K(\theta_0)t}{n_e} \quad (3.27)$$

where

$K(\theta_0)$ = initial hydraulic conductivity in soil moisture zone

The main difference in the two model forms is that the Braester model is an implicit function of soil parameters through $\bar{\theta}_1$ and the Eagleson model is an explicit function of them.

The surface flux expression (3.28) says that moisture will infiltrate deeper into the soil column with heavier rainfall and with time. The denominator is an index of the volume of available pore space in the column. The less initial moisture there is per unit depth the less deep a given moisture volume will infiltrate.

The surface concentration expression (3.27) says that the penetration depth is a function of a 'diffusion' component, $4(D_*t)^{1/2}$, and a gravitational seepage component, $K(\theta_0)t/n_e$. This model has the penetration depth increasing with diffusivity, time and hydraulic

conductivity. Available pore space is accounted for by effective porosity, n_e . Expressing the Equations (3.27) and (3.28) in dimensionless terms allows us to free the expressions from a particular climate or soil type.

The Braester model may be expressed in dimensionless terms. Multiplying both sides of Equation (3.28) by k/D_* and the right side also by k/k and substituting Equations (3.107), (3.124) and (3.108) into the result, we find

$$z^0 \gg N^0 t^0 / (\theta_1 - \theta_0) \quad (5.1)$$

For the Eagleson model, we also multiply both sides by k/D_* , use the assumed relation $K(\theta) = k\theta_e$ and substitute Equations (3.107) and (3.108) into the result to produce

$$z^0 \gg 4t^0{}^{1/2} + t^0(\theta_e/n_e) \quad (5.2)$$

5.3.3 Capillary Fringe Depth

We may be more exact in defining how much deeper the water table should be for the soil water zone to be considered semi-infinite. The basic criterion is that the infiltrated water not penetrate into the capillary fringe. Using the linearizing assumptions of Section 3.5.1, the capillary fringe is described by

$$\theta_e(z^0) = n_e \exp(z^0 - Z^0) \quad (3.133)$$

At the interface between the capillary fringe and the intermediate zone in the soil column (e.g., see Figure 3.8), we assume the influence of the capillary fringe ends when the moisture content

is within one percent of field capacity (e.g., the gravity-drained moisture content). With field capacity given by $\theta_e = 0$ and describing the capillary fringe by Equation (3.133), the influence of the capillary fringe may be neglected for dimensionless depths in the soil column above

$$z_c^0 = Z^0 - 5 \quad (5.3)$$

where

$$\begin{aligned} z_c^0 &= \text{dimensionless depth to the capillary fringe/intermediate} \\ &\quad \text{zone interface (point B on Figure 3.10)} \\ &= kz_c/D_* \end{aligned}$$

with

$$\begin{aligned} z_c &= \text{depth to the interface (or contact depth)} \\ &= Z - 5D_*/k \end{aligned}$$

and where θ_e equals 0.7% of the effective porosity, n_e .

This result states that the capillary fringe influence is negligible for depths in the soil column which are $5D_*/k$ units above the water table, or dimensionless depths which are more than five dimensionless units above the dimensionless water table. For example, for an average diffusivity, $D_* = 4000 \text{ cm}^2/\text{day}$, saturated hydraulic conductivity, $K(1) = 21 \text{ cm/day}$ and effective porosity, $n_e = 0.35$, we calculate $k = 60 \text{ cm/day}$ and $D_*/k = 66.7 \text{ cm}$. If the water table depth, $Z = 5 \text{ meters}$, the contact depth is calculated from Equation (5.3) to be $z_c = 1.67 \text{ meters}$.

5.3.4 Effectively Semi-Infinite Soil Column

If the maximum penetration depth of the infiltrating soil moisture wetting front is less than z_c , we may treat the soil column as semi-infinite. For this case, surface-induced processes (e.g., infiltration) may be analyzed separately from processes occurring at the water table (e.g., drainage) and their effects may be linearly superimposed (cf. Eagleson, 1978c).

Combining the dimensionless contact depth Equation (5.3) with Equations (5.1) and (5.2), we may more concisely define when we may not assume the soil column is effectively semi-infinite. When the climate controls the infiltration rate (e.g., flux surface boundary condition), we use Equation (5.3) in (5.1) to specify that the column may be assumed semi-infinite when

$$z^0 - 5 > N^0 t^0 / (\bar{\theta}_1 - \theta_o) \quad (5.4)$$

When soil controls the infiltration rate (e.g., surface concentration boundary condition), we assume a semi-infinite soil column when

$$z^0 - 5 > 4t^{0/2} + t^0(\theta_{e,o}/n_e) \quad (5.5)$$

where

$\theta_{e,o}$ = initial effective moisture content in soil-water zone

(see Figure 3.8)

For dimensionless time, $t^0 < 1$, the diffusion-term of Equation (5.5), $4t^0{}^{1/2}$, dominates. For smaller initial moisture contents, $\theta_{e,0}$, the gravity term of Equation (5.5), $t^0(\theta_{e,0}(n_e))$, is smaller and the diffusion term dominates for even longer dimensionless time.

5.3.5 Contact Parameters

Defining the diffusion-dominated process by $t^0 < 1$, a single parameter may be used to distinguish when the soil column cannot be assumed to be semi-infinite. Specifying the Boltzmann similarity variable ϕ (see Equation (3.21)) in dimensionless notation by

$$\phi^0 = z^0/t^0{}^{1/2}$$

we may evaluate it at the dimensionless water table depth $z^0 = Z^0$ or at z_c^0 , the dimensionless contact depth, defined by Equation (5.3). For the latter case, the dimensionless similarity contact parameter, ϕ_c^0 , is expressed by

$$\begin{aligned}\phi_c^0 &= z_c^0/t^0{}^{1/2} \\ &= z_c^0/(D_*t)^{1/2}\end{aligned}\tag{5.6}$$

or by using Equation (5.3) in (5.6) it is written

$$\phi_c^0 = (Z^0 - \xi)/t^0{}^{1/2}\tag{5.7}$$

where

Z^0 = dimensionless depth to water table

ϕ_c^0 = dimensionless similarity contact parameter

For a diffusion-dominated soil moisture process ($t^0 < 1$), the soil column may be assumed to be semi-infinite when

$$\phi_c^0 (= \phi_c / D_*^{1/2}) < 4 \quad (5.8)$$

or

$$\phi_c (= z_c / t^{1/2}) < 4D_*^{1/2}$$

where

$$\phi_c = \text{similarity contact parameter [units: (length)(time)}^{-1/2}]$$

For dimensionless times $t^0 < 1$, the dimensionless contact parameter has the value $\phi_c^0 = 4$ at the moment when the wetting front depth of the infiltration process, z_F , reaches the contact depth, z_c . At this moment, the soil column may no longer be assumed to be semi-infinite. The time when $z_F = z_c$ occurs (e.g., Figure 3.10, point B) is in dimensionless notation

$$\begin{aligned} t_c^0 &= z_c^0{}^2 / 16 & t_c^0 < 1 & \quad 5 < Z^0 < 9 \\ &= (Z^0 - 5)^2 / 16 & & \quad (5.9) \end{aligned}$$

where

$$t_c^0 = \text{dimensionless contact time}$$

Dimensionally, contact time is expressed by

$$t_c = z_c^0 / 16D_* = z_{\max}^2 / 16D_* \quad (5.10)$$

where

t_c = contact time, when z_F (or z_{\max}) = z_c

Equation (5.9) requires the assumption that the infiltration process is diffusion-dominated. This restricts the dimensionless time to approximately $t_c^0 < 1$. Substituting $t_c^0 = 1$ into Equation (5.9) and solving for Z^0 results in $Z^0 = 9$. This is the upper limit to the dimensionless water table depth for the diffusion-dominated infiltration process. The limit is larger for average soil-moisture contents less than the effective porosity. In dimensional terms, this limit is $Z = 9D_*/k$. For $Z^0 > 9$, we may find t_c^0 implicitly through Equation (5.5).

It must be noted again that the above analysis is for the surface concentration boundary condition.

For the surface flux boundary condition, we define the dimensionless contact time using Equation (5.4) by

$$t_c^0 = (Z^0 - 5)(\bar{\theta}_1 - \theta_0)/N^0 \quad (5.11)$$

If dimensionless ponding time, t_o^0 , is less than t_c^0 , we may use the climate-controlled infiltration models developed for the semi-infinite domain.

5.3.6 Parameter Modifications for Exfiltration

Though Equations (3.27) and (3.28), describing the penetration depth, z_{\max} , must be modified to account for vegetation, they are applicable for bare soil exfiltration. In this case, z_{\max} represents the drying front penetration depth. For the surface flux induced penetration depth of Equation (3.28), the flux term N represents the evaporation rate. Since N is defined to be positive into the soil

column, it is negative for exfiltration. The term $(\theta_1 - \theta_0)$ is also negative since the moisture content at the land surface is reduced by evaporation. The result is a positive penetration depth.

The diffusive term for the drying front is the same as for the wetting front in Equation (3.27). Gravity also acts in the same direction as it acts on the moisture, θ_0 , in the column at the start of the event, causing motion of moisture toward the capillary fringe. The only difference between infiltration and exfiltration here is the evaluation of D_* and the characteristic time, t .

5.3.7 Sample Problem

An example of the domain determination method for an infiltration problem will give a sense of the dimensions involved. For soil we use the Yolo light clay data of Moore (1939). We use the Clinton, MA, climate data of Eagleson (1978f). From Philip (1966a), $\theta_0 = 0.238$, $n = \theta_1 = .495$, $S = 1.25 \times 10^{-2} \text{ cm sec}^{-1/2}$ (sorptivity, a soil parameter). We find D_* from the expression derived for a semi-infinite domain by Philip (1966a) relating D_* to S for infiltration which is

$$D_* = \pi S^2 / 4 (\theta_1 - \theta_0)^2 \quad (3.29)$$

Also from Philip (1966a), we have

$$k = \frac{K(1) - K_0}{\theta_1 - \theta_0} \quad (3.26b)$$

where we assume $K_0 \approx 0$. For Clinton, MA, $K(1) = 2 \times 10^{-5} \text{ cm/sec}$, and we use the characteristic time $m_{t_r} = 0.32 \text{ day}$, where m_{t_r} is the mean storm duration. Assuming the water table depth at Clinton, MA, is five meters,

the parameters are $D_* = 161 \text{ cm}^2/\text{day}$ and $k = 6.72 \text{ cm/day}$ and the dimensionless parameters are

$$z^0 = \frac{kZ}{D_*} = 20.9$$

$$t^0 = \frac{k^2 m_t r}{D_*} = 0.090$$

From Equation (5.5) for the concentration surface boundary condition

$$15.9 > 1.2 + 0.04 = 1.24$$

and the domain may be treated as semi-infinite. Since the diffusive component clearly dominates ($t^0 = 0.09$), we may use Equations (5.7) to calculate $\phi_c^0 = 70$. Since $70 \gg 4$, the semi-infinite domain assumption is supported by Equation (5.8). Using Equation (3.28) in (5.10), we see that the domain is considered finite only for times, $t \geq 56 \text{ days } (=t_c)$.

Using the mean storm intensity, $m_i = 2.69 \text{ cm/day}$ for Boston, MA (near Clinton, MA) from Eagleson (1978b), we calculate $N^0 = m_i/k$ from Equation (3.124) to be

$$N^0 = 0.4$$

For $n_e = \theta_1 - \theta_0 (-\theta_{wo}) = .257$, $m_i/K(1) = 1.56$, which means ponding may occur for the mean intensity storm, because m_i exceeds the minimum infiltration capacity of the soil, $K(1)$.

The dimensionless contact time with the surface flux boundary condition, assuming $\bar{\theta}_1 = 0.4$ is, from Equation (5.11),

$$t_c^0 = 6.44 \gg 0.09$$

This means that the domain for climate-controlled infiltration may also be assumed to be semi-infinite.

The above results do not exclude the use of a finite domain solution, but instead they allow the use of the simpler, extensively-tested analytical solutions for the semi-infinite domain.

5.3.8 Dominant Forces

The quantities t^0 and Z^0 also contain information about when 'diffusion' and advection dominate in the finite domain. For $t^0 > 1$ and $Z^0 > 1$, $k^2 t > D_*$ and $kZ > D_*$. With $t^0 \gg 1$ advective moisture movement (represented by k) clearly dominates. The constant (gravity-induced) advective flow rate only occurs with a fixed soil moisture profile for the finite domain problem. Therefore, steady state conditions for all the processes modelled in Chapter 4 will occur for dimensionless times greater than $t^0 \approx 1$, except where transpiration is accounted for. Also, we see that 'diffusive' transport dominates for $Z^0 < 1$ ($D_* > kZ$) in the finite soil column.

We see how far into the finite column the surface moisture conditions have penetrated from the relations t^0/Z^{0^2} ($=\phi^{0^{-2}}$) and t^0/Z^0 . These translate into the dimensional terms $D_* t/Z$ and kt/Z . For $\phi^{0^{-2}}$ and t^0/Z^0 greater than unity, moisture flow induced by the surface conditions occurs throughout the soil column.

5.4 Convergence

5.4.1 Series Convergence

Since the solution to the linear problem in the finite domain is in infinite series form, the solution is only exact for an infinite number of terms. For practical purposes, we use enough terms so that the calculated 'approximate' solution has converged arbitrarily close to the true solution. The necessary number of terms depends on the degree of accuracy desired and varies with the type of solution.

The two general convergence criteria employed are reproduction of the exact solution and preservation of the solution form. In general, the exact solution is reproduced for one hundred series terms for all solutions except the soil moisture distribution, where two hundred terms are sufficient in most cases. Where the solution parameters are fitted to data, it is sufficient to preserve the shape of the solution.

Figure 5.1, a plot of depth-averaged moisture content versus dimensionless time for a drainage problem, shows that the solution form is sufficiently preserved using from one to five series terms. This is generally the case for the average moisture content and the exfiltration capacity rate solutions. Fifty series terms are needed for the infiltration capacity rate solution for reasons discussed momentarily. Volumetric quantities require one hundred series terms because the solution is reached through integration which also sums the errors.

The series solution converges faster for shallower dimensionless water table depths. Convergence is the result of higher order harmonics in the series solution which approach zero as the eigenvalue $[\beta_m, (\text{Eqn. (4.13)})]$ increase in value with each series term. As the eigenvalues are

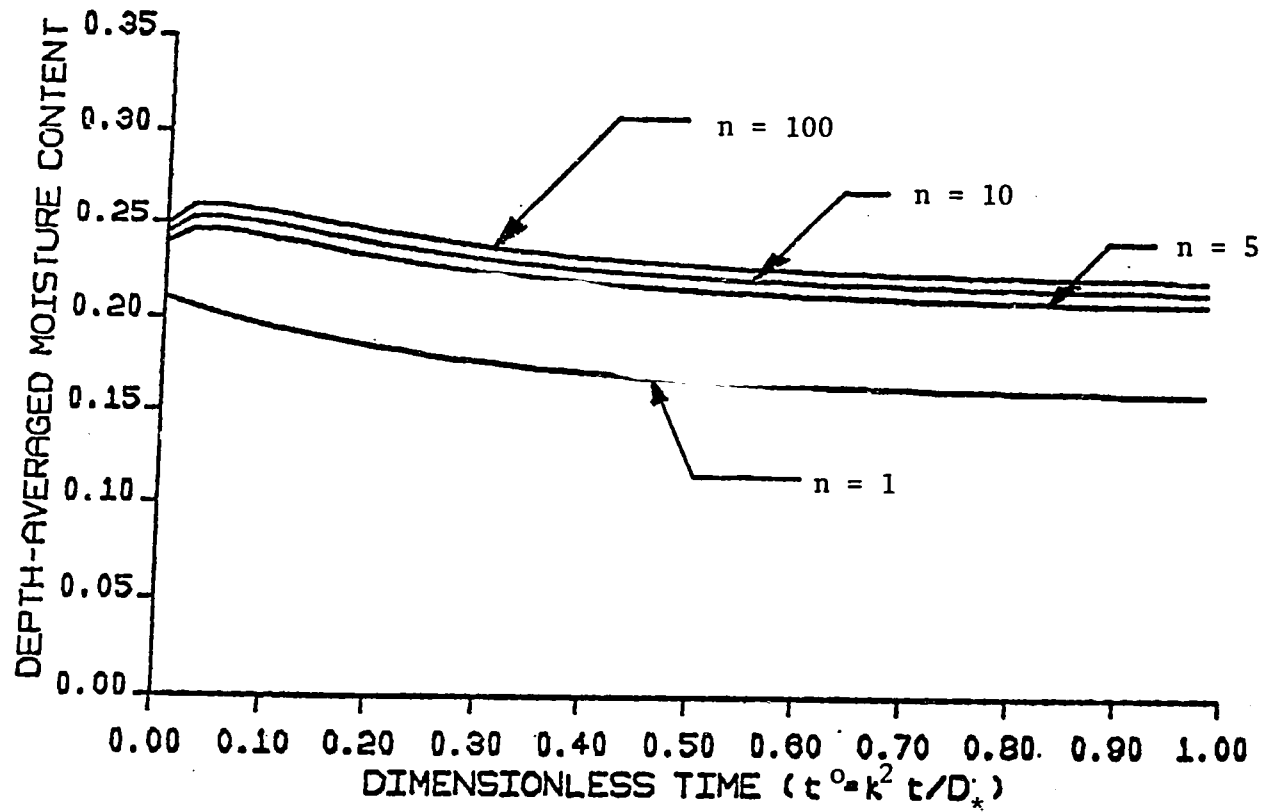


Figure 5.1

SENSITIVITY OF EQUATION (4.166) TO NUMBER OF SERIES TERMS
 FOR A DRAINING SHALLOW SOIL COLUMN
 ($Z_0^0 = 1, e_0^p = 0, n_e = .35, \text{uniform } \theta_0 = .25$)

inversely proportional to the dimensionless column length, the larger column requires more eigenvalues to achieve the same consequences as the shorter column. For dimensionless column lengths $Z^0 > 15$, soil moisture profile solutions require over 1000 series terms for convergence. The flux solutions are still accurate at large depths using 100 series terms. For larger depths, the semi-infinite equations are preferable.

As seen in Figure 5.2, the dimensionless ponding time expression diverges for dimensionless depths greater than 15. This is the result of the invalidity of the assumption of Equation (4.121), which applies only with the faster convergences (fewer series terms) associated with smaller values of Z^0 . For values of $D_* = 4000 \text{ cm}^2/\text{day}$, $k = 40 \text{ cm/day}$ ($k/D_* = 0.01$), the dimensionless water table depth, $Z^0 = 14$ corresponds to a 14 meter deep water table.

Note also from Figure 5.2 that the ponding time solution series converges with about one hundred terms.

Some solutions converge with fewer terms for larger dimensionless times. This is simply the result of the reduced influence of the initial condition at these times and the smoothing of the moisture content distribution due to the diffusion-type governing equation. The uniform initial condition requires many series terms for convergence, as straight lines are difficult to represent by sine and cosine series.

5.4.2 Boundary Convergence

A second limitation of some of the solutions is that they are

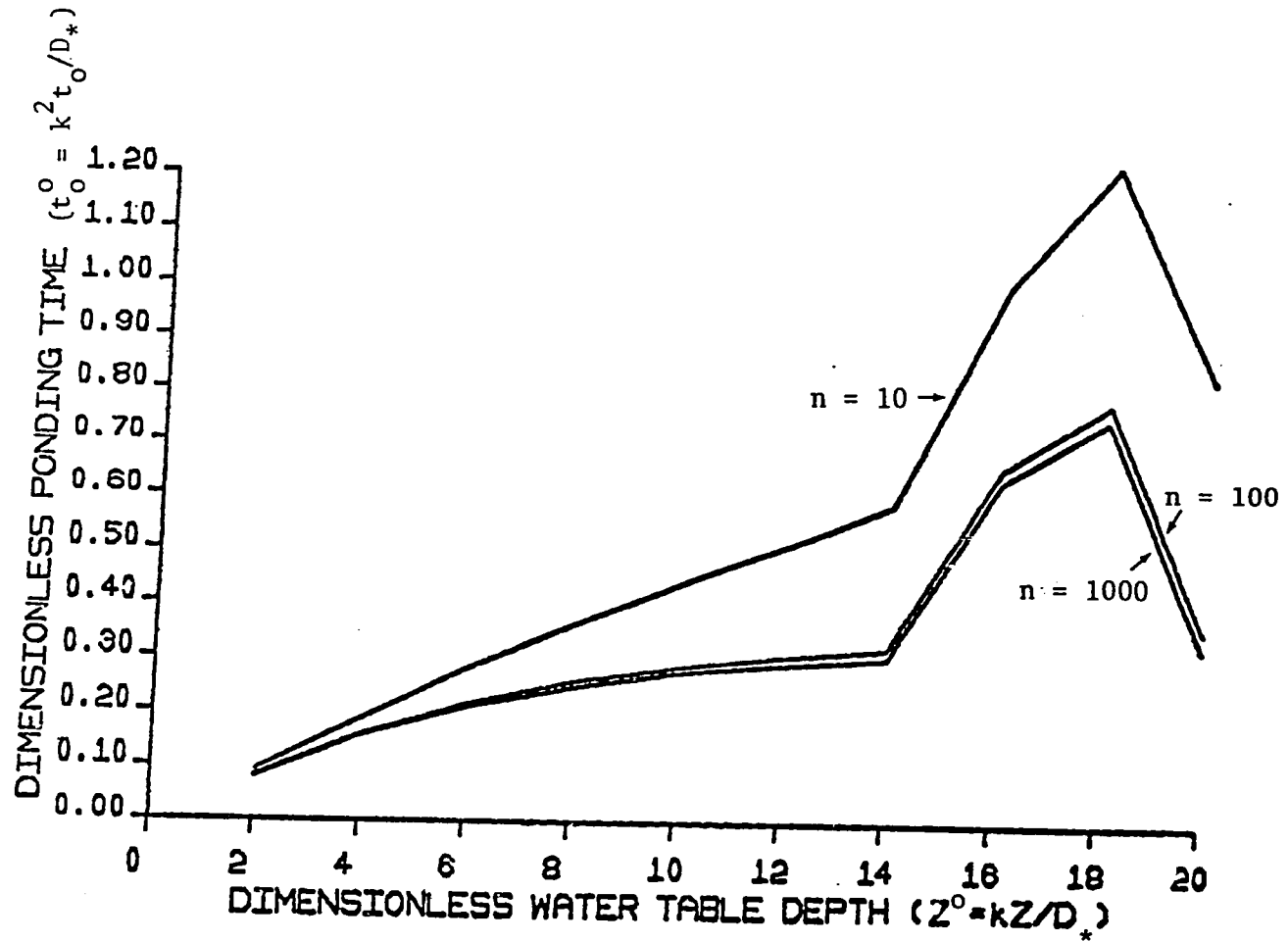


Figure 5.2

SENSITIVITY OF EQUATION (4.122) TO WATER TABLE DEPTH AND NUMBER OF SERIES TERMS FOR INFILTRATION ($i_0^0 = 2$, $n_e = .35$, hydrostatic θ_0)

not valid at or very close to the boundary. This is the case for the moisture content solution at the boundaries where moisture content is fixed at saturation. It is also true for most of the moisture fluxes and volumes at the same boundaries. The dimensionless distance from these boundaries at which the solutions are again valid depends on the number of series terms. For one hundred series terms, the dimensionless distance from the boundary for a reasonable solution is found to be two percent of the dimensionless column length.

Some solutions are invalid at the boundaries because the finite Fourier transform method sets the constant moisture content boundary conditions to zero when solving for the eigenvalues and eigenfunctions of the problem. This solution artifice affects the moisture content distribution and also the boundary fluxes, which are derivatives of the moisture content, and the moisture volumes crossing the boundaries, which are time integrals of the fluxes.

The solutions for exfiltration with the constant surface moisture content are unaffected by the artifice because the surface boundary condition is supposed to be set to zero. Thus the artificial surface boundary condition value equals that used in the actual problem statement. The result is that the series solutions converge much faster for the exfiltration problem than for infiltration. Also, the exfiltration solutions for moisture content, exfiltration capacity and exfiltrated moisture volume are valid at the surface boundary.

In the time domain, the constant concentration boundary flow solutions are undefined at very small dimensionless times. This is due

to the discontinuity at these boundaries between the initial and boundary conditions at $t^0 = 0$. The effects of the initial discontinuity disappear at dimensionless times between $t^0 = 0.001$ and $t^0 = 0.01$.

5.5 Numerical Examples

5.5.1 Soil-Water Depletion

The plots of Figure 5.3 are demonstrations of how the finite soil column may decrease its average water content according to the linear model of soil moisture movement. The processes shown are drainage from the bare surfaced soil column, with no surface moisture loss (curve 1), drainage plus vegetal transpiration (curves 2-4) and drainage plus bare soil evaporation (curve 5). The transpiration plots are for different assumptions of how plants extract soil moisture. The lines plotted are analytical depth-averaged moisture content solutions presented in Section 4.2.7, for the flux surface boundary condition.

5.5.1.1 Drainage

Drainage from a bare surfaced soil column (curve 1) is the simplest moisture removal mechanism, both physically and as an analytical solution ($e_p^0 = 0$). Gravity drains moisture from the soil column, with no moisture loss at the land surface, or through vegetation. In the example, the column is initially 85% saturated, draining to hydrostatic equilibrium (64% saturated for dimensionless water table depth, $Z^0 = 1$) in dimensionless time, $t^0 = 1$. For an average diffusivity $D_* = 2000 \text{ cm}^2/\text{day}$ and $k(= \frac{dK}{d\theta}) = 60 \text{ cm/day}$ (e.g., $K(1) = 21 \text{ cm/day}$ and $n_e = .35$), we find $Z^0 = 1$ and $t^0 = 1$ correspond to $Z(=D_*z^0/k) = 0.33$ meters and

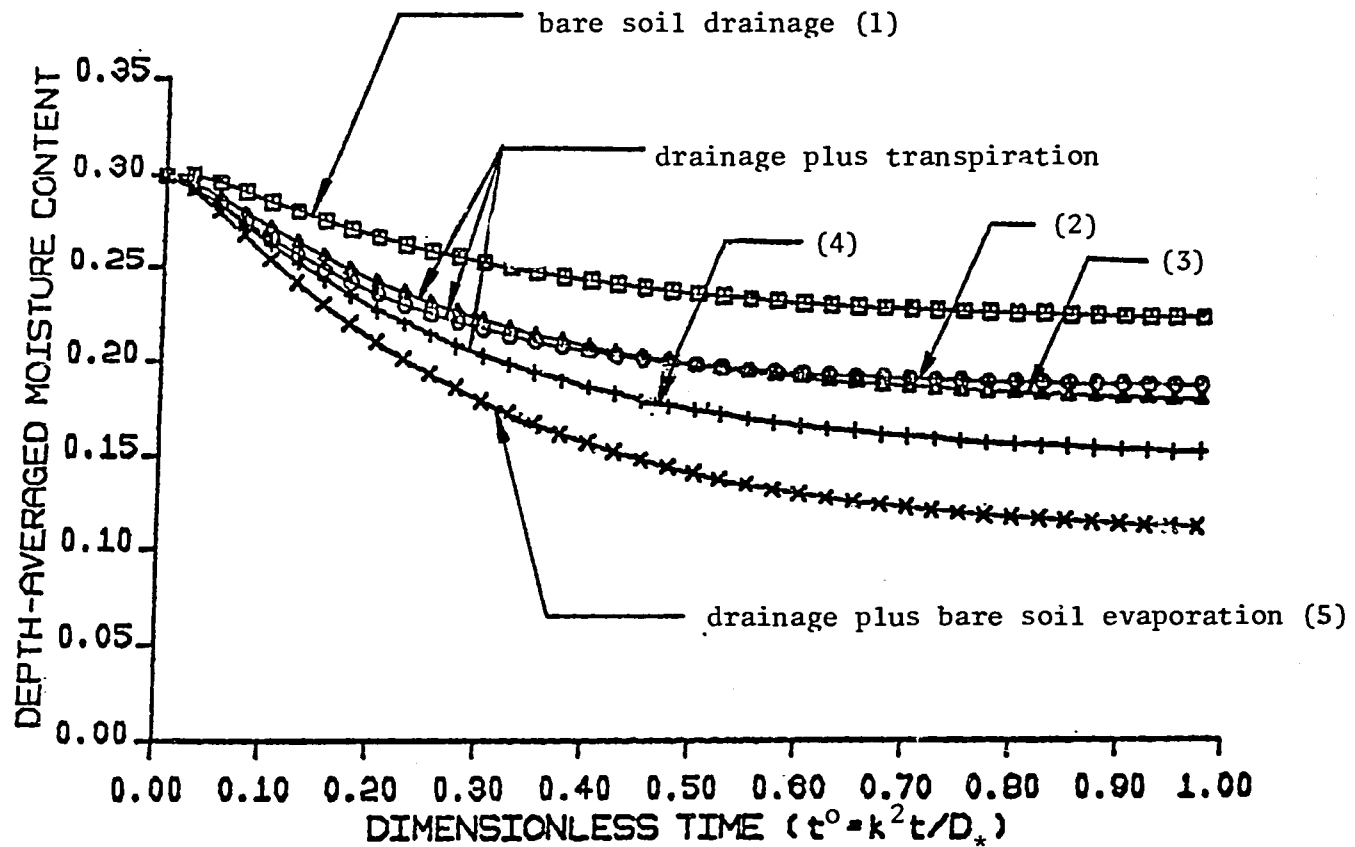


Figure 5.3

SENSITIVITY OF EQUATION (4.166) TO VEGETATION AND SURFACE EVAPORATION
 FOR A DRAINING WET SHALLOW SOIL COLUMN ($Z^0 = 1$, $n^e = .35$, uniform $\theta^0 = .30$, $n = 100$)
 \square $e_p = 0$; \circ eqn. 3.11 $G_{11} = 1$; Δ eqn. 3.113 $G_{11} = .315$, $G_{12}^0 = 1$;
 $+$ eqn. 3.113 $G_{11} = .315$, $G_{12} = 0$; \times $e_p = .315$

$$t(=D_*t^0/k^2) = 0.56 \text{ days.}$$

5.5.1.2 Drainage plus transpiration by plants

The analytical solution for the depth-averaged moisture content with moisture extraction by vegetation along with drainage (but no bare soil loss) is plotted versus dimensionless time in Figure 5.3, curves 2 through 4 (for the flux surface boundary condition, $e_p^0 = 0$). In comparison with gravity drainage alone (curve 1), the major difference is the reduction in moisture content in the column when plant transpiration is incorporated into the solution (compare curve 1 with curves 2-4). It is expected that if transpiring plants are extracting soil moisture in addition to gravity drainage (but with no bare soil surface extraction), that a greater moisture loss occurs than from gravity drainage alone.

The three curves of drainage plus transpiration (Figure 5.3, curves 2-4) are analytical solutions for the average moisture content where the vegetal extraction mechanism is represented by a different model for each plot. Curve 2 uses the Feddes (1976) vegetal extraction function (extraction is proportional to moisture content). Curve 3 incorporates vegetal extraction the strength of which decreases linearly from the land surface to the water table. Curve 4 involves the assumption of a uniform moisture extraction over the depth to the water table. All the models assume the plant roots are uniformly distributed horizontally in space. All the extraction rates (dimensional and dimensionless) must be scaled by the fraction, M , of the land surface covered by vegetation.

By comparing the average moisture content with drainage plus concentration-dependent moisture transpiration (curve 2) with that for drainage plus transpiration decreasing linearly with depth (curve 3) for nearly the same total transpiration rate (the concentration-dependent transpiration rate varies with the average moisture content). We may see how each vegetal extraction model affects the shape of the average moisture content solution. We see that curves 2 and 3 are almost overlapping. Curve 2 has a sharper initial moisture drop and a higher steady state value than curve 3. This is the result of the initially higher transpiration rate for the concentration-dependent vegetal extraction model with an initially greater average moisture content, and the reduced rate for the lower steady state moisture contents. The depth-dependent transpiration rate is constant over time for a given event and water table height.

The transpiration rate may be compared between vegetal extraction models by numerically relating the parameters of the models. The dimensionless parameter (G_1) of the concentration-dependent vegetal extraction model is related to the two dimensionless parameters (G_{11} , G_{12}) of the depth-dependent model as follows:

$$G_1 = (1.11/n_e)G_{11} = (1.25/n_e)G_{12}$$

where

$$G_{12} = 0.89G_{11}$$

$$G_{11} = 1.8 \left(\frac{D^* e_v}{k^2 z_r} \right)$$

and

$$e_v = k_v e_p$$

where

n_e = effective soil porosity

z_r = root zone depth

e_v = maximum vegetal extraction rate

k_v = plant transpiration effectiveness coefficient

e_p = potential evaporation of bare soil

For $D_* = 200 \text{ cm}^2/\text{day}$, $k = 6 \text{ cm/day}$, $k_v = 1$, $M = 1$ (completely vegetated land surface), $e_p = 1.05 \text{ cm/day}$, $n_e = 0.35$ and $Z_r \approx Z = 0.33$ meters, we find $G_{11} = 0.318$, $G_{12} = 0.28$ and $G_1 = 1.0$. The relation $G_{12} = 0.32 G_{11}$ is used in curve 3 of Figure 5.3 (with $G_{11} = 0.315$) in order to match the quantity of moisture lost in curve 2 for dimensionless event duration, $t^0 = 1$. This is done to allow the aforementioned comparison of the shape of the curves of the analytical solutions for the average moisture content.

5.5.1.3 A comparison of drainage and transpiration with drainage and bare soil evaporation

Curves 4 and 5 in Figure 5.3 compare the decaying average soil moisture content analytical solution (flux surface boundary condition) due to drainage and bare soil evaporation (curve 5, no transpiration, $M = 0$, $e_p^0 > 0$) with that due to drainage and vegetal transpiration (curve 4, no bare soil evaporation, $M = 1$, $e_p^0 = 0$). The transpiration model assumes the constant transpiration rate is supported by moisture extracted uniformly over the entire column depth, to the water table,

and that the land surface is completely vegetated ($M = 1$). For $Z^0 = 1$, the dimensionless transpiration rate is $e_v^0 = G_{11} Z^0 = G_{11}$. The dimensionless bare soil evaporation rate for the flux surface boundary condition is e_p^0 , the dimensionless potential evaporation rate (climate-controlled evaporation). In curves 4 and 5, we equate the dimensionless extraction rates $(1-M) e_p^0 = M e_v^0 = .315$.

The result is that there is less soil moisture for the bare soil evaporation-drainage process (curve 5) than for the transpiration-drainage process (curve 4), with identical moisture extraction rates for the evaporation and transpiration processes. The natural conclusion is that less drainage of the soil column occurs under the vegetated land surface than the bare soil land surface; for the same rate of moisture loss to the atmosphere.

The difference in the average moisture content between curves 4 and 5 may result from the different way the soil moisture is redistributed under surface extraction than under a vertically uniform extraction mechanism. Near the water table, the water content is reduced less than near the land surface under surface evaporation. There is no difference in the moisture content reduction between any two depths just considering the uniform vegetal extraction mechanism. But gravity drainage is a function of the moisture content near the water table. Since this is likely to be greater with surface evaporation (curve 5) than with uniform extraction (curve 4), and since the extraction rates are equal, the lower moisture content of curve 5 is very possibly due to the increased gravity drainage.

5.5.2 Infiltration

Of primary interest for the infiltration process are how the ponding time and the infiltration capacity are influenced by the water table.

5.5.2.1 Ponding time

The presence of both the water table and the capillary fringe decreases the ponding time. They limit the volume of pore space into which water may infiltrate. The result is that the zone above the high water table attains a higher moisture content faster than with the deep water table. This means the surface moisture content reaches saturation faster than for the deeper water table, and hence ponding time is shortened.

The ponding time equation (4.122) developed in Section 4.2.4 is consistent with the above analysis, providing an increased ponding time for deeper water tables. Figure 5.2 displays the logarithmically increasing ponding time ($n = 1000$) with the water table depth, asymptotically approaching a value which may be interpreted as the point where the water table is no longer influential. If the water table may be neglected for $Z^0 \geq 16$ ($\theta_1 - \theta_i = 0.15$, $i^0 = 3$) and $t_0^0 = 0.32$, using $D_* = 4000 \text{ cm}^2/\text{day}$ and $k = 40 \text{ cm/day}$, this corresponds to $Z \geq 16$ meters and $t_0 = 0.8$ day.

When considering the problem dimensionally, the $t_0 - Z$ relations will vary depending on how one estimates D_* and k .

How the water table decreases the ponding time is seen in Figure 5.4. This moisture distribution is only for the linearized

model, and does not resemble the non-linear solution. But this idealization shows the capillary fringe slowing the downward moisture movement (by reducing the moisture content/capillary pressure gradient and by its own volume occupying pore space) with the result that the surface pores fill up faster.

Figure 5.5 shows how the ponding equation (4.122) with the approximation (4.121) deviates increasingly with the dimensionless water table depth from the ponding time calculated using the linear model, solving $\theta(0, t_0^0) = n_e$. Though the approximation is not very accurate, it still preserves the essential shape of the relation of ponding time to the water table depth. This facilitates physically-based parameter estimation.

5.5.2.2 Infiltration capacity

The influence of the water table on the infiltration capacity for the linear soil moisture movement model is depicted in dimensionless format in Figure 5.6. One distinctive feature (not shown) is that the initial infiltration rate is higher for the shallow dimensionless water table ($Z^0 = 1$) than for the deep dimensionless water table ($Z^0 = 10$). A part of the reason for this is that the infiltration capacity, according to this model, decreases at a rate inversely proportional to the square of the water table depth (see Appendix A, Equation A.3, for the decay rate expression). Thus, the shallower depth column has a much faster infiltration capacity decay over time than does the deeper column. The other important feature is that this model produces a larger steady state infiltration capacity for the deep dimensionless

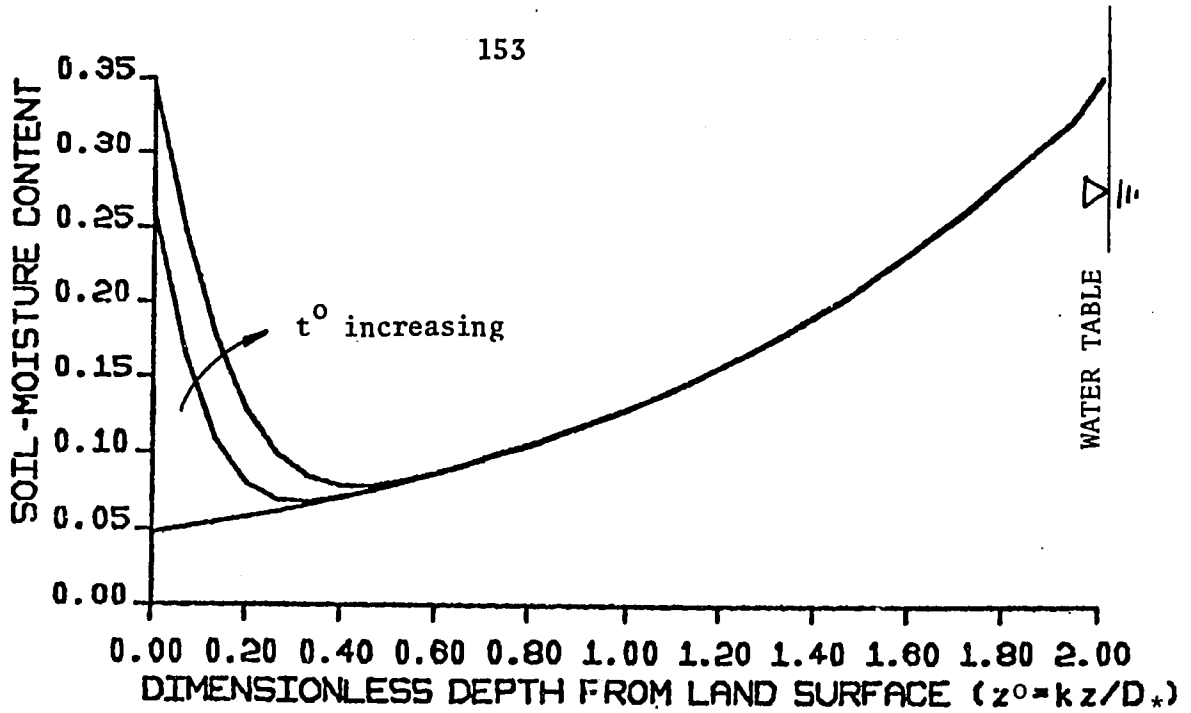


Figure 5.4

INFILTRATION INTO A SHALLOW SOIL COLUMN USING EQUATION (4.68)
 $(Z^0 = 2, i^0 = 2, n_e = .35, \text{hydrostatic } \theta_0, n = 200)$

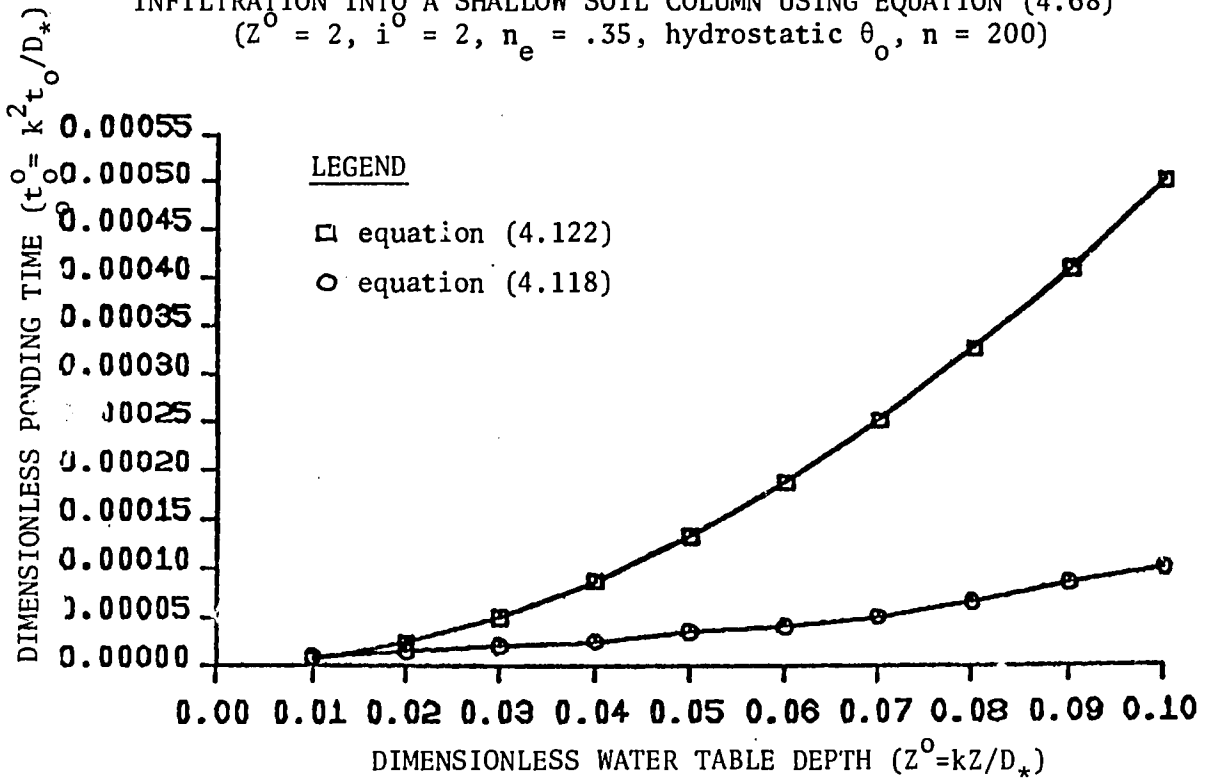


Figure 5.5

SENSITIVITY OF EQUATION (4.122) TO APPROXIMATION (4.121)
 BY COMPARISON WITH EQUATION (4.118) FOR INFILTRATION
 INTO A SHALLOW SOIL COLUMN $(i^0 = 3, n_e = .35, \text{hydrostatic } \theta_0, n = 100)$

water table than for the shallow one. Since steady state infiltration occurs for a saturated soil column in the finite domain, accounting only for liquid moisture movement, the steady state infiltration capacity should be the same for all water table depths and equal to the saturated hydraulic conductivity.

According to the assumptions of this model, the steady state dimensionless flux for the completely saturated column should be equal to the value of the effective porosity. This is apparent from Equation (3.123a), valid over the column length, which states

$$q^0 = \theta_e - \frac{\partial \theta_e}{\partial z} \quad (3.123a)$$

For a saturated soil column, it is obvious that $\partial \theta_e / \partial z \equiv 0$, which leaves $q^0 = \theta_e = n_e$. That this is nearly true for large dimensionless depth is seen in Figure 5.6, where the value of the porosity, n_e is indicated by a dashed line.

The difference between the steady state solutions for different z^0 is attributed to a problem inherent in the Fourier series solution. The original problem solved is for the moisture content. It has already been shown that the solution for q^0 converges most slowly when the Fourier series must approximate a straight line (see Section 5.4.1). It has also been shown that taking the derivative of this solution causes problems at the boundaries and at very early time (see Section 5.4.2). This is a case where the inexact replication of a line (completely saturated column) is reflected in an inexact derivative of that solution to cause a physically inconsistent steady state solution. The

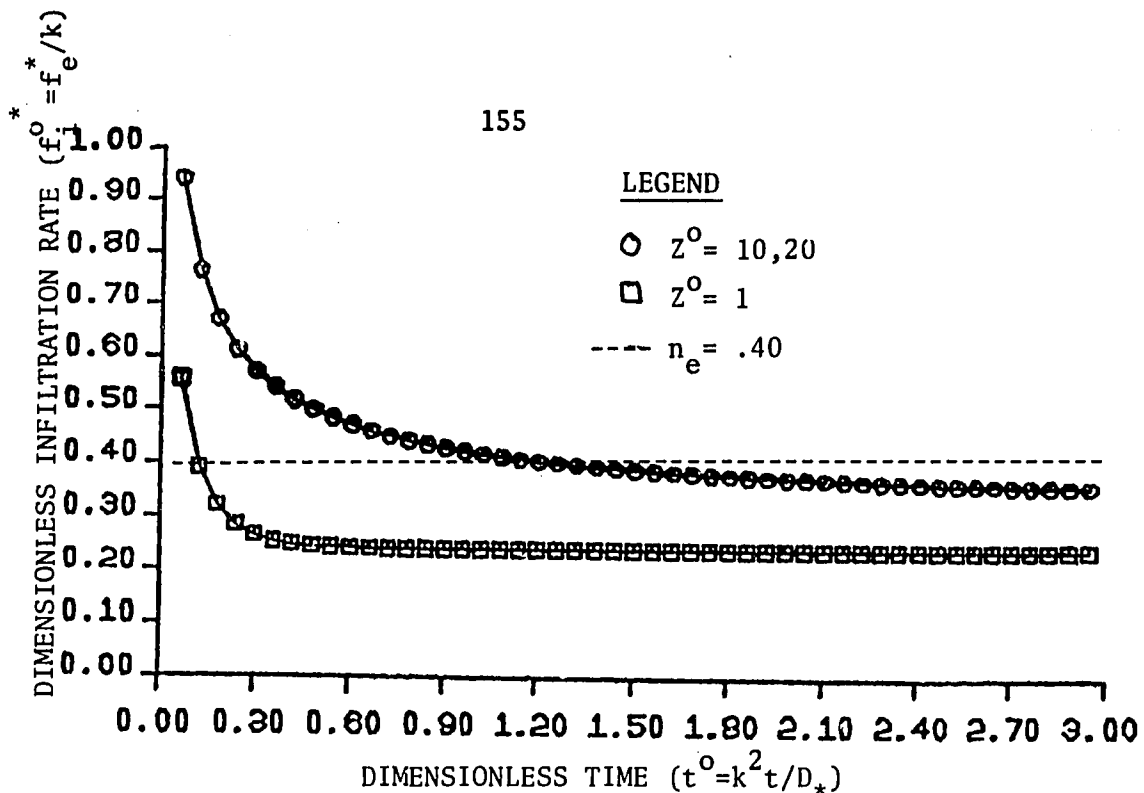


Figure 5.6: SENSITIVITY OF EQUATION (4.114) TO WATER TABLE DEPTH FOR INFILTRATION INTO A SHALLOW SOIL COLUMN ($n_e = .40$, hydrostatic θ_0 , $z^0 = .02Z^0$, $n = 100$)

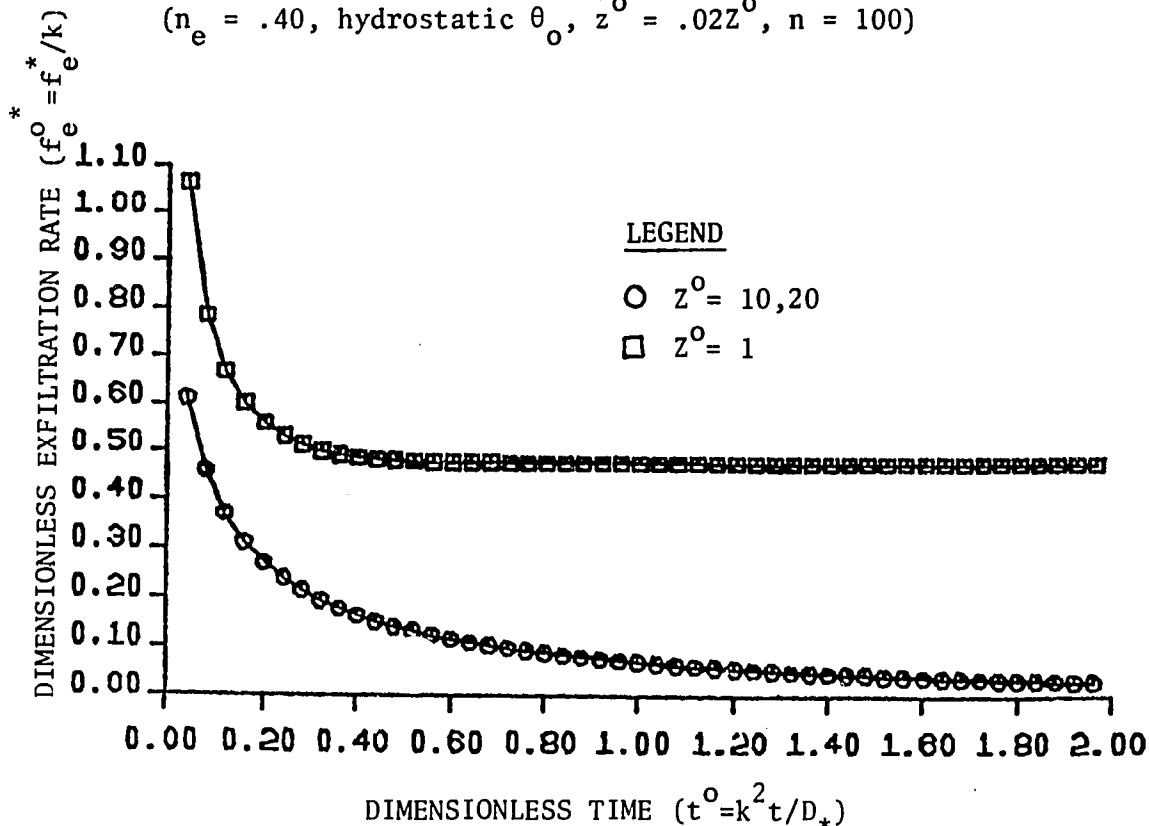


Figure 5.7: SENSITIVITY OF EQUATION (4.135) TO WATER TABLE DEPTH FOR EXFILTRATION FROM A WET SHALLOW SOIL COLUMN ($n_e = .40$, uniform $\theta_0 = .35$, $z^0 = 0$, $n = 101$)

slightly positive steady state value for $\partial\theta/\partial z$ results in a lower than predicted value for q^0 , as seen in Figure 5.6. This problem is apparently worse for shallower dimensionless depths.

Recognizing that this is not a problem affecting the shape of the time-dependency of the flux solution, we may either set the steady state value to n_e , known to be the dimensionless steady state flux rate for the linear model of infiltration, or we may set it to the measured value for each particular soil type, after reducing this value to dimensionless form. The latter method is discussed further in Appendix A.

The series solution for infiltration capacity converges to different solutions depending on whether the number of series terms is even or odd. Only an even number of series terms should be used for this solution. An odd number of terms produces negative values for infiltration capacity.

5.5.3 Water Loss at the Soil Surface; Exfiltration

5.5.3.1 Drying time

Vegetation plays an important role in drying time estimation. Depending on the fraction of vegetated land surface and the mechanism of vegetal extraction of soil moisture, the drying time could be either increased or decreased. Also, as with ponding time, drying time increases logarithmically with the depth to the water table.

For the drying process, the uniform initial condition more realistically models reality than does the hydrostatic initial condition (which is the result of the soil having already been dried).

5.5.3.2 Exfiltration capacity

The analytical equation for bare soil exfiltration capacity (Equation (4.135), dry surface and uniform initial condition) is plotted for two dimensionless water table depths ($Z^0 = 1$, $Z^0 = 10$) in Figure 5.7. It shows a greater rate of decay of the exfiltration capacity and a larger steady state value for the shallow water table. As with infiltration capacity (Section 5.5.2.2), the decay rate is inversely proportional to the square of the dimensionless water table depth, causing a sharper exfiltration capacity decay rate for the shallower water table. The steady state value is the linear model equivalent to the capillary rise versus depth relation of Gardner (1958). It is a result of the moisture content gradient near the land surface for the linear model. The steady state gradient approaches zero for the deeper column as the water table influence becomes negligible.

In general, the exfiltration capacity solution behaves better mathematically than the infiltration capacity solution. It is applicable exactly at the land surface boundary. It converges with fewer series terms and the steady state solution is consistent with the corresponding moisture content distribution. Aside from the explanation of Section 5.4.2, the other cause is that the moisture content distribution is exponential in shape as the solution approaches steady state. This is easier to model with the Fourier series than the linear steady state solution for the infiltration capacity. Still, the solution should only be calculated using an odd number of series terms, which is a property of the type of function characterizing the solution.

5.5.4 Two Period Process: Simulation Prototype

Figure 5.8 depicts the depth-average soil moisture content for a storm-interstorm sequence under climate-control (pre-ponding time and pre-drying time, respectively). The moisture content climbs during the dimensionless rainfall period and falls during the dimensionless bare soil evaporation period. A sequence of these storm-interstorm periods may be generated by the continual input of rainfall and evaporation intensities and event durations. For each event period, a new average diffusivity (D_*) and a new k must be calculated, to account for hysteresis and for the new initial moisture content. The result is that for each event period a given value of $t^0 (=k^2 t/D_*)$ would represent a different value of real time. The simulation could also account for vegetation, using one of the vegetal extraction models discussed in Section 3.2.5.

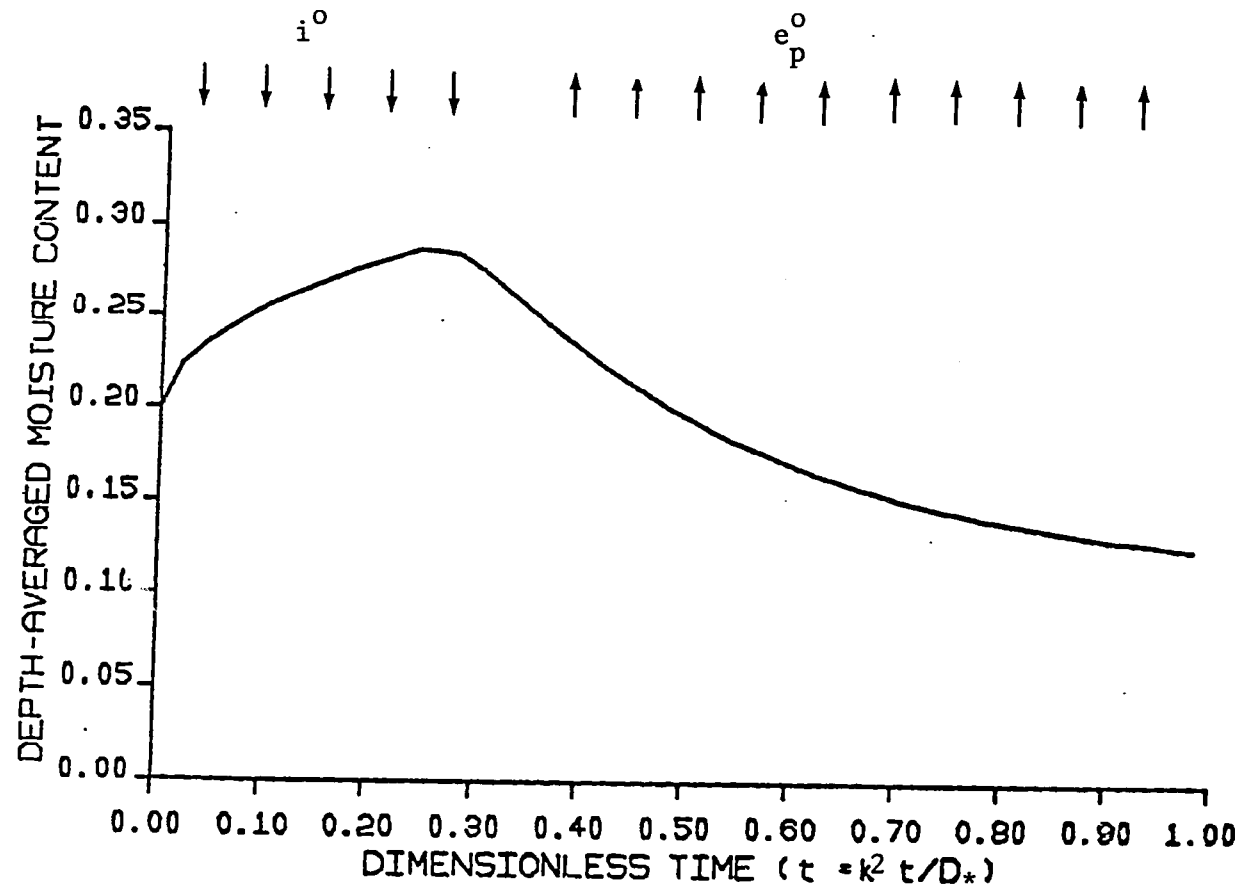


Figure 5.8

STORM-INTERSTORM SEQUENCE USING EQUATION (4.166)
 $(Z^o = 1, i^o = .3, e_p^o = .3, n_e = .35, \text{uniform } \theta_o = .2, n = 100)$

5.6 Comparisons with a Numerical Solution

5.6.1 Introduction

We are interested in seeing for a shallow water table soil how well the linear analytical solutions of Section 4.2 compare with non-linear solutions generated from a numerical model, which more accurately describes the highly non-linear soil-water movement process. The numerical finite-element code, developed by P.D.C. Milly, is a simplified version of the code presented in Milly and Eagleson (1980). The non-linear governing equation is (3.66), with the matric potential, ψ , as the dependent variable.

The essential features of the numerical model are the assumed relationships between moisture content (θ_e), matric potential (ψ) and hydraulic conductivity ($K(\theta)$). This model neglects hysteresis, vapor transport and temperature effects though the comprehensive model of Milly and Eagleson (1980) includes them. Relationships suggested by Brooks and Corey (1966) and used in the numerical model for $\theta(\psi)$ and $K(\theta)$ are (Eagleson, 1978c)

$$\theta = n(\psi/\psi_1)^{-m} \quad (5.12)$$

and

$$K(\theta) = K_1(\theta/n)^c \quad (5.13)$$

where

n = effective porosity

m = pore size distribution index

c = pore disconnectedness index

ψ_1 = matrix potential at effective saturation, $s(=\theta/n)=1$

= bubbling pressure head

K_1 = saturated hydraulic conductivity

The expression for soil-moisture diffusivity implied by this is found from the definition of diffusivity, which is

$$D(\theta) = K(\theta)/(d\theta/d\psi) \quad (5.14)$$

where

$d\theta/d\psi$ = specific moisture capacity

Using the analytical expression for the moisture retention curve, Equation (5.12), we find

$$\frac{d\theta}{d\psi} = -m \theta/\psi \quad (5.15)$$

and, from Equations (5.13) and (5.15) in (5.14), diffusivity is described by

$$D(\theta) = \frac{\psi_1 K_1}{nm} (\theta/n)^d \quad (5.16)$$

where

$$d = c - 1/m - 1$$

= diffusivity index

and

$$m = 2/(c - 3)$$

The constant diffusivity D_* is thus more reasonable for small moisture content perturbations, larger values of θ and soils where d is smaller (e.g., sandy soils).

The relations (5.12), (5.13) and (5.16) are used as the 'reality' against which the analytical, linearized model is measured. However, the analytical expressions are based on laboratory studies of soil properties. Recent evidence suggests that the diffusivity of soils in the field may be much less variable than that measured using the repacked soils of the laboratory. Clothier, et al (1981) have found that 'at wetter water contents, the diffusivity (of the field tested Bungendore fine sand) was indeed the "linear" diffusivity of Philip (1969)'.

5.6.2 Pondered Infiltration into Yolo Light Clay for Two Water Table Depths

5.6.2.1 Parameter estimation

For the linear model of soil moisture movement, we need to evaluate the parameters D_* and k in order to convert the problem from dimensional into dimensionless form. Philip (1966) has developed expressions for these parameters requiring four soil parameters and the average initial moisture content. His expressions are developed by matching the linear and non-linear solutions to the soil-moisture movement equation for large and small times, for the semi-infinite domain. We use these estimates as first guesses for the parameter values for the finite domain problem.

For infiltration we have

$$D_* = \frac{\pi S^2}{4(\theta_1 - \theta_0)^2} \quad (3.29)$$

where

S = sorptivity (soil parameter)

θ_1 = effective saturated moisture content

θ_0 = initial depth-averaged moisture content

and we estimate k by

$$k = \frac{K_1 - K_0}{\theta_1 - \theta_0} \quad (3.26)$$

where

K_1 = saturated hydraulic conductivity (or asymptotic infiltration rate)

K_0 = initial column-averaged hydraulic conductivity

Philip used the field capacity for θ_0 , where $K_0(\theta_0) = 0$. Here we use θ_0 to conserve the initial volume of soil moisture in the column. These estimates of D_* and k do not account for the initial distribution of moisture content. We also assume that $K_0 \ll K_1$ and set $K_0 = 0$, though we could also estimate it from equations such as (5.13). Neglecting K_0 is reasonable for soils closer to clay types and for lower initial moisture contents.

A second model for the average infiltration diffusivity, D_* , developed by Eagleson (1978c) for the semi-infinite domain, using the Brooks and Corey (1966) models for $\psi(\theta)$ and $K(\theta)$ and the Crank (1956) scheme for the weighted average diffusivity,

$$\begin{aligned}
 D_* &= \frac{5K_1 \psi_1 \phi_i(d, s_o)}{3mn} \\
 &= \frac{5k \psi_1 \phi_i(d, s_o)}{3m}
 \end{aligned}
 \tag{5.17}$$

where

s_o = depth-averaged initial degree of effective saturation

$$= \theta_{e,o} / n_e$$

ϕ_i = sorption diffusivity

and may be approximated by the empirical fit

$$\phi_i = [d(1 - s_o)^{1.425 - 0.0375d} + 1.67]^{-1} \tag{5.18}$$

Both models for D_* are only valid for the infiltration process. The basic differences between them are that (3.29) requires two parameters and directly measures the soil sorption through $S = f(D(\theta))$ while (5.17) requires five parameters and assumes an analytical $D(\theta)$ relation. Equation (3.29) will equal (5.17) if $S(D(\theta))$ uses the same $D(\theta)$ relation.

As neither model is derived for the finite domain, it is hard to predict which is better in advance. Relation (5.17) is developed using the same assumed curves for $K(\theta)$ and $\psi(\theta)$ as the numerical model uses to characterize the 'real soil', which suggests it might be a more appropriate parameter choice for this comparison.

5.6.2.2 Soil data

For both the numerical model and to calculate D_* and k , we are using data for Yolo light clay (Moore, 1939), called a 'linear soil' by Philip (1969). From the curve of $D(\theta)$ (independent of water table depth),

Philip (1957a) calculated

$$S = 1.254 \times 10^{-2} \text{ cm sec}^{-1/2}$$

The other data from Moore (1939) are $\theta_1 = .4950$, $\theta_{wo} = .2574$ and $K_1 = 1.229 \times 10^{-5} \text{ cm sec}^{-1}$. For similar type clay soils, we find from Eagleson (1978e) that $\psi_1 = 26 \text{ cm}$ and $c = 12$. We calculate $n(=\theta_1 - \theta_{wo})$ to be 0.26.

We assume for this example that the average initial moisture content is $\theta_{e,o} = 0.13$.

For the same conditions that he developed the diffusivity expression (5.17), Philip (1966) suggested a soil parameter characterization of early time defined by

$$t_{\text{grav}} = \left(\frac{S}{K_1 - K_0} \right)$$

where

t_{grav} = time dividing dominance of capillary and gravity forces

For the above soil data, we calculate t_{grav} to be twelve days. Thus the Yolo light clay soil is dominated by capillary forces for the time frame of interest.

5.6.2.3 Dimensionless parameters

To make time and water table depth dimensionless, we need values for k^2/D_* and k/D_* .

From the Philip expressions, $D_* = 631.41 \text{ cm}^2 \text{ day}^{-1}$ and

$k = 8.17 \text{ cm day}^{-1}$. Thus, $k/D_* = 0.0129 \text{ cm}^{-1}$ and $k^2/D_* = 0.1057 \text{ day}^{-1}$. Thus, for normal rainfall durations of less than one day, we are in early time ($t^0 \leq 0.11$). A typical shallow depth is around 1 meter ($Z^0 = 1.3$).

Using the Eagleson model for comparison, we calculate $d = 6.5$, $\phi_1(d, s_0) = \phi_1(6.5, 0.5) = 0.220$, $k(=K_1/n) = 8.17 \text{ cm day}^{-1}$ (Philip expression for k) and $D_* = 350.84 \text{ cm}^2 \text{ day}^{-1}$ (=44% of D_* from Philip). We have $k/D_* = 0.0233 \text{ cm}^{-1}$ and $k^2/D_* = 0.190 \text{ day}^{-1}$. For a 1-day rainfall event, we find $t^0 = .19$, and for a water table depth of one meter, dimensionless $Z^0 = 2.3$.

5.6.2.4 Volume of infiltrated moisture

In Figure 5.9, we have the analytical, linearized solution [Equation (4.117)] for the infiltrated moisture volume versus time for water table depths of one and two meters. On the same figure are the results of the numerical simulation of the associated non-linear problem. The diffusivity, D_* , and k are estimated from the Philip expressions (3.29) and (3.26). That this is a finite domain case is clear from the sensitivity to the infiltrated volume of moisture to the water table depth.

The analytical linearized solution agrees with the non-linear one in showing less infiltration for the 1 meter water table than the 2 meter one. In fact, the linearized solution reasonably approximates the non-linear one in both cases for times less than 40 hours (1.67 days). In that time period, the largest percent difference for the

2 meter case is 18% and for the 1 meter case it is 33%. The linear solution for $Z = 2\text{m}$ actually improves between 40 and 60 hours, when at 60 hours the two solutions agree exactly. Ultimately, for very large times, greater than 60 hours, the linear and non-linear solutions diverge.

The soil column is calculated to saturate in 2.4 days for the 1m deep column and in 4.3 days for the 2m deep column. Thus, the linear solutions are reasonable before saturation occurs.

The overprediction of the infiltrated volume in early time ($t < 10$ hours) using Philip's D_* is minimized using D_* from Eagleson as seen in Figure 5.10. Agreement between the linear and non-linear models for times less than 40 hours (1.7 days) is excellent with the maximum percent difference being 9%. For times greater than this, the solutions diverge.

One main difference exists between the solutions in Figures 5.9 and 5.10. The analytical solutions using the larger D_* (Figure 5.9) diverge much more quickly than those of Figure 5.10. The latter maintains quite well the small difference in the cumulative infiltrated moisture occurring in the non-linear case between the two water table depths.

A problem, shown in Figure 5.10, is that the infiltration rate for the analytical solutions is larger for $z = 1\text{m}$ than for $z = 2\text{m}$ in early time and switches for times, $t < 10$ hours. In dimensionless terms, this occurs for $t^0 (=k^2t/D_*) \leq 0.0001$, with $Z^0 (=kZ/D_*) = 0(1)$. This is due to the initial surface moisture gradient being higher for the

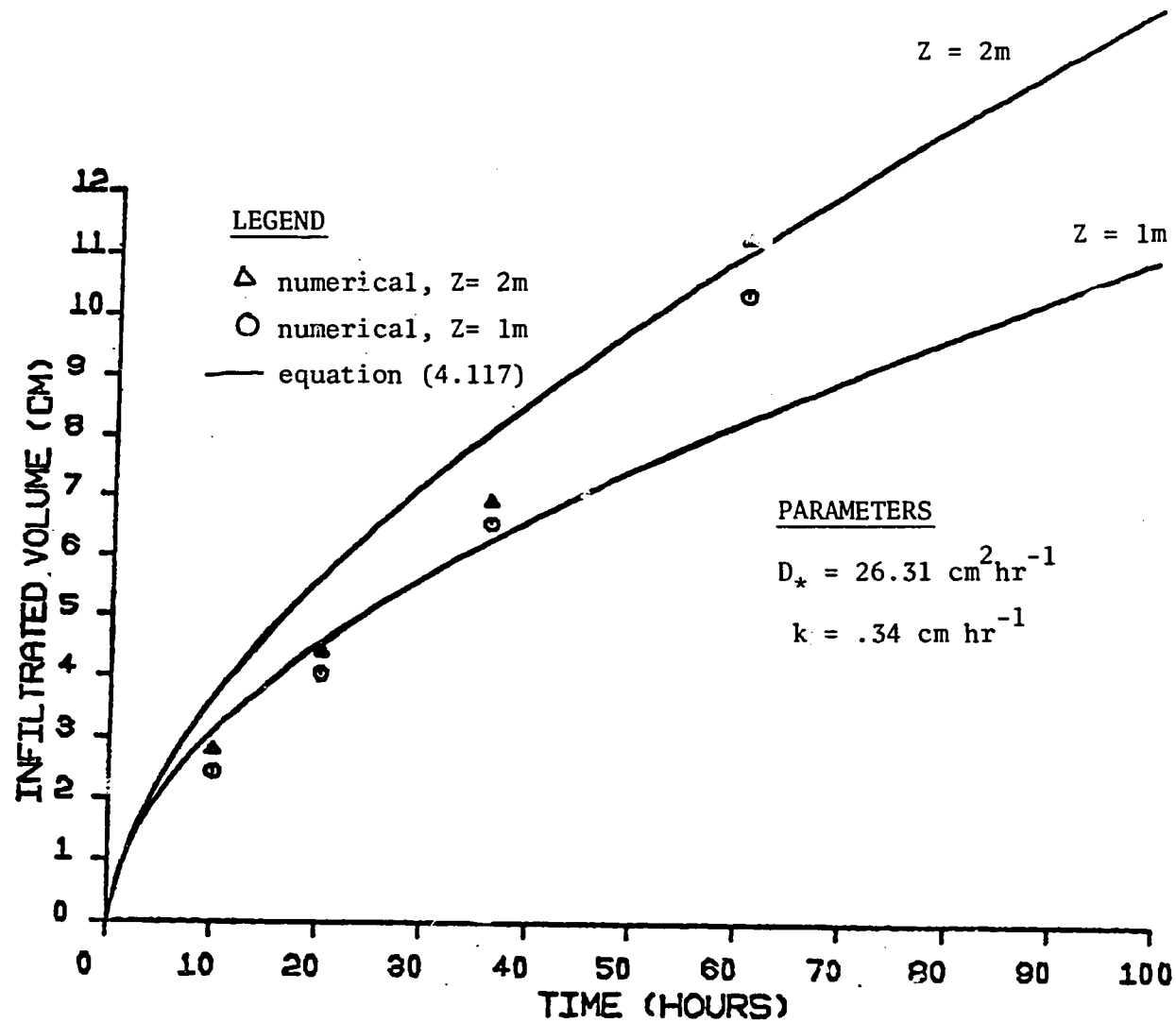


Figure 5.9: CUMULATIVE INFILTRATION COMPARING EQUATION (4.117) WITH THE NUMERICAL NON-LINEAR SOLUTION USING PHILIP'S D_* ($n_e = .26$, hydrostatic θ_o , $n = 100$)

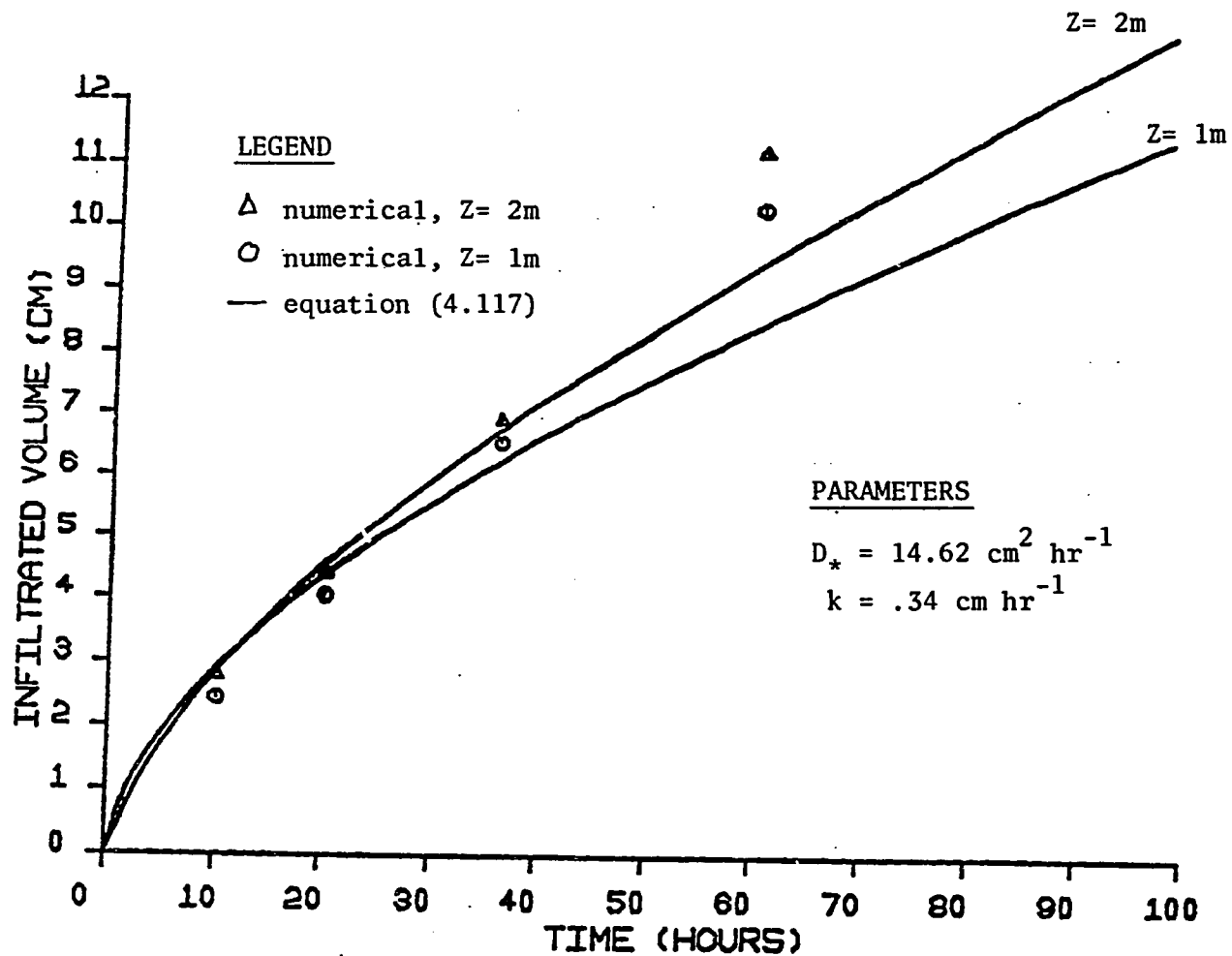


Figure 5.10: CUMULATIVE INFILTRATION COMPARING EQUATION (4.117) WITH THE NUMERICAL NON-LINEAR SOLUTION USING EAGLESON'S D_* ($n_e = .26$, hydrostatic θ_0 , $n = 100$)

shallower water table. It does not happen with the non-linear solution over any time period.

The two estimates of D_* and the one for k need not be the only ones used. We may use these as initial estimates and find the 'best fit' using a criterion such as least squares. We would like to avoid having to fit new values of D_* and k for each water table depth. The estimates used are conveniently independent of the water table depth.

The linearized solution, though detailed and slowly convergent, still is advantageous (compared to the numerical solution) in that it is analytical and dimensionless. The solution form explicitly shows how the water table boundary influences the moisture flow dynamics. In Appendix A, a simplified equation for the infiltration capacity is presented, which is extracted from the form of the complete solution and includes the effect of water table depth.

An important aspect of the linearized model input is that the initial moisture content for the model itself is assumed to be hydrostatically distributed. The depth-averaged value is used to evaluate D_* and k .

5.6.2.5 Average moisture content

Figures 5.11 and 5.12 are the depth averaged moisture contents corresponding to the cumulative infiltration volumes of Figures 5.9 and 5.10. The only difference is that the initial condition for the linear model here is one of uniform moisture content, rather than a hydrostatic distribution. The reason for this difference is that the

initial volume of moisture in the column is exactly preserved in this case, while the hydrostatic initial condition is more suitable for modeling boundary dynamics. The dynamics are more sensitive to the initial moisture distribution and the average content is more sensitive to the initial volume of moisture in the column.

For the average moisture content, the Philip diffusivity (Figure 5.11) provides a better fit to the numerical solution than does the Eagleson diffusivity (Figure 5.12). The Philip estimate consistently underestimates the content less than does the Eagleson estimate. Using the Philip estimator, the percent difference between the linear and non-linear solutions is less than 12% for times less than 20 hours. This is quite surprising since the change in the moisture content for $Z = 1\text{m}$ is 34% of the total content (from $\theta = .13$ to $\theta = .215$). The model is supposed to be more valid for small changes in moisture content.

Both estimates for D_* underestimate the average moisture content. But for times less than 50 hours, Figure 5.11 shows that the difference between moisture content values for the two water table depths at a given time is almost identical between the linear and non-linear models. For example, at $t = 30$ hours, the difference between the moisture contents for the two water table depths is 0.055 for both the linear and non-linear models. Since the linear model approximates the non-linear one better for the larger value of D_* , it is likely a larger, fitted value of D_* may do even better.

Fitting the value of D_* to the numerical data for $Z = 1\text{m}$ results in an excellent matching of the depth-averaged moisture content

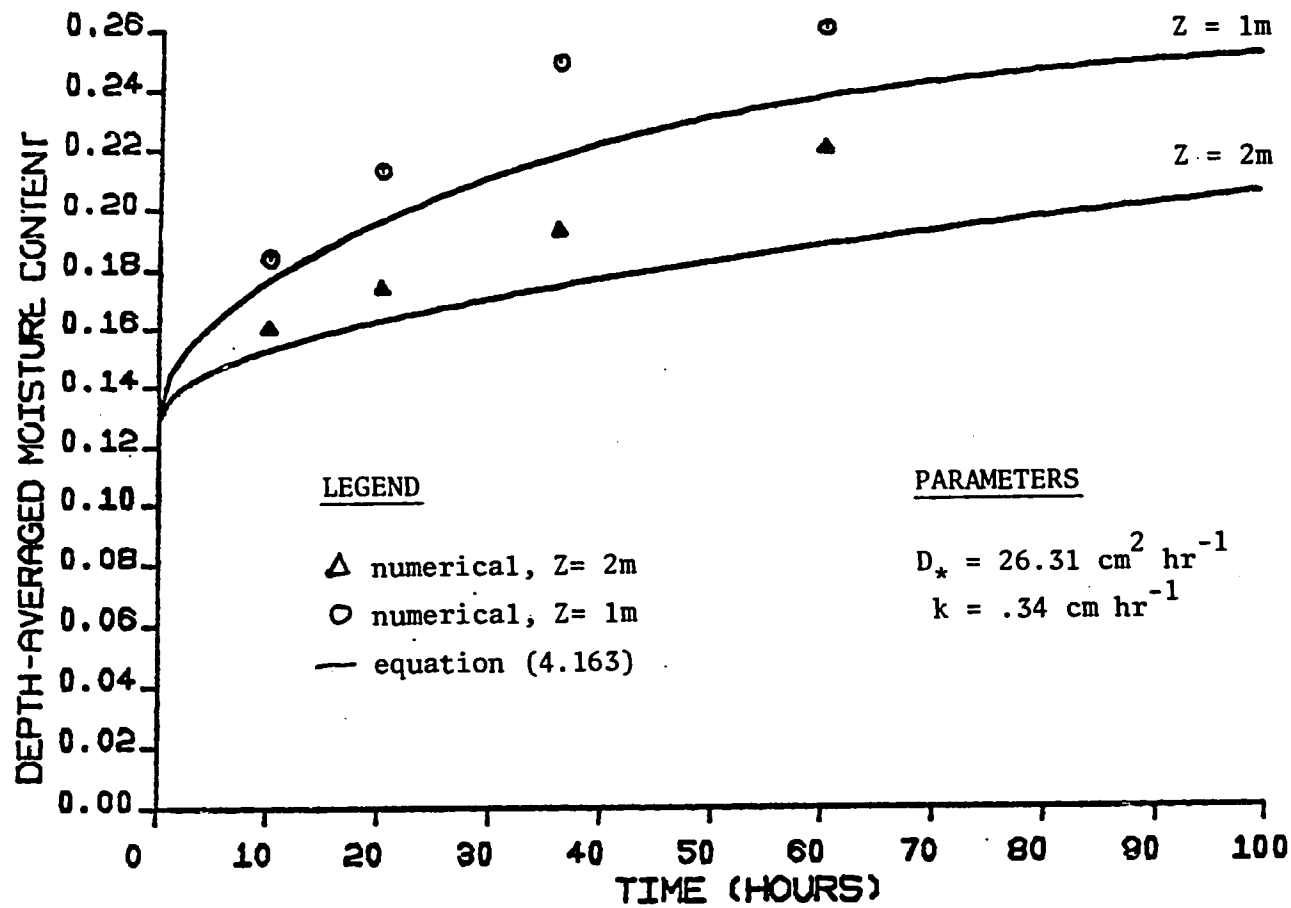


Figure 5.11: BARE SOIL INFILTRATION COMPARING EQUATION (4.167) WITH THE NUMERICAL NON-LINEAR SOLUTION USING PHILIP'S D_* ($n_e = .26$, uniform $\theta_o = .13$, $n = 100$)

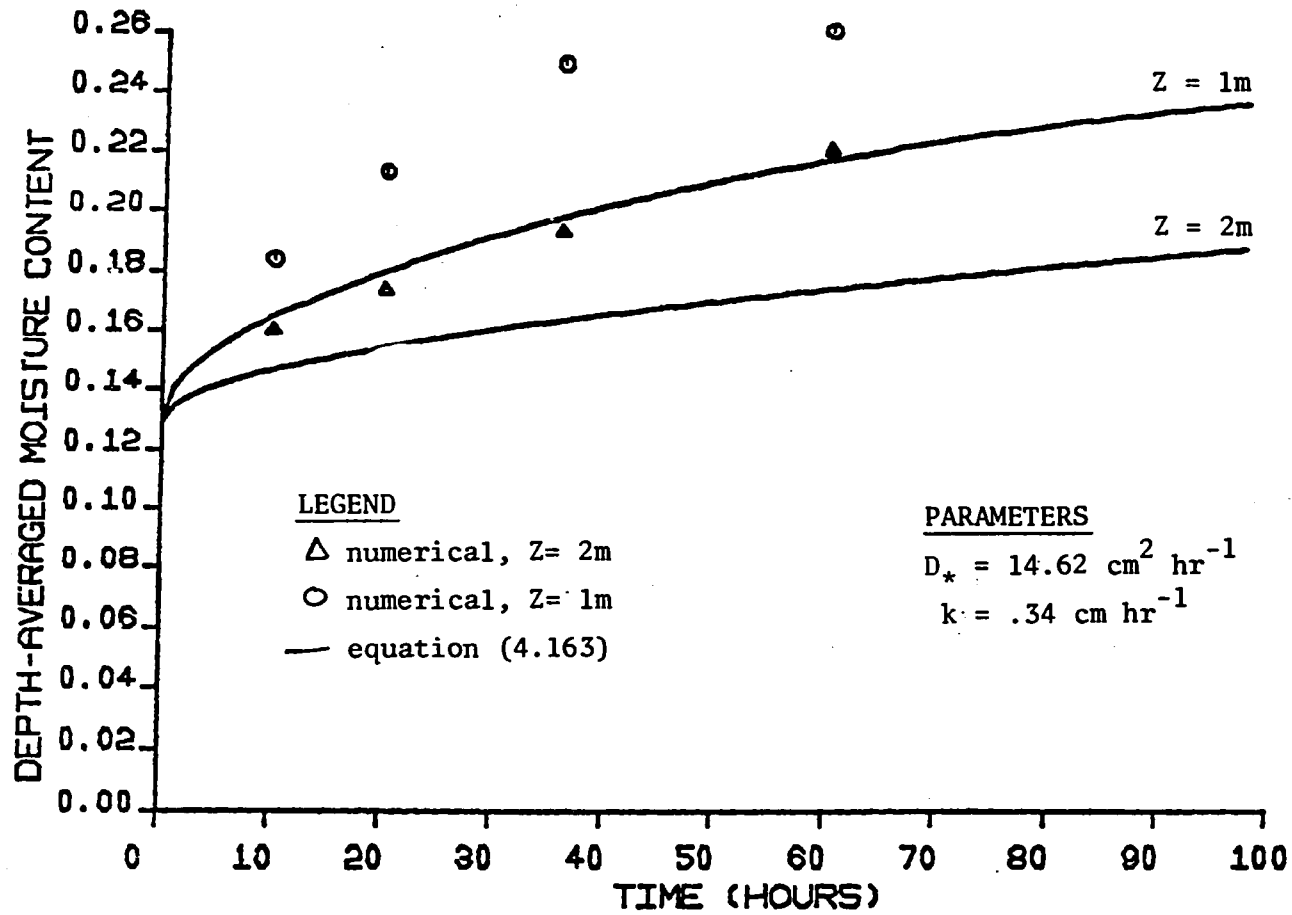


Figure 5.12: BARE SOIL INFILTRATION COMPARING EQUATION (4.167) WITH THE NUMERICAL NON-LINEAR SOLUTION USING EAGLESON'S D_* ($n_e = .26$, uniform $\theta_0 = .13$, $n = 100$)

both for $Z = 1$ meter and $Z = 2$ meters, as shown in Figure 5.13. The maximum percent error between the analytical and numerical models is only 5% for $Z = 2$ meters after more than 60 hours of infiltration and less for $Z = 1$. Also the time the column saturates is accurately predicted for $Z = 1$ meter. All this strongly suggests that the analytical average moisture content solution to the linearized model contains some essential structure of the relation between water table depth and the soil moisture dynamics. The key point is that the diffusivity is fitted only for the one meter water table depth case, yet the same diffusivity yields quite an adequate prediction of average moisture content for the two meter water table depth case. This is not to say another value of D_* would not produce a better fit for $Z = 2$ meters, but we need not rely solely on fitting D_* to model the effects of the water table.

The fitted value of D_* is twice that of the Philip value. This is very close considering how D_* may vary over several orders of magnitude. This lends further support to the method of starting with D_* from Philip or Eagleson and using a best fit value near to the calculated one. What is interesting about this is that the fitting is for one parameter only. We keep k at its calculated value. This supports the suggestion that the process is diffusion (or capillarity) dominated as indicated by t_{grav} in Section 5.6.2.2.

The benefit of all this is that we may study the linearized solution for the depth-averaged moisture content for ponded infiltration into a finite soil column [Equations (4.167) and (4.78)] to better understand the influence of the water table in the unsaturated zone dynamics. Since the average moisture content solutions converge fairly

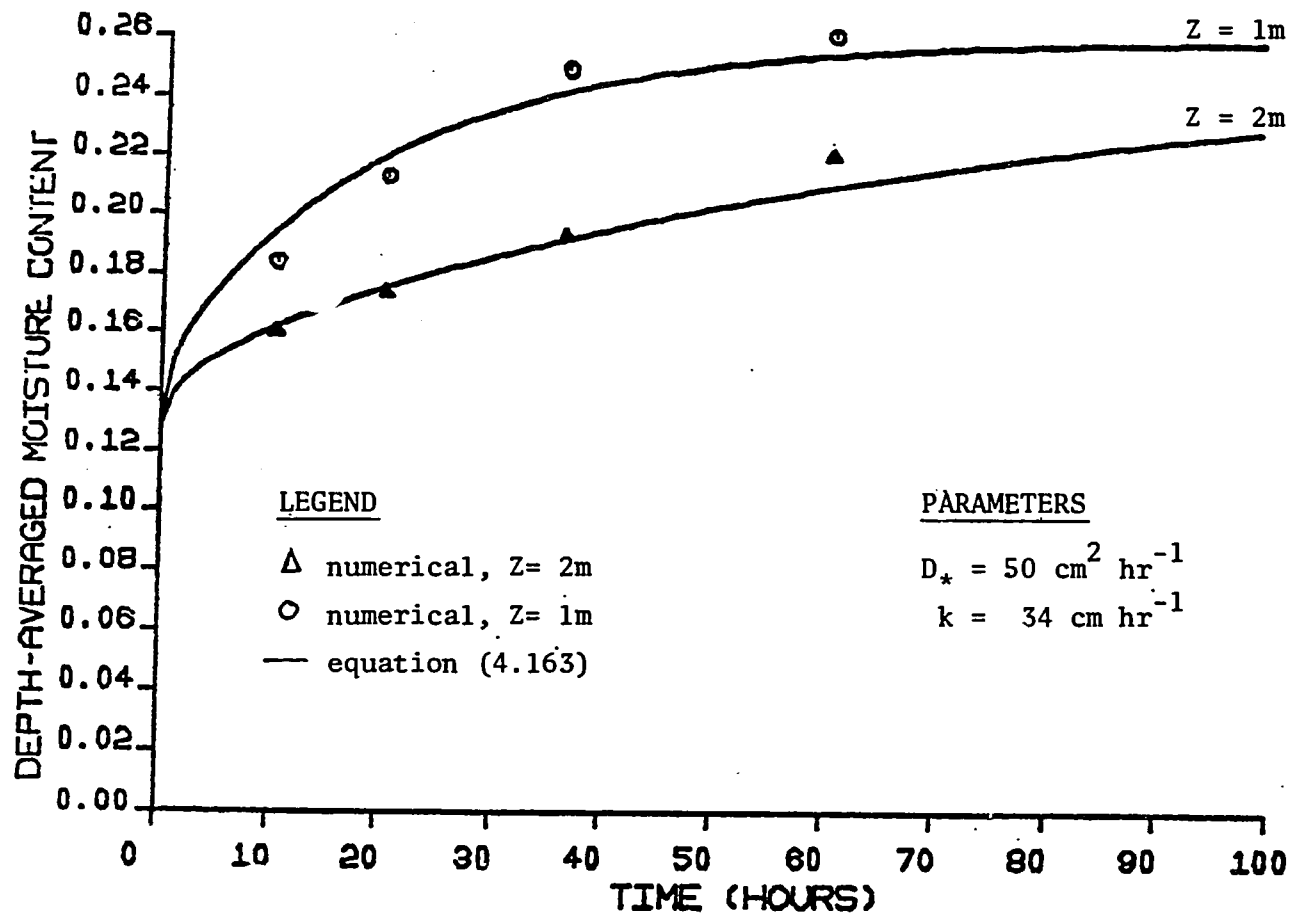


Figure 5.13: BARE SOIL INFILTRATION COMPARING EQUATION (4.167) WITH THE NUMERICAL NON-LINEAR SOLUTION USING FITTED D_* ($n_e = .26$, uniform $\theta_0 = .13$, $n = 100$)

quickly ($n < 10$) we may even be able to extract a useful simplified expression for θ_{AV} directly from the series solution. This also will help in the understanding of the related dynamic equations such as the cumulative infiltration. The fact that this solution is depth-integrated makes it less dependent on moisture distribution than those for the surface and water table fluxes. Since it is much easier to preserve volume rather than moisture distribution with the linear model, it is understandable that this solution gives the most accurate results.

5.6.3 Infiltration of Rainfall (Pre-Ponded) into Yolo Light Clay

5.6.3.1 Ponding time preliminaries

We use the soil data from Section 5.6.2.2 for Yolo Light Clay.

Initial estimates for D_* are again from Eagleson and Philip, as discussed in Section 5.6.2.1. Also there is an expression from Braester (1973) for D_* developed for preponded infiltration. It is

$$D_* = i(1 - e^{-a_2 Z})/a_2 [(\theta_{ss} - \theta_{wo}) - e^{-a_2 Z}(\theta_1 - \theta_{wo})]$$

where

$$a_2 = \frac{k}{D_*}$$

= parameter fitted for analytical $K(\psi)$ expression from

Gardner (1958)

θ_{ss} = maximum moisture content at soil surface

i = rainfall intensity

Z = depth to water table

The Braester expression is derived for $i/K(i) < 1$ (e.g., when ponding time is at infinity). It will not be used here for the

following reasons. First, its depth-dependence requires recalculation for every water table depth. Secondly, it is parameter-intensive, requiring six parameters. Thirdly, we must estimate a_2 such that it is consistent with the relation $a_2 = k/D_*$, making the estimate of D_* somewhat dependent upon itself. Fourth, it is developed by matching the exact and analytical moisture contents in the steady state which is when diffusion is least important in the process. On the other hand, it is the only expression for D_* derived for pre-ponded infiltration into a finite domain. The Philip and Eagleson estimates are more removed from the conditions of their derivation since now we have replaced the surface concentration boundary condition by the third type flux boundary condition.

Values for D_* and k are those of Section 5.6.2.3. We have $k = 8.17 \text{ cm day}^{-1}$. From Philip, $D_* = 631.41 \text{ cm}^2 \text{ day}^{-1}$ and from Eagleson $D_* = 350.84 \text{ cm}^2 \text{ day}^{-1}$. The same values of k/D_* and k^2/D_* result. These are $k/D_* = 0.0129 \text{ cm}^{-1}$ and $k^2/D_* = 0.1057 \text{ day}^{-1}$ from Philip, and $k/D_* = 0.0233 \text{ cm}^{-1}$ and $k^2/D_* = 0.1900 \text{ day}^{-1}$ from Eagleson.

An important feature of the numerical model is that we use a third type (flux) surface boundary condition and input the rainfall rate; we input an event duration much larger than the expected ponding time to ensure that the ponding time will be reached. The analytical solution uses a hydrostatic initial condition as the uniform initial condition produces unrealistically large values for t_0 . The hydrostatic initial condition is also more physically reasonable since ponding time

is sensitive to the value of the surface moisture content and to the shape of the moisture distribution.

5.6.3.2 Ponding time results

By fitting a single parameter to the "data" (i.e., numerical results), a good agreement between the numerical model and the analytical, linear ponding time expression [Equation (4.122), method 1] has been achieved over a wide range of water table depths, as depicted in Figure 5.14. When $i/K_1 = 2$, by setting $i^0 (=i/k) = 3.5$, and using the Philip expressions for k and D_* , we find the percent difference between the numerical and analytical solutions ranges from 63% for the smaller water table depths ($Z \leq 1.0\text{m}$) to 2% for depths around 9 meters. In essence, this is using k as a separate fitted parameter, distinct from its use in D_*/k and D_*/k^2 , where we define $k_1 \equiv k = .025 \text{ cm hr}^{-1}$.

If the value of i^0 is not fitted to the non-linear data, values of the linear ponding time five times greater than the non-linear ones are predicted if the same i/K_1 is used for both the linear and non-linear models. Also, the ponding time expression is sensitive to D_* and k . Using the Eagleson D_* estimate produces larger ponding time estimates than when the Philip estimate is used.

Having fit the parameter $i^0 = i^0(i)$ for a specific value of rainfall intensity, i , we test to see if it must be adjusted for each separate value of i . Using the previously fitted $k_1 (= .025 \text{ cm hr}^{-1})$ and $i/K_1 = 10$ or $i = .4428 \text{ cm/hour}$, we calculate $i^0 \approx 17.5$ and input it into the linear model. The result, also shown in Figure 5.14, gives

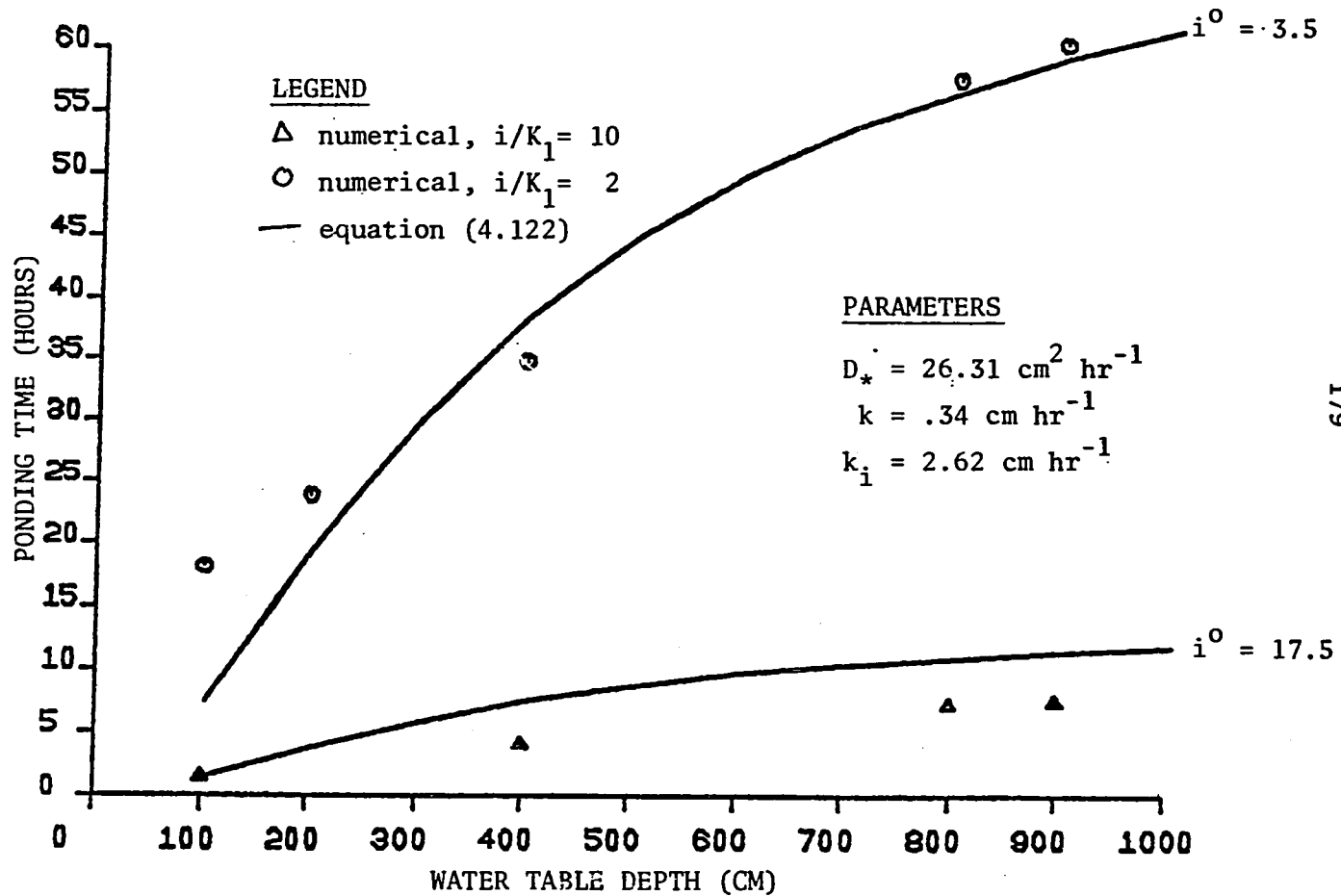


Figure 5.14: INFILTRATION COMPARISON OF PONDING TIME EQUATION (4.122) WITH THE NUMERICAL NON-LINEAR SOLUTION: SENSITIVITY TO WATER TABLE DEPTH AND RAINFALL INTENSITY ($n_e = .26$, hydrostatic θ_0 , Philip's D_* , $n = 100$)

reasonable agreement between the numerical and analytical models. The range of error is from 8% near $Z = 1\text{m}$ to 41% near $Z = 10\text{m}$. We conclude that using D_* and k estimates from Philip and fitting k_i over a range of water table depths we may vary the value of i somewhat without needing to readjust the value of k_i . Thus, the parameters D_* , k and k_i are independent of water table depth and of rainfall intensity.

The reason we need the third parameter, k_i , for the ponding time expression is that the approximations involved in deriving t_0 result in the equation preserving the solution form, if not the ponding time actually predicted by the linear model. The difference is seen in Figure 5.5 for very shallow tables and increases for deeper ones. That the approximate model matches the non-linear reality reasonably well indicates that the approximate solution contains some of the essential structure of the relation between water table depth, rainfall intensity and the ponding time.

The ponding time expression tested here (4.122) is derived from the constant surface flux infiltration model. Ponding occurs when the soil surface first saturates. Surface saturation never occurs when $i/K_1 < 1$. This approximate ponding time solution also indicates this phenomenon. When $i/K_1 < 1$, the argument of the logarithm in the solution dips below zero preventing a solution from being calculated.

The ponding time expression (4.131) developed from the time compression approximation (method 2) does not produce realistic ponding times. The reason is that the solution for the surface infiltration rate does not converge as $t \rightarrow 0$ (see Section 5.4.2), and the ponding

time expression is a function of the initial surface flux. However, the form of the solution is useful in that it expresses ponding time using parameters of the Horton infiltration capacity model. As these parameters are functions of water table depth in the finite domain solution we may explore their structure in order to develop simplified ponding time expressions which include water table effects. This is attempted in Appendix A.

5.6.3.3 Average moisture content for rainfall infiltration

where $i/K_1 < 1$

We can produce a very good agreement between the analytical, linearized solution and the numerical non-linear solution for the average moisture content under rainfall infiltration [Equation (4.166), (4.78)], as seen in Figure 5.15. However we still must use the third, fitting parameter, k_i . Using a rainfall rate of $i/K_1 = 1/2$ for the numerical model, we get a near perfect fit for the linear solution with $i^0 = 0.4$ for $Z = 1$ meter. This corresponds to a fitted value of $k_i = 0.055$ cm hr^{-1} . Using the Philip D_* for $Z = 1$ meter, the maximum percent difference between the linear and non-linear solutions in a 100 hour infiltration period is 5%. For $Z = 2\text{m}$, same parameters produce a fit with a maximum percent difference at 21% in 100 hours and of 10% for the first 50 hours. As with the ponded infiltration average moisture content, the ability of the linear model to predict the average water content for $Z = 2$ meters with the same parameters as for $Z = 1$ meter indicates the linear solution structure contains some important aspects of the dynamic relationship between the water table depth and the

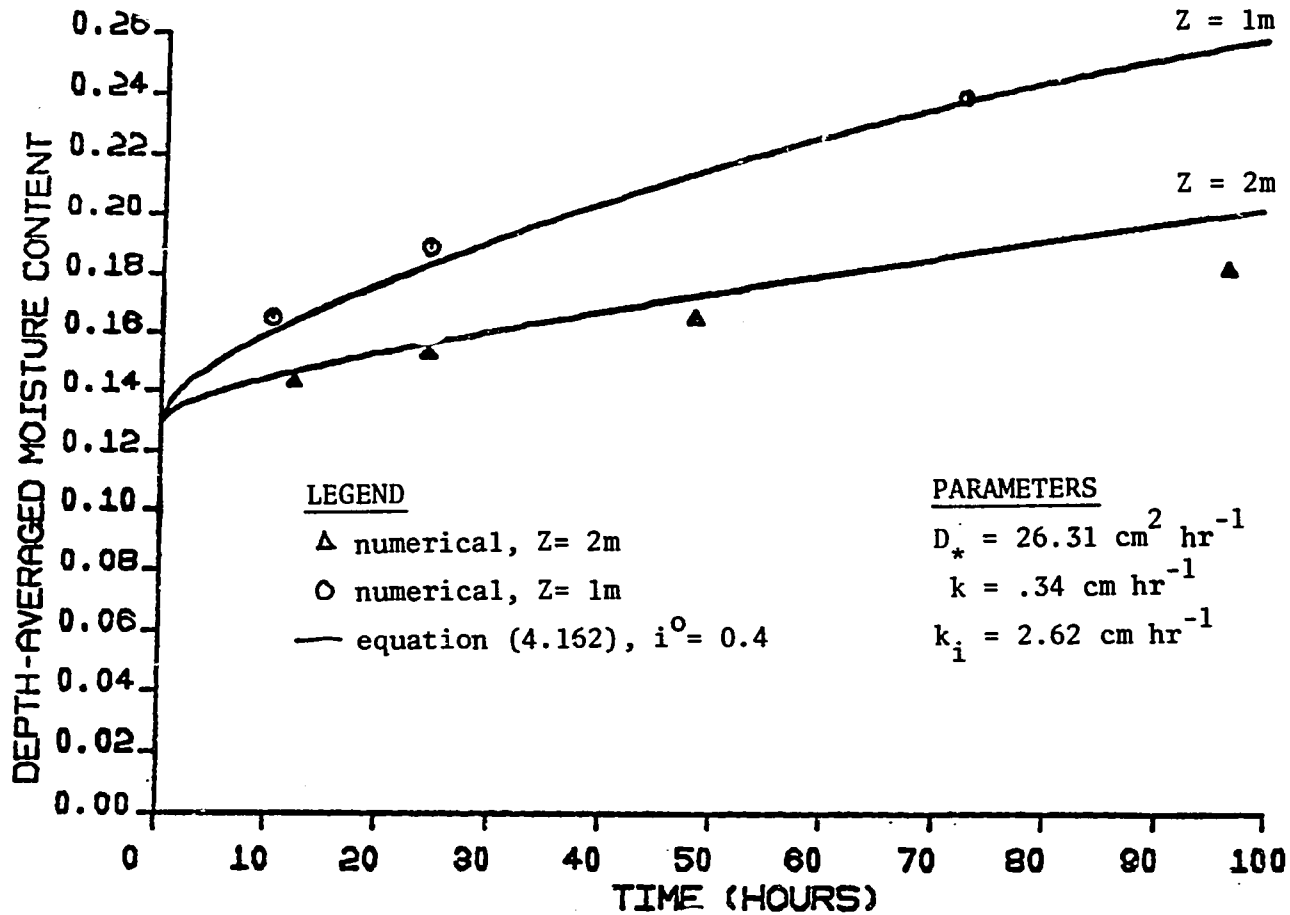


Figure 5.15: INFILTRATION COMPARING EQUATION (4.166) WITH THE NUMERICAL NON-LINEAR SOLUTION USING FITTED i^0 : ($n_e = .26$, uniform $\theta_o = .13$, PHILIP'S D_* , $n = 100$)

average moisture content.

It is both convenient and interesting that the analytical solution fitted the non-linear one so well using physically-based parameter expressions for D_* and k . This is somewhat surprising since the expressions for D_* and k are not only derived for the semi-infinite domain, but also for ponded infiltration.

Chapter 6

CLIMATE-WATER TABLE COUPLING6.1 Introduction

In addition to affecting the hydrologic budget, the saturated and unsaturated soil moisture zones also interact to determine the water table response to regional climatic conditions. Three questions of interest are:

1. How and when does the climate affect the phreatic surface (water table) shape?
2. How and when does the phreatic surface affect the hydrologic budget of the soil moisture zone?
3. How and when do environmental changes affect the water table and hydrologic balance?

This study is concerned with the development of long-term steady-state conditions where the soil moisture zone is distinct from the capillary fringe, unlike the case of the previous chapters. It is also limited to flow in the liquid phase.

One way to determine if the climate is governing the phreatic surface is to derive the water table shape that develops from climatic forcing and compare it to the measured surface. For example, if the climate forcing yields a recharge mound and the observed water table is concave upward, a leaky aquifer or significant pumping may be the cause.

This analysis uses models of the unsaturated and saturated zones with relatively few data requirements and with small computational

costs. The analysis is useful as a preliminary tool to assess long-term results from local climate or project-related changes in the environment such as large drainage or pumping schemes.

6.2 Literature Review

The interactions between climate and the water table are of interest to a wide range of researchers in hydrology. These include the groundwater hydrologist interested in the groundwater quantity available for pumping; the hydrologist interested in surface runoff, and surface water quantity; the agricultural and drainage engineers interested in soil moisture levels and water tables near the land surface; the regional water planner interested in annual and long-term water abstractions; and those involved with groundwater quality, who are interested in the filtering of recharge water in the unsaturated zone (Freeze and Cherry, 1979), (Rushton and Ward, 1979). There are also those investigating the hydrologic impact of non-stationary climates.

All these researchers have different criteria for whether the climate is having an impact on the water table elevation. The criteria are concerned first with what constitutes a change in the water table elevation. This involves both the magnitude of the change and the time scale over which the change occurs. It also concerns whether the change is measured with respect to the land surface or the aquiclude. For example, the agricultural engineer is concerned with the daily small fluctuations of the water table compared with its depth from the land surface. The groundwater resource long range planner is concerned with changes in the long run water supply. Water table changes of concern to

to him must be significant in comparison with the aquifer thickness (Hillel, 1980), (Rennolls et al, 1980), (Vandenberg, 1980), (Metzger and Eagleson, 1980).

The influence of the climate on the water table is evaluated with respect to all the sources of water supplying the aquifer and to the sinks removing water. This involves establishing clear boundaries for the problem between which we measure the water table depth. Next we assess the relative contribution of moisture to or from the water table from each source or sink. These include vertical boundaries such as rivers and contiguous aquifers, and horizontal boundaries including leakage at the bottom and pumping out net recharge at the top (Bear, 1979). Exactly how the climate affects the groundwater table depends on the local topography, geology and soil properties.

The local climate affects the water table in two ways. Local runoff contributes to the river water levels. In a humid climate at least, fluctuations in these levels affect the water table shape. Local climate directly interacts with the water table through net recharge and capillary rise. Where the contributions to the groundwater regime from these sources are significant, they must be reflected in models of the system.

A variety of methods have been used to estimate net recharge to and capillary rise from the water table, but few other than the most complex models have considered the feedback between the groundwater table and the recharge and capillary rise (Kovács, 1969). The standard method of estimating recharge is through the water balance of the soil

moisture zone (Freeze, 1979). Few models account for the capillary rise (Hillel, 1980), and in most of these models recharge is estimated from a water balance that does not consider the soil moisture content. That is, they are empirically, rather than physically based (Kovács, 1969)(Chow, 1963). The equation used is

$$p_N = p - e_T - r_s \quad (6.1)$$

where

p = precipitation rate

e_T = evapotranspiration rate

p_N = recharge rate

r_s = surface runoff

and where p , e_T and r_s are all estimated. Because of the absence of change in soil moisture storage, these models are limited to average annual or long-term estimates. At the other extreme are three-dimensional models of the coupled saturated-unsaturated zones including storage change, with hydraulic head and moisture content as dependent variables and where every change in the climate boundary is felt (Freeze, 1971). This method, while informative about the exact dynamics of soil moisture movement, is expensive to implement and requires much data and costly verification.

For regional groundwater studies or regional studies including the effects of the water table on soil moisture content, a simplified physically-based model of the soil moisture zone dynamics coupled with a simple groundwater model could be a useful middle ground. A physically-

based model may reduce some of the uncertainty associated with recharge rates and phreatic surface levels (Dettinger, 1979). A detailed, physically-based water balance model developed by Eagleson (1978a) provides estimates of average soil moisture levels, either annually or long-term, assuming a stationary climate and no annual storage carryover in either the soil moisture zone, or the groundwater zone. Using the estimated soil moisture content drainage rates are estimated. This model indirectly accounts for the water table level through the capillary rise function. This, in turn, affects the soil moisture content and recharge rate. The model is expanded by Metzger and Eagleson (1980) to account for seasonal and annual storage changes.

The model of Metzger and Eagleson explicitly considers the feedback between groundwater table elevation and the soil water balance. Since its primary concern is with the vertical moisture balance of the unsaturated zone, the groundwater regime is modelled as a linear reservoir.

The goal of the present analysis is to study the feedback effects in more detail, with the primary emphasis on the groundwater zone.

6.3 Problem Formulation and Assumptions

6.3.1 Problem Statement

The problem is to couple a horizontal groundwater flow model with a vertical soil moisture model to assess the effects of their interactions. The horizontal groundwater flow model is derived from Darcy's Law and the continuity equation, as was done for the soil moisture flow

model of the previous analysis.

With an interest in the climate-groundwater interactions, we posit a simple groundwater model, with flow only in the x-direction, bounded by two rivers and recharged from the soil water zone, as shown in Figure 2.3. Using this model, the consequences of changing river levels over time and net accretion from the soil water zone may be studied.

The time-varying non-linear governing equation is

$$\frac{\partial}{\partial x} (K(1)h \frac{\partial h}{\partial x}) + Q_N(s_o, h(x)) = S_y \frac{\partial h}{\partial t} \quad (6.2)$$

where

Q_N = net accretion rate into the aquifer

$K(1)$ = saturated hydraulic conductivity

h = height of water table above reference level

x = distance from boundary where head is h_o

S_y = specific yield of aquifer

s_o = space and time average local soil moisture content

6.3.2 Groundwater Model Assumptions

This model assumes

1. Essentially horizontal flow (Dupuit assumption); valid in the regions

$$2h_o \leq x \leq L - 2h_L \quad (6.3)$$

excluding the regions around the local minimum or maximum water table

levels where

h_0, h_L = boundary heads (river surface elevations) above
reference level

2. Isotropic aquifer

3. Constant specific yield (in time)

A linearized version of this model solved analytically for an infinite domain has been used by Polubarinova-Kochina (1962) to study the growth and damping of a groundwater mound. The model does not consider climate-water table interactions.

The boundary conditions are two potentials which represent rivers assumed fully penetrating to the aquiclude. They are described mathematically by

$$h(0) = h_0(t) \quad (6.4)$$

$$h(L) = h_L(t) \quad (6.5)$$

The initial condition is the assumed initial phreatic surface elevation,

$$h(x, 0) = h_0(x) \quad (6.6)$$

The model implicitly assumes that the specific yield is independent of the water table depth. This assumption is decreasingly accurate as the water table approaches the land surface (Hillel, 1980).

The model of net accretion over the duration of a year is written

$$Q_N(s_0, Z) = m_T P_N - T_1 w \quad (6.7)$$

where

m_T = mean annual rainy season length

T_1 = number of days per year capillary rise occurs

6.3.3 Capillary Rise Model

The steady state capillary rise is derived from Gardner's (1958) solution to the (steady state) diffusion equation for a fixed water table and a dry land surface. The expression is

$$w = K(1) [1 + 1.5(mc-1)^{-1}] [\psi(1)/Z]^{mc}, \quad w/e_p < 1 \quad (6.8)$$

where

m = pore size distribution index

c = pore disconnectedness index

We extend the use of the solution to unsteady cases where steady state capillary rise occurs much sooner than the aquifer response time. Typically capillary rise reaches steady state over a period of days or months while we are interested in annual and longer term water table trends (Skaggs, 1978), (Bear, 1979). For annual or seasonal water table fluctuations when storage changes in the aquifer are significant, we may use the modification of Metzger and Eagleson (1980) which is

$$\bar{w} = [1 + mc(\frac{\Delta Z}{Z})] w_0, \quad \frac{\Delta Z}{Z} \ll 1 \quad (6.9)$$

where

\bar{w} = seasonal (annual) average capillary rise rate

w_0 = long-term average capillary rise rate

ΔZ = water table fluctuations from the long-term mean

Z = long-term average water table depth

6.3.4 Percolation Rate Model

The percolation rate model, derived from the Brooks and Corey (1964) model of the effective intrinsic permeability, states

$$p_N(s_o) = K(1)s_o^c \quad (6.10)$$

The space and time average soil moisture content, s_o , is computed from a statistical-dynamic formulation of the water budget for an arbitrary hydrologic system (Eagleson, 1978a-f). It is a dimensionless, analytical representation of the one-dimensional annual water balance based on simplified models of the various interacting hydrologic subprocesses.

The model assumptions are the following (Eagleson, 1978a):

1. General

- a. One-dimensional analysis (only vertical processes) is used
- b. No consideration is given to snow or ice.
- c. All processes are stationary in the long-term average.

2. Precipitation

- a. Storm series is represented by Poisson arrivals of independent and identically distributed rectangular pulses.
- b. Average interstorm period is much greater than average storm duration.
- c. Interstorm period and storm duration are statistically independent.

3. Soils

- a. Soils are homogeneous.
- b. Movement of water vapor is not considered.
- c. Column is effectively semi-infinite as far as surface processes are concerned.
- d. Infiltration, exfiltration, percolation, and capillary rise from water table are formulated separately and their fluxes are linearly superimposed.
- e. Carryover moisture storage (or deficit) from storm to interstorm period (and vice versa) is neglected with internal moisture at the start of every period being s_0 , the space and time average in the surface boundary layer.

4. Vegetation (natural systems only)

- a. Transpiration occurs at the potential rate.
- b. Rate of soil moisture extraction by the root system is a constant throughout the soil volume above the maximum root depth.
- c. Canopy density seeks a short-term equilibrium state at which soil moisture is a maximum.
- d. In water-limited systems, species evolve in the long term toward maximum water use.

5. Infiltration and surface runoff

- a. No surface inflows from outside the region are considered.
- b. Storm intensity and duration are statistically independent.

6. Evapotranspiration

- a. Vegetation transpires at the potential rate.
- b. Potential rate of evaporation averaged over the interstorm period has a negligible coefficient of variation during the rainy season.

7. Percolation to water table

- a. Percolation is steady throughout rainy season at a rate determined by the average soil moisture, s_0 .
- b. Percolation is zero during dry season.

→ 8. Capillary rise from the water table

- a. Potential rate of evaporation is much greater than rate of capillary rise from water table.
- b. Dry surface matrix potential is much greater than saturated matrix potential.

→ 9. Miscellaneous

- a. Water table is constant (no carryover groundwater storage from year-to-year).
- b. Relation among annual water balance components is given to the first order by the relation among the average annual quantities.

The basic soil moisture zone water balance is

$$P_A = E_{T_A}(s_0, w, M) + R_{S_A}(s_0, w) + R_{g_A}(s_0, w) \quad (6.11)$$

where

- P_A = annual precipitation volume
 R_{sA} = annual surface runoff volume
 E_{TA} = annual evapotranspiration volume
 R_{gA} = annual groundwater runoff volume

Here

$$R_{gA} = m_{\tau} P_N(s_o) - T_1 w(Z) \quad (6.12)$$

6.4 Analytical Solutions

6.4.1 Steady State Flow with Accretion

To check the finite difference model for numerical convergence, a solution is developed for the case of steady state flow in a phreatic aquifer with accretion. Using Darcy's Law in the continuity equation, the governing equation for a homogeneous, isotropic medium is

$$K(1) \frac{d}{dx} \left(h \frac{dh}{dx} \right) + Q_v = 0 \quad (6.13)$$

where

$$Q_v = \text{uniform, distributed accretion rate}$$

and the boundary conditions are stated in Equations (6.4) and (6.5).

Q_v may include percolation, capillary rise, pumping and leakage, provided they are constant and uniformly distributed in space.

The solution to Equation (6.13) subject to Equations (6.4) and (6.5) is

$$h^2 = \frac{Q_v}{K(1)} x(x - L) - \frac{x}{L} (h_o^2 - h_L^2) + h_o^2 \quad (6.14)$$

When $h_o = h_L$, Equation (6.15) reduces to

$$K(1)(h^2 - h_o^2) - Q_v x(x - L) = 0 \quad (6.15)$$

In this case, one of the boundary conditions may be replaced by

$$\frac{dh}{dx} = 0 \quad x = L/2 \quad (6.16)$$

From Equation (6.14) in Darcy's Law, the volumetric flow rate is

$$Q(x) = \frac{K(1)}{2L} (h_o^2 - h_L^2) + Q_v L/2 - x \quad (6.17)$$

where the dimensions of $Q(x)$ are $(\text{length})^2 (\text{time})^{-1}$.

Equation (6.17) preserves mass balance which is

$$Q(o) - Q(L) = Q_v L \quad (6.18)$$

The extreme water table height between the boundaries is found from the condition

$$Q(x) = 0 \quad \text{at} \quad x = x_m \quad (6.19)$$

where

x_m = distance from $x = 0$ to the location of extreme water table height

The solution is

$$x_m = \frac{K(1)}{2Q_v L} (h_o^2 - h_L^2) + L/2 \quad (6.20)$$

which is substituted into Equation (6.15) to find h_m . When $h_o = h_L$, $x_m = L/2$.

6.4.2 Steady State Flow with Accretion and Point Pumping

Solution (6.14) may be modified to include the effect of pumping from a point source. To do this, a boundary condition is added at the pumping or recharging well location. This condition is

$$h(x) = h_a \quad 0 < a < L \quad (6.21)$$

where

a = well location

h_a = water table height at the well

The value of h_a is found by solving the continuity equation at $x = a$, which is

$$Q_p = Q_{p_I}(h_a) - Q_{p_{II}}(h_a) \quad (6.22)$$

where

Q_{p_I} = volumetric flow rate contribution from reservoir h_o to the well

$Q_{p_{II}}$ = volumetric flow rate contribution from reservoir h_L
 Q_p = pumping rate at the well

For the region $0 \leq x \leq a$, $Q_{p_I} = Q(a)$ which is evaluated from Equation (6.17), replacing h_L by h_a . For the region $a \leq x \leq L$, the volumetric flow rate is

$$Q(x) = \frac{Q_v}{2} (a + L - 2x) - \frac{K(1)}{2} \left(\frac{h_L^2 - h_a^2}{L - a} \right) \quad (6.23)$$

Substituting Equations (6.17) and (6.23) into Equation (6.22), we find

$$h_a^2 = \left[\frac{K(1)}{2} \left(\frac{h_o^2}{2} + \frac{h_L^2}{L-a} \right) - \frac{Q_v L}{2} - Q_p \right] / \left[\frac{K(1)}{2} \left(\frac{1}{a} + \frac{1}{L-a} \right) \right] \quad (6.24)$$

The condition $h_a \geq 0$ restricts Q_p to

$$Q_p < \frac{K(1)}{2} \left(\frac{h_o^2}{a} + \frac{h_L^2}{L-a} \right) - \frac{Q_v L}{2} \quad (6.25)$$

The phreatic surface is described by Equation (6.14) for the region $0 \leq x \leq a$ and by

$$h^2(x) = \frac{Q_v}{K(1)} (x-a)(x-L) + (h_L^2 - h_a^2) \left(\frac{L-x}{L-a} \right) + h_L^2 \quad (6.26)$$

for $a \leq x \leq L$.

6.4.3 Transient Flow with Accretion

We linearize Equation (6.2) to permit an analytical solution, reducing the governing equation to

$$\bar{T} \frac{\partial^2 h}{\partial x^2} + Q_v = S_y \frac{\partial h}{\partial t} \quad (6.27)$$

where

$$\begin{aligned} S_y &= \text{specific yield} \\ &= n_e \end{aligned}$$

and

$$\begin{aligned} \bar{T} &= \text{linearized transmissivity} \\ &= K(1)\bar{h} \end{aligned} \quad (6.28)$$

where

\bar{h} = average phreatic surface elevation

For this model, we assume the water table fluctuations are small compared with \bar{h} .

With boundary conditions (6.4) and (6.5) and a uniform phreatic surface initial condition described by

$$h(x, 0)/h_o = 1 + \left(\frac{h_L}{h_o} - 1\right) \left(\frac{x}{L}\right) \quad (6.29)$$

the solution (by finite Fourier transforms: Section 4.1.1) is

$$h(x, t) = h_o \left[1 + \left(\frac{h_L}{h_o} - 1\right) \left(\frac{x}{L}\right) \right] + h_t(x, t) \quad (6.30)$$

where

$$h_t(x, t) = \sum_{m=0}^{\infty} K(\beta_m, z) \exp(-\alpha \beta_m^2 t) [\bar{F}(\beta_m)] + \int_0^t \exp(\alpha \beta_m^2 t') A(\beta_m, t') dt' \quad (6.31)$$

with

$$K(\beta_m, z) = \left(\frac{2}{L}\right)^{1/2} \sin \beta_m z \quad (6.32)$$

$$\bar{F} = \left(\frac{2}{L}\right)^{1/2} \int_0^L \sin \beta_m x [h_o + (h_L - h_o)x/L] dx \quad (6.33)$$

$$A = \alpha \left(\frac{2}{L}\right)^{1/2} \int_0^L [Q_v(\sin \beta_m z)/\bar{T}] dx \quad (6.34)$$

and

$$\alpha = \bar{T}/S_y \quad (6.35)$$

An alternative solution is found in Carslaw and Jaeger (1959, ch. 3).

6.5 Finite Difference Model

6.5.1 Discretization Procedure

We discretize the governing equation (6.2) for the groundwater system using an implicit finite difference form. Starting at time, k , and block-centered node, i , the time derivative is represented by

$$\frac{\partial h}{\partial t} \approx \frac{1}{\Delta t} [h_{i,k+1} - h_{i,k}] \quad (6.35)$$

where

t = time step between times k and $k+1$

The space-derivative evaluated at time $k+1/2$ and location $i+1/2$ is represented by

$$\left(T \frac{\partial h}{\partial x}\right)_{i+1/2,k+1/2} \approx T_{i+1/2,k+1/2} \left(\frac{h_{i+1,k+1/2} - h_{i,k+1/2}}{\Delta x}\right) \quad (6.36)$$

where

$$\begin{aligned} T &= \text{transmissivity} \\ &= Kh \end{aligned} \quad (6.37)$$

and

Δx = distance between locations i and $i+1$

We let $h_{i,k+1/2}$ be the arithmetic average of the water table elevation at times k and $k+1$, which is for node $i+1$

$$h_{i+1,k+1/2} \approx \frac{1}{2} (h_{i+1,k+1/2} + h_{i+1,k}) \quad (6.38)$$

The outer spatial derivative is represented by a central difference approximation, which is for location i and time $k+1/2$

$$\frac{\partial}{\partial x} \left(T \frac{\partial h}{\partial x} \right)_{i,k+1/2} \approx \frac{\left(T \frac{\partial h}{\partial x} \right)_{i+1/2,k+1/2} - \left(T \frac{\partial h}{\partial x} \right)_{i-1/2,k+1/2}}{\Delta x} \quad (6.39)$$

We approximate the accretion rate, $Q_N(s_o, h)$ at location i by

$$Q_N \approx Q_{N_i,k+1/2} \quad (6.40)$$

Substituting Equations (6.38) and (6.36) into Equation (6.39) and Equations (6.35), (6.39) and (6.40) into Equation (6.2), the resulting discretized governing equation for node i and time $k+1/2$ is

$$\begin{aligned} & \frac{1}{2(\Delta x)^2} [T_{i+1/2,k+1/2} (h_{i+1,k+1} + h_{i+1,k}) - (T_{i+1/2,k+1/2} \\ & + T_{i-1/2,k+1/2}) (h_{i,k+1} + h_{i,k}) + T_{i-1/2,k+1/2} (h_{i-1,k+1} + h_{i-1,k})] \\ & + Q_{N_i,k+1/2} = \frac{1}{\Delta t} [S_y (h_{i,k+1} - h_{i,k})] \quad (6.41) \\ & \qquad \qquad \qquad i = 1, 2, \dots, N; k = 1, 2, \dots \end{aligned}$$

We use the harmonic average for the transmissivity in the space domain to insure continuity between nodes (Bear, 1979), which is

$$T_{i\pm 1/2,k+1/2} = \left(\frac{\Delta x_i + \Delta x_{i\pm 1}}{x_i/T_i + x_{i\pm 1}/T_{i\pm 1}} \right)_{k+1/2} \quad (6.42)$$

In general, since both the transmissivity and the accretion rate are functions of the dependent variable, h , we must solve iteratively for the water table level at each time step to check for convergence.

We first assume

$$T_{i,k+1/2} \approx T_{i,k}(h_{i,k}) \quad (6.43)$$

and

$$Q_{N_{i,k+1/2}} \approx Q_{N_{i,k}}(h_{i,k}) \quad (6.44)$$

We solve for $h_{i,k+1}$ and update $T_{i,k+1/2}$ and $Q_{N_{i,k+1/2}}$ using the arithmetic time average,

$$T_{i,k+1/2} \approx \frac{1}{2} (T_{i,k} + T_{i,k+1}) \quad (6.45)$$

and

$$Q_{N_{i,k+1/2}} \approx \frac{1}{2} (Q_{N_{i,k}} + Q_{N_{i,k+1}}) \quad (6.46)$$

We solve again for $h_{i,k+1}$ using the updated values for T and Q_N and iterate until

$$h_{i,k+1,m} \approx h_{i,k+1,m+1} \quad (6.47)$$

within an acceptable error level. Here

m = iteration number

Very few, if any, iterations should be required because the time-step should be small compared with the time domain of interest and the water balance model assumes the water table is unchanging or changing very slowly over the time period of interest.

The implicit scheme is used for the governing equation because it is unconditionally stable, meaning as Δt goes to zero the F-D solution converges to the true solution.

The boundary conditions, Equations (6.4) and (6.5) are assigned to fictitious nodes and represented by

$$h_o(t) \approx h_{o,k} \quad (6.48)$$

$$h_L(t) \approx h_{N+1,k}$$

We now have one governing equation per location node 1 through N and fixed water levels at nodes 0 and N+1. This set of N equations and N unknowns is solved by matrix methods. In matrix notation, the phreatic surface elevation at time k is written

$$[\underline{h}]'_k = \begin{vmatrix} h_{o,k} \\ h_{1,k} \\ \cdot \\ \cdot \\ h_{N,k} \\ h_{N+1,k} \end{vmatrix} \quad (6.49)$$

where

$[\underline{h}]'_k = (N+2) \times 1$ matrix of phreatic surface elevations including boundaries

The governing equation for N+2 nodes is represented in matrix notation by

$$[\underline{A}]' ([\underline{h}]'_{k+1} - [\underline{h}]'_k) = [\underline{B}]'_{k+1/2} ([\underline{h}]'_{k+1} + [\underline{h}]'_k) + [\underline{f}]'_{k+1/2} \quad (6.50)$$

$$[\underline{f}]'_{k+1/2} = \begin{bmatrix} Q_{N,0} \\ Q_{N,1} \\ \vdots \\ Q_i \\ \vdots \\ Q_N \\ Q_{N+1} \end{bmatrix} \quad (6.53)$$

where

$[\underline{f}]'$ = (N+2) x 1 matrix of net accretion values

We use our knowledge of the boundary conditions and matrix manipulation techniques to reduce the (N+2)x(N+2) matrices to NxN matrices and the (N+2) x 1 matrices to Nx1 matrices. In the process two new matrices are created to account for the boundary conditions. The resulting governing equation is

$$[\underline{A}]_{k+1/2}([\underline{h}]_{k+1} - [\underline{h}]_k) = [\underline{B}]_{k+1/2}([\underline{h}]_{k+1} + [\underline{h}]_k) + [\underline{f}]_{k+1/2} + [\underline{g}]_{k+1} + [\underline{g}]_k \quad (6.54)$$

where

$$[\underline{A}] = \begin{bmatrix} (S_y/\Delta t)_1 & & & 0 \\ & \ddots & & \\ 0 & & \ddots & \\ & & & (S_y/\Delta t)_N \end{bmatrix} \quad (6.55)$$

To use a standard matrix solver on the governing equation, we need it in the form

$$[C][x] = [b] \quad (6.63)$$

Equation (6.54) may be rewritten in this form as

$$([A] - [B])_{k+1/2} [h]_{k+1} = ([A] + [B])_{k+1/2} [h]_k + [f]_{k+1/2} + [g]_{k+1} + [g]_k \quad (6.64)$$

which means we may use a matrix solver such as the Thomas algorithm to forecast future phreatic surfaces, h_{k+1} . To do so, we let

$$[C] = ([A] - [B])_{k+1/2} \quad (6.65)$$

$$[b] = ([A] + [B])_{k+1/2} [h]_k + [f]_{k+1/2} + [g]_{k+1} + [g]_k \quad (6.66)$$

$$[x] = [h]_{k+1} \quad (6.67)$$

The problem is completely formulated with the assignment of the initial condition and landform shape. Their matrix forms are

$$[h]_0 = \text{initial water table elevation}$$

and

$$[H]_0 = \text{landform elevation}$$

The landform elevation is needed to calculate the water table depths necessary to solve for the capillary rise.

The formulation of the model permits variable distances between nodes and time steps. It also permits the aquifer properties to be inhomogeneous. Pumping and leakage may be included by modifying the accretion matrix.

The model assumes the water balance of the soil water zone is performed over the distance Δx and per unit width of the aquifer.

6.5.2 Iteration Procedure

The procedure for calculating successive water table elevations contains the steps:

1. calculate the soil moisture content over a range of water table depths. Either interpolate values of the content for depths not calculated or fit a curve to the data for use in the groundwater model.
2. input the landsurface shape function, $H(x)$
3. assign an initial water table elevation, $h_0(x)$
4. calculate the water table depth from Equation (6.3)
5. calculate matrices $[f]$, $[g]$ and $[A]$ from the water balance results, the boundary conditions, parameters and space and time steps
6. calculate $[B]_0$ from $[h]_0$
7. solve for $[h]_1$ sequentially until the steady state $[h]_{ss}$ is reached, using the matrix solver and the previous $[h]_i$ as the known phreatic surface elevation.

Any parameter or boundary condition, including $H(x)$, may change its value at any time to simulate changing conditions. Step one eliminates the need to recalculate s_0 from the water balance for each Z at each time step.

The solution procedure is simplified by compacting the $[A]$ and $[B]$ matrices by using their symmetric natures (Milly and Eagleson, 1980, p. 115). Matrix $[A]$ is condensed into

$$[A]^* = \begin{bmatrix} S_y/\Delta t & 0 \\ \cdot & \cdot \\ \cdot & \cdot \\ \cdot & \cdot \\ S_y/\Delta t & 0 \end{bmatrix} \quad (6.68)$$

and matrix $[B]$ into

$$[B]^* = \begin{bmatrix} B_{2,1} & B_{1,2} \\ \cdot & \cdot \\ \cdot & \cdot \\ \cdot & \cdot \\ \cdot & B_{1,N} \\ B_{2,N} & 0 \end{bmatrix} \quad (6.69)$$

where

$$B_{2,i} = B_2 \text{ for the } i\text{th node}$$

and

$$\begin{aligned} B_{1,i} &= B_{3,i-1} \\ &= B_1 \text{ for the } i\text{th node} \end{aligned}$$

6.5.3 Convergence Requirement

While the implicit finite-difference scheme is unconditionally stable, it would only converge to the true solution as $\Delta t \rightarrow 0$. A physically-based time-step specification reduces the guesswork in choosing one which is small enough to prevent large water table changes per time-step and large enough to minimize computational costs. Following Bear (1979, ch. 10), we start with a water balance for an

incremental slice of the aquifer domain. The water balance per unit width of aquifer is

$$\Delta t [Q_{IN_i} - Q_{OUT_i} + Q_{N_i}] = S_y \Delta x_i (h_i^{t+\Delta t} - h_i^t) \quad (6.70)$$

where

- Q_{IN_i} = volumetric flow rate into increment i
- Q_{OUT_i} = volumetric flow rate out of increment i
- Q_v = volumetric accretion, pumping and leakage rates
- h_i^t = water table height for increment i and time t

The dimensions of Q are $(\text{length})^2(\text{time})^{-1}$.

Assuming $T = Kh \approx \text{const.}$, $\Delta x_i = \text{const.} = \Delta x$, $S_y = \text{const.}$ and using Darcy's Law in Equation (6.70), we may restate Equation (6.70) as

$$\Delta t [T(h_{i+1} - 2h_i + h_{i-1})/\Delta x + Q_v] = S_y \Delta x (h_i^{t+\Delta t} - h_i^t) \quad (6.71)$$

We restrict the one time-step change in water table elevation to the initial depth to the water table by setting $h_{i+1} = h_{i-1} = 0$ and $h_i^t = -Z_i$. (Z_i = initial water table depth.) This sets the limits $-Z_i \leq h_i^{t+\Delta t} \leq 0$. Substituting these values and limits into Equation (6.71) results in

$$0 \leq \Delta t \left[\frac{T}{S_y} (\Delta x)^{-2} + \frac{Q_v}{2Z_i S_y \Delta x} \right] \leq \frac{1}{2} \quad (6.72)$$

Letting $Q_v = Q'_N + Q_p$, where $Q'_N = Q_N \Delta x$ and Q_p is the distributed pumping rate, and substituting Equation (6.10) for Q_N , we have an upper bound on the time step which is

$$\Delta t \leq (\beta/2) \left[\frac{T}{S_y} (\Delta x)^{-2} + \frac{K(1)}{S_y} (2Z_i)^{-1} \right] \quad (6.73)$$

where

β = arbitrary scaling factor

6.6 Results

6.6.1 Similarity Parameters

Certain parameters of the water balance model and the groundwater flow model simplify the analysis and evaluation of the results. For the water balance from the Eagleson model (1978a-f), the parameter describing the sensitivity of the percolation rate to the soil moisture content is

$$K(s_o)/K(1) = s_o^c \quad (6.74)$$

where

c = pore disconnectedness index

The parameter is derived from the Brooks and Corey (1966) model of the hydraulic conductivity.

The index of water table influence, a parameter of the climate and soil, indicates when the water table is too high for its effects to be superimposable in the water balance. When

$$\gamma = w/K(1) \geq 0(1) \quad (6.75)$$

the water balance model is no longer valid. We define

γ = index of water table influence

The relation for w assumes a dry land surface which is invalid for $w/e_p > 1$. The resultant water balance for $w/e_p > 1$ is also invalid.

Thus we restrict γ to

$$\gamma \leq \gamma_{\max}$$

where

$$\gamma_{\max} = e_p / K(1) \quad (6.76)$$

and

e_p = potential evapotranspiration

w = capillary rise rate

The potential influence of the water table on the volume of groundwater recharge is measured by

$$\Lambda = T_1 w / m_T K(1) \quad (6.77)$$

where

Λ = groundwater loss index

m_T = average rainy season length

T_1 = number of days/year capillary rise occurs

The actual volumetric contribution of the water table to the water balance is measured by

$$\Lambda(s_o, Z) = T_1 w(Z) / m_T K(s_o) \quad (6.78)$$

$$= T_1 w / m_T K(1) s_o^c \quad (6.79)$$

which may vary considerably from Λ depending on s_o and c .

The maximum value of this parameter is defined by

$$\Lambda_m(s_o) = T_{1p} e / m_{\tau} K(1) s_o^c \quad (6.80)$$

The primary parameter of the groundwater system, derived from a mass balance of a cross-section of the phreatic aquifer, is t/τ where

$$\begin{aligned} \tau &= \text{characteristic residence time of water in aquifer} \\ &= S_y L / K(1) \end{aligned} \quad (6.81)$$

and

$$\begin{aligned} S_y &= \text{specific yield of the aquifer} \\ L &= \text{length of aquifer} \end{aligned}$$

This parameter is also a measure of the time scale over which the boundaries of the aquifer interact. When

$$t/\tau \geq 0(1) \quad (6.82)$$

the boundaries are completely interacting.

The parameter $(h_o - h_L)/L$ provides a measure of the average hydraulic gradient of the groundwater system. If

$$(h_o - h_L)/L \geq 0(.01) \quad (6.83)$$

the Dupuit approximation of essentially horizontal flow may be invalid.

The parameter x/L is a convenient measure of distance where
 x = distance from reservoir of height, h_o

6.6.2 Water Balance Results

6.6.2.1 Climate-induced water table shape

Examination of the value of the net accretion to a water table,

represented by $\Lambda(s_o)$ or $\Lambda_m(s_o)$, produces much information about the shape of the water table and the influence of climate on its shape. We define $\Lambda_m(s_o)$ as the index of potential climate-induced water table shape, a climate-soil-vegetation parameter, where s_o is the long-term steady state soil moisture. With $\Lambda_m(s_o)$ expressed by Equation (6.80), only when $\Lambda_m(s_o) \geq 1$ is a climate-induced steady state water table depression possible. Conversely, only when $\Lambda_m(s_o) < 1$ is a climate-induced steady state swamp possible. A climate-induced water table depression is formed when the capillary rise rate exceeds the percolation rate.

The index of climate-induced local water table shape, $\Lambda(s_o)$, a climate-soil-vegetation parameter defined by Equation (6.79), indicates whether a region (in which the water table is shaped by climate rather than aquifer properties) actually has a recharge mound, or a water table depression. When

$$\Lambda(s_o) \geq 1 \quad : \quad \text{climate-induced water table depression} \quad (6.84)$$

$$\Lambda(s_o) \leq 1 \quad : \quad \text{climate-induced recharge mound} \quad (6.85)$$

The special case of $\Lambda(s_o) = 1$ indicates the location of the maximum climate-induced water table depression or mound. The local extremum is defined by

$$\frac{\partial h(x)}{\partial x} = 0 \quad (6.86)$$

Equation (6.86) states that no horizontal flow crosses the extremum section, as was also noted by Equations (6.16) and (6.19). For a long-term steady state water table, shaped solely by the local climate,

neglecting pumping and leakage, the water balance at the extremum section also restricts vertical flow to

$$Q_N = 0 \quad (6.87)$$

where

Q_N = vertical recharge and capillary rise rates

Substituting Equation (6.7) for Q_N in Equation (6.87) results in

$$T_1 w = m_\tau p_N \quad (6.88)$$

or

$$\Lambda(s_o) = 1 \quad (6.89)$$

Substituting Equations (6.8) and (6.10) into Equation (6.88) yields a useful $s_o(Z)$ relation. First we have

$$T_1 K(1) B[\psi(1)/Z]^{mc} = m_\tau K(1) s_o^c \quad (6.90)$$

which is rewritten as

$$s_o = (T_1/m_\tau)^{1/c} B^{1/c} [\psi(1)/Z]^m \quad (6.91)$$

where

$$B = 1 + 1.5(mc - 1)^{-1} \quad (6.92)$$

This $s_o(Z)$ relation for $\Lambda(s_o) = 1$ is a function of the soil type through m , c , $\psi(1)$ where $c = c(m)$. It is a function of climate

through m_τ (and through e_p when $\Lambda(s_o) = \Lambda_{\max}(s_o)$). This relation assumes a fixed water table.

Equation (6.91) is plotted in Figures 6.1 and 6.2 for the four representative soils of Table 6.1. In Figure 6.1, we use $m_\tau = T_1$ and in Figure 6.2, we use $m_\tau = T_1/2$. These cover the range of most rainy season lengths. Since $s_o = s_o(w)$, a maximum value of s_o occurs for $w = e_p$. To eliminate this climate dependence, we set e_p (in each case) such that the maximum soil moisture is $s_o = 1$. For $m_\tau = T_1$, the plotted equations are, for the soil data of Table 6.1 and $w < e_p$

$$s_o = 0.74 Z^{-.222} \quad \text{Clay} \quad (6.93)$$

$$s_o = 0.66 Z^{-.286} \quad \text{Clay loam} \quad (6.94)$$

$$s_o = 1.50 Z^{-.667} \quad \text{Silt loam} \quad (6.95)$$

$$s_o = 4.24 Z^{-2} \quad \text{Sandy loam} \quad (6.96)$$

Each relation, $s_o(Z)$ for a given soil type, m_τ and e_p is referred to as a chart. Care must be made in using these to define the s_o at which $w = e_p$. Values of s_o for water table depths from the land surface where $w > e_p$ are invalid. The cutoff minimum valid water table depth is defined by

$$Z = \psi(1) \left(\frac{e_p}{BK(1)} \right)^{-1/mc} \quad (6.97)$$

The most appropriate use of these charts is to ascertain whether a measured water table depression is climate-induced. For a given soil type, e_p , m_τ and the measured maximum water table depression,

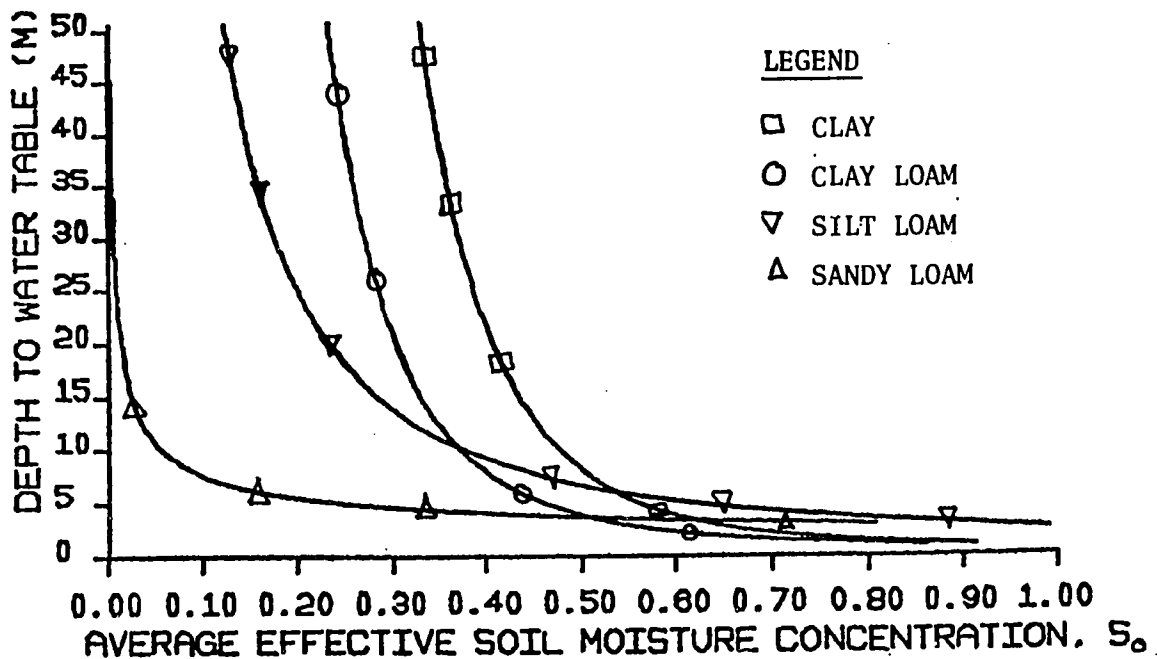


Figure 6.1

WATER BALANCE EQUILIBRIUM WITH NO NET ANNUAL RECHARGE AND A YEAR LONG RAINY SEASON ($\Lambda = 1$)

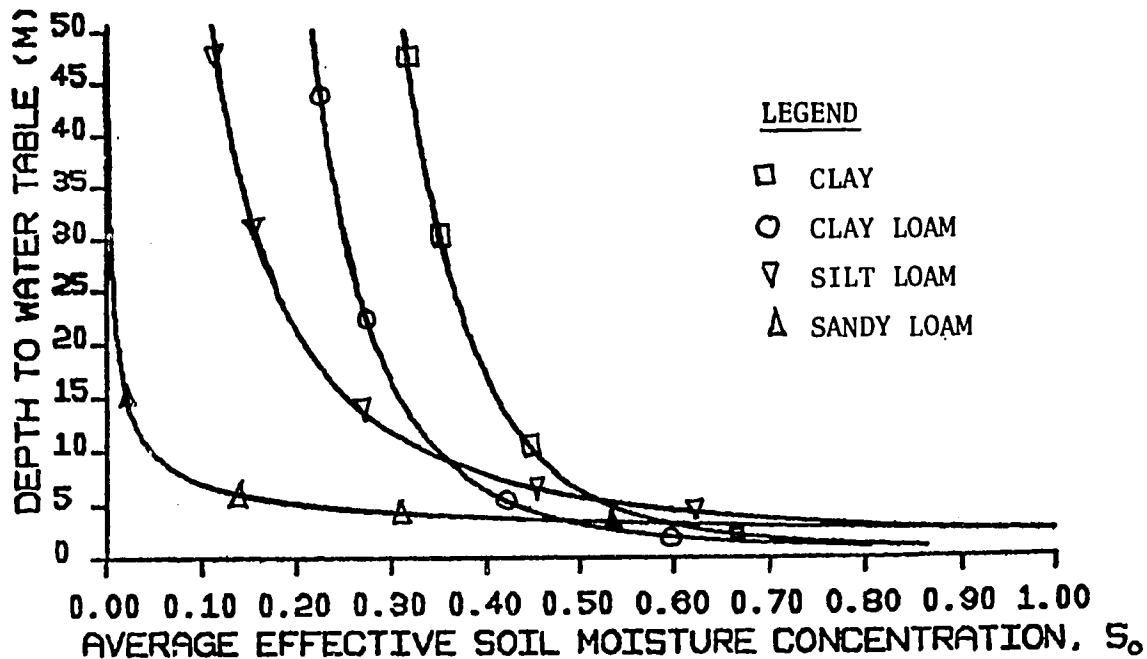


Figure 6.2

WATER BALANCE EQUILIBRIUM WITH NO NET ANNUAL RECHARGE AND A HALF YEAR RAINY SEASON ($\Lambda = 1$)

the corresponding long-term average soil moisture content is as given by Figure 6.1 and Equations (6.93) to (6.96). This is associated with the type of climate-soil-vegetation system (CSVs) necessary to drive the water table to that depth from climate forcing alone. To the extent that the s_o calculated from the water balance is greater than the value from this chart, alternative mechanisms, such as pumping or leakage are responsible for the depression. When $\Lambda_m(s_o) > 1$, the climate plays at least some role in the depression formation, however. When the s_o calculated from the water balance is less than that from the chart, either the water table has not reached its climate-induced maximum depth or the hydraulic conductivity of the aquifer is large so that equilibrium between the flow from the boundaries and net water loss is reached before $Q_N = 0$.

The charts (Figure 6.1) are also useful to determine whether a recharge mound is climate-controlled or transmissivity controlled. When $\Lambda_m(s_o) < 1$, the recharge mound is limited by the hydraulic conductivity of the soil. When $\Lambda_m(s_o) > 1$, the water table will rise until $\Lambda(s_o) = 1$ unless steady state has not yet been reached or recharge is in equilibrium with the flow to the boundaries (as in the water table depression case). The charts are used in the same way for recharge mounds as for the water table depressions.

The charts may also be used to deduce s_o in some cases. Knowing Z , e_p and m_τ , if we suspect the depression or mound is climate-controlled and $\Lambda_m(s_o) \geq 1$; we may find the corresponding s_o from the chart.

	Clay	Clay Loam	Silty Loam	Sandy Loam
m	.222(12)	.286(10)	.667(6)	2(4)
$\psi(1)$ (cm)	25	19	166	200
K(1) (cm/s)	8.28×10^{-6}	2.32×10^{-5}	9.94×10^{-5}	2.08×10^{-4}
n_e	.45	.35	.35	.25

Table 6.1

SOIL PARAMETERS

[Eagleson, 1978c]

An example of this method is taken from the El-Gizera (EG) region of Sudan (between the White and Blue Niles south of Khartoum), a region of irrigated agriculture. A maximum water table depression of 100 meters has been measured. Available data for the actual soil are given in Table 6.2 and lie between the clay-loam and the silty-loam of Table 6.1. For the listed m_T , the condition $\Lambda(s_o) = 1$ is fulfilled by the relation

$$s_o = 1.18Z^{-.388} \quad w < e_p$$

From Figure 6.3, a climate-induced water table depression of 100 meters requires a soil moisture content of 0.2 or less. The calculated El-Gizera water balance using the data from Table 6.2 and $Z = 100$ gives $s_o = 0.4$. This indicates that the climate could account for only a 15 meter steady state depression and we must look to another mechanism to account for the bulk of the depression. We must also note that liquid moisture capillary rise may not be sustainable for such large water table depressions anyway.

For this example, the restriction $w/e_p < 1$ limits $Z \leq 3.92$ m and $s_o \leq 0.695$, using Equation (6.97).

6.6.2.3 Water table-dependent quantities for CSV systems

Each climate-soil-vegetal system (CSV) has curves of $s_o(Z)$, $p_N(Z)$ and $w(Z)$ from which are derived curves of $Q_N(Z) = p_N - w$ which indicate the sensitivity of the water balance and the accretion rate to the water table depth. These curves answer the questions of when the water balance may neglect the water table and when net accretion into the

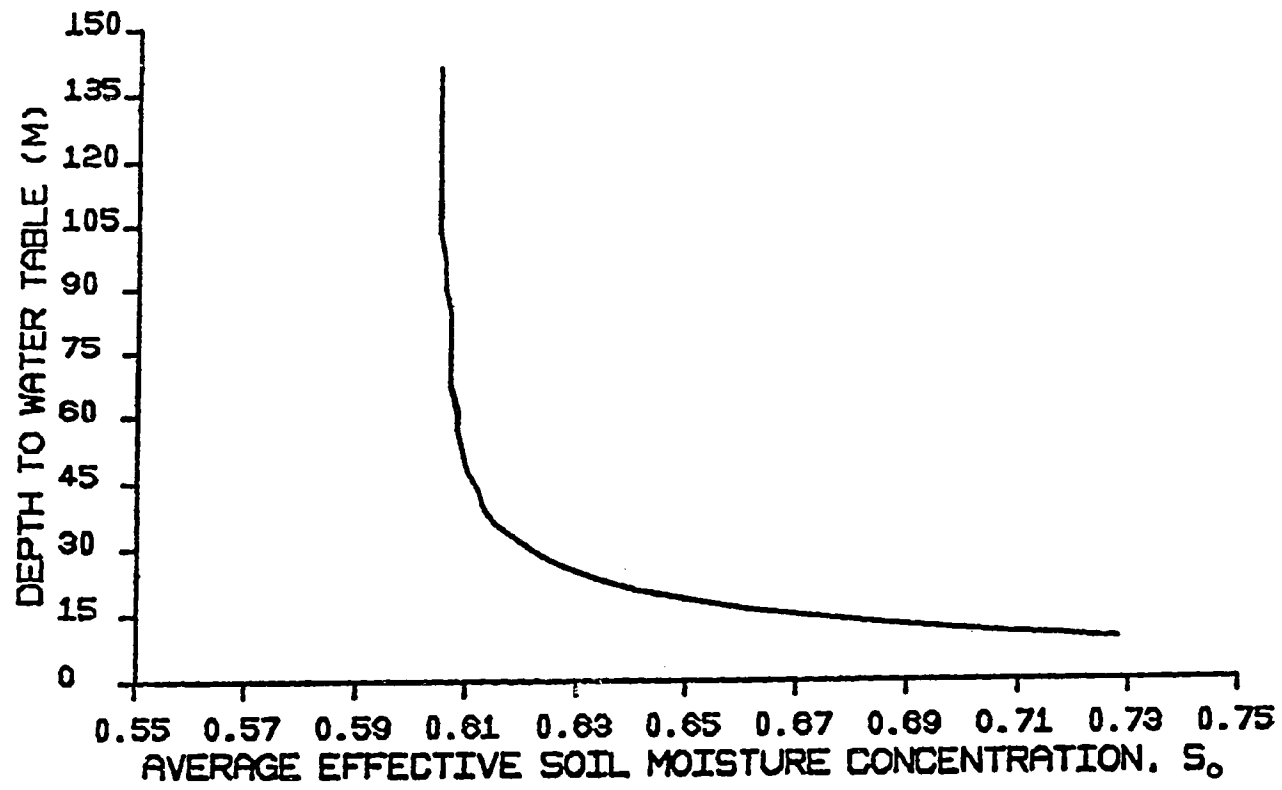


Figure 6.3

WATER BALANCE EQUILIBRIUM WITH NO NET ANNUAL RECHARGE
 FOR EL-GIZERA SOIL ($\Lambda = 1$, $T_1 = 157$ days, $e_p = 1.6$ m/year)

groundwater system may be assumed uniformly distributed in space. They also show the maximum water table depth for which a climate-controlled steady state water table depression or recharge mound will occur.

Curves of $s_o(Z)$, $p_N(Z)$, $w(Z)$ and $Q_N(Z)$ are presented in Figures 6.4 to 6.11 for a wide range of CSVS. The data used are listed in Table 6.2. The Bahr el Ghazal region and the Machar Marshes are large swamplands in the south of Sudan. The Bahr el Ghazal data are averaged for six catchments surrounding the central swampland using the physical parameters given by Chan and Eagleson (1980). The Machar data are averaged from five catchments (El-Hemry, 1980).

Figures 6.4 to 6.8 show how the steady state water balance, represented by s_o , varies with the water table depth. The moisture content decreases with lower water tables because the soil moisture supplies the evaporation demand not supplied by the deeper water table.

The steady state soil moisture content is bounded by a maximum

$$\lim_{Z \rightarrow Z_{\min}} s_o(w) = s_{o,\max}(e_p) \quad Z = Z_{\min} \text{ for } s_o < 1$$

and a minimum

$$\lim_{Z \rightarrow \infty} s_o(w) = s_{o,\min}(0) \quad Z_{\max} \leq Z$$

where Z_{\min} may be exactly calculated from Equation (6.97) and the associated s_o is found from the water balance with $Z = Z_{\min}$.

A comparison of $s_o(Z)$ for a sub-humid climate and an arid one reveals trends in the sensitivity of the water balance to the water table depth. Figures 6.4 and 6.5 show that s_o varies over a wider range of

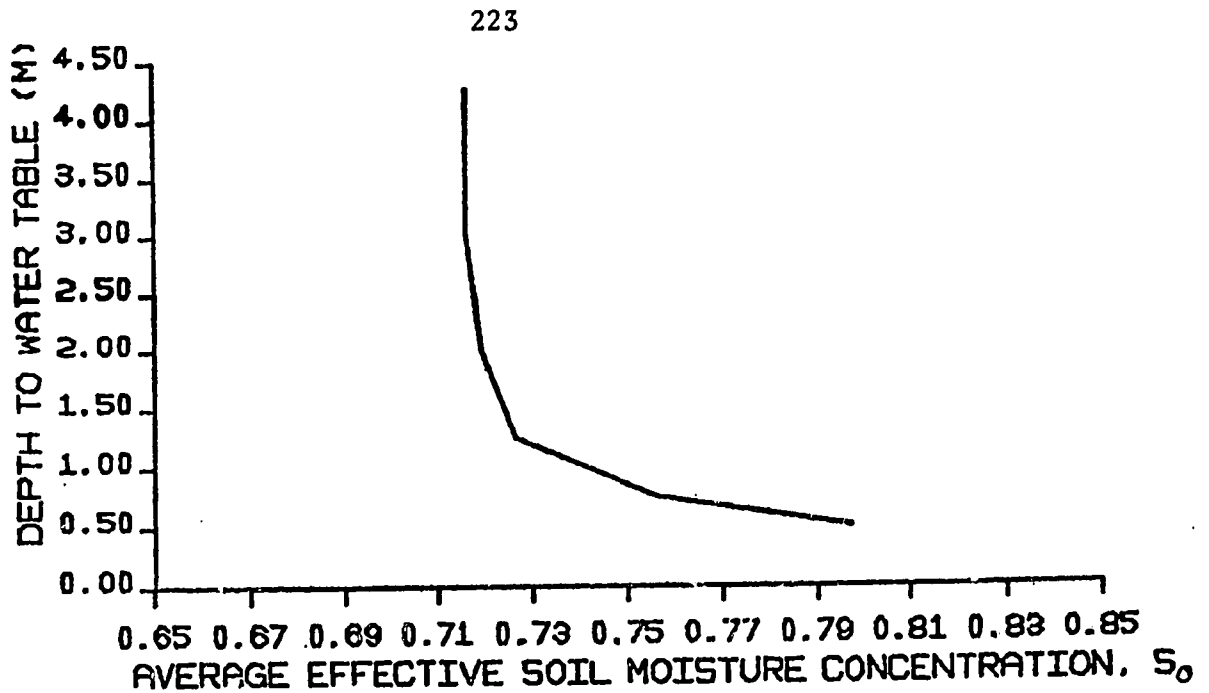


Figure 6.4

WATER TABLE-DEPENDENT WATER BALANCE, CLINTON, MA

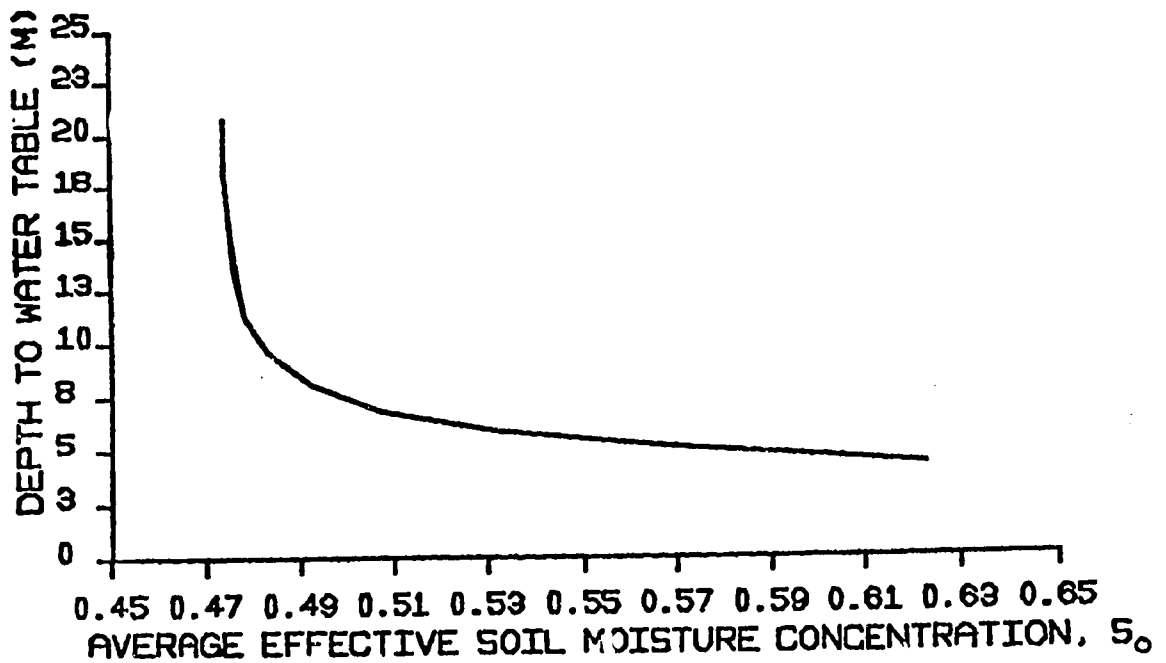


Figure 6.5

WATER TABLE-DEPENDENT WATER BALANCE, SANTA PAULA, CA

values and is dependent on Z for deeper water tables with an arid climate. For the arid climate (Santa Paula, CA), $0.47 < s_0 < 0.62$ and Z is influential for about 10 meters. For the sub-humid climate (Clinton, MA), $0.72 \leq s_0 < 0.8$ and Z is important for the first two meters.

These results are physically reasonable. One expects higher s_0 values with more precipitation and moisture contributions from deeper water tables with larger potential evaporation rates. The influence of deeper water tables for Santa Paula is also due to the larger value of $\psi(1)$, a soil property.

The effects of an unusual CSVS are seen in the $s_0(Z)$ relation for the Bahr el Ghazal region plotted in Figure 6.6. The result of a large evaporation rate and an unusual soil type is a water balance that is sensitive to water table depths of over 100 meters.

The very arid climate of the El-Gizera CSVS demonstrates a great sensitivity of the water balance to the water table depth but negligible sensitivity to the quantity of vegetal cover, M . Figure 6.7 shows that the $s_0(Z)$ relation is identical regardless of whether the vegetal cover has a fixed value or an "optimal" value chosen (Eagleson, 1978) to maximize soil moisture, M_0 . This observation is only valid for values of M close to M_0 . Figure 6.8 is the plotted $s_0(Z)$ relation with the optimal vegetal cover for each s_0 as noted on the graph.

The water table depths used in the steady state water balance to generate Figures 6.4 to 6.8 are themselves the result of an equilibrium achieved between the climatic conditions, local geometries, and the properties of the soil, particularly the aquifer conductivity.

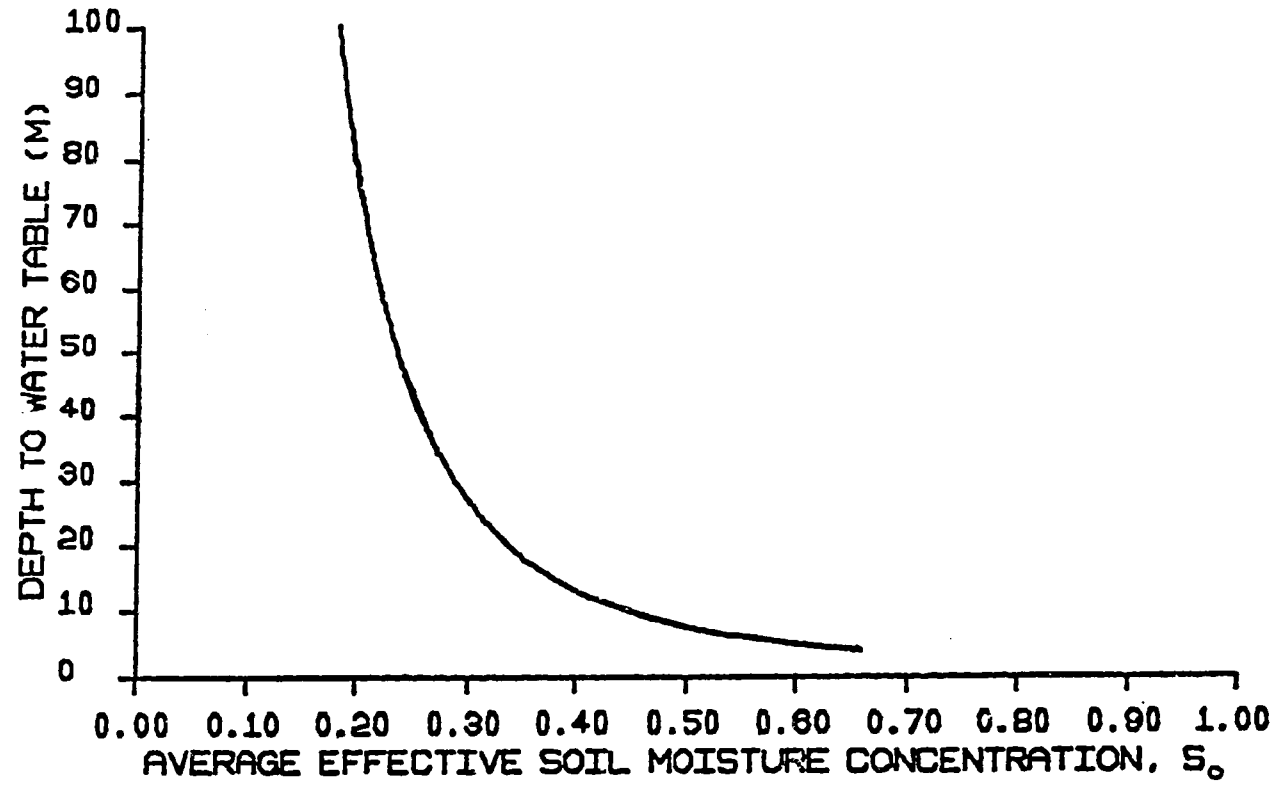


Figure 6.6

WATER TABLE-DEPENDENT WATER BALANCE, BAHR EL GHAZAL

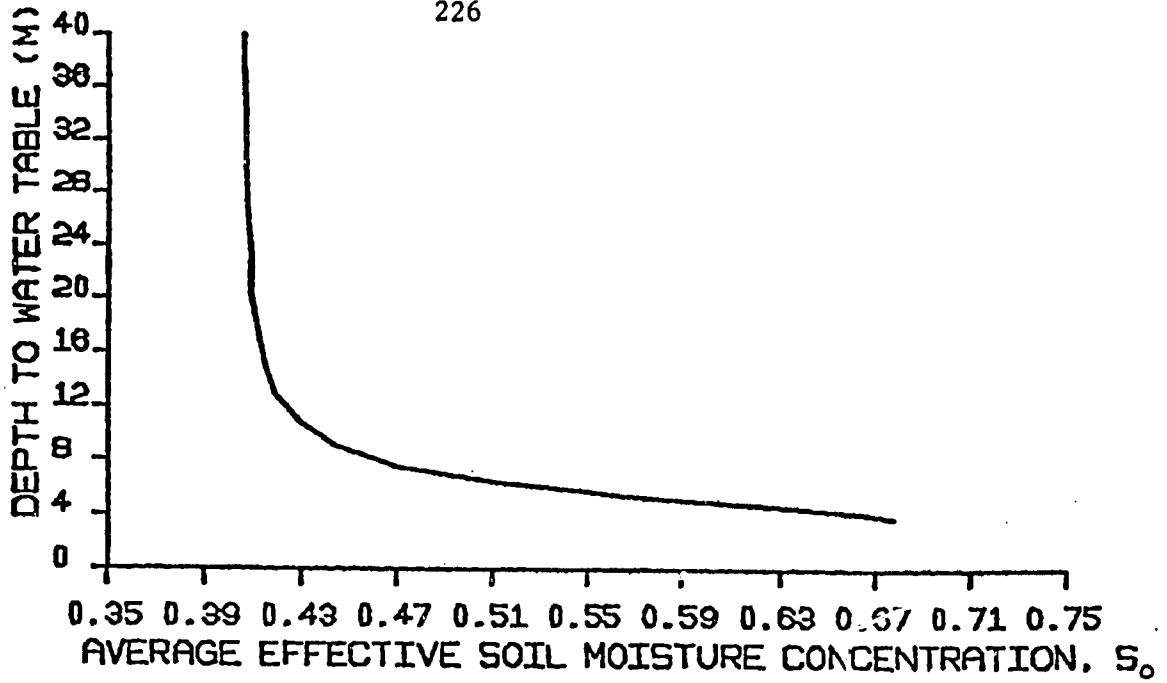


Figure 6.7

WATER TABLE-DEPENDENT WATER BALANCE, FL-GIZERA, SUDAN

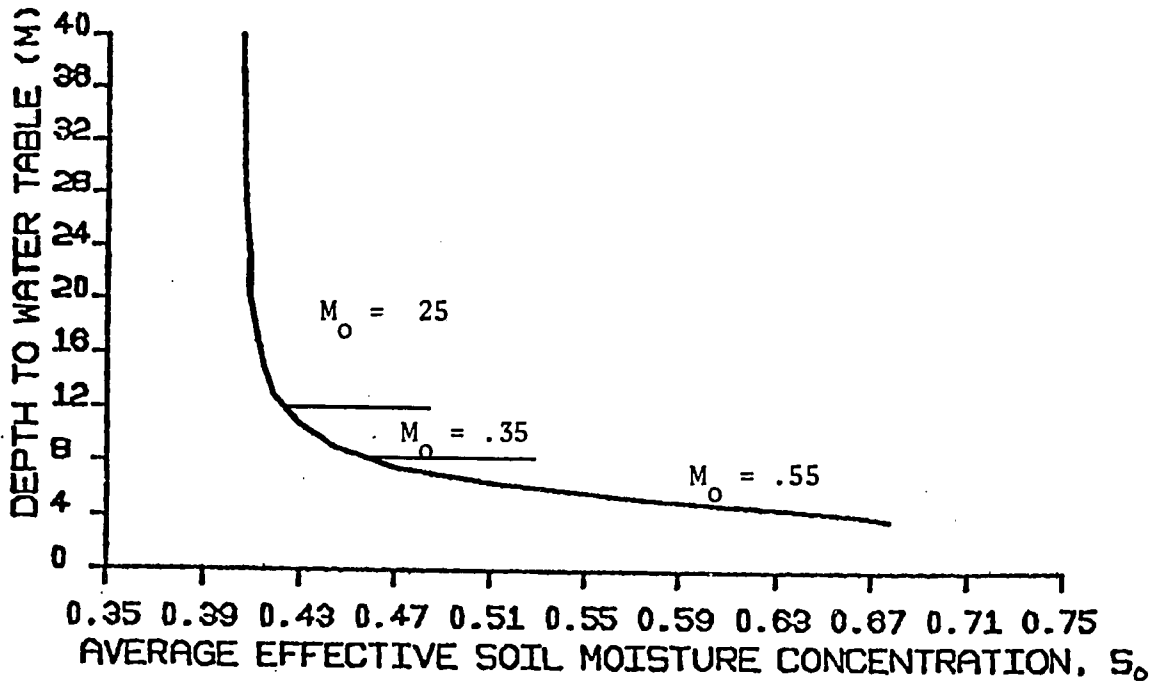


Figure 6.8

WATER TABLE-DEPENDENT WATER BALANCE, EL-GIZERA ($M = M_o$)

	El-Gizera	Santa Paula, CA	Machar Marshes	Clinton, MA	Bahr el Ghazal
<u>Climate</u>					
P_s (cm)	41.61	53.4	90	94.1	118.1
m_v	49.1	15.7	75	109	81.4
m_H (cm)	.85	3.4	1.21	.86	1.44
m_{tr} (days)	.063	1.43	.05	.32	.05
m_{tr}^r (days)	3.2	10.42	2.61	3	3.08
m_{tr}^b (days)	157	212	197	365	255
m_i (cm/hr)	.565	.100	1.01	.084	1.20
κ	1.16	.25	.47	.50	.97
e_p (cm/hr)	.0183	.0114	.013	.0063	.0175
h_o (cm)	.15	.10	1.13	.10	.30
\bar{T}_a (°C)	29.74	13.8	27.5	8.4	26.3
<u>Soil</u>					
n_e	.35	.35	.35	.35	.35
$m(c)$.388(8.2)	.20(13)	.286(10)	.667(6)	.28(10.1)
$K(1)$ (cm/sec)	2.32×10^{-4}	$1. \times 10^{-4}$	$1. \times 10^{-4}$	$2. \times 10^{-5}$	4.5×10^{-4}
$\psi(1)$ (cm)	100	166	65	19	129
<u>Vegetation</u> (initial values)					
k_v	1.02	1.	1.	1.	1.
M	.3	.4	.4	.8	.78

Table 6.2
WATER BALANCE DATA

Source: El-Gizera (Cairo U., Dept. of Hydrology); Santa Paula, CA and Clinton, MA (Eagleson, 1978e,f); Machar Marshes (El-Hemry and Eagleson, 1980); Bahr el Ghazal (Chan and Eagleson, 1980)

The basic question when analyzing $Q_N(Z)$ is when may we assume $Q_N(Z)$ to be independent of water table depth. Comparing Figures 6.9 and 6.4 for a sub-humid climate shows as expected that Q_N is dependent on water table depth over the same depth range as is $s_o(Z)$. We may assume $Q_N = \text{const.}$ for $Z > 4$ meters for the sub-humid Clinton, MA, CSVS and for $Z > 18$ meters for the arid Santa Paula, CA, CSVS.

Figures 6.9 and 6.10 show that the accretion rate, Q_N , increases with Z because the capillary rise decreases faster than does the percolation rate with increasing depth to the water table.

Figures 6.11 and 6.12 are for a case where $\Lambda_m(s_o) > 1$, the El-Gizera CSVS. For elevations above that at which $\Lambda(s_o) = 1$ (Figure 6.11) there is a net water loss. Below this depth (Figure 6.12), there is a net water table recharge. For the net water loss case, Q_N follows the shape of the capillary rise (Figure 6.11).

The water balance data for the above curves are generated from a computer program written in FORTRAN by Chan (1980) and modified to vary the water table depth and allow for negative groundwater runoff.

6.6.3 Results of Coupled Groundwater-Water Balance Models

6.6.3.1 Methodology

The water balance model generates a file of water table depths and accretion rates to or from the water table. This is input into the groundwater finite-difference model.

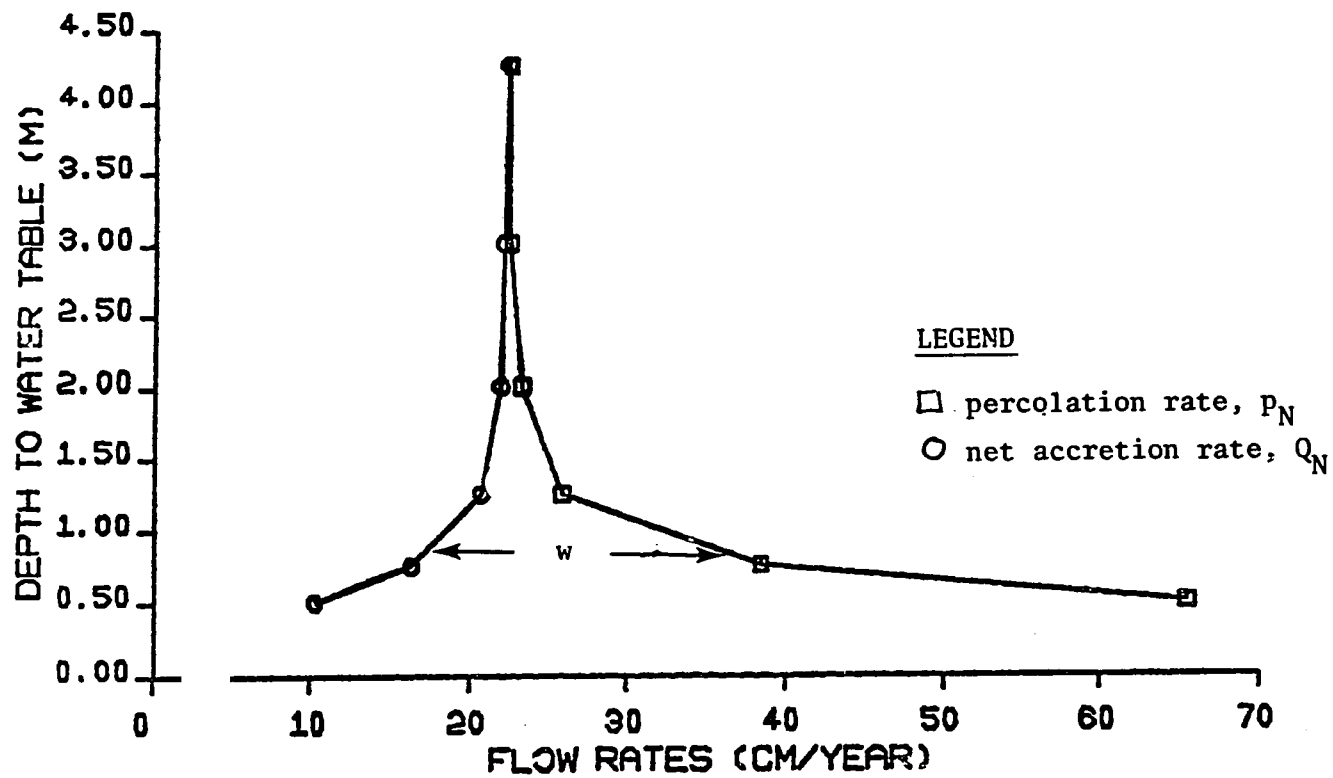


Figure 6.9

WATER TABLE-DEPENDENT RECHARGE RATES, CLINTON, MA.

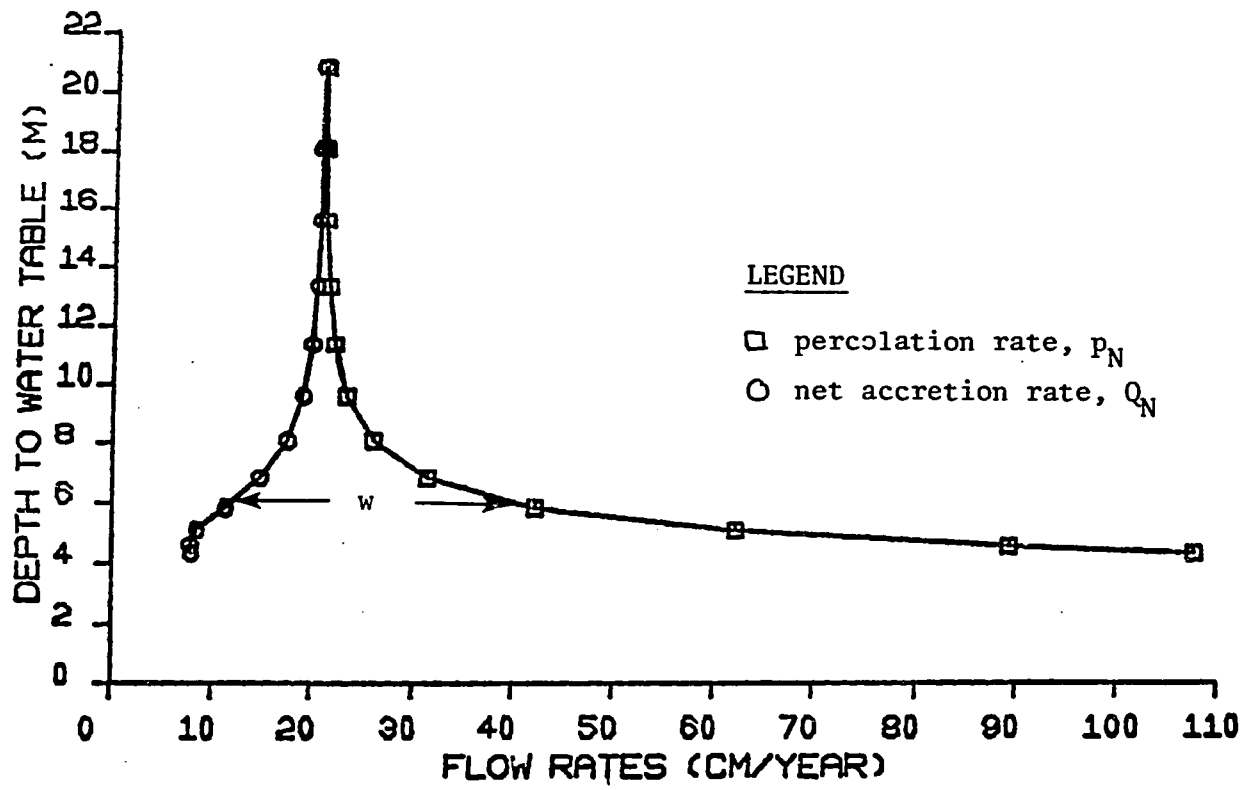


Figure 6.10

WATER TABLE-DEPENDENT RECHARGE RATES, SANTA PAULA, CA.

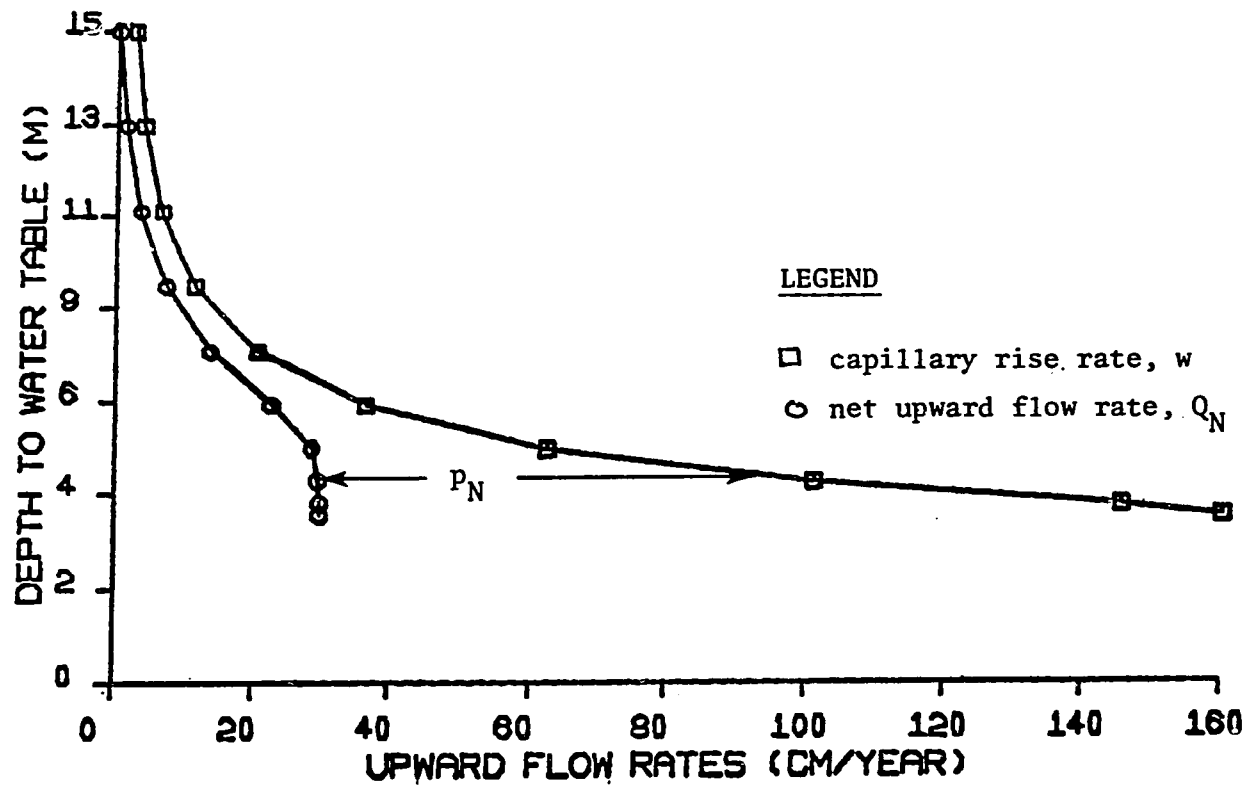


Figure 6.11

WATER TABLE-DEPENDENT WATER LOSS RATES, EL-GIZERA, SUDAN

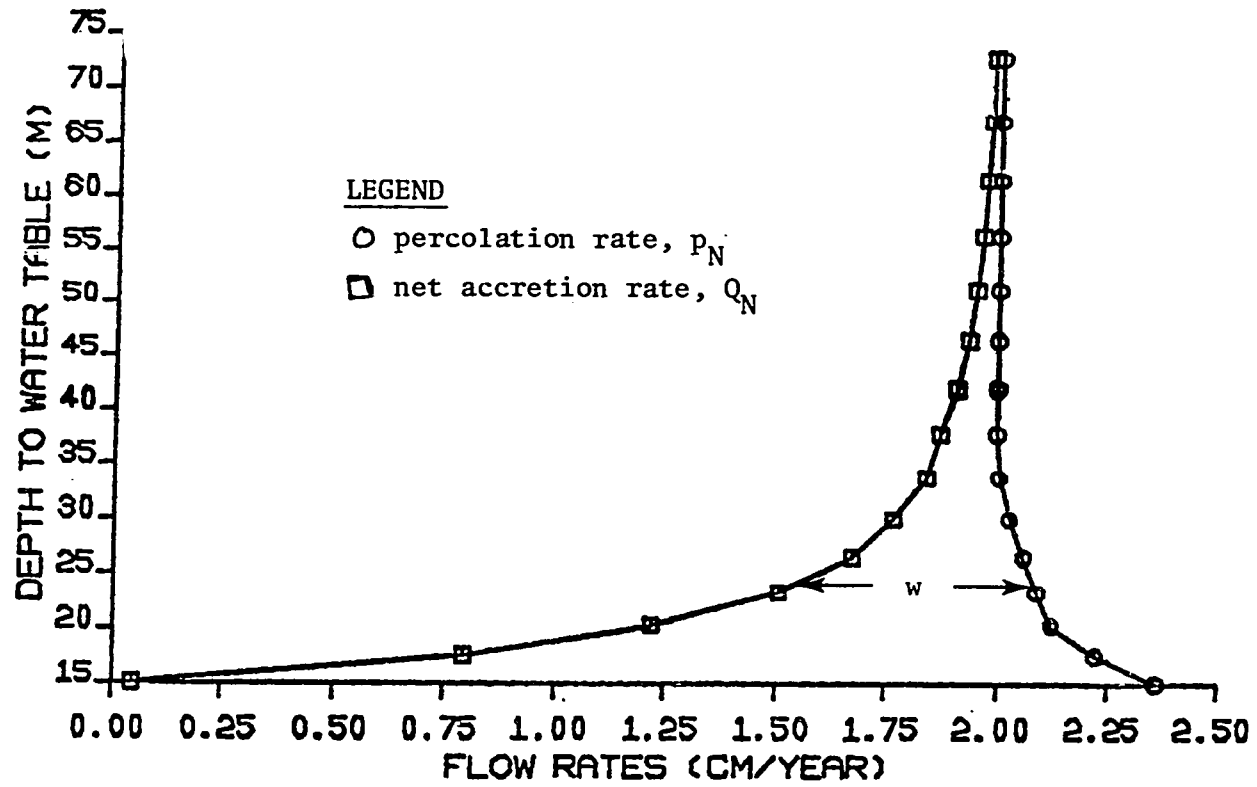


Figure 6.12

WATER TABLE-DEPENDENT RECHARGE RATES, EL-GIZERA, SUDAN

6.3.3.2 Results

Tests of the coupled groundwater-water balance model show the dependence of the shape and depth of a steady state water table depression on the distance between the lateral boundaries (rivers in this case) and on the aquifer hydraulic conductivity. A comparison of Figures 6.13 and 6.14 using the El-Gizera CSVS data of Table 6.2 and the aquifer data of Table 6.3 shows that the water table is flatter and deeper for the larger distance between the rivers. Comparing Figures 6.14 and 6.15 for the same distance between rivers but different $K(1)$ shows that the steady state water table is deeper for the smaller $K(1)$.

These results are sensible when considering what mechanisms result in steady state water table configurations. In this example, the only water sources are the rivers and aquifer storage and the only water demand is from the climate.

Starting from a horizontal phreatic surface at $t = 0$, the water table falls initially at a rate which is uniform everywhere except close to the rivers where a gradient is formed. This gradient causes flow from the rivers toward the center. Until this flow (and accompanying gradient) reaches any interior section, climate demand at that section can only be met through extractions from aquifer storage which produce a falling local water table. Depending upon the dimensions and conductivities involved, the falling water table may reduce climate demand to zero (i.e., $p_N = w$) before the encroaching gradient-induced river flow reaches the section. Such a case is climate-controlled and there will be a section of horizontal phreatic surface in the steady state (see for example Figure 6.13).

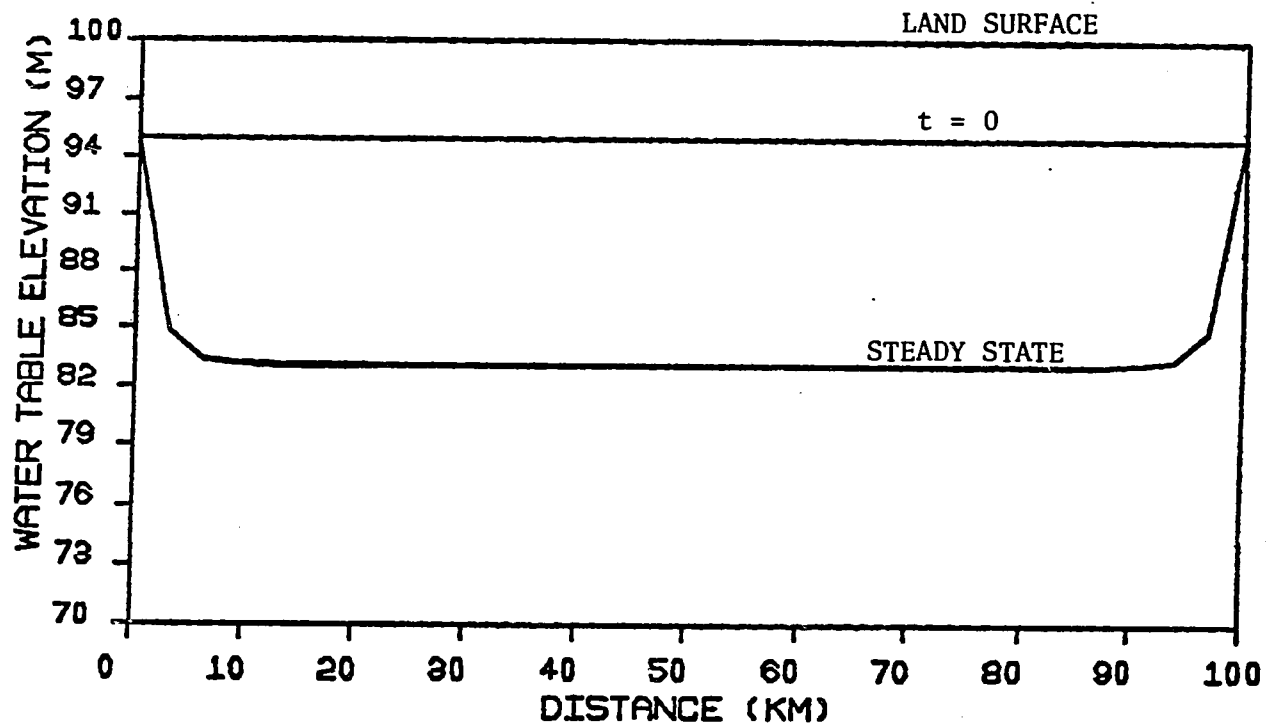


Figure 6.13

CLIMATE-INDUCED STEADY-STATE WATER TABLE DEPRESSION, EL-GIZERA, SUDAN
 (L = 100 km, $K_1 = 73$ m/year, t = 500 years)

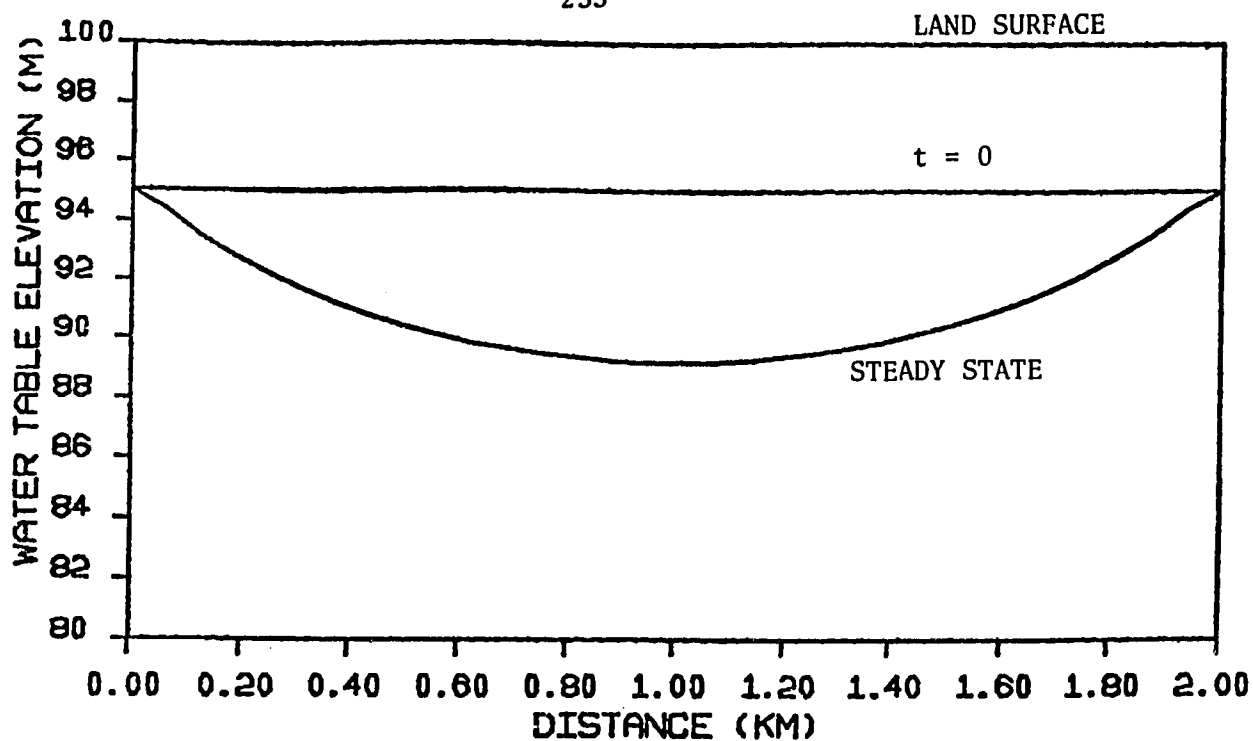


Figure 6.14

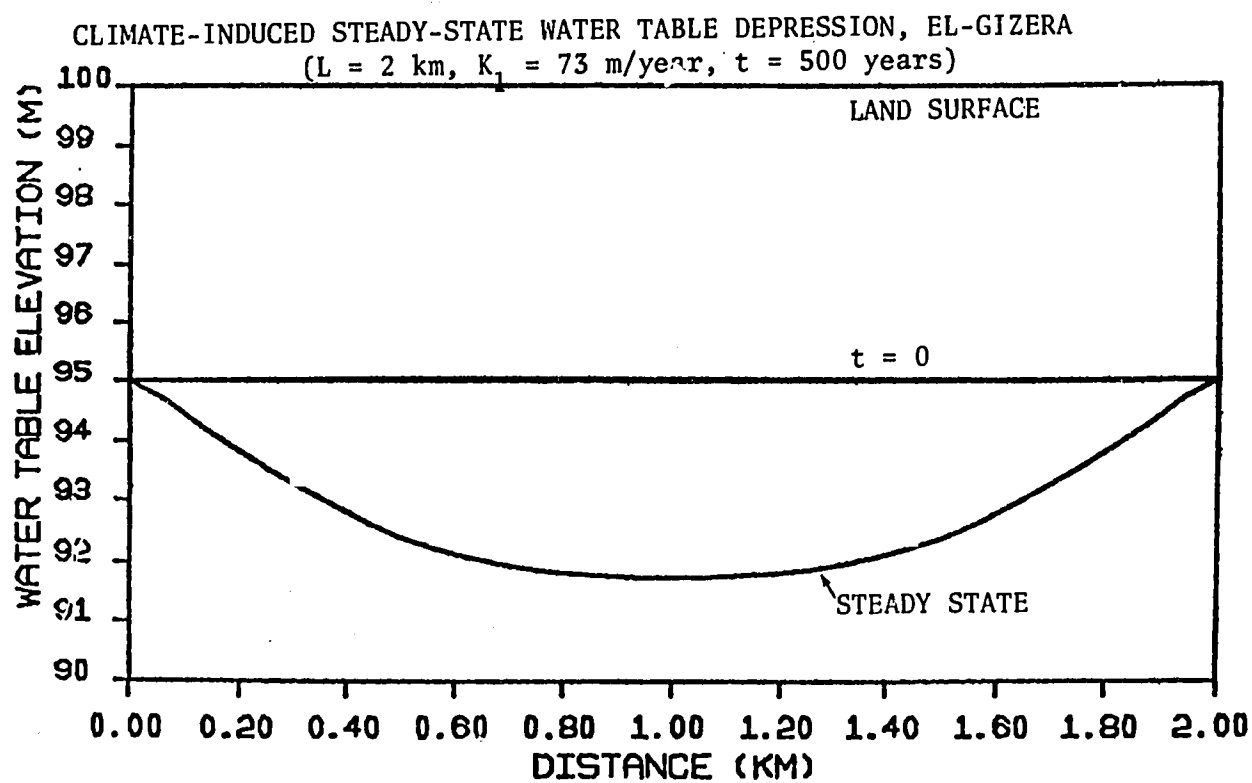


Figure 6.15

CLIMATE-INDUCED STEADY-STATE WATER TABLE DEPRESSION, EL-GIZERA
($L = 2$ km, $K_1 = 365$ m/year, $t = 500$ years)

If flow from the two rivers reaches the center of the aquifer then the entire phreatic surface is curved. Such a case is called gradient-controlled. The steady state maximum depression is less than in the climate-controlled case, and at the section of maximum depth $w > p_N$. When $K(1)$ is large, the flow supplies the entire aquifer length more quickly than when $K(1)$ is small. Also, when the aquifer length is smaller the water flow from the rivers supplies the entire aquifer sooner.

A comparison of Figures 6.13 and 6.14 also shows that the variability of Q_N with water table depth is more important with shorter aquifer lengths. For shorter lengths, there is much more variability of Z with respect to x .

In all three cases, it takes about 500 years for the new steady state water table to develop.

The shape of the steady state water table is also dependent on the land surface shape and on the initial water table slope. The steady state water table shape in Figure 6.16 follows that of the land surface. The result is a central mound in a generally-depressed water table. The effect of the sloped initial water table is the shift of the extreme water table depths in the direction of the initial water flow.

The question of what causes a 100 meter water table depression in the El-Gizera region of Sudan is possibly answered if pumping is added to the water demands on the aquifer. It is shown in Figure 6.17 that a pumping rate of $1 \times 10^5 \text{ m}^2/\text{yr}$ applied over a 42-year period for the 100 km distance between the Blue and White Niles produces a water table drop of about 100 m starting from an initially shallow water table and a gentle

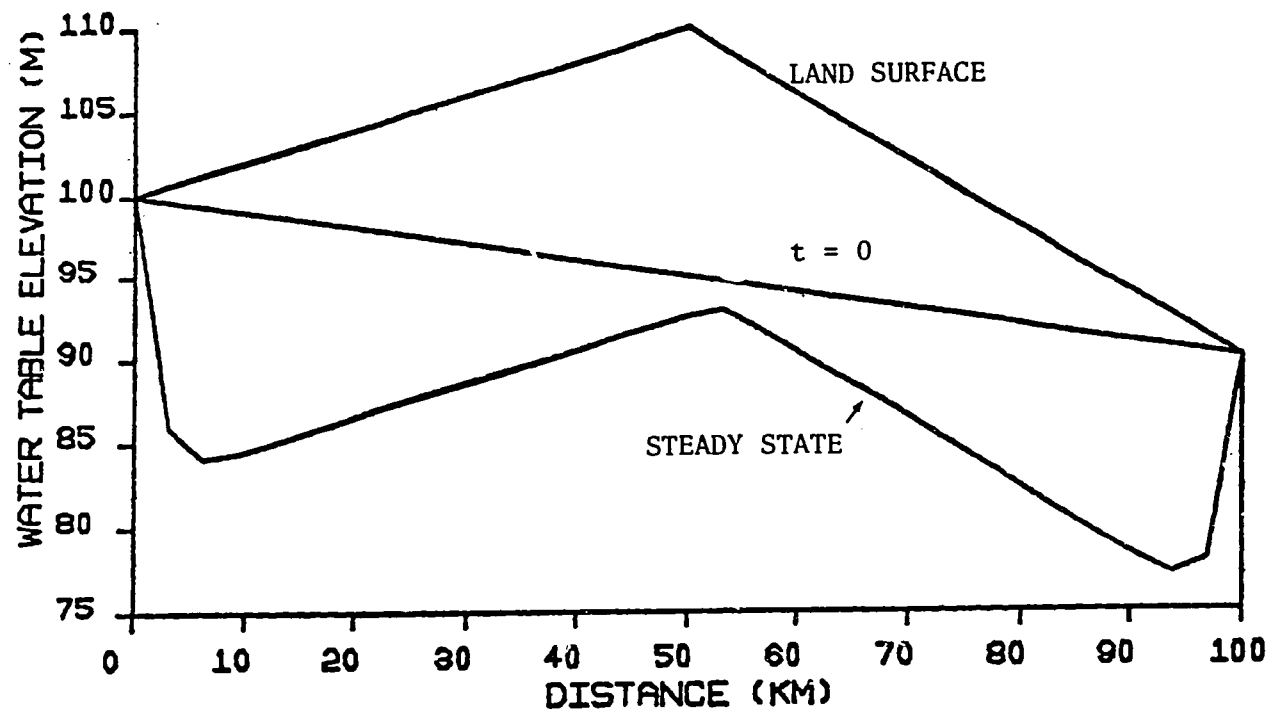


Figure 6.16

CLIMATE-INDUCED STEADY-STATE WATER TABLE SHAPE
 WITH NON-UNIFORM LAND SURFACE AND INITIAL WATER TABLE SLOPE, EL-GIZERA, SUDAN
 ($L = 100$ km, $K_1 = 73$ m/year, $t = 500$ years)

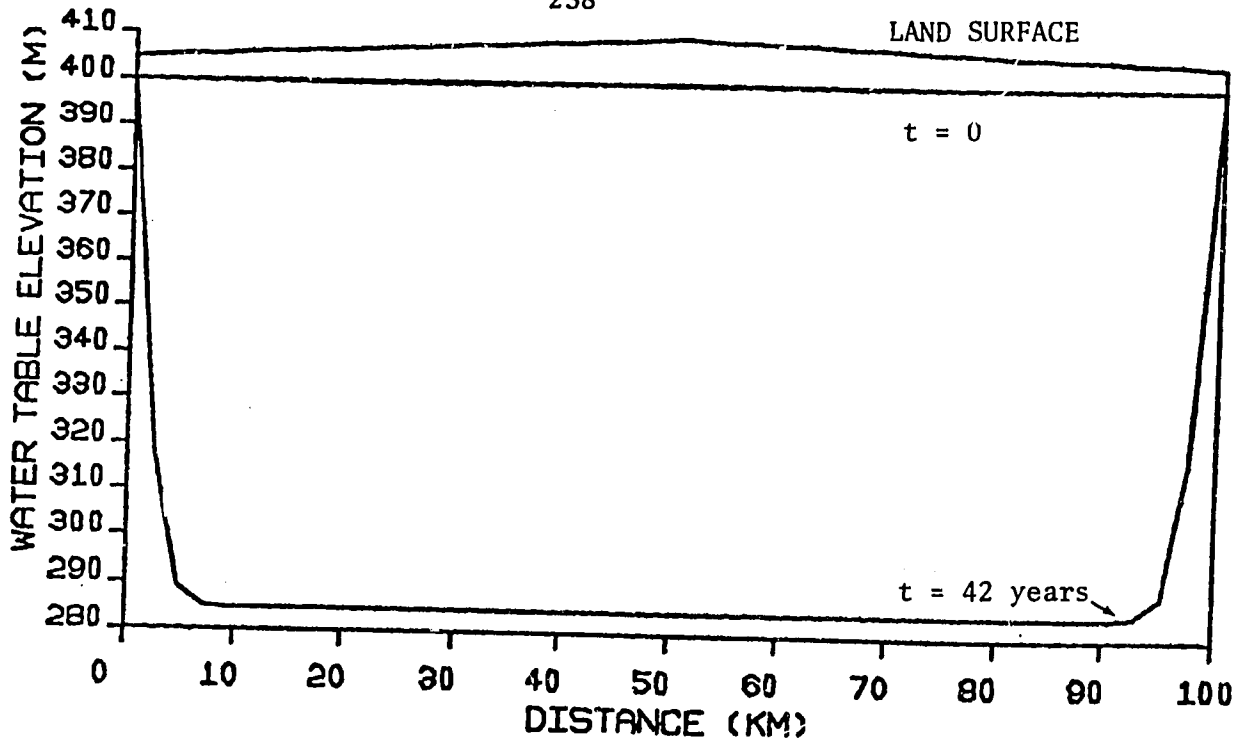


Figure 6.17

WATER TABLE DEPRESSION DUE TO PUMPING, EL-GIZERA, SUDAN
 ($L = 100$ km, $K_1 = 73$ m/year, $Q_p = 1$ m/yr, $t = 42$ yr)

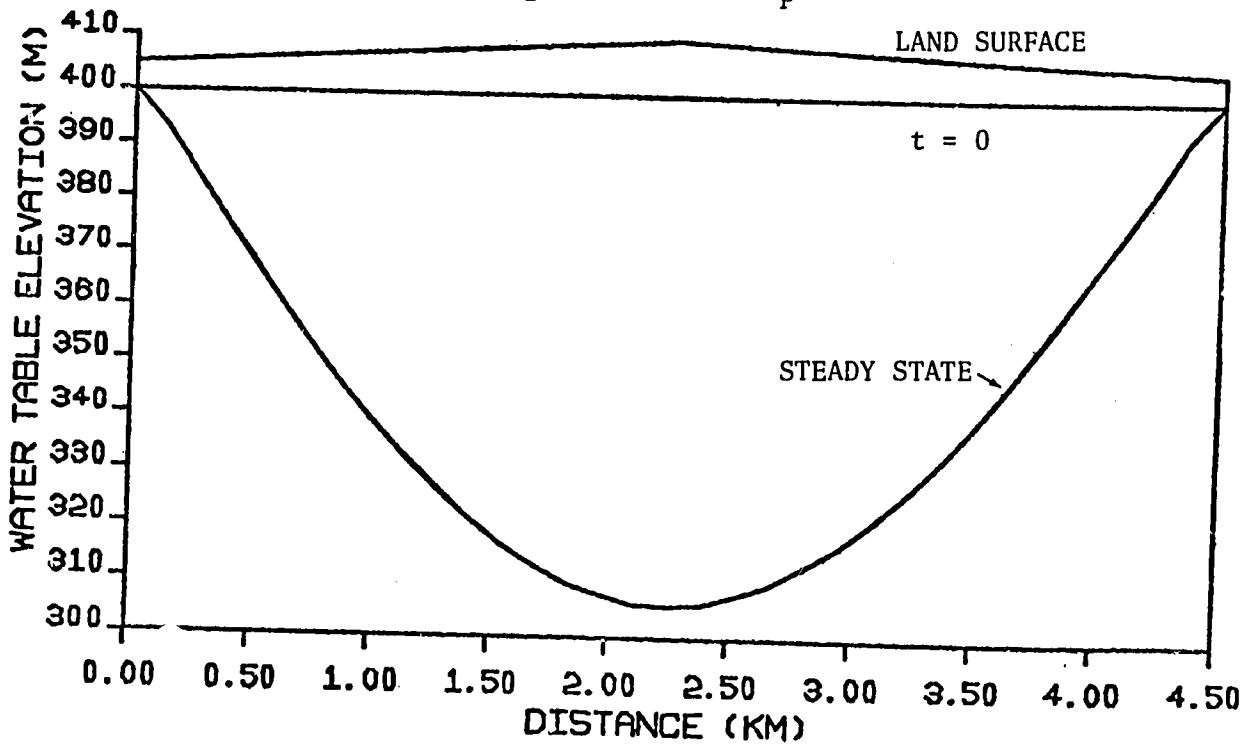


Figure 6.18

STEADY-STATE WATER TABLE DEPRESSION DUE TO PUMPING, EL-GIZERA, SUDAN
 ($L = 4.5$ km, $K_1 = 73$ m/year, $Q_p = 1$ m/yr, $t = 50$ yr)

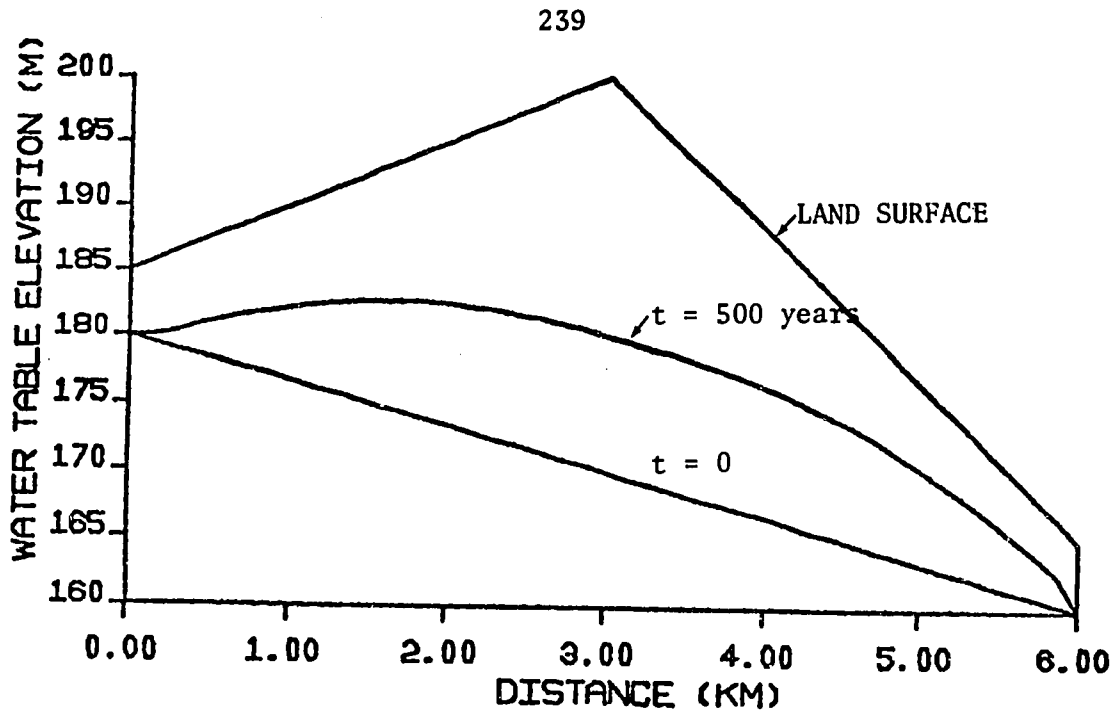


Figure 6.19

STEADY-STATE RECHARGE MOUND; BAHR EL GHAZAL, SUDAN
 ($L = 6$ km, $K_1 = 142$ m/year, $t = 500$ years)

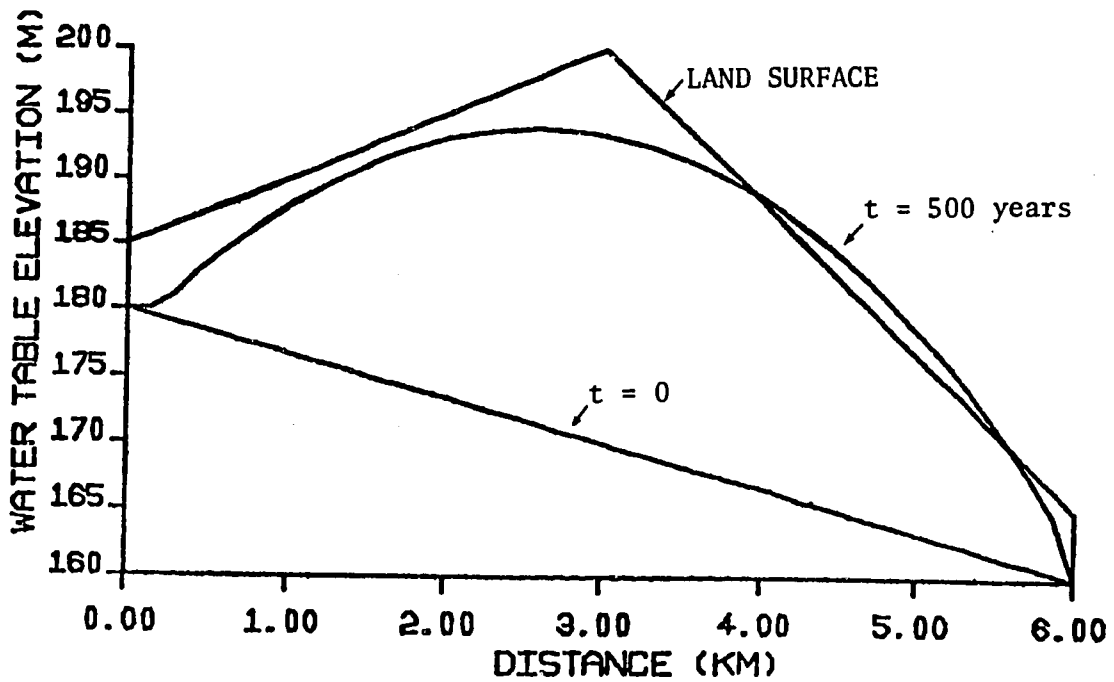


Figure 6.20

STEADY-STATE RECHARGE MOUND; BAHR EL GHAZAL, SUDAN
 ($L = 6$ km, $K_1 = 71$ m/year, $t = 500$ years)

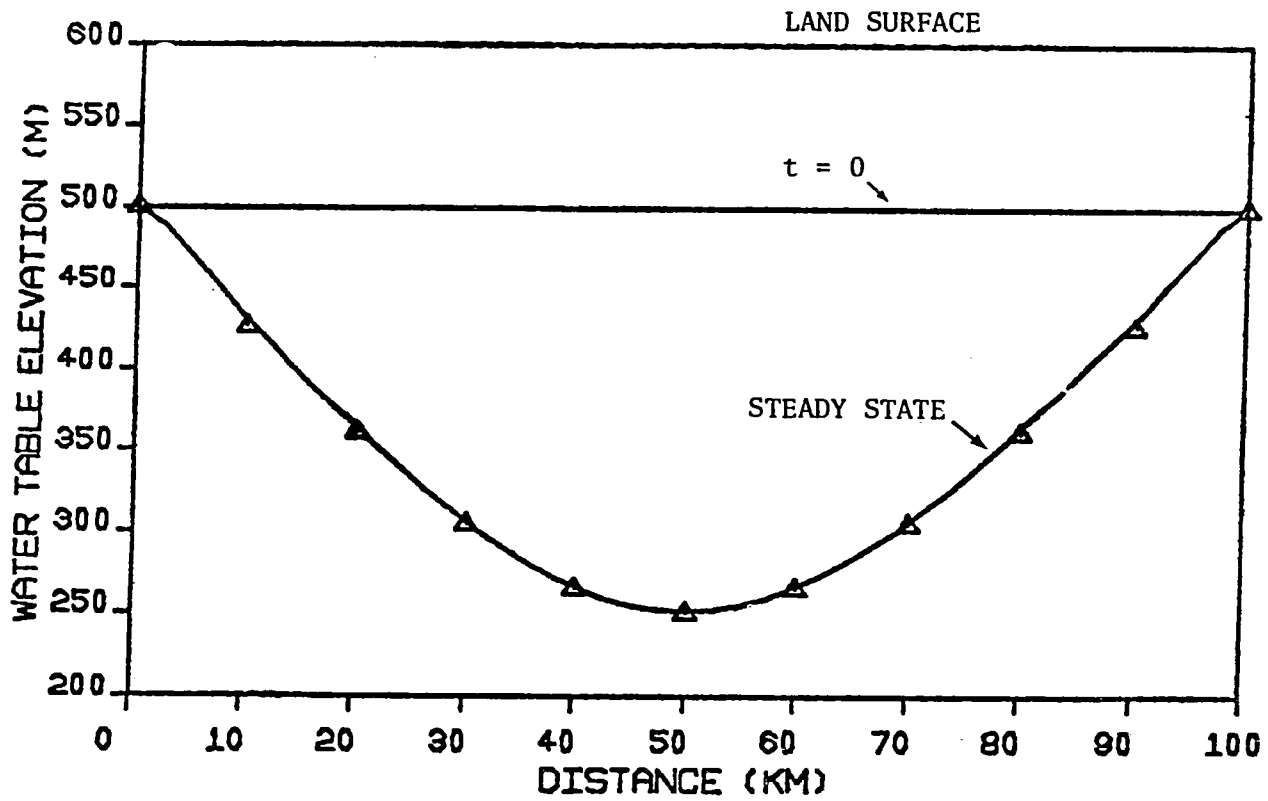


Figure 6.21

COMPARISON OF STEADY-STATE WATER TABLE SHAPE
 BETWEEN THE FINITE DIFFERENCE MODEL AND EQUATION (6.15)
 ($L = 100$ km, $K_1 = 126.1$ m/year, $Q_N = .01$ m/year)

land surface grade. For such a short duration of pumping and such a large distance between rivers, the pumping primarily removes water directly from aquifer storage.

Including both climate and pumping effects results in a larger water table depression than if just pumping is applied, since it was shown in Section 6.6.2.3 that climate demand alone produces a 15 m water table depression.

For a narrower aquifer, the given pumping rate may reach steady state with the river water supply over the 42-year duration. For a five kilometer long aquifer, the steady state maximum water table depression is 90 meters, as seen in Figure 6.18.

For aquifers with recharge mounds, the shape and height of the recharge mound are partially determined by the distance between the boundaries and the hydraulic conductivity. A comparison of Figures 6.19 and 6.20 shows how a swampland may form when lateral hydraulic conductivity is small. This occurs when the climate water supply rate exceeds the aquifer's capability to remove the water to the river. In general, the recharge mound rises until either the recharge rate equals the lateral flow rate or the swampland forms and excess water runs off across the surface.

6.6.3.3 Convergence

To test the model for numerical convergence, we compare the finite-difference solution with an analytical steady state solution from Section 6.4. The comparison between Equation (3.14) and the finite-difference solution as shown in Figure (6.21) indicates the model

Figure:	6.13	6.14	6.15	6.16	6.17	6.18	6.19	6.20	6.21
K(1) (m/yr)	73	73	365	73	73	73	142	71	126.1
S _y	.35	.35	.35	.35	.35	.35	.35	.35	.35
e _p (m/yr)	1.6	1.6	1.6	1.6	0	0	1.53	0	0
B	1.69	1.69	1.69	1.69	0	0	1.82	0	0
ψ(1) (m)	1.0	1.0	1.0	1.0	0	0	1.29	0	0
mc	3.16	3.16	3.16	3.16	0	0	2.83	0	0
L (km)	100	2	2	100	100	4.5	6	6	100
h _o (m)	95	95	95	100	400	400	180	180	500
h _L (m)	95	95	95	90	400	400	160	160	500
β	1	1	1	1	1	1	1	1	1
t _f (yr)	1000	1000	1000	1000	1000	1000	1000	1000	1000
nn	31	31	31	31	41	41	41	31	31
H _o (m)	100	100	100	100	405	405	185	180	600
H _c (m)	100	100	100	110	410	410	200	200	600
H _L (m)	100	100	100	90	405	405	165	165	600
Q _p (m/yr)	0	0	0	0	1	1	0	0	0
Q _N (m/yr)	0	0	0	0	0	0	0	0	01

Table 6.3

GROUNDWATER MODEL INPUTS

convergences to the true solution for time steps on the order of the physically-based time step used.

Chapter 7

SUMMARY, CONCLUSIONS AND RECOMMENDATIONS7.1 Summary

The specific objectives of Section 2.2 were fulfilled in the context of a larger objective; the understanding of the interactions between the water table and the unsaturated zone. In part one of this work (Chapters 3-5), the program consisted of three steps:

1. There are comments on the applicability of the hydrologic equations of the soil-water zone developed for semi-infinite soil columns, and for finite columns (Sections 3.1-3.3).

2. There is the deduction and the solution of the linearized soil-water movement problem (Sections 3.4 to 4.2) for high water tables and including some effects of vegetation.

3. Solutions for the infiltration case were examined and compared with the non-linear approximation of reality. Additionally, dimensionless expressions were derived to indicate when a finite domain analysis is needed.

The second aspect of this work (Chapter 6) includes the development of quantitative relationships between soil-water content (s_0), water table depth (Z) and the net accretion to the groundwater (Q_N) (Section 6.6.2) for a wide range of soil types and climates. We have shown when the soil water balance influences the phreatic surface shape and under what conditions that shape will be convex or concave. We have demonstrated how lateral transmissivity may dominate groundwater flow and force the creation of a swampland.

Several parameters of the groundwater-unsaturated zone regions were developed and shown to simplify the definition of when and to what effect climate governs the phreatic surface shape.

7.2 Conclusions

The linearization of the soil-water movement equation is productive in terms of generating dimensionless expressions for the hydrologic aspects of the soil-water zone. The dimensionless parameters have been particularly useful in expressing the relationship between the water table and the hydrologic processes (see Section 5.2).

In comparison with a numerical model, the linear analytical expressions for infiltrated volume, ponding time and particularly for average moisture content are reasonable representations of the non-linear solutions. This demonstrates the theoretical utility of the linearizing process because of the analytical representation of the soil physics. The equations for the average moisture content are shown to be adequate substitutes for the numerical non-linear solution in problems of practical interest (e.g., drainage and agricultural studies).

Limitations on the analytical models are due to the linearization, and the convergence of the series solution. One must be careful not to use the linear solution in domains where its validity has not been substantiated (e.g., ponding time for $Z^0 > 16$, or for large changes in moisture content).

The expressions indicating the validity of the assumption of the semi-infinite domain are promising indices of when a domain is not realistically semi-infinite.

Much of the work of part one is an extension of the literature which uses linearization to handle problems of high water tables and to analytically account for the influence of vegetation. The solution technique used (and rarely referred to in the soil physics literature) has been shown to be productive in terms of generating analytical solutions to a wide range of problems.

Concerning direct application of the equations of Chapter 4 or Appendix A in water balance models, only the average soil moisture model for infiltration seems reasonable at this time. Analysis of the high water table is a relatively undeveloped field of study and more comparisons with field studies is advisable, particularly with respect to the effects of entrapped air. However, many of the equations developed are likely to be appropriate based on the results presented in Chapter 5.

The equations of Chapter 6 coupling water table, average soil-water content and the accretion rate are useful on the annual or larger time scale. They are based on realistic physics of non-linear soil-moisture movement.

The basic conclusion for Chapter 6 is that the water table plays a significant role in many water balance problems and should not be immediately assumed negligible. Convenient equations, presented in Chapters 5 and 6, permit ready assessment of when the water table may safely be neglected.

7.3 Recommendations for Future Research

1. The incorporation of water table effects on the unsaturated zone hydrology and soil-moisture dynamics is a ripe field for future work,

including field studies and theory. More analytical expressions need to be developed for cases of interest in agriculture and drainage (including 2D and 3D).

2. The equations developed herein need to be compared with data from field studies and numerical studies for the cases not considered in Chapter 5 (especially exfiltration and the solutions for vegetated soils).

3. Computer cpu time comparisons between the slowly converging analytical solutions and the non-linear numerical solutions should be undertaken.

4. Effort should be directed at developing and testing simplified expressions for the hydrologic processes, such as are suggested in Appendix A.

5. The analysis of Chapter 6 should be modified for annual, seasonal and daily water table fluctuations for use in short term agricultural and drainage studies.

6. The essence of this work has been to replace empirical hydrological expressions with physically-based ones. This spirit should continue in future investigations of the high water table case. Accurate modelling of the high water table condition is theoretically satisfying and could result in better drainage schemes for greater agricultural output and environmental safety.

REFERENCES

- Ambramowitz, M. and I. A. Stegun, ed., Handbook of Mathematical Functions, National Bureau of Standards, Applied Math. Series No. 55, U.S. Dept. of Commerce, 1972.
- Aggelides, S. and E. G. Youngs, The dependence of the parameters in the Green and Ampt infiltration equation on the initial water content in draining and wetting states, Water Resources Res., 14(5), 857-862, 1978.
- Anat, A., H. R. Duke and A. T. Corey, Steady Upward Flow from Water Tables, Colorado State Univ. Hydrology Paper No. 7, 1965.
- Babu, D. K., Infiltration analysis and perturbation methods, 1. Absorption with exponential diffusivity, Water Resources Res., 12(1), 89-93, 1976.
- Baumann, P., Technical Development in Groundwater Recharge, Advances in Hydroscience, Vol. 2, Academic Press, New York, 1966.
- Bear, J., Dynamics of Fluids in Porous Media, American Elsevier, New York, 1972.
- Bear, J., Hydraulics of Groundwater, McGraw-Hill, New York, 1979.
- Ben-Asher, J., D. O. Lomen and A. W. Warrick, Linear and non-linear models of infiltration from a point source, Soil Sci. Soc. Am. J., 42, 3-6, 1978.
- Bond, W. J. and N. Collis-George, Poned infiltration into simple soil systems: 1. The saturation and transition zones in the moisture content profile, Soil Sci., 131(4), 202-209, 1981.
- Bond, W. J. and N. Collis-George, Poned infiltration into simple soil systems: 3. The behavior of infiltration rate with time, Soil Sci., 131(6), 327-333, 1981.
- Bouwer, H., Infiltration of water into non-uniform soil, J. Irrig. and Drainage Div., ASCE, 95(IR4), 451-462, 1969.
- Boyce, W. E. and R. C. DiPrima, Elementary Differential Equations, 3rd Ed., John Wiley and Sons, New York, 1977.
- Braester, C., Moisture variation at the soil surface and the advance of the wetting front during infiltration at constant flux, Water Resources Res., 9(3), 687-694, 1973.

- Braester, C., G. Dagan, S. P. Neuman, and D. Zaslavsky, A survey of the equations and solutions of unsaturated flow in porous media, Tech. Rept. Technion - Israel Inst. of Technology, Haifa, Israel, 1971.
- Braester, C., Reply, Water Resources Res., 12(2), 314, 1976.
- Brakensiek, D. L. and C. A. Onstad, Parameter estimation of the Green and Ampt infiltration equation, Water Resources Res., 13(6), 1009-1012, 1977.
- Brooks, R. H. and A. T. Corey, Hydraulic properties of porous media, Colo. State Univ. Hydrol. Paper No. 3, 1964.
- Brutsaert, W., The concise formulation of diffusive sorption of water in a dry soil, Water Resources Res., 12(6), 1118-1124, 1976.
- Carrier, G. F. and C. E. Pearson, Partial Differential Equations, Academic Press, New York, 1976.
- Carslaw, H. S. and J. C. Jaeger, Conduction of Heat in Solids, 2nd ed., Oxford Univ. Press, London, 1959.
- Chan, S.-O. and P. S. Eagleson, Water Balance Studies of the Bahr El Ghazal Swamp, Cairo University-M.I.T. Technology and Planning Program, Technology Adaptation Program Report No. 80-14, 1980.
- Childs, E. C., Soil Moisture Theory, in Advances in Hydroscience (V.T. Chow, ed.), Vol. 4, 73-117, Academic Press, New York, 1967.
- Childs, E. C., An Introduction to The Physical Basis of Soil Water Phenomena, John Wiley, New York, 1969.
- Childs, E. C., Concepts of soil water phenomena, Soil Sci., 113(4), 246-253, 1972.
- Childs, E. C. and M. Bybordi, The vertical movement of water in stratified porous material - 1. infiltration, Water Resources Res., 5(2), 446-459, 1969.
- Chow, V. T., ed., Handbook of Applied Hydrology, McGraw-Hill, New York, 1964.
- Chubarov, V. N., The Method of Groundwater Recharge Evaluation in Sand Desert by Investigation of Moisture Exchange in Zone of Aeration, I.A.S.H. Symposium on Water in the Unsaturated Zone, Vol. 2, 809-821, 1969.
- Clapp, R. B. and G. M. Hornberger, Empirical equations for some soil hydraulic properties, Water Resources Res., 14(4), 601-604, 1978.

- Cleary, R. W., Notes on Finite Fourier Transforms, Princeton Univ., 1977.
- Cleary, R. W. and D. D. Adrian, Analytical studies of the convective-dispersive equation for cation adsorption in soils, Soil Sci. Soc. Am. Proc., 37(2), 197-199, 1973.
- Clothier, B. E., J. H. Knight, and I. White, Burger's equation: application to field constant-flux infiltration, Soil Sci., 132(4), 255-261, 1981.
- Collis-George, N., A laboratory study of infiltration-advance, Soil Sci. 117(5), 282-287, 1974.
- Collis-George, N., Infiltration Equation for Simple-Soil Systems, Water Resources Res., 13(2), 395-403, 1977.
- Corey, G. L. and A. T. Corey, Similitude for Drainage of Soils, Proc. ASCE, J. Irrig. & Drainage Div., No. IR3, Paper No. 5462, 3-23, 1967.
- Crank, J., Mathematics of Diffusion, Oxford Univ. Press, New York, 1975.
- Curtis, A. A. and K. K. Watson, Numerical analysis of infiltration into a sand profile bounded by a capillary fringe, Water Resources Res. 16(2), 365-371, 1980.
- Dettinger, M. D., Numerical Modelling of Aquifer Systems under Uncertainty: A Second Moment Analysis, S. M. Thesis, M.I.T., 1979.
- DeWiest, R.J.M., Geohydrology, John Wiley and Sons Inc., New York, 1965.
- Domenico, P. A., Concepts and Models in Groundwater Hydrology, McGraw-Hill, New York, 1972.
- Dooge, J.C.I., Linear Theory of Hydrologic Systems, Technical Bull. 1468, U.S.D.A., 1973.
- Dooge, J.C.I., Effect of water table on infiltration rate, Personal Communication with P. S. Eagleson, 1977.
- Eagleson, P. S., Dynamic Hydrology, McGraw-Hill, New York, 1970.
- Eagleson, P. S., Climate, Soil and the Water Balance, M.I.T., Department of Civil Engineering, 1977.
- Eagleson, P. S., Climate, soil and vegetation 1. Introduction to water balance dynamics, Water Resources Res., 14(5), 1978a.

- Eagleson, P. S., Climate, soil and vegetation 2. The distribution of annual precipitation derived from observed storm sequences, Water Resources Res., 14(5), 1978b.
- Eagleson, P. S., Climate, soil and vegetation 3. A simplified model of soil moisture movement in the liquid phase, Water Resources Res., 14(5), 1978c.
- Eagleson, P. S., Climate, soil and vegetation 4. The expected value of annual evapotranspiration, Water Resources Res., 14(5), 1978d.
- Eagleson, P. S., Climate, soil and vegetation 5. A derived distribution of storm surface runoff, Water Resources Res., 14(5), 1978e.
- Eagleson, P. S., Climate, soil and vegetation 6. Dynamics of the annual water balance, Water Resources Res., 14(5), 1978f.
- El-Hemry, I. I. and P. S. Eagleson, Water Balance Estimates of the Machar Marshes, Cairo Univ.-M.I.T. Technology and Planning Program, Technology Adaptation Program Rept. No. 80-3, 1980.
- Elrick, D. E. and K. B. Laryea, Sorption of water in soils: a comparison of techniques for solving the diffusion equation, Soil Sci., 128(6), 369-374, 1979.
- Ernst, L. F., Determination of storage coefficients from observations of groundwater levels, Symposium on Water in the Unsaturated Zone, Vol. 2, 966-989, 1969.
- Feddes, R. A., P. Kowalik, K. Kolinska-Malinka, H. Zavadny, Simulation of field water uptake by plants using a soil water dependent root extraction function, J. Hydrology, 31, 13-26, 1976.
- Feddes, R. A., P. Kowalik and H. Zavadny, Simulation of Field Water Use and Crop Yield, John Wiley and Sons, 1978.
- Fleming, G., Computer Simulation Techniques in Hydrology, Elsevier, New York, 1977.
- Freeze, R. A., Three-dimensional, transient, saturated-unsaturated flow in a groundwater basin, Water Resources Res., 7(2), 347-366, 1971.
- Freeze, R. A. and J. A. Cherry, Groundwater, Prentice-Hall, New Jersey, 1979.
- Gardner, W. R. and W. R. Gardner, Relation of water application to evaporation and storage of soil water, Soil Sci. Soc. Am. Proc., 33, 192-196, 1969.

- Gardner, W. R., Some steady state solutions of the unsaturated moisture flow equation with application to evaporation from a water table, Soil Sci., 85(4), 228-232, 1958.
- Gardner, W. R., Solutions of the Flow Equation for the Drying of Soils and Other Porous Media, Soil Sci. Soc. Am. Proc., 23(3), 183-187, 1959.
- Gardner, W. R., Approximate solution of a non-steady-state drainage problem, Soil Sci. Soc. Am. Proc., 129-132, 1962.
- Gardner, W. R. and Fireman, M., Laboratory studies of evaporation from soil columns in the presence of a water table, Soil Sci., 85, 244-249, 1958.
- Gardner, W. R. and Mayhugh, M. S., Solutions and tests of the diffusion equation for the movement of water in soil, Soil Sci. Soc. Am. Proc., 22, 197-201, 1958.
- Gardner, W. R. and Widsoe, J. A., Movement of soil moisture, Soil Sci., 11, 215-232, 1921.
- Ghosh, R. K., Modelling infiltration, Soil Sci., 130(6), 297-302, 1980.
- Gradshteyn, I. S. and I. M. Ryzhik, Table of Integrals, Series and Products, Academic Press, New York, 1965.
- Green, W. H. and Ampt, G. A., Studies on soil physics. Part I - the flow of air and water through soils, J. Agric. Sci., 4, 1-24, 1911.
- Hayhoe, H., Analysis of a diffusion model for plant root growth and an application to plant soil-water uptake, Soil Sci., 131(6), 334-343, 1981.
- Hedstrom, W. E., A. T. Corey, and H. R. Duke, Models for Subsurface Drainage, Colo. State Univ. Hydrology Paper No. 48, Apr. 1971.
- Hildebrand, F. B., Advanced Calculus for Applications, Prentice-Hall, Inc., New Jersey, 1976.
- Hillel, D., Simulation of evaporation from bare soil under steady and diurnally fluctuating evaporativity, Soil Sci., 120(3), 230-237, 1975.
- Hillel, D., Computer Simulation of Soil-Water Dynamics, International Development Research Centre, Ottawa, 1977.
- Hillel, D., Applications of Soil Physics, Academic Press, New York, 1980.

- Hillel, D. and W. R. Gardner, Steady infiltration into crust-topped profiles, Soil Sci., 108, 137-142, 1969.
- Horton, R. E., An approach toward physical interpretation of infiltration capacity, Proc. Soil Sci. Soc. Am., 5, 399-417, 1939.
- International Mathematical and Statistical Librarian, Inc. (IMSL), Library 2, Edition 6, 1977 (subroutines zbrent, leglph).
- Irmay, S., Solution of the non-linear diffusion equation with a gravity term in hydrology, I.A.S.H. Symposium on Water in the Unsaturated Zone, Vol. 1, Wageningen, 1969.
- Jaworski, J., Evapotranspiration of plants and fluctuation of the groundwater table, I.A.S.H. Symposium on Water in the Unsaturated Zone, Vol. 2, 730-738, Wageningen, 1969.
- Kirkham, D. and Powers, W. L., Advanced Soil Physics, Wiley-Interscience, New York, 1972.
- Klute, A., A numerical method for solving the flow equation for water in unsaturated materials, Soil Sci., 73(2), 105-116, 1952a.
- Klute, A., Some theoretical aspects of the flow of water in unsaturated soils, Soil Sci. Soc. Am. Proc., 16(2), 144-148, 1952b.
- Knight, J. H. and J. R. Philip, On solving the unsaturated flow equation: 2. critique of Parlange's method, Soil Sci., 116(6), 407-416, 1974.
- Kostiakov, A. N., On the dynamics of the coefficient of water-percolation in soils and on the necessity for studying it from a dynamic point of view for purposes of amelioration, Trans. 6th Comm. Intern. Soc. Soil Sci., Russian Part A, 17-21, 1932.
- Kovács, G., Relationship between infiltration and groundwater household, I.A.S.H. Symposium on Water in the Unsaturated Zone, Vol. 2, 801-809, Wageningen, 1969.
- Kutilek, M., Constant-rainfall infiltration, Journal of Hydrology, 45, 289-303, 1980.
- Laliberte, G. E., A. T. Corey and R. H. Brooks, Properties of Unsaturated Porous Media, Colo. State Univ. Hydrology Paper No. 17, 1966.
- Laroussi, C. and L. De Backer, Physical interpretation of the diffusion equation parameters according to Markov's stochastic processes theory, Soil Sci., 120(3), 169-173, 1975.
- Laroussi, C., G. Vandervoerde and L. De Backer, Experimental investigation of the diffusivity coefficient, Soil Sci., 120(4), 249-255, 1975.

- Lomen, D. O. and A. W. Warrick, Solution of the one-dimensional linear moisture flow equation with implicit water extraction functions, Soil Sci. Soc. Am. J., 40, 342-345, 1976.
- Lomen, D. O. and A. W. Warrick, Linearized moisture flow with loss at the soil surface, Soil Sci. Soc. Am. J., 42, 396-400, 1978.
- Lomen, D. O. and A. W. Warrick, Time-dependent solutions to the one-dimensional linearized moisture flow equation with water extraction, J. Hydrol., 39, 59-67, 1978.
- Luthin, J. N., Some observations on flow in the capillary fringe, in Symposium on Water in the Unsaturated Zone, Vol. 2, 905-909, 1969.
- Luthin, J. N. and J. W. Holmes, An Analysis of the flow in a shallow, linear aquifer and of the approach to a new equilibrium after intake, J. Geophys. Res., 65(5), 1573-1576, 1960.
- Malik, B. S., C. Larroussi and L. W. De Backer, Physical components of the diffusivity coefficient, Soil Sci. Soc. Am. Proc., 43(4), 633-637, 1979.
- Mein, R. G. and Larson, C. L., Modelling infiltration during a steady rain, Water Resources Res., 9(2), 384-394, 1973.
- Mein, R. G. and D. A. Farrell, Determination of wetting front suction in the Green-Ampt equation, Soil Sci. Soc. Am. Proc., 38, 872-876, 1974.
- Metzger, B. H. and P. S. Eagleson, The Effects of Annual Storage and Random Potential Evapotranspiration on the One-Dimensional Annual Water Balance, M.I.T. Department of Civil Engineering, Ralph M. Parsons Laboratory for Water Resources and Hydrodynamics, Tech. Rept. No. 251, 1980.
- Milly, P.C.D. and P. S. Eagleson, The Coupled Transport of Water and Heat in a Vertical Soil Column under Atmospheric Excitation, M.I.T. Department of Civil Engineering, Ralph M. Parsons Laboratory for Water Resources and Hydrodynamics, Technical Report No. 258, 1980.
- Molz, F. J., Models of water transport in the soil-plant system: a review, Water Resources Res., 17(5), 1245-1260, 1981.
- Molz, F. J. and I. Remson, Extraction term models of soil moisture use by transpiring plants, Water Resources Res., 6, 1346-1356, 1970.
- Moore, R. E., Water conduction from shallow water tables, Hilgardia, 12(6), 383-426, 1939.

- Morel-Seytoux, H. J. and J. Khanji, Derivation of an equation of infiltration, Water Resources Res., 10(4), 795-800, 1974.
- Nimah, M. N. and R. J. Hanks, Model for estimating soil water, plant, and atmospheric interrelations: 1. description and sensitivity, Soil Sci. Soc. Am. Proc., 37, 522-527, 1973.
- Nimah, M. N. and R. J. Hanks, Model for estimating soil water, plant, and atmospheric interrelations: 2. field test of model, Soil Sci. Soc. Am. Proc., 37, 528-532, 1973.
- Ölcer, N. Y., On the theory of conductive heat transfer in finite regions, Int. J. Heat, Mass Transfer, 7, 307-314, 1964.
- Ölcer, N. Y., On the theory of conductive heat transfer in finite regions with boundary conditions of the second kind, Int. J. Heat, Mass Transfer, 8, 529-556, 1965.
- Ozisik, M. N., Integral transform in the solution of heat-conduction equation in the cartesian coordinate system, American Society of Mechanical Engineers, reprint No. 67-WA/HT-36, 1967.
- Parlange, J.-Y., Theory of water movement in soils: 1. one-dimensional absorption, Soil Sci., 111(2), 134-137, 1971a.
- Parlange, J.-Y., Theory of water movement in soils: 2. one-dimensional infiltration, Soil Sci., 111(3), 170-174, 1971b.
- Parlange, J.-Y., Theory of water movement in soils: 6. effect of water depth over soil, Soil Sci., 113(5), 308-312, 1972a.
- Parlange, J.-Y., Theory of water movement in soils: 8. one-dimensional infiltration with constant flux at the surface, Soil Sci., 114(1), 1-4, 1972b.
- Parlange, J.-Y., Theory of water movement in soils: 11. conclusion and discussion of some recent developments, Soil Sci., 119(2), 158-161, 1975a.
- Parlange, J.-Y., A note on the Green and Ampt equation, Soil Sci., 119(4), 466-467, 1975b.
- Parlange, J.-Y., Comment on 'Moisture Variation at the Soil Surface and the Advance of the Wetting Front during Infiltration at Constant Flux' by Carol Braester, Water Resources Res., 12(2), 313, 1976.
- Parlange, J.-Y. and D. E. Aylor, Theory of water movement in soils:
a. the dynamics of capillary rise, Soil Sci., 114(2), 79-81, 1972.

- Parlange, J.-Y. and D. E. Aylor, Response of an unsaturated soil to forest transpiration, Water Resources Res., 11, 319-323, 1975.
- Parlange, J.-Y. and D. K. Babu, On solving the non-linear diffusion equation - a comparison of perturbation, iterative and optimal techniques for an arbitrary diffusivity, Water Resources Res., 13(1), 213-214, 1977.
- Peck, A. J., R. J. Luxmoore and J. L. Stolzy, Effects of spatial variability of soil hydraulic properties in water budget modelling, Water Resources Res., 13(2), 348-354, 1977.
- Penman, H. L., Role of vegetation in soil water problems, in Symposium on Water in the Unsaturated Zone, Vol. 1, UNESCO-IASH, Belgium, 1969.
- Perroux, K. M., D. E. Smiles and I. White, Water movement in uniform soils during constant flux infiltration, Soil Sci. Am. J., 45, 237-240, 1981.
- Philip, J. R., An infiltration equation with physical significance, Soil Sci., 77, 153-157, 1954.
- Philip, J. R., The theory of infiltration 1. The infiltration equation and its solution, Soil Sci., 83, 345-357, 1957a.
- Philip, J. R., The theory of infiltration 2. The profile at infinity, Soil Sci., 83(6), 435-448, 1957b.
- Philip, J. R., The theory of infiltration 4. Sorptivity and algebraic infiltration equations, Soil Sci., 84, 257-264, 1957c.
- Philip, J. R., Theory of Infiltration, in Advances in Hydrosociences (V. T. Chow, ed.), 5, Academic Press, New York, 215-296, 1969a.
- Philip, J. R., A linearization technique for the study of infiltration, I.A.S.H. Symposium on Water in the Unsaturated Zone, Vol. 1, Wageningen, 471-478, 1969b.
- Philip, J. R., The dynamics of capillary rise, I.A.S.H. Symposium on Water in the Unsaturated Zone, Vol. 2, Wageningen, 559-564, 1969c.
- Philip, J. R., On solving the unsaturated flow equation 1. The flux-concentration relation, Soil Sci., 116(3), 328-335, 1973.
- Philip, J. R. and J. H. Knight, On solving the unsaturated flow equation: 3. New quasi-analytical technique, Soil Sci., 117(1), 1-13, 1974.
- Pinder, G. F. and W. G. Gray, Finite Element Simulation in Surface and Sursurface Hydrology, Academic Press, New York, 1977.

- Polubarinova-Kochina, P.-Y., Theory of Groundwater Movement, Princeton University Press, Princeton, NJ, 1962.
- Raats, P.A.C., Analytical solutions of a simplified flow equation, Trans. ASAE, 19, 683-689, 1976.
- Rainville, E. D. and Bedient, P. E., Elementary Differential Equations, 4th ed., The Macmillan Co., London, 1969.
- Reeves, M. and E. E. Miller, Estimating infiltration for erratic rainfall, Water Resources Res., 11(1), 102-110, 1975.
- Remson, I., Hornberger, G. M., Molz, F. J., Numerical Methods in Subsurface Hydrology, Wiley Interscience, New York, 1971.
- Rennolls, K., R. Cornell, V. Tee, A descriptive model of the relationship between rainfall and soil water table, J. Hydrol. 47, 103-114, 1980.
- Ripple, C. D., J. Rubin, and T. E. A. van Hylckama, Estimating steady-state evaporation rates from bare soils under conditions of high water table, Geological Survey Water-Supply Paper 2019-A, 1968.
- Rubin, J. and R. Steinhardt, Soil water relations during rain infiltration: I. theory, Proc. Soil Sci. Soc. Am., 27, 246-251, 1963.
- Rushton, K. R. and C. Ward, The estimation of groundwater recharge, J. Hydrol., 41, 345-361, 1979.
- Salem, M. H., Water Balance of El-Gizera Land between the White Nile and the Blue Nile, Unpublished manuscript, Cairo Univ., Dept. of Hydrology, Cairo, Egypt, 1981.
- Sharma, M. L., G. A. Gander, C. G. Hunt, Spatial variability of infiltration in a watershed, J. Hydrol. 45, 101-122, 1980.
- Skaggs, R. W., A Water Management Model for Shallow Water Table Soils, Water Res. Research Inst. Rept. #134, Univ. N. Carolina, 1978.
- Smiles, D. E., K. M. Perroux and S. J. Segelin, Adsorption of water by soil: some effects of a saturated zone, Soil Sci. Am. J., 44, 1153-1158, 1980.
- Smith, R. E. and J.-Y. Parlange, A parameter-efficient hydrologic infiltration model, Water Resources Res., 14(3), 533-538, 1978.
- Stallman, R. W., Flow in the zone of aeration, in Advances in Hydroscience, Vol. 4, Academic Press, New York, 1968.
- Swartendruver, D., The flow of water in unsaturated soils, in Flow through Porous Media (ed., R. J. M. DeWiest), Academic Press, New York, 1969.

- Swartzendruber, D., Infiltration of constant flux rainfall into soil as analyzed by the approach of Green and Ampt, Soil Sci., 117(5), 272-281, 1974.
- Swartzendruber, D., and E. G. Youngs, Note: a comparison of physically-based infiltration equations, Soil Sci., 117(3), 165-167, 1974.
- Thornthwaite, C. W., An approach toward a rational classification of climate, Geog. Rev., 33, 55-94, 1948.
- Vachaud, G., J. P. Gaudet and V. Kuraz, Air and water flow during ponded infiltration in a vertical bounded column, J. Hydrol., 22(1/2), 89-108, 1974.
- Vachaud, G., M. Vauclin, M. Wakil and D. Khanji, Effect of air pressure during water flow in an unsaturated, stratified vertical column of soil, in Fund. of Transp. Phenom. in Porous Media, IAHR-ISSS, Vol. 1, 1972.
- Vandenberg, A., Regional groundwater motion response to an oscillating water table, J. Hydrol., 47, 333-348, 1980.
- van Hylckama, T.E.A., Evaporation from vegetated and fallow soils, Water Resources Res., 2(1), 99-103, 1966.
- Visser, W. C., Unsaturated soil moisture conditions studied from field observations, in Symposium on Water in the Unsaturated Zone, Vol. 2, 952-966, 1969.
- Warrick, A. W., Analytical solutions to the one-dimensional linearized moisture flow equation for arbitrary input, Soil Sci., 120(2), 79-84, 1975.
- Watson, K. K., A note on the field use of a thematically derived infiltration equation, J. Geophysical Research, 64(10), 1959.
- Warrick, Lomen and Amoozegar-Fard, Linearized moisture flow with root extraction for 3D steady conditions, Soil Sci. Soc. Am. J., 44, 911-914, 1980.
- Whistler, F. D. and H. Bouwer, Comparison of methods for calculating vertical drainage and infiltration for soils, J. Hydrol., 10, 1-19, 1970.
- Whistler, F. D., A. Klute and R. J. Millington, Analysis of steady state evapotranspiration from a soil column, Soil Sci. Soc. Am. Proc., 32(2), 167-174, 1968a.
- White, I., Measured and approximate flux-concentration relations for absorption of water by soil, Soil Sci. Soc. Am. J., 43, 1074-1080, 1979.

- White, I., D. E. Smiles and K. M. Perroux, Absorption of water by soil: the constant flux boundary condition, Soil Sci. Soc. Am. J., 43, 659-664, 1979.
- Wisler, C. O. and E. F. Brater, Hydrology, John Wiley and Sons, New York, 1949.
- Youngs, E. G., The drainage of liquids from porous media, J. Geophysical Research, 65(12), 4025-5040, 1960.
- Zachmann, D. W., H. R. Gardner and P. C. DuChateau, A mathematical treatment of the initial stages of druing of a soil column, Soil Sci. Soc. Am. J., 44, 235-238, 1980.
- Zaradny, H., Boundary conditions in modelling water flow in unsaturated soils, Soil Sci., 125(2), 75-82, 1978.

Appendix A

SIMPLIFIED INFILTRATION EQUATIONS FOR HIGH WATER TABLE

The goal here is to incorporate the influence of the water table on the infiltration rate and ponding time using simpler expressions motivated by the series solutions of Sections 4.2.3 and 4.2.4.

A.1 Similarity to Horton's Infiltration Law

The expressions for infiltration capacity derived in Section 4.2.3 are of the form of the Horton infiltration equation, (1939), which is

$$f_i^*(t) = (f_{i,i}^* - f_{i,ss}^*)e^{-k_1 t} + f_{i,ss}^* \quad (\text{A.1})$$

where, for the uniform initial condition

$$\lim_{t \rightarrow 0} \lim_{z^0 \rightarrow 0} f_{i,i}^* = \frac{K_1}{2} - \frac{2D_*}{z} \sum_0^{\infty} \left(\frac{m\pi}{z^0}\right)^2 \left(\cos \frac{m\pi z^0}{z^0}\right) \theta_0 [1 - (-1)^n e^{-z^0/2}] / \left[\left(\frac{m\pi}{z^0}\right)^2 + \frac{1}{4}\right] \quad (\text{A.2})$$

$$\lim_{t \rightarrow \infty} \lim_{z \rightarrow \infty} f_{i,ss}^* = \frac{K_1}{2} - \frac{2D_*}{z} \sum_0^{\infty} \left(\frac{m\pi}{z^0}\right)^2 \left(\cos \frac{m\pi z^0}{z^0}\right) \theta_1 [1 - (-1)^n e^{-z^0/2}] / \left[\left(\frac{m\pi}{z^0}\right)^2 + \frac{1}{4}\right] \quad (\text{A.3})$$

$$k_1 = (m\pi/z^0)^2 + 1/4 \quad (\text{A.4})$$

with

$$\begin{aligned} f_{i,i}^* &= \text{initial infiltration rate} \\ f_{i,ss}^* &= \text{ultimate infiltration rate} \\ k_1 &= \text{rate of infiltration decay} \end{aligned}$$

The expressions are only valid in the limits of time and space

because of the convergence problems mentioned in Sections (5.4.1), (5.4.2) and (5.5.3).

We may simplify Equations (A.2), (A.3) and (A.4) for small dimensionless depths, when $\left(\frac{\pi}{Z^0}\right)^2 \gg 1/4$ or $Z^0 < 2\pi$, to

$$\lim_{t \rightarrow 0} \lim_{z^0 \rightarrow 0} f_{i,i}^* = \frac{K_1}{2} - \frac{2D_*}{Z} \sum_0^{\infty} \cos\left(\frac{n\pi z^0}{Z^0}\right) \theta_0 [1 - (-1)^n e^{-Z^0/2}] \quad (\text{A.5})$$

$$\lim_{t \rightarrow \infty} \lim_{z^0 \rightarrow 0} f_{i,ss}^* = \frac{K_1}{2} - \frac{2D_*}{Z} \sum_0^{\infty} \cos\left(\frac{n\pi z^0}{Z^0}\right) \theta_1 [1 - (-1)^n e^{-Z^0/2}] \quad (\text{A.6})$$

and

$$k_1 = (n\pi/Z^0)^2 \quad (\text{A.7})$$

Horton's infiltration law does not appear to have been derived previously (including gravity) from the basic equation of soil physics. Instead, it was proposed as an analogy to the decay process. This analysis relates the Horton parameters to those of the soil, the soil moisture state and the water table depth based on the linearized soil moisture movement equation solved for the finite one-dimensional domain. The relations are

$$f_i = f_i(K_1, D_*, Z, \theta_0, \theta_1)$$

$$f_{ss} = f_{ss}(K_1, D_*, Z, \theta_1)$$

and

$$k_1 = k_1(K_1, D_*, Z, \theta_1)$$

Showing the similarity between the Horton equation and the linearized solution aids in understanding both models of infiltration. Research on the Horton equation has shown the Horton model to decay to the steady state more slowly than the actual process and resultingly to overpredict the surface runoff (Collis-George, 1977). This is to be expected of the linear model solution. On the other hand, knowledge of the composition of the Horton parameters and the assumptions underlying the derivation of them for the finite domain, linear model (Sections 3.4 and 3.5) places the Horton equation on a sounder physical basis. The connection between the two suggests that the Horton equation might be a good model for the infiltration capacity in a shallow water table situation.

A.2 Infiltration Law for Shallow Water Table Conditions

To use the Horton model, we may either fit the parameters for the range of water table depths or explicitly account for the depth-dependence. In the latter case, we consider the following, based on the results of tests using the numerical model of Milly (Section 5.6).

1. $f_{i,ss}^*$ occurs at soil column saturation. It is thus the depth-independent saturated column vertical flow rate (e.g., saturated hydraulic conductivity).
2. The initial infiltration rate is larger for deeper soil columns.
3. The infiltration rate of a soil column is independent of the water table depth for a sufficiently deep column.

The component of Equations (A.2) and (A.3) which fulfills the above criteria is the first series term ($n=0$) expression $1 - e^{-Z^0/2}$. To generalize the expression, we replace $Z^0/2$ by $P_1 Z$, where we have replaced $k/2D_*$ by a fitting parameter, P_1 . The modified Horton expression proposed is

$$f_i^*(t) = (1 + e^{-P_1 Z})(f_{i,i}^* - f_{i,ss}^*)e^{-k_1 t} + f_{i,ss}^* \quad (A.8)$$

where

P_1 = model parameter

Z = water table depth

The linearized model suggests other modifications of the Horton equation which may be added if this proves inadequate.

A.3 Ponding Time Using Horton's Law

Instead of using the Philip infiltration law in the time-compression approximation to derive a ponding time expression, we may use Horton's infiltration law. The cumulative infiltration expression corresponding to the rate expression (A.1) is

$$I(t) = \left(\frac{f_{i,i}^* - f_{i,ss}^*}{k_1} \right) (1 - e^{-k_1 t}) + f_{i,ss}^* \quad (A.9)$$

Matching the actual cumulative infiltration at ponding time, t_o , with that derived from this model at time, t^* , we express $t_o(t^*)$ by

$$t_o = \frac{1}{i} \left| \frac{(f_{i,i}^* - f_{i,ss}^*)}{k_1} (1 - e^{-k_1 t^*}) + f_{i,ss}^* t^* \right| \quad (A.10)$$

where

i = rainfall rate

Assuming $f_i^*(t^*) = i$, we invert Equation (A.1) to write

$$t^* = \frac{1}{k_1} \ln \left| \frac{f_{i,i}^* - f_{i,ss}^*}{i - f_{i,ss}^*} \right| \quad (\text{A.11})$$

Substituting Equation (A.11) into (A.10) results in the ponding time expression for the Horton infiltration law which is

$$t_o = \left| f_{i,i}^* - i + f_{i,ss}^* \ln \left(\frac{f_{i,i}^* - f_{i,ss}^*}{i - f_{i,ss}^*} \right) \right| / k_1 i \quad , \quad t_o \geq 0 \quad (\text{A.12})$$

For $i = f_{i,i}^* > f_{i,ss}^*$, ponding time occurs instantaneously from this model. For $f_{i,i}^* > i > f_{i,ss}^*$, ponding time is negative. This is interpreted to mean that saturation of the soil surface occurs very quickly as i approaches $f_{i,i}^*$ and is assumed to occur instantaneously for heavier rainstorms.

A.4 Ponding Time for Shallow Water Table Conditions

We incorporate the water table influence with the same modification as in Section A.2. The result is

$$t_o = \left| f_{i,i}^* (1 - e^{-P_1 Z}) - i + f_{i,ss}^* \ln \left(\frac{(f_{i,i}^* - f_{i,ss}^*) (1 - e^{-P_1 Z})}{i - f_{i,ss}^*} \right) \right| / k_1 i \quad (\text{A.13})$$

Both the expression for ponding time and for the infiltration capacity need to be tested against real soil data or a numerical model. They are both functions of four parameters: P_1 , f_i , f_{ss} and k_1 .

Appendix B

Listing of Computer Code

C IIBC INDEX FOR ZERO BOUNDARY CONDITION VALUE
 C IIC INDEX FOR INITIAL CONDITION TYPE
 C IS INDEX FOR EVENT TYPE
 C IPLT INDEX FOR PLOTTED OUTPUT (MULTICS SOFTWARE SYSTEM)
 C ITAB INDEX FOR TABULATED OUTPUT
 C IVEG INDEX FOR VEGETATION MODEL TYPE
 C IP__ INDEX OF PLOT TYPE
 C =
 C FS SURFACE FLUX
 C VS SURFACE IN/EXFILTRATION VOLUME
 C VW MOISTURE QUANTITY CROSSING WATER TABLE
 C VSS VOLUME OF SOIL MOISTURE STORAGE
 C EV VOLUME OF TRANSPIRED MOISTURE
 C TO PONDING TIME
 C KTH LINEAR HYDRAULIC CONDUCTIVITY COEFFICIENT (K(1)/N; CM/HR)
 C N__ INDEX FOR NUMBER OF SIMULATIONS VARYING PARAMETER __
 C NL__ INDEX FOR LOGARITHMIC (=2) OR INCREMENTAL (=1) SCALE
 C NN__ INDEX FOR POWER OF LOG10
 C ZN__ INDEX FOR MULTIPLICATION FACTOR OF INCREMENTAL SCALE
 C =
 C ZL DEPTH TO WATER TABLE
 C FL RAINFALL OR EVAPORATION RATE
 C IC INDEX FOR AVERAGE INITIAL MOISTURE CONTENT
 C TS TIME STEP INDEX
 C VG INDEX FOR CONC. DEPENDENT VEGETATION MODEL PARAMETER
 C NLT SCALE INDEX (2=LOG10,1=INCREMENTAL)
 C NNT MULTIPLICATION FACTOR OR LOG10 POWER INDEX
 C NOT INDEX FOR NO. OF SIMULATIONS VARYING NO. OF SERIES TERMS
 C NZT INDEX FOR NUMBER OF CALCULATED DEPTHS
 C PL PERCENT OF WATER TABLE DEPTH FROM BOUNDARIES TO
 C EVALUATE FLUXES
 C THO INITIAL AVERAGE MOISTURE CONTENT
 C TH1 SURFACE CONCENTRATION BOUNDARY CONDITON VALUE
 C ZHO SINUSOIDAL INITIAL CONDITION PARAMETER
 C ZIIC STARTING VALUE FOR UNIFORM INITIAL CONDITION
 C ZNE EFFECTIVE POROSITY

CC

C 2.0
 C TYPE DECLARATION

CC

REAL THETA (100, 100) , ZTHETA (100) , ZZ (100) , KTH, D, ZL, G, DIST, TIME (100) ,
 &FB (1000) , F14 (1000) , F15 (1000) , ZJ1 (1000) , ZJ2 (1000) , FS (100) , VS (100) ,
 &DF (1000) , F11 (1000) , CF (1000) , TO (1000) , F8 (1000) , CZT (1000) , CZB (1000) ,
 &Q11 (1000) , QSS1 (1000) , THAV (100) , ATO (100) , SUM, FW (100) , VW (100) ,
 &VSS (100) , EV (100) , LEN (100)
 INTEGER IZ, IT

```

COMMON EIGB(4000),P1,IBC
EXTERNAL PLOT_(DESCRIPTORS),PLOT_$SETUP(DESCRIPTORS),PLOT_$SCALE
&(DESCRIPTORS),F
C
CCCCCCCCCCCCCCCCCCCCCCCCCCCCCCCCCCCCCCCCCCCCCCCCCCCCCCCCCCCCCCCC
C
C      3.0
C      DEFINE OUTPUT DATA FILE
C
CCCCCCCCCCCCCCCCCCCCCCCCCCCCCCCCCCCCCCCCCCCCCCCCCCCCCCCCCCCCCCCC
C
      PRINT, ' INPUT IXX '
      READ(5,*) IXX
C
CCCCCCCCCCCCCCCCCCCCCCCCCCCCCCCCCCCCCCCCCCCCCCCCCCCCCCCCCCCCCCCC
C
C      2.0
C      INPUT PARAMETERS OF PHYSICAL SYSTEM.
C
CCCCCCCCCCCCCCCCCCCCCCCCCCCCCCCCCCCCCCCCCCCCCCCCCCCCCCCCCCCCCCCC
C
      WRITE(6,10)
10      FORMAT(' INPUT ZNE,D,K ')
      READ(5,) ZNE,D,KTH
C
CCCCCCCCCCCCCCCCCCCCCCCCCCCCCCCCCCCCCCCCCCCCCCCCCCCCCCCCCCCCCCCC
C
C      2.0
C      INPUT GEOMETRICAL PARAMETERS
C
CCCCCCCCCCCCCCCCCCCCCCCCCCCCCCCCCCCCCCCCCCCCCCCCCCCCCCCCCCCCCCCC
C
      PRINT, ' INPUT NO. DEPTH STEPS;SCALE TYPE(LN=2) '
      READ(5,) NZL,NLZL
      PRINT, ' INPUT SCALE '
      IF(NLZL.EQ.2) READ(5,) NNZL
      IF(NLZL.NE.2) READ(5,) ZNZL
C
CCCCCCCCCCCCCCCCCCCCCCCCCCCCCCCCCCCCCCCCCCCCCCCCCCCCCCCCCCCCCCCC
C
C      2.0
C      INPUT INITIAL CONDITIONS
C      (UNIFORM=1,SINUSOIDAL=2,HYDROSTATIC=3)
C
CCCCCCCCCCCCCCCCCCCCCCCCCCCCCCCCCCCCCCCCCCCCCCCCCCCCCCCCCCCCCCCC
C
      NIC=1
      WRITE(6,52)
52      FORMAT(' UNIF=1,SIN=2,EXP=3 ')
      READ(5,) IIC

```



```

C
C   3.0
C   TO CALCULATE ONLY PONDING TIME SET ITO=1 AND TO NEGLECT PONDING
C   TIME SET ITO=2
C
CCCCCCCCCCCCCCCCCCCCCCCCCCCCCCCCCCCCCCCCCCCCCCCCCCCCCCCCCCCC
C
C   WRITE (6,29)
29  FORMAT(' TO ONLY=1,NOT TO=2 ')
C   READ (5,) ITO
C   IF (ITO.EQ.1) GO TO 35
C
CCCCCCCCCCCCCCCCCCCCCCCCCCCCCCCCCCCCCCCCCCCCCCCCCCCCCCCCCCCC
C
C   3.0
C   CALCULATE MOISTURE DISTRIBUTION?
C
CCCCCCCCCCCCCCCCCCCCCCCCCCCCCCCCCCCCCCCCCCCCCCCCCCCCCCCCCCCC
C
C   WRITE (6,33)
33  FORMAT(' DISTRIBUTION=1 ')
C   READ (5,) IDS
C   IF (IDS.NE.1) GO TO 35
C
CCCCCCCCCCCCCCCCCCCCCCCCCCCCCCCCCCCCCCCCCCCCCCCCCCCCCCCCCCCC
C
C   3.0
C   INPUT THE NUMBER OF NODES AT WHICH THE CONTINUOUS SOLUTION IS
C   TO BE EVALUATED OVER THE UNSATURATED ZONE DEPTH
C
CCCCCCCCCCCCCCCCCCCCCCCCCCCCCCCCCCCCCCCCCCCCCCCCCCCCCCCCCCCC
C
C   WRITE (6,37)
37  FORMAT(' INPUT NO.NODES ')
C   READ (5,) NZT
35  CONTINUE
C
CCCCCCCCCCCCCCCCCCCCCCCCCCCCCCCCCCCCCCCCCCCCCCCCCCCCCCCCCCCC
C
C   2.0
C   VARY NUMBER OF SERIES TERMS,SURFACE FLUX RATE,WATER TABLE DEPTH,
C   INITIAL CONDITION VALUE,VEGETATION COEFFICIENT VALUE
C
CCCCCCCCCCCCCCCCCCCCCCCCCCCCCCCCCCCCCCCCCCCCCCCCCCCCCCCCCCCC
C
C   DO 55 IN=1,NOT
C   IF (NLT.EQ.2) NT=10** (IN-NNT)
C   IF (NLT.NE.2) NT=NNT*IN
C   DO 50 IFL=1,NFL
C   IF (NLFL.EQ.2) FL=10.** (IFL-NNFL)

```



```

C      2.0
C      CALCULATE THE EIGENVALUES OF THE PROBLEM
C
C
C
C      CALL EIGVAL (NT,PI,ZL)
C
C
C
C      2.0
C      INITIALIZE EIGENVALUE RELATED VECTORS
C
C
C
C      ATT=0.
C      THI=0.
C      THSS=0.
C      SQI=0.
C      SQSS=0.
C      QI=0.
C      QSS=0.
C
C
C
C      2.0
C      CALCULATE THE EIGENVALUE DEPENDENT TERMS
C
C
C
C      DO 100 N=1,NT
C      BN=EIGB (N)
C      BN2=BN*BN
C      Z1=(-1.)**N
C      A1=BN2+0.25
C      A3=A1+G1
C      IF (IBC.EQ.1) DF (N)=0.5*(ZL*A1+0.5)/A1
C      F1=BN*E1+SIN (BN*ZL)
C      F3=A1*SIN (BN*ZL) -BN*COS (BN*ZL)
C      F2=BN*E1*(ZL+1/A1)+F3/A1
C      F5=1-Z1*E1
C      F6=1/A1-Z1*E1*(ZL+1/A1)
C      CZT (N)=COS (BN*Z2)
C      CZB (N)=COS (BN*(ZL-Z2))
C
C
C
C      2.0
C      CALCULATE THE TRANSFORMED INITIAL CONDITION
C
C
C

```

```

C
C      2.0
C      CALCULATE HYDROSTATIC INITIAL CONDITION
C
CCCCCCCCCCCCCCCCCCCCCCCCCCCCCCCCCCCCCCCCCCCCCCCCCCCCCCCCCCCCCCCC
C
      FB(N)=0.
      IF (IIC.NE.3) GO TO 92
      IF (IBC.EQ.1) FB(N)=ZNE*BN*E1/A1
      IF (IBC.EQ.1) GO TO 96
      F8(N)=E2-Z1*E1
      FB(N)=ZNE*BN*F8(N)/A1
C
CCCCCCCCCCCCCCCCCCCCCCCCCCCCCCCCCCCCCCCCCCCCCCCCCCCCCCCCCCCCCCCC
C
      2.0
      CALCULATE UNIFORM INITIAL CONDITION
C
CCCCCCCCCCCCCCCCCCCCCCCCCCCCCCCCCCCCCCCCCCCCCCCCCCCCCCCCCCCCCCCC
C
92      IF (IIC.NE.1) GO TO 94
      IF (IBC.NE.1) GO TO 93
      FB(N)=THO*F1/A1
93      IF (IBC.NE.2) GO TO 96
      FB(N)=THO*BN*F5/A1
C
CCCCCCCCCCCCCCCCCCCCCCCCCCCCCCCCCCCCCCCCCCCCCCCCCCCCCCCCCCCCCCCC
C
      2.0
      CALCULATE SINUSOIDAL INITIAL CONDITION
      (CAUTION: NEEDS FURTHER TESTING)
C
CCCCCCCCCCCCCCCCCCCCCCCCCCCCCCCCCCCCCCCCCCCCCCCCCCCCCCCCCCCCCCCC
C
94      IF (IIC.NE.2) GO TO 96
      IF (IBC.NE.1) GO TO 95
      F4=0.5*(E1+1)
      PZB1=(PI/ZL-BN)
      PZB2=(PI/ZL+BN)
      F41=(F4-PZB1)/(0.25+PZB1)**2
      F42=(F4+PZB2)/(0.25+PZB2)**2
      FB(N)=(PFS2*F2+ZHO*F1)/A1+ACAP*(F41-F42)/2.
95      IF (IBC.NE.2) GO TO 96
      F7=1+Z1*E1
      F71=(N+1)*F7/(0.25+EIGB(N+1)*EIGB(N+1))
      IF (N.EQ.1) F72=0.
      IF (N.NE.1) F72=(N-1)*F7/(0.25+EIGB(N-1)*EIGB(N-1))
      FB(N)=(ZHO*BN*F5+PFS2*F6)/A1+PI*ACAP*(F71-F72)
96      CONTINUE
C

```



```

C
C      2.0
C      CALCULATE PONDING/DRYING TIME FOR CONCENTRATION BC
C
CCCCCCCCCCCCCCCCCCCCCCCCCCCCCCCCCCCCCCCCCCCCCCCCCCCCCCCCCCCCCCCC
C
      IF (IBC.NE.2) GO TO 106
      QI=TH1/2.-QI
      QSS=TH1/2.-QSS
      ATT=(FL-QSS)/(QI-QSS)
      IF (ITO.EQ.2) GO TO 107
      ATO (IZL) = (FL-QI-QSS*A LOG (ATT)) / (FL*P41)
106   CONTINUE
      IF (IPLT.EQ.1) GO TO 107
      WRITE (6,105) FL,ZL,ATO (IZL)
105   FORMAT (' INTENSITY=',F6.2,3X,' DEPTH=',F6.2,3X,'
&PONDING TIME=',F6.4)
107   CONTINUE
      IF (ITO.EQ.1) GO TO 34
C
CCCCCCCCCCCCCCCCCCCCCCCCCCCCCCCCCCCCCCCCCCCCCCCCCCCCCCCCCCCCCCCC
C
C      2.0
C      CALCULATE THE VALUE OF THE MASS BALANCE COEFFICIENTS AND TERMS
C
CCCCCCCCCCCCCCCCCCCCCCCCCCCCCCCCCCCCCCCCCCCCCCCCCCCCCCCCCCCCCCCC
C
C      2.0
C      CALCULATE THE RESULTS OVER THE TIME DOMAIN
C
CCCCCCCCCCCCCCCCCCCCCCCCCCCCCCCCCCCCCCCCCCCCCCCCCCCCCCCCCCCCCCCC
C
      DO 400 IT=1,NTS
      IF (NLTS.EQ.2) T=10.*(IT-NNTS)
      IF (NLTS.NE.2) T=ZNTS*(IT-1.)
C
CCCCCCCCCCCCCCCCCCCCCCCCCCCCCCCCCCCCCCCCCCCCCCCCCCCCCCCCCCCCCCCC
C
C      2.0
C      CALCULATE THE SERIES TERMS FOR THE TIME DEPENDENT PARAMETERS
C
CCCCCCCCCCCCCCCCCCCCCCCCCCCCCCCCCCCCCCCCCCCCCCCCCCCCCCCCCCCCCCCC
C
      SJC=0.
      SVC=0.
      SBF=0.
      SBBF=0.
      SBC=0.
      SBBC=0.
      SVSF=0.

```


IF (IBC.EQ.2) FS (IT)=TH1/2.-SJC

C
CC

C
C 2.0
C SURFACE VOLUMES

C
CC

C
IF (IBC.EQ.1) VS (IT)=FL*T
IF (IBC.EQ.2) VS (IT)=TH1*T/2.-SVC

C
CC

C
C 2.0
C WATER TABLE FLUXES

C
CC

C
IF (IBC.EQ.1) FW (IT)=ZNE/2.+E3*SBF
IF (IBC.EQ.2) FW (IT)=ZNE/2.-E3*SBC

C
CC

C
C 2.0
C WATER TABLE VOLUMES

C
CC

C
IF (IBC.EQ.1) VW (IT)=ZNE*T/2.+E3*SBBF
IF (IBC.EQ.2) VW (IT)=ZNE*T/2.-E3*SBBC

C
CC

C
C 2.0
C SOIL MOISTURE STORAGE

C
CC

C
IF (IBC.EQ.1) VSS (IT)=SVSF
IF (IBC.EQ.2) VSS (IT)=SVSC
THAV (IT)=VSS (IT)/ZL

C
CC

C
C 2.0
C VEGETAL TRANSPIRATION

C
CC

C


```

IF (ITAB.NE.1) GO TO 450
DO 410 IT=1,NTS
IF (NLTS.EQ.2) TIME (IT)=10.** (IT-NNTS)
IF (NLTS.NE.2) TIME (IT)=ZNTS*(IT-1.)
410 CONTINUE
WRITE (6,415) ZL,THI,THAV(1)
415 FORMAT (' DEPTH=',F8.2, ' IC=',F5.2, ' IC=',F5.3)
WRITE (6,420) (TIME (IT),IT=1,NTS)
420 FORMAT (' TIME ',4X,10 (2X,F8.3))
WRITE (6,430) (FS (IT),IT=1,NTS)
WRITE (6,431) (VS (IT),IT=1,NTS)
WRITE (6,432) (FW (IT),IT=1,NTS)
WRITE (6,433) (VW (IT),IT=1,NTS)
WRITE (6,434) (VSS (IT),IT=1,NTS)
WRITE (6,435) (EV (IT),IT=1,NTS)
430 FORMAT (' FS (T) =',2X,10 (2X,F8.3))
431 FORMAT (' VS (T) =',2X,10 (2X,F8.3))
432 FORMAT (' FW (T) =',2X,10 (2X,F8.3))
433 FORMAT (' VW (T) =',2X,10 (2X,F8.3))
434 FORMAT (' VSS (T) =',1X,10 (2X,F8.3))
435 FORMAT (' EV (T) =',2X,10 (2X,F8.3))
IF (IDS.NE.1) GO TO 450

C
CCCCCCCCCCCCCCCCCCCCCCCCCCCCCCCCCCCCCCCCCCCCCCCCCCCCCCCCCCCCCCCC
C
C      2.0
C      TABULAR MOISTURE DISTRIBUTION DISPLAY
C
CCCCCCCCCCCCCCCCCCCCCCCCCCCCCCCCCCCCCCCCCCCCCCCCCCCCCCCCCCCCCCCC
C
DO 600 IT=1,NTS
IF (NLTS.EQ.2) TIME (IT)=10.** (IT-NNTS)
IF (NLTS.NE.2) TIME (IT)=ZNTS*(IT-1.)
600 CONTINUE
WRITE (6,620) (TIME (IT),IT=1,NTS)
620 FORMAT (' TIME ',4X,10 (2X,F5.2))
DO 630 IZ=1,NZT
DIST=(IZ-1.)*ZL/(NZT-1.)
WRITE (6,640) DIST,(THETA (IZ,IT),IT=1,NTS)
640 FORMAT (2X,F5.1,2X,10 (2X,F5.3))
630 CONTINUE
450 CONTINUE

C
CCCCCCCCCCCCCCCCCCCCCCCCCCCCCCCCCCCCCCCCCCCCCCCCCCCCCCCCCCCCCCCC
C
C      2.0
C      STORAGE OF DATA IN FILE IXX AND GRAPHICAL DATA DISPLAY
C      USING MULTICS SOFTWARE SYSTEM
C      (MOISTURE DISTRIBUTION, SURFACE VOLUMES, AVERAGE MOISTURE CONTENT
C      AND PONDING TIME ARE DIMENSIONAL. ALL OTHERS ARE DIMENSIONLESS.)

```

```

C
CCCCCCCCCCCCCCCCCCCCCCCCCCCCCCCCCCCCCCCCCCCCCCCCCCCCCCCCCCCCCCCC
C
  IF (IPLT.NE.1) GO TO 800
  IF (IDS.NE.1) GO TO 705
  DK=D/KTH
  DK2=D/(KTH*KTH)
  ZL=DK*ZL
  DO 700 IT=1,NTS
  DO 690 IZ=1,NZT
  Z=(IZ-1.)*ZL/(NZT-1.)
  ZTHETA (IZ)=THETA (IZ,IT)
  ZZ (IZ)=Z
690  CONTINUE
  IF (IIBC.NE.1) ZTHETA (NZT)=ZNE
  IF (IIBC.EQ.1) GO TO 91
  IF (IBC.EQ.1) GO TO 91
  IF (IS.EQ.1) ZTHETA (1)=ZNE
91  CONTINUE
  IF (IT.NE.1) GO TO 680
  CALL PLOT_$SETUP (' SOIL MOISTURE DISTRIBUTION ', 'DEPTH', '
&MOISTURE CONTENT ',1,0EO,0,0)
  CALL PLOT_$SCALE (0.,ZL,0.,ZNE)
680  CONTINUE
  CALL PLOT_(ZZ,ZTHETA,NZT,1,' ')
  DO 701 IZ=1,NZT
  ZZ (IZ)=ZZ (IZ)/DK
  WRITE (IXX,*) ZZ (IZ),ZTHETA (IZ)
701  CONTINUE
700  CONTINUE
705  CONTINUE
  IF (IPLT.NE.1) GO TO 800
  DK2=D/(KTH*KTH)
  DK=D/KTH
  DO 710 IT=1,NTS
  TIME (IT)=ZNTS*(IT-1.)
  IF (IPVSS.EQ.1) TIME (IT)=DK2*TIME (IT)
  IF (IPVS.EQ.1) TIME (IT)=DK2*TIME (IT)
  VS (IT)=DK*VS (IT)
710  CONTINUE
  IF (IPFS.EQ.1) GO TO 712
  GO TO 714
712  CONTINUE
  DO 716 IT=1,NTS
  IF (IT.EQ.1) GO TO 716
  FS (IT-1)=FS (IT)
  IF (IS.EQ.2) FS (IT-1)=-FS (IT-1)
  TIME (IT-1)=ZNTS*(IT-1.)
  WRITE (IXX,*) TIME (IT-1),FS (IT-1)
716  CONTINUE

```

```

714 CONTINUE
    IF (IPFS.NE.1) GO TO 720
    IF (IN.NE.1) GO TO 715
    IF (IZL.NE.1) GO TO 715
    IF (IFL.NE.1) GO TO 715
    IF (IVG.NE.1) GO TO 715
    IF (IJC.NE.1) GO TO 715
    CALL PLOT_$SETUP(' FLUX ', 'TIME ', 'FLUX ', 1, OEO, 0, 0)
    CALL PLOT_$SCALE (0., TIME (NTS), 0., FS (1)+.25)
715 CONTINUE
    CALL PLOT_ (TIME, FS, (NTS-1), 2, '+')
720 CONTINUE
    IF (IPVS.NE.1) GO TO 730
    IF (IN.NE.1) GO TO 725
    IF (IZL.NE.1) GO TO 725
    IF (IFL.NE.1) GO TO 725
    IF (IVG.NE.1) GO TO 725
    IF (IJC.NE.1) GO TO 725
    CALL PLOT_$SETUP(' ', 'TIME (HOURS) ', 'VOLUME (CM) ', 1, OEO, 0, 0)
725 CONTINUE
    CALL PLOT_ (TIME, VS, NTS, 0, '+')
730 CONTINUE
    IF (IPVS.NE.1) GO TO 734
    DO 731 IT=1, NTS
    WRITE (IXX, *) TIME (IT), VS (IT)
731 CONTINUE
734 CONTINUE
    IF (IPVSS.NE.1) GO TO 740
    IF (IN.NE.1) GO TO 735
    IF (IZL.NE.1) GO TO 735
    IF (IFL.NE.1) GO TO 735
    IF (IVG.NE.1) GO TO 735
    IF (IJC.NE.1) GO TO 735
    CALL PLOT_$SETUP(' ', 'TIME (HOURS) ', ' ', 1, OEO, 0, 0)
    CALL PLOT_$SCALE (0., TIME (NTS), 0., ZNE)
735 CONTINUE
    CALL PLOT_ (TIME, THAV, NTS, 0, '+')
    IF (IPVSS.NE.1) GO TO 744
    DO 741 IT=1, NTS
    WRITE (IXX, *) TIME (IT), THAV (IT)
741 CONTINUE
744 CONTINUE
740 CONTINUE
    IF (IPVW.NE.1) GO TO 750
    IF (IN.NE.1) GO TO 745
    IF (IZL.NE.1) GO TO 745
    IF (IFL.NE.1) GO TO 745
    IF (IVG.NE.1) GO TO 745
    IF (IJC.NE.1) GO TO 745
    CALL PLOT_$SETUP(' WATER TABLE VOLUME ', 'TIME ', 'VOLUME ', 1, OEO, 1, 0)

```

```

745  CONTINUE
      CALL PLOT_(TIME,VW,NTS,0,'+')
750  CONTINUE
      IF(IPEV.NE.1) GO TO 760
      IF(IN.NE.1) GO TO 755
      IF(IZL.NE.1) GO TO 755
      IF(IFL.NE.1) GO TO 755
      IF(IVG.NE.1) GO TO 755
      IF(IJC.NE.1) GO TO 755
      CALL PLOT_$(SETUP(' TRANSP.RATE ', 'TIME ', 'VOLUME ',1,0EO,1,0)
755  CONTINUE
      CALL PLOT_(TIME,EV,NZL,0,'+')
760  CONTINUE
800  CONTINUE
34   CONTINUE
54   CONTINUE
20   CONTINUE
C
CCCCCCCCCCCCCCCCCCCCCCCCCCCCCCCCCCCCCCCCCCCCCCCCCCCCCCCCCCCCCCCCCCCC
C
C      2.0
C      GRAPHICALLY DISPLAY AND STORE DIMENSIONAL PONDING TIME DATA
C
CCCCCCCCCCCCCCCCCCCCCCCCCCCCCCCCCCCCCCCCCCCCCCCCCCCCCCCCCCCCCCCCCCCC
C
      IF(IPLT.NE.1) GO TO 50
      IF(IPTO.NE.1) GO TO 50
      DK=D/KTH
      DK2=D/(KTH*KTH)
      DO 910 IZL=1,NZL
      LEN(IZL)=ZNZL*IZL
      LEN(IZL)=DK*LEN(IZL)
      ATO(IZL)=DK2*ATO(IZL)
910  CONTINUE
      IF(IFL.NE.1) GO TO 915
      IF(IN.NE.1) GO TO 915
      CALL PLOT_$(SETUP(' ', 'WATER TABLE DEPTH (CM) ', ' TO (HRS) ',
&1,0EO,0,0)
      CALL PLOT_$(SCALE(0.,LEN(NZL),0.,ATO(NZL))
915  CONTINUE
      CALL PLOT_(LEN,ATO,NZL,2,'+')
      DO 1001 IZL=1,NZL
      LEN(IZL)=LEN(IZL)/DK
      ATO(IZL)=ATO(IZL)/DK2
      WRITE(IXX,*) LEN(IZL),ATO(IZL)
1001 CONTINUE
50   CONTINUE
55   CONTINUE
      READ(5, )
1000 CONTINUE

```